

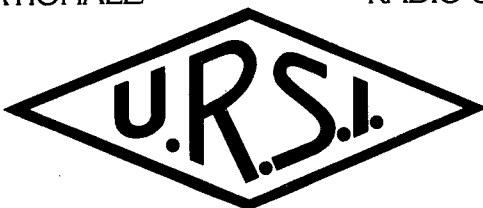
Conseil national de la recherche
National Research Council
du / of
Canada

National Academies of Science
and Engineering
National Research Council
United States of America

COMITÉS NATIONAUX / NATIONAL COMMITTEES

UNION RADIO
SCIENTIFIQUE
INTERNATIONALE

INTERNATIONAL UNION
OF
RADIO SCIENCE



COLLOQUE RADIO
SCIENTIFIQUE
NORD-AMÉRICAIN

NORTH AMERICAN
RADIO SCIENCE
MEETING

QUÉBEC, JUIN / JUNE 2-6, 1980

Parrainé par / Sponsored by
URSI / CNC - USNC / URSI

tenu conjointement avec / held jointly with

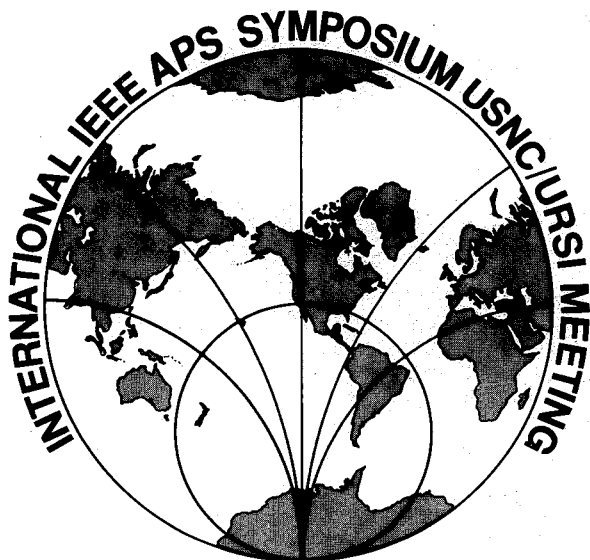
Symposium international de
la Société
Antennes et Propagation

International Symposium
of
Antennas and Propagation Society

Institute of Electrical and Electronics Engineers

UNIVERSITÉ LAVAL
CITÉ UNIVERSITAIRE
QUÉBEC, CANADA

**COME TO LOS ANGELES
IN 1981**



**17-19 JUNE 1981
AT THE
BONAVENTURE HOTEL
LOS ANGELES, CALIFORNIA**

**FOR INFORMATION WRITE TO:
PROFESSOR R. S. ELLIOTT
7732 BOELTER HALL
UCLA
LOS ANGELES, CALIFORNIA 90024**

Programme
et
Résumés

Program
and
Abstracts

United States of America - Canada
National Committees - Comités Nationaux

Union Radio Scientifique / International Union of
Internationale Radio Science



Colloque Radio Scientifique
Nord-Américain

North American Radio
Science Meeting

Juin/June 2-6, 1980

tenue conjointement avec/held jointly with

Symposium International de
la Société
Antennes et Propagation

International Symposium
of
Antennas and Propagation Society

Québec, Canada

AVIS

On pourra se procurer le programme et le résumé des communications présentées au Colloque Radio Scientifique Nord-Américain de l'URSI en écrivant à l'adresse suivante:

Symposium IEEE/URSI 1980
Département de Génie Electrique
Université Laval
Cité Universitaire
Québec, Canada
G1K 7P4

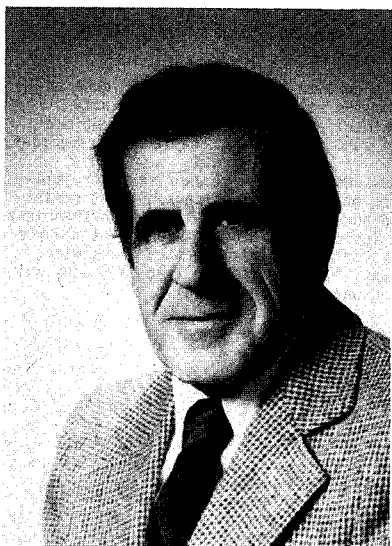
Le texte intégral des communications ne sera pas publié dans une édition spéciale. Il est fort possible néanmoins qu'un auteur, de sa propre initiative, fasse publier son texte; en ce cas, on devra s'adresser à lui pour en obtenir une copie. A noter, de plus, que les comités nationaux assurent l'entière responsabilité des colloques qui, comme celui-ci, ne sont pas organisés par le comité international de l'URSI. Il ne faut donc pas s'adresser au Secrétariat international pour obtenir copie des programmes ou des résumés.

NOTE

Program and Abstracts of the North American Radio Science Meeting are available from:

Symposium IEEE/URSI 1980
Département de Génie Electrique
Université Laval
Cité Universitaire
Québec, Canada
G1K 7P4

The full papers are not published in any collected format; requests for them should be addressed to the authors who may have them published on their own initiative. Please note that these meetings are national and they are not organized by international URSI, nor are the program available from the international Secretariat.



BIENVENUE
A QUEBEC

WELCOME
TO QUEBEC

The Steering Committee of the 1980 APS-URSI joint symposium and the Canadian members of both societies welcome you to the city of Quebec and the campus of "Université Laval". We trust that, during your visit, not only will you derive great professional benefit from the broad scope of the technical sessions that reflect the most recent advances in the field of electromagnetics, but that you will also take the time to enjoy the splendid attractions that your host city can provide.

Quebec has retained the French character of its beginnings along with an elegance that lend it a unique charm. It is the oldest city in Canada and holds the lion's share of historical monuments. Nowhere are these features more evident than in the heart of the old city, where the Conference banquet will take place, at the magnificent Château Frontenac. The program includes a number of sightseeing tours to sites of exceptional scenic beauty and to areas that are typically French-Canadian.

Le comité directeur du Congrès de 1980 des deux sociétés savantes AP-S et URSI est heureux de se joindre aux membres canadiens de chacune d'elles pour vous souhaiter la bienvenue à Québec et à l'Université Laval, où se tiendront les réunions.

Nous sommes confiants que votre séjour ici, en plus de vous être utile du côté professionnel, vous apportera aussi des moments de détente. L'éventail très vaste des sujets traités par les conférenciers ne manquera pas, sans doute, de vous intéresser et il est sûr que les attraits multiples de la ville qui vous accueille, sauront aussi vous plaire.

Fidèle à ses origines, notre ville a sauvegardé le cachet d'élégance lié à sa culture française et c'est ce qui fait son charme. C'est la ville la plus ancienne du Canada, encore entourée par ses vieilles murailles, où abondent les monuments historiques. Ces caractéristiques ne sont, nulle part, plus évidentes qu'au coeur même du vieux Québec.

Finally, we wish to express our appreciation and sincere gratitude to all those who have helped to make this symposium a success: the speakers and the session chairmen, the members of the organizing committees and their chairmen, Université Laval and all our supporters.

où le banquet traditionnel du Congrès doit avoir lieu, en l'enceinte du Château Frontenac.

Le programme comprend aussi quelques excursions vers des sites d'une beauté vraiment exceptionnelle, en des régions qui sont typiquement canadiennes-françaises.

Nous désirons, enfin, exprimer notre sincère gratitude à tous ceux qui ont contribué au succès du Congrès: les conférenciers et les directeurs de sessions, les membres des comités organisateurs et leurs directeurs, l'Université Laval et tous ceux qui nous ont donné leur appui.

MEMBRES/MEMBERSHIP

Officiers/Officers

Président/Chairman

Dr. F.J.F. Osborne

Président sortant/Past Chairman

Dr. R.E. Barrington

Secrétaire/Secretary

Dr. J.Y. Wong

Présidents des Commissions du CNC/URSI/Chairmen of the CNC/URSI Commissions

Commission A

Dr. D. Morris

Commission B

Dr. J.A. Cummins

Commission C

Dr. P.H. Wittke

Commission D

Dr. A.R. Boothroyd

Commission E

Dr. Bhartendu

Commission F

Dr. K.S. McCormick

Commission G

Vacant/Presently unfilled

Commission H

Dr. R. Gagné

Commission J

Mr. N.W. Broten

MEMBERSHIP

United States National Committee

INTERNATIONAL UNION OF RADIO SCIENCE

Chairman:	Dr. C. Gordon Little*
Vice-Chairman:	Mr. George H. Hagn*
Secretary:	Dr. Thomas B.A. Senior*
Immediate Past Chairman:	Dr. John V. Evans*

Members Representing Societies, Groups and Institutions:

American Geophysical Union	Dr. Christopher T. Russell
Bioelectromagnetics Society	Dr. James C. Lin
Institute of Electrical & Electronic Engineering	Dr. Ernst Weber
IEEE Antennas & Propagation Society	Dr. Alan W. Love
IEEE Communications Society	Dr. Amos Joel
IEEE Information Theory Group	Dr. Aaron D. Wyner
IEEE Microwave Theory & Techniques Society	Dr. Kenneth J. Button
IEEE Quantum Electronics Society	Dr. Robert A. Bartolini
Optical Society of America	Dr. Steven F. Clifford

Liaison Representatives from Government Agencies:

National Telecommunications & Information Administration	Mr. Samuel E. Probst
National Science Foundation	Dr. Vernon Pankonin
Department of Commerce	(Vacant)
National Aeronautics & Space Administration	Dr. Erwin R. Schmerling
Federal Communications Commission	(Vacant)
Department of Defense	Mr. Emil Paroulek
Department of the Army	Major Robert Clayton, Jr.
Department of the Navy	Dr. Leo Young
Department of the Air Force	Dr. Allan C. Schell

Members-at-large:	Dr. Donald E. Barrick
	Dr. George W. Swenson, Jr.
	Dr. Leonard S. Taylor

* Member of USNC-URSI Executive Committee

Chairmen of the USNC-URSI Commissions:

Commission A	Dr. Raymond C. Baird
Commission B	Prof. Georges A. Deschamps
Commission C	Prof. Mischa Schwartz
Commission D	Dr. Kenneth J. Button
Commission E	Dr. Arthur D. Spaulding
Commission F	Dr. Robert K. Crane
Commission G	Dr. Jules Aarons
Commission H	Dr. Robert W. Fredricks
Commission J	Dr. Alan T. Moffet

Officers of URSI resident in the United States:
(including Honorary Presidents)

Vice-President	Prof. William E. Gordon*
Honorary President	Prof. Henry G. Booker*

Chairmen and Vice-Chairmen of
Commissions of URSI resident
in the United States:

Chairman of Commission B	Prof. Leopold B. Felsen
Vice-Chairman of Commission C	Prof. Jack K. Wolf
Chairman of Commission E	Mr. George H. Hagn
Chairman of Commission F	Prof. Alan T. Waterman, Jr.
Chairman of Commission H	Dr. Frederick W. Crawford

Foreign Secretary of the U.S.
National Academy of Sciences

Dr. Thomas F. Malone

Chairman, Office of Physical
Sciences-NRC

Dr. Ralph O. Simmons

NRC Staff Officer

Mr. Richard Y. Dow

Honorary Members:

Dr. Harold H. Beverage
Prof. Arthur H. Waynick

* Member of USNC-URSI Executive Committee

DESCRIPTION

DE

L'UNION RADIO SCIENTIFIQUE INTERNATIONALE

L'Union Radio Scientifique Internationale est l'une des dix-huit unions scientifiques organisées sous les auspices du Conseil International des Unions Scientifiques (CIUS). On la désigne généralement par son acronyme: l'URSI. Ses buts sont les suivants: (1) stimuler et coordonner, à l'échelle internationale, les études dans le domaine de la radioélectricité scientifique; (2) de promouvoir et d'organiser les recherches exigeant une coopération internationale, ainsi que la discussion et la diffusion des résultats de ces recherches; (3) d'encourager l'adoption de méthodes de mesure communes, ainsi que la comparaison et l'étalonnage des instruments de mesure utilisés dans les travaux scientifiques; (4) de stimuler et de coordonner les études des aspects scientifiques des télécommunications utilisant les ondes électromagnétiques guidées et non guidées. L'URSI est un organisme administratif dont la fonction est de promouvoir la poursuite des objectifs décrits plus haut. La partie technique des travaux se fait, en majeure partie, au sein des Comités nationaux des pays membres.

Les officiers de l'Union Internationale sont:

Président:	W.N. Christiansen (Australie)
Président sortant:	M.J. Voge (France)
Vice-Présidents:	W.E. Gordon (Etats-Unis) A.P. Mitra (Indes) A. Smolinski (Pologne) F.L.H.M. Stumpers (Pays-Bas)
Secrétaire Général:	J. Van Bladel (Belgique)
Présidents Honoraires:	H.G. Booker (Etats-Unis) M.B. Decaux (France) W. Dieminger (Allemagne de l'Ouest) J.A. Ratcliffe (Royaume-Uni) R.L. Smith-Rose (Royaume-Uni)

Le bureau du Secrétaire Général et le siège du Conseil de l'URSI sont situés à l'adresse suivante: Avenue de Lancaster 32, B-1180 Bruxelles, Belgique. Les ressources financières de l'URSI proviennent principalement des contributions fournies par les 36 pays qui en font partie. Une aide financière supplémentaire, provenant de l'Unesco, lui est aussi accordée par l'intermédiaire de l'ICSU.

L'URSI, lors de sa XIXième Assemblée Générale, tenue au mois d'août 1978, à Helsinki, en Finlande, comprenait neuf groupements, appelés "Commissions", qui ont pour fonction de canaliser les recherches qui se poursuivent dans les principaux domaines de la radio-électricité scientifique. La liste des neuf Commissions, le champ d'étude de chacune avec le nom du président actuel sont donnés ci-dessous:

Commission A	Métrieologie électromagnétique S. Okamura (Japon)
Commission B	Ondes et champs L.B. Felsen (Etats-Unis)
Commission C	Signaux et Systèmes V. Zima (Tchécoslovaquie)
Commission D	Physique électronique W.G. Farnell (Canada)
Commission E	Bruits et brouillages électromagnétiques G.H. Hagn (Etats-Unis)
Commission F	Phénomènes ondulatoires dans les milieux non-ionisés A.T. Waterman, Jr. (Etats-Unis)
Commission G	Radio électricité ionosphérique et propagation B. Hultqvist (Suède)
Commission H	Ondes dans les plasmas F.W. Crawford (Etats-Unis)
Commission J	Radioastronomie H. Tanaka (Japon)

A tous les trois ans, l'URSI organise un congrès que l'on appelle Assemblée Générale. La prochaine, qui sera la XXIème, se tiendra à Washington, D.C., au mois d'août 1981. Les compte rendus des Assemblées Générales sont rédigés par le Secrétariat qui se charge aussi de leur distribution. L'URSI organise, en outre, des Conférences Internationales sur des sujets d'étude particuliers, ressortissant au domaine de l'une des neuf Commissions, ou même de plusieurs d'entre elles. Enfin, de concert avec d'autres Unions Scientifiques, l'URSI organise aussi des colloques, à l'échelle internationale sur des sujets d'intérêt commun.

La radioélectricité se distingue des autres domaines de recherches scientifiques par la caractéristique suivante: elle se prête mieux que toute autre à l'élaboration de programmes de recherches à l'échelle internationale, du fait que les phénomènes à étudier ne sont pas confinés au territoire d'un seul pays mais se propagent souvent sur une vaste portion du globe terrestre, et ceci, sans toutefois échapper au contrôle des expérimentateurs.

On sait aussi que les recherches qui ont pour domaine l'exploration de l'espace ou l'observation du milieu spatial ne seraient pas possibles sans la radioélectricité. La radio-astronomie, en particulier, s'occupe exclusivement des phénomènes de radiation cosmiques. En tout ceci, l'URSI joue un rôle important, puisqu'elle offre à tous les chercheurs qui s'occupent des multiples aspects de la radioélectricité l'organisme qui leur permet de communiquer entre eux.

Les congrès qu'elle organise et les travaux de ses nombreux comités stimulent la recherche en favorisant la discussion entre chercheurs et la diffusion des résultats de leurs recherches.

DESCRIPTION OF THE
INTERNATIONAL UNION OF RADIO SCIENCE

The International Union of Radio Science is one of 18 world scientific unions organized under the International Council of Scientific Unions (ICSU). It is commonly designated as URSI (from its French name, Union Radio Scientifique Internationale). Its aims are (1) to promote the scientific study of radio communications, (2) to aid and organize radio research requiring cooperation on an international scale and to encourage the discussion and publication of the results (3) to facilitate agreement upon common methods of measurement and the standardization of measuring instruments, and (4) to stimulate and to coordinate studies of the scientific aspects unguided. The International Union itself is an organizational framework to aid in promoting these objectives. The actual technical work is largely done by the National Committees in the various countries.

The officers of the International Union are:

President:	W.N. Christiansen (Australia)
Past President:	M.J. Voge (France)
Vice-Presidents:	W.E. Gordon (USA) A.P. Mitra (India) A. Smolinski (Poland) F.L.H.M. Stumpers (Netherlands)
Secretary General:	J. Van Bladel (Belgium)
Honorary Presidents:	H.G. Booker (USA) M.B. Decaux (France) W. Dieminger (West Germany) J.A. Ratcliffe (UK) R.L. Smith-Rose (UK)

The Secretary General's office and the headquarters of the organization are located at Avenue de Lancaster 32, B-1180 Brussels, Belgium. The Union is supported by contributions (dues) from 36 member countries. Additional funds for symposia and other scientific activities of the Union are provided by ICSU from contributions received for this purpose from UNESCO.

The International Union, as of the XIXth General Assembly held in Helsinki, Finland in August, 1978, has nine bodies called Commissions for centralizing studies in the principal technical fields. The names of the Commissions and their chairmen follow.

Commission A	Electromagnetic Metrology S. Okamura (Japan)
Commission B	Fields and Waves L.B. Felsen (USA)
Commission C	Signals and Systems V. Zima (Czechoslovakia)
Commission D	Physical Electronics W.G. Farnell (Canada)
Commission E	Electromagnetic Noise and Interference G.H. Hagn (USA)
Commission F	Wave Phenomena in Non-Ionized Media A.T. Waterman, Jr. (USA)
Commission G	Ionospheric Radio and Propagation B. Hultqvist (Sweden)
Commission H	Waves in Plasmas F.W. Crawford (USA)
Commission J	Radio Astronomy H. Tanaka (Japan)

Every three years the International Union holds a meeting called the General Assembly, and the next is the XXth, to be held in Washington, D.C., in August, 1981. The Secretariat prepares and distributes the Proceedings of these General Assemblies. The International Union arranges international symposia on specific subjects pertaining to the work of one Commission or to several Commissions, and also cooperates with other Unions in international symposia on subjects of joint interest.

Radio is unique among the fields of scientific work in having a specific adaptability to large-scale international research programs, since many of the phenomena that must be studied are world-wide in extent and yet are in a measure subject to control by experimenters. Exploration of space and the extension of scientific observations to the space environment are dependent on radio for their research. One branch, radio astronomy, involves cosmic phenomena. URSI has in all this a distinct field of usefulness in furnishing a meeting ground for the numerous workers in the manifold aspects of radio research; its meetings and committee activities furnish valuable means of promoting research through exchange of ideas.

STEERING COMMITTEE/COMITE DIRECTEUR

J.A. Cummins, chairman/président			
G.G. Armitage	G.Y. Delisle	N. Nachman	J.R. Wait
K.G. Balmain	S. Kubina	F.J.F. Osborne	J.Y. Wong
J.P. Bouchard	M. Lecours	T.B.A. Senior	G.L. Yip

LOCAL ARRANGEMENT COMMITTEE/COMITE D'ORGANISATION LOCALE

D. Angers	G.Y. Delisle	H. Kourilko	M. Pelletier
J.P. Bouchard	B. Faure	M. Lecours	A. Pomerleau
J.A. Cummins	R. Gagné	J.P. Lefèvre	B. Tousignant

PUBLICATIONS COMMITTEE/COMITE DES PUBLICATIONS

M. Lecours, G.Y. Delisle, F. Kirouac, J.P. Bouchard, J.A. Cummins

TECHNICAL PROGRAM COMMITTEE/COMITE DU PROGRAMME

J. Aarons	R.K. Crane	E.V. Jull	T.B.A. Senior
R.C. Baird	J.A. Cummins	G. Lyon	M. Schwartz
Bhartendu	G.A. Deschamps	R.J. Mailloux	A.D. Spaulding
A.R. Boothroyd	R.W. Fredricks	K.S. McCormick	J.R. Wait
N.W. Broten	R. Gagné	A.T. Moffet	P.H. Wittke
K.J. Button	R.A. Hurd	D. Morris	G.L. Yip

1980 MEETING
CONDENSED PROGRAM

ROOM

SUNDAY, JUNE 1

- 4:00 p.m. IEEE/AP-S Wave Propagation Standards Committee Meeting
Pavillon Vachon, 1045
- 6:30 p.m. USNC/URSI Executive Committee Dinner and Meeting
Pavillon Pollack, Salon des professeurs
- 8:00 p.m. USNC/URSI Business Meeting
Pavillon Pollack, Salon des professeurs

MONDAY, JUNE 2

8:30 - 12:00 a.m.

- | | | |
|--------|---|--------|
| B.1 | Scattering I | DKN 1A |
| AP.1 | Millimetre Wave Antennas | DKN 1D |
| A | Bio Electromagnetics | DKN 2A |
| B.2/AP | Special Session on Optical Communications I -
Fiber and Guided Wave Optics I | DKN 2B |
| J.1/AP | Very Long Baseline Interferometry | DKN 2D |

8:30 - 10:25 a.m.

- | | | |
|------|--------------------------|--------|
| AP.2 | Dipole and Slot Antennas | DKN 1E |
|------|--------------------------|--------|

1:30 - 5:00 p.m.

- | | | |
|-------|---|----------|
| B.3 | High Frequency Scattering | DKN 1A |
| B.4 | Wire Antennas I | DKN 1B |
| AP.3 | Satellite Antennas | DKN 1D |
| AP.4 | Adaptive Antenna Systems | DKN 1E |
| C.1/D | Special Session on Optical Communications II -
Devices and Systems | DKN 2B |
| F.1 | Remote Sensing - Active | DKN 2C |
| J.2 | Radar Astronomy | DKN 2D |
| B.5 | Guided Waves (poster session) | DKN 1271 |

5:30 - 7:00 p.m.

Cocktails - Geological Garden

- 7:00 p.m. IEEE/AP-S Wave Propagation Standards Committee Meeting
Pavillon Vachon, 1045

TUESDAY, JUNE 3

ROOM

9:00 - 12:00 a.m.

Session Plénière/Plenary Session

DEVELOPPEMENTS RADIO-SCIENTIFIQUES AU CANADA

RADIO SCIENCE IN CANADA

Théâtre de la Cité Universitaire

12:00 - noon

AP-S Reviewers' Luncheon
Pavillon Pollack, Salon des Professeurs

1:30 - 5:00 p.m.

B.6	Special Session on Electromagnetic Earth Induction from Overhead Conductors	DKN 1B
AP.5	Phased Arrays	DKN 1D
AP.6	Scattering and Diffraction	DKN 1E
G.1	Ionospheric Modification and Irregularities	DKN 2A
B.7/AP	Special Session on Optical Communications III - Fiber and Guided Wave Optics II	DKN 2B
F.2	Remote Sensing - Passive	DKN 2C
J.3	Spectrometry and Technical Development	DKN 2D
AP.7	Horn Antennas (poster session)	DKN 1271
5:00 p.m.	AP-S Local Chapter Chairmen's Meeting Pavillon Pollack, Salon du recteur	
5:30 p.m.	Commission B Business Meeting	DKN 1248
5:30 p.m.	Commission F Business Meeting	DKN 1252
5:30 p.m.	IEEE Geoscience and Remote Sensing Society Meeting	DKN 1255
6:00 p.m.	AP-S Ad. Com. Meeting Pavillon Pollack, Salon des professeurs	

WEDNESDAY, JUNE 4

ROOM

8:30 - 12:00 a.m.

B.8	Analytical and Numerical Techniques	DKN 1A
B.9	Random Media	DKN 1B
AP/B.10	HF-to-UHF Arrays	DKN 1D
H.1	Measurements of Magnetospheric and Space Plasmas: Probes, VLF and HF	DKN 1E
C.2	Satellite and Radio Transmission	DKN 2A
B.11/AP	Special Session on Optical Communications IV - Fiber and Guided Wave Optics III	DKN 2B
F.3	Radiative Transfer Theory and Remote Sensing of Lightning	DKN 2C
G.2	M. Lindeman Phillips Memorial Session on Ionosonde Techniques	DKN 2E
AP.8	Antenna Measurements and Calculations (poster session)	DKN 1271

8:30 - 10:00 a.m.

J.4	Radio Stars	DKN 2D
-----	-------------	--------

10:30 - 12:00 a.m.

A/J.5	Measurements of Large Antennas	DKN 2D
-------	--------------------------------	--------

1:30 - 5:00 p.m.

AP/B.12	Transients	DKN 1A
B.13	Special Session on Inverse Scattering-I Theoretical Approaches	DKN 1B
AP.9	Antenna Synthesis	DKN 1D
G.3	Ionogram Interpretations, Ionospheric Drifts, and Dispersion	DKN 2A
C.3	Signal Processing	DKN 2B
F.4/AP	Surface/Underground Propagation	DKN 2C
H.2	Plasma Related Theoretical Studies	DKN 2D
J.6	Radio Astronomy Antennas	DKN 2E
AP.12	Satellite Antenna Systems (poster session)	DKN 1271

1:30 - 3:25 p.m.

AP.10	Radar and Direction - Finding	DKN 1E
-------	-------------------------------	--------

3:40 - 5:00 p.m.

AP.11	Adaptive and Active Antennas	DKN 1E
-------	------------------------------	--------

7:30 p.m. Conference Banquet, Château Frontenac
Open bar from 6:30 p.m.

THURSDAY, JUNE 5

ROOM

8:30 - 12:00 a.m.

B.14	Scattering II	DKN 1A
B.15/AP	Special Session on Inverse Scattering-II Transient Signature Interpretation	DKN 1B
AP.13	Reflector Antennas I	DKN 1D
AP.14	Vehicular Antennas	DKN 1E
E	Noise and Interference, Characterization and Measurement	DKN 2A
F.5/AP	Line-of-Sight Propagation	DKN 2C

1:30 - 5:00 p.m.

B.16	Special Topics	DKN 1B
AP.15	Offset Reflector and Lens Antenna	DKN 1D
AP.16	Microstrip Antennas	DKN 1E
AP.17	GTD and Ray Methods	DKN 2A
F.6/AP	Precipitation Attenuation and Depolarization	DKN 2C
B.17/AP	Special Session on Inverse Scattering-III poster session on Electromagnetic Imaging	DKN 1271
5:00 p.m.	Panel on Electromagnetics Consulting	DKN 1255
5:30 p.m.	Commission G Business Meeting	DKN 1248
5:30 p.m.	Commission H Business Meeting	DKN 1252
5:30 p.m.	CNC/URSI Commission B Business Meeting	VCH 1045
8:00 p.m.	USNC/URSI Executive Committee Meeting	VCH 1045
7:30 p.m.	Wine and Cheese Pavillon Pollack	

FRIDAY, JUNE 6

8:30 - 12:00 a.m.

B.18	Reflector Antennas II	DKN 1A
B.19	Special Session on Inverse Scattering-IV Geophysical Sounding	DKN 1B
AP/B.20	Microstrip Antennas and Arrays (poster session)	DKN 1271
AP.18	Wire Antennas II	DKN 1E

TABLE DES MATIERES/TABLE OF CONTENTS

URSI	pages	1	-	359
Index alphabétique des auteurs/Author Index		360	-	366

TUESDAY MORNING
June 3, 9:00 - 12:00

RADIO SCIENCE IN CANADA
DEVELOPPEMENTS RADIO-SCIENTIFIQUES AU CANADA

Théâtre de la Cité Universitaire

Session Plénière / URSI/AP-S Plenary Session

A la mémoire de / Dedicated to the Memory of
J.H. Chapman

Président / Chairman: J.R. Wait
U.S. Department of Commerce
NOAA, ERL
Boulder, Co.

Introduction / Opening remarks: J.A. Cummins
Président, Comité directeur
Steering Committee chairman
Université Laval
Québec, P.Q.

Mot de bienvenue / Welcome: J.-G. Paquet
Recteur
Université Laval

	<u>Page</u>
1. CANADIAN SATELLITES FOR IONOSPHERIC STUDIES AND DOMESTIC COMMUNICATIONS, C.A. Franklin, Department of Communications, Ottawa, Ontario.	2
2. IONOSPHERIC PROPAGATION, R.E. Barrington, Department of Communications, Ottawa, Ontario.	3
3. ADVANCES IN VLBI, J.L. Yen, Department of Electrical Engineering, University of Toronto, Toronto, Ontario.	4
4. EM METHODS OF ORE PROSPECTING: A STATUS REPORT, G.F. West, Department of Physics, University of Toronto, Toronto, Ontario.	5

MONDAY MORNING

June 2, 08:30 - 12:00

BIO ELECTROMAGNETICS

DKN 2A

Session A

Chairman: D. Morris
Division of Physics
National Research Council, Ottawa

Page

1. DEVELOPMENTAL ANOMALIES INDUCED BY PULSED MICROWAVE RADIATION, G. d'Ambrosio, F.A. Di Meglio, G. Ferrara, Istituto Elettrotecnico, University of Naples, Italy, and A. Tranfaglia, Istituto di Entomologia Agraria, University of Naples, Italy. 7
2. IRRADIATION OF PROLATE SPHEROIDAL MODELS OF HUMANS AND ANIMALS IN THE NEAR FIELD OF A SMALL LOOP ANTENNA, A. Lakhtakia, M.F. Iskander, C.H. Durney and H. Massoudi, University of Utah, Salt-Lake City, Utah 84112, U.S.A. 8
3. RAYONNEMENT DE GUIDES RECTANGULAIRES EN PRESENCE DE MILIEUX STRATIFIES - APPLICATION AUX SONDAS BIOMEDICALES, J. Audet, J.Ch. Bolomey, Ch. Pichot, Laboratoire des Signaux et Systèmes, Groupe d'Electromagnétisme - C.N.R.S. - E.S.E., Plateau du Moulon, 91190 Gif-sur-Yvette, France, and M. Robillard, M. Chive, Y. Leroy, Centre Hyperfréquences et Semiconducteurs, L.A. au C.N.R.S., n° 287, Université de Lille I, B.P. 39, 59650 Villeneuve d'Ascq, France. 9
4. EDGE-TRACKING OF CARDIAC STRUCTURES. A METHOD FOR TRACKING OF THE EDGES OF CARDIAC STRUCTURES, J. Kuhfeld, L. Roemer, Electrical Engineering Department, the University of Akron, Akron, Ohio 44325, and G. Malindzak, Northeastern Ohio Universities, College of Medicine, Rootstown, Ohio 44272, U.S.A. 10
5. FREQUENCY DOMAIN PROFILE RECONSTRUCTION FOR TISSUE CHARACTERIZATION, C.Q. Lee and L.F. Sio, Communications Laboratory, Department of Information Engineering, University of Illinois at Chicago Circle, Box 4348, Chicago, Illinois 60680, U.S.A. 11

WEDNESDAY MORNING
June 4, 10:30 - 12:00

MEASUREMENTS OF LARGE ANTENNAS

DKN 2D

Combined Session A/J.5

Chairman: W.J. English
Intelsat
Washington, D.C.

	<u>Page</u>
1. MEASUREMENT METHOD OF EARTH STATION ANTENNA POLARIZATION CHARACTERISTICS, T. Satoh and F. Makita, Kokusai Denshin Denwa Co., Ltd., Tokyo, Japan.	13
2. PROBING AMPLITUDE, PHASE AND POLARIZATION OF MICROWAVE FIELD DISTRIBUTIONS IN REAL-TIME, R.J. King and Y.H. Yen, Dept. of Electrical and Computer Engineering, University of Wisconsin, Madison, Wisconsin, 53706.	14
3. NEAR FIELD ANTENNA MEASUREMENTS AT TEXAS INSTRUMENTS, J.P. Montgomery and S. Sanzgeri, Texas Instruments Incorporated, Dallas, Texas 75266.	15
4. MEASUREMENT OF LARGE ANTENNA SURFACE DISTORTION, R.S. Neiswander, TRW, Defense and Space Systems Group, One Space Park, Redondo Beach, California 90278.	16

MONDAY MORNING

June 2, 08:30 - 12:00

SCATTERING I

DKN IA

Session B.1

Chairman: R.E. Collin
Case Western Reserve University
Cleveland, Ohio.

	<u>Page</u>
1. ELECTROMAGNETIC SCATTERING BY TWO PARALLEL PROLATE SPHEROIDS, B.P. Sinha and R.H. MacPhie, Department of Electrical Engineering, University of Waterloo, Waterloo, Ontario N2L 3G1	18
2. SCATTERING BY A FINITE RESISTIVE PLATE, Thomas B.A. Senior, Radiation Laboratory, The University of Michigan, Ann Arbor, Michigan 48109, U.S.A.	19
3. SCATTERING FROM "INTERNALLY THICK" RESISTIVE STRIPS, K.M. Mitzner, Aircraft Group, Northrop Corporation, Hawthorne, California 90250, U.S.A.	20
4. COMBINED INTEGRAL EQUATION - FINITE ELEMENT SOLUTION TO ELECTROMAGNETIC SCATTERING BY A MISSILE WITH PLUME, M.A. Morgan and K.G. Gray, Department of Electrical Engineering, Naval Postgraduate School, Monterey, CA 93940, U.S.A.	21
5. RESONANCES OF THIN-WALLED PENETRABLE SCATTERERS, E.M. Kennaugh, The Ohio State University, ElectroScience Laboratory, Department of Electrical Engineering, Columbus, Ohio 43212, U.S.A.	22
6. PROPERTIES OF PLANAR MULTILAYER DIELECTRIC STRUCTURES, Herbert Feldman and Benjamin Rulf, the MITRE Corporation, Bedford, MA 01730, U.S.A.	23
7. WAVE REFLECTION FROM AN ANISOTROPIC MEDIUM: A COORDINATE-FREE APPROACH, Hollis C. Chen, Department of Electrical Engineering, Ohio University, Athens, Ohio 45701, U.S.A.	24
8. COMPUTATION OF THE EQUIVALENT CAPACITANCE FOR A WIRE PASSING THROUGH AN APERTURE IN A CONDUCTING SCREEN, D. Kajfez, C.M. Butler, T. Zbontar, University of Mississippi, University, MS 38677, U.S.A.	25
9. EXPERIMENTAL DETERMINATION OF THE EQUIVALENT CAPACITANCE FOR A WIRE PASSING THROUGH AN APERTURE IN A CONDUCTING SCREEN, D. Kajfez, T. Zbontar, C.M. Butler, University of Mississippi, University, MS 38677, U.S.A.	26

MONDAY MORNING

June 2, 8:30 - 12:00

SPECIAL SESSION ON OPTICAL COMMUNICATIONS 1

FIBER AND GUIDED WAVE OPTICS 1

DKN 2B

Combined Session B.2 / AP-S

Chairman and Organizer: G.L. Yip
McGill University
Montréal, Québec

	<u>Page</u>
1. MULTIMODE OPTICAL FIBERS: PROFILE CONTROL AND ANALYSIS, (Invited), H.M. Presby, Bell Laboratories, Crawford Hill Laboratory, Holmdel, N.J. 07733, U.S.A.	28
2. OPTICS IN WAVEGUIDES AND THE GENERALIZED RULE OF REFRACTIVE INDEX, (Invited), P.K. Tien, Bell Telephone Laboratories, Holmdel, N.J. 07733, U.S.A.	29
3. PROPAGATION IN GRADED-INDEX WAVEGUIDES: A REVIEW OF TECHNIQUES, (Invited), Leopold B. Felsen, Polytechnic Institute of New York, Department of Electrical Engineering, Route 110, Farmingdale, N.Y. 11735.	30
4. ANALYSIS OF INHOMOGENEOUS OPTICAL WAVEGUIDES USING COLLOCATION METHOD, T.H. Nguyen and G.L. Yip, Department of Electrical Engineering, McGill University, Montreal, Quebec H3A 2A7, Canada.	31
5. PULSE PERFORMANCE OF GRADED-INDEX OPTICAL WAVEGUIDES UNDER EQUAL AND DIFFERENTIAL EXCITATION, G.A.E. Crone, RF Technology Center, ERA Technology, Ltd., Leatherhead, Surrey, U.K. and J.M. Arnold, Department of Electrical Engineering, University of Nottingham, Nottingham NG7 2ND, U.K.	32
6. ASYMPTOTIC ANALYSIS OF INHOMOGENEOUS PLANAR AND CYLINDRICAL DIELECTRIC WAVEGUIDES, J.M. Arnold, Department of Electrical Engineering, University of Nottingham, Nottingham NG7 2RD, U.K.	33
7. PROPAGATION CONSTANT AND GROUP DELAY OF GUIDED MODES IN GRADED INDEX FIBERS: EVANESCENT WAVE THEORY (EWT) COMBINED WITH NONLINEAR TRANSFORMATION TECHNIQUES, G. Jacobsen, Electromagnetics Institute, Technical University of Denmark, DK-2800, Lyngby, Denmark.	34
8. TANDEM EFFECTS IN α -TYPE FIBERS, Paolo Galeati, Vittorio Rizzoli and Carlo G. Somena, Istituto di Elettronica, Università di Bologna, Villa Griffone, Pontecchio Marconi, Bologna, Italy.	35
9. EFFECTS OF A CENTRAL DIP ON THE TIME DISPERSION CHARACTERISTICS OF GRADED-INDEX OPTICAL FIBERS, G. Cancellieri, P. Fantini, M. Mezzetti, Fondazione G. Marconi, Villa Griffone, Pontecchio Marconi, Bologna, Italy.	27

MONDAY AFTERNOON
June 2, 1:30 - 5:00

HIGH FREQUENCY SCATTERING

DKN 1A

Session B.3

Chairman: T.B.A. Senior
University of Michigan
Ann Arbor, MI.

Page

1. A RADAR CROSS SECTION STUDY OF SIMPLE SHAPES BY UTD METHOD, J. Huang and C.L. Yu, Code 3313, Naval Weapons Center, China Lake, CA 93555, U.S.A. 37
2. A HIGH FREQUENCY ANALYSIS OF THE BACKSCATTER FROM FINNED CYLINDERS OF FINITE LENGTH, T. Jirapunth, P.H. Pathak and R.G. Kouyoumjian, The ElectroScience Laboratory, the Ohio State University, 1320 Kinnear Road, Columbus, Ohio 43212, U.S.A. 38
3. AN EXTENSION OF THE UNIFORM GTD TO THE DIFFRACTION BY A WEDGE ILLUMINATED BY A DIPOLE CLOSE TO ITS EDGE, R. Tiberio and G. Pelosi, Istituto di Elettronica, University of Florence, Florence, Italy, and R.G. Kouyoumjian, Department of Electrical Engineering, ElectroScience Laboratory, the Ohio State University, Columbus, Ohio 43212, U.S.A. 39
4. PREDICTION OF CAVITY AND NATURAL RESONANCE FREQUENCIES BY GTD, E.M. Kennaugh, the Ohio State University, ElectroScience Laboratory, Department of Electrical Engineering, Columbus, Ohio 43212, U.S.A. 40
5. DETERMINATION OF RADIATION PATTERN OF CONICAL ANTENNAS BY THE GEOMETRICAL THEORY OF DIFFRACTION, J.Ch. Bolomey, J. Cashman, S. El Habiby, Laboratoire des Signaux et Systèmes, Groupe d'Electromagnétisme, C.N.R.S. - E.S.E., Plateau du Moulon, 91190 Gif-sur-Yvette, France. 41
6. HIGH FREQUENCY SCATTERING FROM AIRCRAFT MODELED BY FLAT PLATES AND CONE FRUSTA, E.C. Burt, G.A. Dike, R.F. Wallenberg, Syracuse Research Corporation, Merrill Lane, Syracuse, New York 13210, U.S.A. 42
7. MASLOV METHOD AND ASYMPTOTIC FOURIER TRANSFORM, R.W. Ziolkowski and G.A. Deschamps, Department of Electrical Engineering, University of Illinois, Urbana, Illinois 61801, U.S.A. 43
8. ON THE EVALUATION OF CERTAIN HALF-PLANE DIFFRACTION INTEGRALS NEAR SHADOW BOUNDARIES, R.J. Pogorzelski, TRW Defense and Space Systems Group, One Space Park, Redondo Beach, California 90278, U.S.A. 44

MONDAY AFTERNOON
June 2, 1:30 - 5:00

WIRE ANTENNAS 1

DKN IB

Session B.4

Chairman: W. Tilston
Til-Tek
Richmond Hill, Ontario

	<u>Page</u>
1. CURRENT DISTRIBUTIONS, INPUT IMPEDANCES, AND RADIATION PATTERNS OF WIRE ANTENNAS, J.D. Lilly, C.A. Balanis, Department of Electrical Engineering, West Virginia University, Morgantown, W.Va. 26506, U.S.A.	46
2. NETWORK ANALOGS OF WIRE ANTENNA-FORMULATION, T.H. Lehman and E.I. Coffey, The BDM Corporation, Albuquerque, New Mexico, U.S.A.	47
3. NETWORK ANALOGS OF WIRE ANTENNA - APPLICATIONS, E.B. Mann, W.R. Zimmerman and T.H. Lehman, The BDM Corporation, Albuquerque, New Mexico, U.S.A.	48
4. THE INSULATED CONDUCTOR IN A RELATIVELY DENSE MEDIUM AS A TRANSMISSION LINE AND RADIATOR, R.W.P. King, Gordon McKay Laboratory, Harvard University, Cambridge, MA. 92138, U.S.A.	49
5. ANALYTICAL SOLUTIONS FOR THE CURRENTS ON AN ELECTRICALLY THICK TUBULAR RECEIVING ANTENNA, L.W. Rispin and D.C. Chang, Electromagnetics Laboratory, Department of Electrical Engineering, University of Colorado, Boulder, Co. 80309, U.S.A.	50
6. A FILAMENTARY MULTIPOLE MODEL FOR CYLINDRICAL ANTENNAS, T. Jason Chou, General Electric Co., Electronics Laboratory, Syracuse, N.Y. 13210, and Arlon T. Adams, Department of Electrical and Computer Engineering, Syracuse University, Syracuse, N.Y. 13210, U.S.A.	51
7. THE ANALYSIS OF THE FIELD RESPONSE OF SOLID WIRES EXCITED BY CURRENT FILAMENTS ON THE ENDCAPS, K.R. Demarest, Lafayette College, Department of Electrical Engineering, Easton, Pennsylvania 18042, U.S.A.	52
8. TRANSIENT NEAR-FIELDS OF LINEAR ANTENNAS, P. Fellingner, K.L. Langenberg, K.D. Rech, Teoretische Elektrotechnik, Fachrichtung 12.2, Universität des Saarlandes, D-6600 Saarbrücken, FRG.	53
9. A NEW TYPE OF ANTENNA "GAUSS-CURVE DIPOLE", Zhou Chao-Dong, Zhou Liang-Ming and Yang En-Yao, Northwest Telecommunication Engineering Institute, Xi-an, Shaansi, China.	54
10. BACKWARD-WAVE YAGI HYBRID ANTENNA, W.K. Kahn, Naval Research Laboratory, Washington, D.C., U.S.A.	55

MONDAY AFTERNOON

June 2, 1:30 - 5:00

GUIDED WAVES

DKN 1271

Session B.5

POSTER SESSION

Chairman: R. Gagné
Université Laval
Québec, Qué.

	<u>Page</u>
1. COUPLED-MODE ANALYSIS OF STEEP WAVEGUIDE TRANSITIONS, S.S. Saad, Andrew Corporation, Orland Park, Illinois 60462, A.A. Kamal, Cairo University, Cairo, Egypt and S.A. Marshali, National Research Center, Cairo, Egypt.	57
2. ANALYSIS OF AN ANNULAR SLOT IN A RADIAL WAVEGUIDE WITH AN INTERIOR TRUNCATED DIELECTRIC, T.L. Keshavamurthy and C.M. Butler, Department of Electrical Engineering, University of Mississippi, University, MS. 38677.	58
3. ANALYSIS OF COAXIAL TO RADIAL WAVEGUIDE JUNCTION, C.M. Butler and T.L. Keshavamurthy, Department of Electrical Engineering, University of Mississippi, University, MS. 38677.	59
4. CARACTERISATION ELECTROMAGNETIQUE DE DISCONTINUITES SIMPLES OU MULTIPLES SUR UN GUIDE DIELECTRIQUE EN BOITIER, M. Petenzi et P. Gelin, Centre Hyperfréquences et Semiconducteurs, Laboratoire associé au C.N.R.S., n° 287, Université de Lille I - Bâtiment P4, 59655 Villeneuve d'Ascq Cedex, France.	60
5. ANALYSIS OF LEAKY COAXIAL CABLES USED IN MINE COMMUNICATIONS, R.S. Tomar, Department of Electrical Engineering, Indian Institute of Technology, Kanpur, India, and Atakananda Paul, Visiting Assistant Professor, Department of Electrical Engineering, Northeastern University, Boston, Mass. 02115.	61
6. INTEGRAL EQUATION FORMULATION FOR MODE CONVERSION AND RADIATION FROM DISCONTINUITY IN OPEN-BOUNDARY WAVEGUIDE, S.V. Hsu, E-Systems Inc., Garland, Texas 75042, and D.P. Nyquist, Department of Electrical Engineering and Systems Science, Michigan State University, East Lansing, Michigan 48824.	62
7. FIELD CONFIGURATION OF FUNDAMENTAL AND HIGHER ORDER MODES IN FIN LINES OBTAINED WITH THE TLM-METHOD, Wolfgang J.R. Hoefer and Yi-Chi Shih, Faculty of Science and Engineering, University of Ottawa, Ottawa, Ontario K1N 6N5.	63

B.5 Poster Session (cont.)

	<u>Page</u>
8. MODE THEORY OF UNIFORM WAVEGUIDES FILLED WITH DIELECTRIC INHOMOGENEOUS ALONG ONE DIRECTION ONLY, Lin Weigan, Chengdu Institute of Radio Engineering, Chengdu, Sichuan, People's Republic of China.	64
9. RECOMMENDATION AND REFERENCE TABLE OF RIGID ELLIPTICAL WAVEGUIDE DATA, Lin Weigan, Chengdu Institute of Radio Engineering, Chengdu, Sichuan, People's Republic of China.	65
10. PROPERTIES OF ANISOTROPIC DIELECTRIC TUBE WAVEGUIDES, D.K. Paul, B.B. Chaudhuri, Electrical Engineering Department, I.I.T., Kanpur, India.	66
11. CALCUL DES COEFFICIENTS DE LA MATRICE SCATTERING D'UNE FOURCHETTE MICROSTRIP APPLICATION AUX COUPLEURS BRANCH-LINES, J. Citerne, E. Cosnard, U.S.T.I. C.H.S. LA n° 287 C.N.R.S. 59655 Villeneuve d'Ascq Cedex, France.	67

TUESDAY AFTERNOON
June 3, 1:30 - 5:00

SPECIAL SESSION ON ELECTROMAGNETIC EARTH
INDUCTION FROM OVERHEAD CONDUCTORS

DKN 1B

Session B.6

Chairman: W.R. Goddard
University of Manitoba
Winnipeg, Manitoba

Organizer: J.R. Wait
U.S. Department of Commerce
NOAA, ERL
Boulder, Co.

	<u>Page</u>
1. INDUCED CURRENT ON AN INFINITE HORIZONTAL WIRE ABOVE EARTH BY A CLOUD TO GROUND LIGHTNING DISCHARGE, R.G. Olsen, Department of Electrical Engineering, Washington State University, Pullman, Washington 99164.	69
2. INDUCED CURRENTS ON AN OVERHEAD TRANSMISSION LINE DUE TO LOCAL ELECTROMAGNETIC SOURCES, D.C. Chang, Ahmad Hoorfar and E.F. Kuester, Electromagnetics Laboratory, Department of Electrical Engineering, University of Colorado, Boulder, Co. 80309.	70
3. ELECTROMAGNETIC EARTH INDUCTION FROM AN OVERHEAD LINE CURRENT PARALLEL TO THE GROUND, O.A. Aboul-Atta, L. Shafai and M.Z. Tarnawewky, Department of Electrical Engineering, University of Manitoba, Winnipeg, Manitoba R3T 2N2.	71
4. EFFECT OF A BURIED CABLE ON THE FIELDS OF A VMD ON THE GROUND SURFACE, Adel Z. Botros and Samir F. Mahmoud, Electronics and Communications Department, Cairo University, Giza, Egypt.	72
5. ON THE IMAGE REPRESENTATION OF THE FIELDS OF A LINE CURRENT SOURCE ABOVE FINITELY CONDUCTING EARTH, A. Mohsen, Department of Electrical Engineering, the University of Manitoba, Winnipeg, Manitoba.	73
6. MEASUREMENT AND ANALYSIS OF CONTROLLED POWERLINE VLF RADIATION FROM THE HV-DC LINE FROM RADISON TO DORSEY, MANITOBA, W.M. Boerner, W.R. Goddard, AEM Laboratory, Department of Electrical Engineering, University of Manitoba, Winnipeg, Manitoba, J. Cole, Communications Laboratory Information Engineering Department, UICC, Chicago, Illinois 60680, and C. Thio, Systems Planning Division, Manitoba-Hydro, Winnipeg, Manitoba.	74

B.6 (cont.)

	<u>Page</u>
7. ELECTROMAGNETIC EARTH INDUCTION FROM M.T. MEASUREMENTS AT EUSEBIO, A STATION UNDER EQUATORIAL ELECTROJETS, N.B. Trivedi and E.G. de Souza, Instituto de Pesquisa Espaciais, INPE, Conselho Nacional de Desenvolvimento Cientifico e Tecnologico, CNPQ, C.P. 515, 12200 S.J. dos Campos, S.P., Brazil.	75
8. ANALYSIS OF BURIED PIPELINE VOLTAGES DUE TO 60 Hz AC INDUCTIVE COUPLING, Allen Taflove, IIT Research Institute, 10 West 35th Street, Chicago, Illinois 60616.	76

TUESDAY AFTERNOON
June 3, 1:30 - 5:00

SPECIAL SESSION ON OPTICAL COMMUNICATIONS III
FIBER AND GUIDED WAVE OPTICS II

DKN 2B

Combined Session B.7/AP-S

Chairman: C. Yeh
U.C.L.A.
Los Angeles, CA.

Organizer: G.L. Yip
McGill University
Montréal, Québec

	<u>Page</u>
1. OPTICAL WAVEGUIDE THEORY, C. Yeh, Electrical Sciences and Engineering Department, University of California, Los Angeles, CA. 90024.	78
2. ON WEAK-COUPPLING THEORY OF OPTICAL FIBER AND FILM WAVEGUIDES, Huang Hung-chia, Shanghai University of Science and Technology, Shanghai, China.	79
3. COUPLED MODES WITH RANDOM PROPAGATION CONSTANTS, H.E. Rowe and I.M. Mach, Bell Laboratories, Crawford Hill Laboratory, Holmdel, N.J. 07733.	80
4. BOUNDARY FORMULATION OF PROPAGATION PROBLEMS IN GUIDING STRUCTURES FOR INTEGRATED OPTICS, V. Daniele, I. Montrosset and R. Zich, CESPÀ (CNR) and Istituto Elettronica e Telecomunicazioni, Politecnico di Torino, Corso Duca degli Abruzzi 24, 10129 Torino, Italy.	77
5. INFLUENCE DE LA CONFIGURATION DES ELECTRODES DE COMMANDE SUR L'EFFICACITE D'UN COMMUTATEUR ELECTROOPTIQUE DU TYPE BOA, F. Favre, Centre National d'Etudes des Télécommunications (CNET), Lannion, France.	81
6. FILTER CHARACTERISTICS OF IMPERFECT PERIODIC STRUCTURES, D.L. Jaggard and G.T. Warhola, Department of Electrical Engineering, University of Utah, Salt-Lake City, Utah 84112.	82
7. POLARIZATION PROPERTIES OF SINGLE MODE FIBERS, Cynthia P. Smith, Hughes Research Laboratories, Malibu, CA., and Giorgio Franceschetti, University of Naples, Italy.	77
8. ELLIPTICAL OPTICAL FIBERS, S.R. Rengarajan and J.E. Lewis, Department of Electrical Engineering, University of New Brunswick, Fredericton, N.B. E3B 5A3.	83

B.7 (cont.)

	<u>Page</u>
9. MULTIMODE OPTICAL FIBERS WITH NON CIRCULAR CROSS SECTION, M. Brenci, P.F. Checcacci, R. Falciai, A.M. Scheggi, Istituto di Ricerca sulle Onde Elettromagnetiche of CNR, Firenze, Italy.	84
10. NON-CIRCULAR OPTICAL WAVEGUIDES AND MODAL CHOICE, Yang Shuwen, Chengdu Institute of Radio Engineering, Jian She Road, Chengdu, China.	85

WEDNESDAY MORNING
June 4, 8:30 - 12:00

ANALYTICAL AND NUMERICAL TECHNIQUES
DKN 1A

Session B.8

Chairman: P. Silvester
McGill University
Montréal, Québec

	<u>Page</u>
1. FINITE ELEMENT METHOD FOR SOLVING THREE-DIMENSIONAL ELECTROMAGNETIC DISCONTINUITY PROBLEMS, G.L. Maile, RF Technology Centre, ERA Technology Ltd., Cleeve Road, Leatherland, Surrey, England KT2 7SA, and R.L. Ferrari, Cambridge University, Engineering Department, Trumpington Street, Cambridge, England CB2 1PZ.	87
2. NUMERICAL MODELING OF ARBITRARY BODIES WITH TRILATERAL SURFACE PATCHES USING THE ELECTRICAL FIELD INTEGRAL EQUATION, J.J.H. Wang, Engineering Experiment Station, Georgia Institute of Technology, Atlanta, Georgia 30332.	88
3. SOLVING A CLASS OF OPEN AND CLOSED DISCONTINUITY PROBLEMS WITHOUT MATRIX INVERSION, R. Mittra and C.H. Tsao, Department of Electrical Engineering, University of Illinois, Urbana, Ill. 61801.	89
4. NUMERICAL ASPECTS OF AN EFFICIENT SCHEME FOR COMPUTING THE REFLECTED FIELD FROM A SMOOTH ARBITRARY SURFACE, A.M. Rushdi and T. Mittra, Department of Electrical Engineering, University of Illinois, Urbana, Ill. 61801.	90
5. ON THE EVALUATION OF SOMMERFELD INTEGRALS BY A MODIFIED FILON'S METHOD, H.J. Price and T.C. Kalahdar Rao, Mission Research Corporation, 1400 San Mateo boulevard S.E., Suite A., Albuquerque, New Mexico 87108.	91
6. A NUMERICAL TECHNIQUE FOR CALCULATING INTERACTIONS BETWEEN WIRES AND SURFACES, W.A. Imbriale, Jet Propulsion Laboratory, 4800 Oak Grove Drive, California Institute of Technology, Pasadena, CA. 91103, and R.J. Pogorzelski, TRW Defense and Space Systems Group, Redondo Beach, CA. 90278.	92
7. THE UNIMOMENT - MONTE CARLO METHOD APPLIED TO TWO-DIMENSIONAL INTERIOR BOUNDARY-VALUE PROBLEMS, R.W. Campbell, Martin Marietta Corporation, Aerospace Division, Denver, Co. 80201.	93
8. A HYBRID FD-TD/MOM APPROACH TO THE ELECTROMAGNETIC COUPLING AND APERTURE PENETRATION, Allen Taflove and Korada Umashankar, IIT Research Institute, 10 West 35th Street, Chicago, Ill. 60616.	94

B.8 (cont.)

	<u>Page</u>
9. DFNA - THE DIRECT FORM OF NETWORK ANALOGS, E.L. Coffey and T.H. Lehman, The BDM Corporation, Albuquerque, New Mexico.	95
10. MATRIX SIZE REDUCTION FOR MICROSTRIP CIRCUITS, Y.L. Chow and M. Tutt, Department of Electrical Engineering, University of Waterloo, Waterloo, Ontario, N2L 3G1.	96

WEDNESDAY MORNING

June 4, 8:30 - 12:00

RANDOM MEDIA

DKN 1B

Session B.9

Chairman: A. Ishimaru
University of Washington
Seattle, WA.

	<u>Page</u>
1. BEAM WAVE INTENSITY FLUCTUATIONS IN WEAK AND STRONG ATMOSPHERIC TURBULENCE, J. Carl Leader, McDonnell Douglas Research Laboratories, P.O.Box 516, St.Louis, Mo. 63166.	98
2. RADIO SCINTILLATIONS DURING OCCULTATIONS BY TURBULENT PLANETARY ATMOSPHERES, Richard Woo, Jet Propulsion Laboratory, California Institute of Technology, 4800 Oak Grove Drive, Pasadena, CA. 91103, Akira Ishimaru, Department of Electrical Engineering, University of Washington, Seattle WA. 98195, and Fang-Chou Yang, Dikewood Corporation, Los Angeles, CA. 90024.	99
3. EFFECTIVE PROPAGATION CHARACTERISTICS OF DISCRETE RANDOM MEDIA, V.N. Bringi, H. Direskeneli, V.K. Varadan, V.V. Varadan and T.A. Seliga, Wave Propagation Group, Department of Electrical Engineering, and the Atmospheric Sciences Program, The Ohio State University, Columbus, Ohio 43210.	100
4. DIFFUSION OF A BEAM WAVE IN RANDOM DISCRETE SCATTERS, Akira Ishimaru, Rudolf Cheung and Yasuo Kuga, Department of Electrical Engineering, University of Washington, Seattle, WA. 98195.	101
5. COHERENT WAVE PROPAGATION THROUGH A SPARSE CONCENTRATION OF PARTICLES, G.S. Brown, Applied Sciences Associates, Inc., 105 East Chatham St., Apex, North Carolina 27502.	102
6. MULTIPLE PHASE-SCREEN CALCULATION OF THE TEMPORAL BEHAVIOR OF STOCHASTIC WAVES, D.L. Knepp, Mission Research Corporation, P.O. Drawer 719, Santa Barbara, CA. 93102.	103
7. FULL-WAVE SOLUTIONS FOR THE DEPOLARIZATION OF THE SCATTERED RADIATION FIELDS BY ROUGH SURFACES OF ARBITRARY SLOPE, Ezekiel Bahar, Electrical Engineering Department, University of Nebraska, Lincoln, Nebraska 68588.	104
8. ELECTROMAGNETIC SCATTERING FROM ROUGH SURFACES BASED ON STATISTICAL CHARACTERIZATION OF THE TERRAIN, R.J. Papa and J.F. Lennon, Deputy for Electronic Technology, Rome Air Development Center, Electromagnetic Sciences Division, Hanscom AFB, Mass. 01731.	105

WEDNESDAY MORNING
June 4, 8:30 - 12:00

HF - TO - UHF ARRAYS

DKN ID

Combined Session AP-S/B.10

Chairman: H.V. Cottony
5204 Wilson Lane
Bethesda, MD.

Page

1. A BROADBAND CAVITY ANTENNA WITH A STEERABLE CARDIOID PATTERN, B.A. Munk and C.J. Larson, Ohio State University, Columbus, Ohio. 106
2. THE TERMINATED RADIAL ARRAY AS A HIGH FREQUENCY SCANNING BEAM ANTENNA, D.W. Griffin, University of Adelaide, South Australia. 106
3. OPTIMUM PATTERN SHAPE OF SHORTWAVE ANTENNAS FROM RADIO-LINK COMPUTATIONS, A. Stark, Rohde & Schwarz, Munich, Germany. 106
4. A NEW COMBINED ANTENNA AND PROPAGATION MODEL, S. Chang, IIT Research Institute, ECAC, Anapolis, MD. 106
5. A COMPACT REACTIVELY STEERED ANTENNA ARRAY, R.J. Dinger, W.D. Meyers, Naval Research Laboratory, Washington, D.C. 106
6. MINIATURIZATION TECHNIQUES FOR HF LOG-PERIODIC DIPOLE ARRAYS, H. Shnitkin, Norden Systems, Norwalk, Connecticut. 106
7. A WIDEBAND CORNER-REFLECTOR ANTENNA FOR 240 TO 400 MHz, J.L. Wong and H.E. King, The Aerospace Corporation, Los Angeles, CA. 106
8. THE DIRECTIVITY OF ANTENNA ARRAY EXCITED BY WEIGHTED WALSH CURRENT, Xie Chu-Fang, Chengdu Institute of Radio Engineering, Chengdu, Sichuan, China. 107
9. PHASE-FREQUENCY SCANNABLE TRAVELING WAVE ARRAYS, H.J. Stalzer, Jr., Manhattan College, Riverdale, N.Y., A. Hessel and J. Shmoys, Polytechnic Institute of New York, Farmingdale, N.Y. 108
10. USE OF A QUAD ARRAY TO GENERATE AN APPARENT TARGET POSITION, D.C. Wu and R.E. Suratt, Naval Research Laboratories, Washington, D.C. 109

WEDNESDAY MORNING
June 4, 8:30 - 12:00

SPECIAL SESSION ON OPTICAL COMMUNICATIONS IV
FIBER AND GUIDED WAVE OPTICS III

DKN 2B

Combined Session B.11/AP-S

Chairman: L.B. Felsen
Polytechnic Institute of New York
Farmingdale, N.Y.

Organizer: G.L. Yip
McGill University
Montréal, Québec

	<u>Page</u>
1. FLAT DISC, RADIALLY NON-HOMOGENEOUS, LENS, S. Cornbleet, Department of Physics, University of Surrey, Guildford, England.	111
2. ELECTROMAGNETIC WAVE PROPAGATING IN UNIFORM WAVEGUIDES CONTAINING INHOMOGENEOUS DIELECTRIC, Lin Weigan, Chengdu Institute of Radio Engineering, Chengdu, Sichuan, China.	112
3. FIRST-ORDER CORRECTIONS TO EXPRESSIONS FOR PARAXIAL BEAM PROPAGATION IN MULTIMODE PARALLEL-PLATE OR DIELECTRIC-SLAB WAVEGUIDES, E.F. Kuester and D.C. Chang, Electromagnetics Laboratory, Department of Electrical Engineering, University of Colorado, Boulder, Co. 80309.	113
4. CALCULATION OF DISPERSION FOR TWO OPTICAL FIBER PROFILES BY THE PROPAGATING BEAM TECHNIQUE, M.D. Feit and J.A. Fleck, Jr., Lawrence Laboratory, University of California, Livermore, CA. 94550.	110
5. MULTIMODE PROPAGATION IN ANISOTROPIC OPTICAL WAVEGUIDES, D.K. Paul, Gordon McKay Laboratory, Harvard University, Cambridge, Mass 02138, and R.K. Shevgaonkar, Electrical Engineering Department, IIT, Kanpur, India.	114
6. BANDWIDTH PREDICTION OF AN OPTICAL ROUTE, G.S. Gupta, RF Technology Centre, ERA Technology Ltd, Leatherhead, Surrey, England, and P.J.B. Clarricoats, Electrical Engineering Department, Queen Mary College, London E-1, England.	115
7. MODAL INTERFERENCE OF LASER LIGHT EMITTED FROM AN OPTICAL FIBER, Masaaki Imai, Department of Engineering Science, Hokkaido University, Sapporo, 060 Japan.	116
8. ANALYSE ET MESURE DU BRUIT MODAL DANS UNE LIAISON PAR FIBRE OPTIQUE MULTIMODE COMPRENANT UN CONNECTEUR OU UN COUPLEUR, Y. Tremblay, K.O. Hill et B.S. Kawasaki, Centre de Recherches sur les Communications, Ministère des Communications, Ottawa, Ontario K2H 8S2.	117

B.11 (cont.)

	<u>Page</u>
9. SIGNAL PROPAGATION IN THE MULTIMODE OPTICAL WAVEGUIDE AS A RANDOM MEDIUM, K. Itoh, K. Tatekura and H. Itoh, Department of Electronic Engineering, Hokkaido University, Sapporo, 060 Japan.	110
10. COMBINED MICROBEND AND WAVELENGTH DEPENDANT LOSS EVALUATION FOR SINGLE AND MULTI-MODE FIBERS, Santanu Das, Department of Electrical Engineering, University of Alberta, Edmonton, Alberta.	118

WEDNESDAY AFTERNOON

June 4, 1:30 - 5:00

TRANSIENTS

DKN 1A

Combined Session AP-S/B.12

Chairman: D.L. Moffatt
The Ohio State University
Columbus, Ohio

	<u>Page</u>
1. TIME-DOMAIN ELECTRIC FIELD INTEGRAL EQUATION APPROACH TO THE SOLUTION OF TRANSIENT SCATTERING BY ARBITRARILY-SHAPED OBJECTS, S.M. Rao, D.R. Wilton and A.W. Glisson, University of Mississippi, Mississippi.	121
2. TIME-DOMAIN CALCULATION OF AIRCRAFT MODEL RESPONSE, C.L. Bennett and H. Mieras, Sperry Research Center, Sudbury, Massachusetts.	122
3. TRANSIENT SCATTERING FROM CURVED THIN WIRES BY THE FINITE ELEMENT METHOD, T.C. Tong and A. Sankar, TRW Defense and Space Systems Group, Redondo Beach, California.	119
4. TIME-DOMAIN INTEGRAL EQUATION APPROACH TO EM SCATTERING BY DIELECTRIC SOLIDS, H. Mieras and C.L. Bennett, Sperry Research Center, Sudbury, Massachusetts, and R. Lyons, University of Michigan, Ann Arbor, Michigan.	119
5. DIFFRACTION EN REGIME TRANSITOIRE PAR DES OBSTACLES CONDUCTEURS OU DIELECTRIQUES, B. Jecko and A. Papiernik, Université de Limoges, Limoges, France.	119
6. ON DEMONSTRATING BASIC ELECTROMAGNETIC PHENOMENA USING TIME-DOMAIN SOLUTIONS, E.K. Miller, University of California, Livermore, California, J.A. Landt, University of California, Los Alamos, New Mexico, F.J. Deadrick and G.J. Burke, University of California, Livermore, California.	119
7. TIME-DOMAIN SEM, W.A. Davis, Virginia Polytechnic Institute and State University, Blacksburg, Virginia and J.T. Cordaro, University of New Mexico, Albuquerque, New Mexico.	119
8. THE DIFFERENTIAL FORM OF NETWORK ANALOGS: APPLICATIONS TO EMP AND SGEMP EXTERNAL RESPONSE PROBLEMS, W.R. Zimmerman, T.H. Lehman, E.L. Coffey and R.L. Hutchins, The BDM Corporation, Albuquerque, New Mexico.	119

	<u>Page</u>
9. TRANSIENT RESPONSE OF MULTICONDUCTOR TRANSMISSION LINES EXCITED BY A NONUNIFORM ELECTROMAGNETIC FIELD, A.K. Agarwal and H.J. Price, Mission Research Corporation, Albuquerque, New Mexico and S.H. Gurbaxani, University of New Mexico, Albuquerque, New Mexico.	120
10. NUMERICAL REPRESENTATION OF TRANSMISSION LINE EQUATIONS BY INTEGRATION ALONG CHARACTERISTICS IN THE PRESENCE OF A REALISTIC GROUND PLANE, H.J. Price and T.C. Kaladhar Rao, Mission Research Corporation, Albuquerque, New Mexico.	120

WEDNESDAY AFTERNOON

June 4, 1:30 - 5:00

SPECIAL SESSION ON INVERSE SCATTERING - I
THEORETICAL APPROACHES

DKN 1B

Session B.13

Chairman: C.L. Bennett
Sperry Research Center
Sudbury, MA

Organizer: W.M. Boerner
U.I.C.C.
Chicago, IL

	<u>Page</u>
1. THE NONEXISTENCE OF NON-RADIATING SOURCES AND THE UNIQUENESS OF THE SOLUTION TO THE INVERSE SCATTERING PROBLEM, W. Ross Stone, Megatak Corporation, 1055 Shafter Street, San Diego, California 92106.	124
2. A WELL-POSED ANALYTIC CLOSED FORM SOLUTION OF THE EXACT INVERSE SCATTERING INTEGRAL EQUATION, N.N. Bojarski, Newport Beach, California 92660.	125
3. MULTI-DIMENSIONAL INVERSE SCATTERING FOR THE REDUCED WAVE EQUATION, V.H. Weston, Purdue University, West Lafayette, Indiana 47907.	126
4. AN EXAMPLE OF RESOLVING THE NONUNIQUENESS IN AN INVERSE SCATTERING PROBLEM, R.J. Krueger, Department of Mathematics and Statistics University of Nebraska, Lincoln, Nebraska 68588.	127
5. INVERSE SCATTERING AND THE BORN APPROXIMATION, R.E. Kleinman, Applied Mathematics Institute, University of Delaware, Newark, Delaware 19711, U.S.A., and B.D. Sleeman, Depart of Mathematics, University of Dundee, Dundee, Scotland DD1 4HN.	128
6. THE APPLICABILITY OF AN INVERSE METHOD FOR RECONSTRUCTION OF ELECTRON DENSITY PROFILES, M.H. Reilly and A.K. Jordan, Naval Research Laboratory, Washington, D.C. 20375.	129
7. RESONANCES OF A DIELECTRICALLY COATED CONDUCTING SPHERE: SURFACE WAVES AND THE INVERSE SCATTERING PROBLEM, P.J. Moser, J. Diarmuid Murphy, A. Nagl and H. Uberall, Department of Physics, Catholic University, Washington, D.C. 20064, and G. C. Gaunaud Naval Surface Weapons Center, White Oak, Silver Spring, Maryland 20910.	130
8. A THEORETICAL AND NUMERICAL METHOD FOR INVERSE SCATTERING PROBLEMS IN ELECTROMAGNETICS, A. Roger, Laboratoire d'Optique Electromagnétique, E.R.A. au CNRS, No. 597, Faculté des Sciences et Techniques, Centre de St-Jérôme, 13397 Marseille Cedex 4, France.	131

THURSDAY MORNING
June 5, 8:30 - 12:00

SCATTERING II

DKN 1A

Session B.14

Chairman: Y.L. Chow
University of Waterloo
Waterloo, Ontario

	<u>Page</u>
1. SMALL APERTURE COUPLING BETWEEN DIS-SIMILAR REGIONS, R.E. Collin, Electrical Engineering and Applied Physics Department, Case Institute of Technology, Case Western Reserve University, Cleveland, Ohio 44106.	133
2. APPROXIMATE SOLUTIONS FOR TRANSMISSION THROUGH ELECTRICALLY SMALL APERTURES, R.F. Harrington, Department of Electrical Engineering, Syracuse University, Syracuse, New York 13210.	134
3. APERTURE-COUPLED FIELDS IN ASYMMETRIC BODIES, L.N. Medgyesi-Mitschang, McDonnell Douglas Research Laboratories, St. Louis, Missouri 63166.	135
4. LOW FREQUENCY SCATTERING FROM A CIRCULAR TUBE OF FINITE LENGTH, P. Parhami and S. Govind, TRW Defense and Space Systems Group, One Space Park, Redondo Beach, California 90278.	136
5. SCATTERING BY ROTATING OSCILLATING TARGETS, R.E. Kleinman and R.B. Mack, Applied Mathematics Institute, University of Delaware, Newark, Delaware 19711.	137
6. SIMPLE INTERPRETATIONS OF SCATTERED FIELD OF SPHERES BY OPTIMIZED SIMULATED IMAGES, Y.L. Chow and M. Tutt, Department of Electrical Engineering, University of Waterloo, Waterloo, Ontario N2L 3G1.	138
7. NATURAL MODE RESONANCES OF DIELECTRIC OBJECTS, P.W. Barber, Department of Electrical Engineering, University of Utah, Salt Lake City, Utah 84112, U.S.A., and R.K. Chang, Department of Electrical Engineering and Applied Sciences, Yale University, New Haven, Connecticut 96520.	139
8. SEM ANALYSIS OF SCATTERING FROM AN INFINITE PERIODIC ARRAY, D.H. Herndon, E.W. Smith and E.J. Dombroski, Harris Corporation, Government Electronic Systems Division, P.O. Box 37, Melbourne, Florida 32901.	140

B.14 (cont.)

	<u>Page</u>
9. A SINGULARITY EXPANSION METHOD ANALYSIS OF TWO FINITE LENGTH THIN CYLINDERS OF ARBITRARY ORIENTATION, D. Maynard Schmale, Lloyd S. Riggs and T.H. Shumpert, Electrical Engineering Department, Auburn University, Auburn, Alabama 36830.	141
10. SEM EQUIVALENT CIRCUIT SYNTHESIS FOR THE SPHERICAL ANTENNA, K.A. Michalski and L.W. Pearson, Department of Electrical Engineering, University of Kentucky, Lexington, Kentucky 40506.	142

THURSDAY MORNING
June 5, 8:30 - 12:00

SPECIAL SESSION ON INVERSE SCATTERING - II
TRANSIENT SIGNATURE INTERPRETATION

DKN 1B

Combined Session B.15/AP-S

Chairman and Organizer : W.M. Boerner
U.I.C.C.
Chicago, IL

	<u>Page</u>
1. PROBING OF PLANE AND CYLINDRICALLY STRATIFIED MEDIUM - BIOMEDICAL AND GEOPHYSICAL APPLICATIONS, J. Audet, J. Ch. Bolomey, B. Duchene, D. Lesselier, Ch. Pichot, W. Tabbara, Laboratoire des Signaux et Systèmes - Groupe d'Electromagnétisme, C.N.R.S. - E.S.E., Plateau du Moulon, 91190 Gif-sur-Yvette, France.	144
2. INTERACTIVE SOLUTION OF THE TIME-DOMAIN INVERSE SCATTERING PROBLEM FOR AN INHOMOGENEOUS, LOSSY DIELECTRIC SLAB, A.G. Tjihuis, Department of Electrical Engineering, Delft University of Technology, P.O.Box 5031, 2600 GA Delft, The Netherlands.	143
3. SEM APPROACH TO THE TRANSIENT SCATTERING BY AN INHOMOGENEOUS, LOSSY DIELECTRIC SLAB, A.G. Tjihuis and H. Block, Department of Electrical Engineering, Delft University of Technology, P.O. Box 5031, 2600 GA Delft, The Netherlands.	143
4. ELIMINATION OF UNDESIRE NATURAL RESONANCES FOR IMPROVED TARGET IDENTIFICATION, J. Volakis and L. Peters, Jr., The Ohio State University, ElectroScience Laboratory, Department of Electrical Engineering, Columbus, Ohio 43212.	145
5. RADAR WAVEFORM SYNTHESIS METHOD - A NEW RADAR DETECTION SCHEME, Kun-Mu Chen, Department of Electrical Engineering and System Science, Michigan State University, East Lansing, Michigan 48824.	143
6. DECISION THEORETIC TARGET CLASSIFICATION, J.P. Toomey and C.L. Bennett, Sperry Research Center, 100 North Road, Sudbury, Massachusetts 01776.	146
7. CLASSIFICATION TECHNIQUES IN INVERSE SCATTERING, A.A. Ksienski, The Ohio State University, ElectroScience Laboratory, Department of Electrical Engineering, Columbus, Ohio 43212, U.S.A., and Heng-Cheng Lin, Harris Corporation, Melbourne, Florida 32901.	147
8. THE USE OF NEAREST NEIGHBOR AND LINEAR DISCRIMINANT TECHNIQUES FOR SHIP IDENTIFICATION USING HF RADAR, E.K. Walton, The Ohio State University, ElectroScience Laboratory, Department of Electrical Engineering, Columbus, Ohio 43212.	148

THURSDAY AFTERNOON

June 5, 1:30 - 5:00

SPECIAL TOPICS

DKN 1B

Session B.16

Chairman: R. MacPhie
University of Waterloo
Waterloo, Ontario

	<u>Page</u>
1. ELECTROMAGNETIC FIELDS OF A DIPOLE SUBMERGED IN A TWO-LAYER CONDUCTING MEDIUM IN THE ELF REGIME, T.M. Habashy, J.A. Kong, W.C. Chew, Department of Electrical Engineering and Computer Science, and Research Laboratory of Electronics, Massachusetts Institute of Technology, Cambridge, Massachusetts 92139.	150
2. A NEW QUASISTATIC REPRESENTATION FOR HORIZONTAL MAGNETIC DIPOLES NEAR A LOSSY HALF-SPACE, J.N. Brittingham, Lawrence Livermore Laboratory, Livermore, California 94550.	151
3. ANTENNES EPAISSES DE REVOLUTION: APPLICATION AU COUPLAGE DES COMPOSANTS ET AUX CAPTEURS LARGE BANDE, J.Ch. Bolomey, S. El Habiby, F. Hillaire et D. Lesselier, Laboratoire des Signaux et Systèmes, Groupe d'Electromagnétisme, C.N.R.S. - E.S.E., Plateau du Moulon, 91190 Gif-sur-Yvette, France.	152
4. MAPPING THE ELECTRIC FIELD INSIDE A FINITE DIELECTRIC CYLINDER, R. Bansal, R.W.P. King and T.T. Wu, Gordon McKay Laboratory, Harvard University, Cambridge, Massachusetts 02138.	153
5. RELATIONS BETWEEN THE ANTENNA AND SCATTERING CHARACTERISTICS IN TERMS OF MEASURABLE PARAMETERS, C.W. Choi and J.J.H. Wang, Engineering Experiment Station, Georgia Institute of Technology, Atlanta, Georgia 30332.	154
6. LASER INDUCED EXCITATION OF THE CHARACTERISTIC MODES OF METAL OBJECTS, W.H. Peake and J.G. Meadors, The Ohio State University ElectroScience Laboratory, Department of Electrical Engineering, Columbus, Ohio 43212.	155
7. SATURATION EFFECTS IN COHERENT ANTI-STROKES RAMAN SPECTROSCOPY (CARS), H. Weil, The University of Michigan, Department of Electrical and Computer Engineering, Ann Arbor, Michigan 49109, U.S.A., and P.W. Schrieber, U.S. Air Force, Aero Propulsion Laboratory, Wright Patterson AFB 45433, U.S.A.	156
8. TRANSIENT CORONA EFFECTS ON WIRE OVER THE GROUND, K.C. Chen, Air Force Weapons Laboratory, Kirtland AFB, New Mexico 87117.	157

B.16 (cont.)

- | | <u>Page</u> |
|---|-------------|
| 9. ELECTROMAGNETIC THEORY OF MULTI-LAYERED SHIELDS WITH PARTICULAR REFERENCE TO ELECTRICAL BONDING BETWEEN SHIELDS, K.S.H. Lee, Dikewood Corporation, Santa Monica, CA. | 158 |

THURSDAY AFTERNOON
June 5, 1:30 - 5:00

SPECIAL SESSION ON INVERSE SCATTERING III
DKN 1271

Combined Session B.17/AP-S

POSTER SESSION on ELECTROMAGNETIC IMAGING

Chairman: N.N. Bojarski
Newport Beach, CA.

Organizer: W.M. Boerner
UICC
Chicago, Ill.

	<u>Page</u>
1. THE PHASE RETRIEVAL PROBLEM, L.S. Taylor, Electrical Engineering Department, University of Maryland, College Park, MD. 20742.	160
2. CODED APERTURE IMAGING WITH SPATIAL FREQUENCY REDUNDANCY, S.C. Som, Applied Physics Department, Calcutta University, 92 Acharya Prafullachandra Road, Calcutta - 700009, India.	161
3. DETERMINATION OF PROPERTIES OF AN OBJECT FROM ITS TRANSIENT EDDY CURRENT RESPONSE, Y. Das and J.E. McFee, Defense Research Establishment Suffield, Ralston, Alberta T0J 2N0.	162
4. A TIME-DOMAIN MONOSTATIC INVERSE SCATTERING SCHEME, S.K. Chaudhuri and P.A. Lenz, Department of Electrical Engineering, University of Waterloo, Waterloo, Ontario N2L 3G1.	159
5. AN APPLICATION OF GEOMETRICAL THEORY OF DIFFRACTION (GTD) AND PHYSICAL OPTICS TO OBJECT IDENTIFICATION THROUGH INVERSE SCATTERING ANALYSIS, G.A. Dike, E.C. Burt and R.F. Wallenberg, Syracuse Research Corporation, Merrill Lane, Syracuse, N.Y. 13210.	159
6. SYNTHETIC IMAGING COHERENT BACKSCATTERING, J.S. Yu, Applied Physics Division 2353, Sandia Laboratories, Albuquerque, N.M. 87185.	163
7. THREE METHODS FOR MICROWAVE IMAGING OF BURIED, DIELECTRIC ANOMALIES, C. Tricoles, E.L. Rope, R.A. Hayward, General Dynamics Electronics Division, P.O.Box 81127, San Diego, CA. 92138.	164
8. A TARGET REFERENCE TECHNIQUE FOR FREQUENCY DIVERSITY IMAGING, N.H. Farhat and T.H. Chu, University of Pennsylvania, The Moore School of Electrical Engineering, Philadelphia, PA. 19104, and C.K. Chan, M.I.T. Lincoln Laboratory, Lexington, Mass.	165

	<u>Page</u>
9. EXTENSION OF PHYSICAL OPTICS INVERSE SCATTERING USING POLARIZATION UTILIZATION, W.M. Boerner, AEM Laboratory, Department of Electrical Engineering, University of Manitoba, Winnipeg, Manitoba R3T 2N2, and C.M. Ho, Communications Laboratory, Information Engineering Department, SE0-1104, UICC, P.O.Box 4348, Chicago, Ill. 60680.	159
10. NONCONVERGENCE RESULTS FOR THE APPLICATION OF THE MOMENT METHOD (GALLERKIN'S METHOD) FOR SOME SIMPLE PROBLEMS, T.K. Sarkar, Department of Electrical Engineering, Rochester Institute of Technology, Rochester, N.Y. 14623.	159

FRIDAY MORNING

June 6, 8:30 - 12:00

REFLECTOR ANTENNAS II

DKN 1A

Session B.18

Chairman: G.Y. Delisle
Université Laval
Québec, P.Q.

	<u>Page</u>
1. IMPROVING SCAN CAPABILITY OF PARABOLIC REFLECTORS BY USING CLUSTER FEEDS, S.W. Lee, Department of Electrical Engineering, University of Illinois, Urbana, Ill. 61801, and P. Cramer, Jr., K. Woo, Jet Propulsion Laboratory, California Institute of Technology, 4800 Oak Grove Drive, Pasadena, CA. 91103.	167
2. DUAL OFFSET REFLECTOR ANTENNAS - GO VERSUS GTD, Y. Rahmat-Samii and C. Coyle, Jet Propulsion Laboratory, 4800 Oak Grove Drive, California Institute of Technology, Pasadena, CA. 91103.	168
3. SIMPLE FORMULAS FOR DESIGNING AN OFFSET MULTIBEAM PARABOLIC REFLECTOR, S.W. Lee, Department of Electrical Engineering, University of Illinois, Urbana, Ill. 61801, and Y. Rahmat-Samii, Jet Propulsion Laboratory, 4800 Oak Grove Drive, California Institute of Technology, Pasadena, CA. 91103.	169
4. BACK-HEMISPHERE PATTERN COMPUTATION FOR REFLECTOR ANTENNAS USING SPECTRAL THEORY OF DIFFRACTION, W.L. Ko, and R. Mittra, Department of Electrical Engineering, University of Illinois, Urbana, Ill. 61801.	170
5. THE ELECTROMAGNETIC EFFECTS OF ELECTRICALLY SMALL CONDUCTING WIRES LOCATED IN THE APERTURE OF THE MAYPOLE REFLECTING ANTENNA, J.C. Brand, E.W. Smith and R.T. Hower, Harris Government Systems Group, P.O.Box 37, Melbourne, Fl. 32901.	171
6. RF CONSIDERATIONS OF SUBREFLECTOR SUPPORTS FOR CASSEGRAIN ANTENNA SYSTEMS, J.C. Brand and E.W. Smith, Harris Government Systems Group, P.O.Box 37, Melbourne, Fl. 32901.	172
7. ANALYSIS OF CURVED RADOMES BY RAY TECHNIQUES, S.W. Lee, R. Mittra, V. Jamnejad and M. Sheshadri, Department of Electrical Engineering, University of Illinois, Urbana, Ill. 61801.	173
8. BOUNDARY VALUE PROBLEMS OF ANTENNAS IN THE METALLIC CYLINDRICAL WEDGE REGIONS, Mao Kang-hou, P.O.Box 3923, Peking, China.	174

B.18 (cont.)

	<u>Page</u>
9. DESIGN AND ANALYSIS OF A MEANDERLINE POLARIZER, J.P. Montgomery, Texas Instruments Incorporated, Dallas, Texas 75226.	175
10. RADIATION CHARACTERISTICS OF DIELECTRIC SPHERE LOADED CORRUGATED CONICAL HORN, R.A. Nair and S.C. Gupta, Department of Electrical Engineering, College of Engineering, University of Mosul, Mosul, Iraq.	176

FRIDAY MORNING

June 6, 8:30 - 12:00

SPECIAL SESSION ON INVERSE SCATTERING IV
GEOPHYSICAL SOUNDING

DKN 1B

Session B.19

Chairman: Leon Peters, Jr.
The Ohio State University
Columbus, Ohio

Organizer: W.M. Boerner
UICC
Chicago, Ill.

Page

1. MAXIMUM ENTROPY INVERSION OF UNDERGROUND ELECTROMAGNETIC AND SEISMIC DATA, R.M. Bevensee, Lawrence Livermore Laboratory, Livermore, CA. 94550. 178
2. EXACT-INVERSE SCATTERING FOR PIECE-WISE CONTINUOUS MEDIA, N.N. Bojar-ski, Newport Beach, California 92660. 179
3. INTERPRETATION OF DATA FROM THE UTEM EM PROSPECTING SYSTEM, G.F. West, Geophysics Laboratory, Department of Physics, University of Toronto, Toronto, Ontario, and Y. Lamontagne, Lamontagne Geophysics Ltd., 740 Spadina Avenue, Toronto, Ontario. 180
4. GEOTOMOGRAPHY APPLIED TO NUCLEAR WASTE REPOSITORY SITE ASSESSMENT, R.J. Lytle, J.T. Okada, E.F. Laine, Lawrence Livermore Laboratory, Livermore, CA. 94550. 181
5. DETECTION AND IDENTIFICATION OF BURIED FERROUS OBJECTS BY MEASUREMENT OF THEIR ASSOCIATED MAGNETOSTATIC FIELDS, J.E. McFee and Y. Das, Defense Research Establishment Suffield, Ralston, Alberta T0J 2N0. 182
6. SELF-CONSISTENT EVALUATIONS OF COMPLEX CONSTITUTIVE PARAMETERS, J.S. Yu, Applied Physics Division 2353, Sandia Laboratories, Albuquerque, N.M. 87185. 183
7. ANTENNA DESIGN FOR GEOPHYSICAL APPLICATIONS, H.M. Buettner, Lawrence Livermore Laboratory, Livermore, CA. 94550. 184
8. THE DESIGN OF A RADIO FREQUENCY PROBE FOR USE IN HYDROCARBON EXPLO-RATION, G.S. Huchital, Schlumberger-Doll Research, P.O.Box 307, Ridgefield, CT. 06877. 185

FRIDAY MORNING
June 6, 8:30 - 12:00

MICROSTRIP ANTENNAS AND ARRAYS
DKN 1271

Combined Session AP-S/URSI-B.20
POSTER SESSION

Chairman: R.E. Munson
Ball Aerospace
Boulder, Co.

	<u>Page</u>
1. CALCULATED AND MEASURED PERIMETER FIELD DISTRIBUTIONS FOR MICROSTRIP ANTENNAS, K.R. Carver, New Mexico State University, Las Cruces, N.M.	186
2. THE CIRCULARLY POLARIZED ELLIPTICAL PRINTED-CIRCUIT ANTENNA, S.A. Long and L.C. Shen, University of Houston, Houston, Texas,	186
3. CHARACTERISTICS OF A CAVITY BACKED ANNULAR SLOT ARRAY, A. Shoamaneh, F. Rahman and L. Shafai, University of Manitoba, Winnipeg, Manitoba.	186
4. CALCULATION OF H-PLANE MUTUAL COUPLING BETWEEN RECTANGULAR MICROSTRIP ANTENNAS, A.R. Sindoris, Harry Diamond Laboratories, Adelphi, MD., C.M. Krowne, North Carolina State University, Raleigh, N.C.	186
5. A 7.5 GHz MICROSTRIP PHASED ARRAY FOR AIRCRAFT TO SATELLITE COMMUNICATION, F.W. Cipolla, Ball Aerospace Systems Division, Boulder, Co., and L.P. Trapani, Griffiss Air Force Base, N.Y.	186
6. ANALYTICAL AND EXPERIMENTAL INVESTIGATION OF XP-FILM MATERIAL FOR HARDENED PRINTED DIPOLE ARRAY DESIGN, R.S. Chu, S.Y. Peng, R. Tang and N.S. Wong, Hughes Aircraft Company, Fullerton, California.	186
7. MUTUAL COUPLING BETWEEN RECTANGULAR AND CIRCULAR MICROSTRIP ELEMENTS, R.P. Jedlicka, M.T. Poe and K.R. Carver, New Mexico State University, Las Cruces, N.M.	186
8. DESIGN OF COLLINEAR LONGITUDINAL SLOT ARRAYS FED BY BOXED STRIPLINE, P.K. Park, Hughes Missile Systems, Canoga Park, CA., and R.S. Elliott, UCLA, Los Angeles, CA.	187
9. REDUCING BACKLOBES FROM MICROSTRIP ARRAYS, M. Shields, Ball Aerospace Systems, Division, Boulder, Co.	187
10. APPROXIMATIVE COMPUTATION OF MUTUAL COUPLING BETWEEN MICROSTRIP RESONATORS, E. Van Lil, A. Van de Capelle, K.U. Leuven, Afd. Microgolven en Lasers, Heverlee, Belgium.	188

B.20 (cont.)

	<u>Page</u>
11. IMPEDANCE-MATCHING OF MICROSTRIP RESONATOR ANTENNAS, H.F. Pues and A.R. Van de Capelle, K.U. Leuven, Department Elektrotechniek, Heverlee, Belgium.	189
12. INPUT IMPEDANCE AND RADIATION CHARACTERISTICS OF A CIRCULAR MICROSTRIP ANTENNA, W.C. Chew, J.A. Kong, M.I.T., Cambridge, Mass.	190
13. HANKEL TRANSFORM DOMAIN ANALYSIS OF OPEN CIRCULAR MICROSTRIP RADIATING STRUCTURES, K. Araki, T. Itoh, University of Texas, Austin, TX. and Y. Naito, Tokyo Institute of Technology, Tokyo, Japan.	191

MONDAY AFTERNOON

June 2, 1:30 - 5:00

SPECIAL SESSION ON OPTICAL COMMUNICATIONS II

DEVICES AND SYSTEMS

DKN 2B

Combined Session C.1/D

Chairman: A.R. Boothroyd
Carleton University
Ottawa, Ontario

Organizers: A.R. Boothroyd P.H. Wittke
Carleton University Queen's University
Ottawa, Ontario Kingston, Ontario

	<u>Page</u>
1. OPTICAL FIBER SYSTEMS: PROGRESS AND PROSPECTS, (Invited), C. Kao, ITT Electro-optical Products Division, Roanoke, VA.	194
2. RECENT ADVANCES IN LIGHT SOURCES FOR OPTICAL COMMUNICATIONS, (Invited), H. Kressel, RCA Laboratories, Princeton, N.J.	195
3. PHOTODETECTORS FOR FIBER OPTICAL COMMUNICATIONS, (Invited), J. Conradi, Bell-Northern Research, Ottawa, Ontario.	196
4. NARROW STRIPE LASERS FOR LINEAR APPLICATIONS, C. Lindström and P. Tihanyi, Institute of Microwave Technology, Stockholm, Sweden.	197
5. CHANNELLED SUBSTRATE LASERS PREPARED USING A COMBINATION OF ORGANOMETALLIC PYROLYSIS AND LIQUID PHASE EPITAXY, J.P. Noad, C.M. Look and A.J. SpringThorpe, Bell-Northern Research, P.O.Box 3511, Station C, Ottawa, Ontario K1Y 4H7.	198
6. OSCILLATION CHARACTERISTICS OF ACTIVE ALMOST PERIODIC STRUCTURES, C.T. Warhola and D.J. Jaggard, Department of Electrical Engineering, University of Utah, Salt-Lake City, Utah 84112.	199
7. BANDWIDTH CHARACTERIZATION OF FIBER LINKS, R. Iyer and A. Javed, Bell-Northern Research, P.O.Box 3511, Station C, Ottawa, Ontario K1Y 4H7.	200
8. OPTICAL WAVELENGTH INTERSATELLITE COMMUNICATIONS SYSTEMS, A.K. Sinha, COMSAT, Communications Satellite Corporation, 950 L'Enfant Plaza, S.W., Washington, D.C. 20024.	201
9. A BASEBAND VIDEO AND FM AUDIO FIBER OPTICAL COMMUNICATION SYSTEM FOR EDUCATIONAL AND DEMONSTRATION PURPOSES, K.J. Clowes and G.L. Yip, Department of Electrical Engineering, McGill University, Montreal, Qué. H3A 2A7.	202

10. TRANSMISSION OF 18 TV CHANNELS OVER A 1-km ANALOG FIBER OPTICAL COMMUNICATION SYSTEM, K.J. Clowes and G.L. Yip, Department of Electrical Engineering, McGill University, Montreal, Qué. H3A 2A7, J.C. Dagenais, Télécâble Vidéotron, St-Hubert, Qué., H. Stephenne, Service de la Recherche, Ministère des Communications, Québec. 203

WEDNESDAY MORNING
June 4, 8:30 - 12:00

SATELLITE AND RADIO TRANSMISSION

DKN 2A

Session C.2

Chairman: J.F. Hayes
McGill University
Montréal, Québec

	<u>Page</u>
1. OPTIMUM SATELLITE FREQUENCY ESTIMATES FOR CANADA AND THE UNITED-STATES, P.F. Christopher, MITRE Technical Staff, D97, Mail Stop B190, The MITRE Corporation, Bedford, Mass. 01730.	205
2. VIDEO COCHANNEL INTERFERENCE INTO DIGITAL COMMUNICATION SATELLITE SYSTEMS, P. Constantinou, Telesat Canada, 333 River Road, Ottawa, Ontario K1L 8B9.	206
3. NEW MODULATION PERFORMANCE PARAMETER FOR DUAL-POLARIZED SATELLITE COMMUNICATION SYSTEMS, Lin-Shan Lee, Department of Electrical Engineering, National Taiwan University, Taipei, Taiwan.	207
4. SIMULATED IMPULSE RESPONSE OF AIRCRAFT OBSTRUCTION OF DIGITAL LINKS, H.S. Hayre, Electrical Engineering Department, Wave Propagation Laboratory, University of Houston, Houston, TX 77004.	208
5. BANDLIMITING DISTORTION IN TRANSMITTING VIDEO AUDIO, AND DIGITAL SIGNALS OVER RADIO RELAY LINKS, A.A. Ali, Manitoba Telephone System, Winnipeg, Manitoba.	209
6. IS ANGLE DIVERSITY BETTER THAN FREQUENCY DIVERSITY?, P. Monsen, Signatron, Inc., 12 Hartwell Avenue, Lexington, Mass. 02173.	210
7. MAXIMUM LIKELIHOOD SEQUENCE ESTIMATION OVER UNKNOWN MULTIPATH CHANNELS, Sally Norvell, Naval Ocean Systems Center, Code 8142, San Diego, CA. 92152.	211
8. THEORETICAL AND EXPERIMENTAL FOUNDATIONS OF MICROWAVE YIG $0 - \pi$ MODULATOR, Xiang Xunxian, Microwave Remote Sensing Laboratory, Huazhong Institute of Technology, Wuhan, China.	212
9. HARMONIC STABILIZATION - A NOVEL CONCEPT FOR BROADBANDING TRAPATT-AMPLIFIERS, M. Heller, Lehrstuhl für Technische Elektronik der Technischen Universität München, West Germany.	213
10. HIGH TEMPERATURE ELECTRONICS AND APPLICATIONS TO BALLOON BEACONS AND LONG LIFE TRANSPONDERS FOR VENUS, R.F. Jurgens, A.I. Zygielbaum, Jet Propulsion Laboratory, 4800 Oak Grove Drive, Pasadena, CA. 91103, and J. Blamont, Service d'Aéronomie du Centre National de la Recherche Scientifique, 91370 Verrières du Buisson, France.	214

WEDNESDAY AFTERNOON

June 4, 1:30 - 5:00

SIGNAL PROCESSING

DKN 2B

Session C.3

Chairman: P.H. Wittke
Queen's University
Kingston, Ontario

	<u>Page</u>
1. CORRELATION FUNCTION OF OUTPUT OF BANDPASS NONLINEARITY, Nelson M. Blachman, GTE Sylvia Systems Group, P.O. Box 188, Mountain View, California 94042.	216
2. TRANSFER FUNCTIONS OF MILDLY NONLINEAR CIRCUITS, J.J. Busgang, Signatron Inc., 12 Hartwell Avenue, Lexington, Michigan 02173.	217
3. FALSE ALARM PROBABILITIES FOR A LOGARITHMIC DETECTOR FOLLOWED BY A SUMMER, J.L. Ekstrom, HRB-Singer Inc., 2100 Reston Avenue, Reston, Virginia 22091.	218
4. AN ADDENDUM TO BAYES' THEOREM, J.S. Avrin, The Aerospace Corporation El Segundo, Post Office Box 92957, Los Angeles, California 90245.	219
5. DESIGN OF SIGNAL SETS WITH SPECIFIED CORRELATION PROPERTIES, T.P. McGree and G.R. Cooper, School of Electrical Engineering, Purdue University, West Lafayette, Indiana 47907.	220
6. THE APPLICATION OF TSENG-SARKAR WINDOW TO SPECTRAL ESTIMATION, Tapan K. Sarkar and Fung-I Tseng, Department of Electrical Engineering, Rochester Institute of Technology, Rochester, New York 14623.	221
7. SERIAL HF MODEM USING ADAPTIVE ANTENNA TO CANCEL MULTIPATH-EXPERIMENTAL RESULTS, P.M. Hansen, Naval Ocean Systems Center, Antennas and RF Distribution, Code 8112, San Diego, California 92152.	222

THURSDAY MORNING
June 5, 8:30 - 12:00

NOISE AND INTERFERENCE,
CHARACTERIZATION AND MEASUREMENT

DKN 2A

Session E

Chairman: Bhartendu
Environment Canada
Downsview, Ontario

	<u>Page</u>
1. RADIO EMISSION FROM LIGHTNING STEPPED LEADER, J.B. Smyth, D.C. Smyth and J. Durment, Smyth Associates, 3555 Aero Court, San Diego, California 92123.	224
2. HORIZONTALLY AND VERTICALLY POLARIZED VLF ATMOSPHERIC RADIO NOISE AT ELEVATED RECEIVERS, F.J. Kelly, J.P. Hauser and F.J. Rhoads, Naval Research Laboratory, Washington, D.C. 20375.	225
3. LIGHTNING AND NUCLEAR ELECTROMAGNETIC INTERFERENCE ENVIRONMENTS AND SUPPRESSION TECHNIQUES TO PROTECT ELECTRONIC SYSTEMS, G.H. Joshi, Raytheon - Missile Systems Division, Bedford, Massachusetts 01730, U.S.A., and J. Dando, J. Beilfuss, Harry Diamond Laboratories, Woodbridge, Virginia.	226
4. STATISTICS OF ELECTROMAGNETIC NOISE DUE TO H.V. POWER LINES, A.U.H. Sheikh, University of Caryounis, Benghazi, Libya, and J.D. Parsons, University of Birmingham, Birmingham, England.	227
5. AMPLITUDE AND PHASE STRUCTURE OF FIELDS IN "DEGRADED" ANECHOIC ENCLOSURES FOR E.M. INTERFERENCE MEASUREMENTS, S.R. Mishra and T.J.F. Pavlasek, Electrical Engineering, McGill University, Montreal, Quebec H3A 2A7.	228
6. WINDMILL INTERFERENCE TO TELEVISION RECEPTION, D.L. Sengupta and Thomas B.A. Senior, Radiation Laboratory, The University of Michigan, Ann Arbor, Michigan 48109.	229
7. SPATIAL FILTERING TECHNIQUES APPLIED TO NETWORK INTERFERENCE PROBLEMS, G.J. Brown, Naval Ocean Systems Center, Code 8142, San Diego, California 92152.	230
8. ETUDE EXPERIMENTALE DES TRAJETS MULTIPLES PAR UNE METHODE BISTATIQUE DE SYNTHÈSE D'OUVERTURE, J. Dorey, Y. Blanchard and D. Medynski, Office National d'Etudes et de Recherches Aérospatiales, 29 Avenue de la Division Leclerc, Châtillon-sous-Bagneux (Hauts de Seine), O.N.E.R.A., 92320 Châtillon, France.	231

MONDAY AFTERNOON
June 2, 1:30 - 5:00

REMOTE SENSING - ACTIVE

DKN 2C

Session F.1

Chairman: Kenneth Hardy
Environmental Research and Technology Incorp.
Concord, MA.

Page

1. THE SAR-SEEN SEA: A SPECIAL CASE, R.O. Harger, Department of Electrical Engineering, University of Maryland, College Park, MD 20742. 233
2. THE DEPENDENCE OF THE BACKSCATTERED SIGNAL AUTOCORRELATION FUNCTION ON WATER SURFACE SCATTERING COEFFICIENT AND ORBITAL VELOCITY VARIATIONS AND PLATFORM VELOCITY, D.E. Weissman, Hofstra University, Hempstead, N.Y. 11550, and J.G. Kim, Old Dominion University, Norfolk, VI 23508. 234
3. MULTIFREQUENCY RADAR SEA RETURN, F.B. Dyer, R.N. Trebits and N.C. Currie, Engineering Experiment Station, Georgia Institute of Technology, Atlanta, Georgia 30332. 235
4. ATMOSPHERIC DUCTING AND CLUTTER EFFECTS ON RF WAVE PROPAGATION OVER THE OCEAN SURFACE, Frank T. Wu, Wai-Mao P. Yu, Alexis Shlanta, Michelson Laboratory, Naval Weapons Center, China Lake, CA. 93555. 236
5. CONCEPTUAL PROBLEMS IN LOW-ANGLE SCATTER FROM THE SEA, L.B. Wetzel, Naval Research Laboratory, Washington, D.C. 02375. 237
6. MEASUREMENTS OF THE VELOCITY CORRELATION FUNCTIONS IN THE PLANETARY BOUNDARY LAYER WITH A PULSE DOPPLER RADAR, Dunsan S. Zrnac and Glenn Smythe, National Severe Storms Laboratory, 1313 Halley Circle, Norman, Oklahoma 73069. 238
7. REMOTE SENSING OF TORNADIC STORM BASED ON HF RADIO WAVE FROM IONOSPHERE AND IR IMAGERY FROM GOES SATELLITE, R.J. Hung, the University of Alabama in Huntsville, Huntsville, AL. 35807, R.E. Smith, NASA/ Marshall Space Flight Center, AL. 35812. 239
8. FREQUENCY VARIATION OF VEGETATION CLUTTER, F.T. Ulaby, Remote Sensing Laboratory, University of Kansas, Center for Research, Inc., Lawrence, Kansas 66045. 240

	<u>Page</u>
9. COMBINED ACTIVE-PASSIVE MICROWAVE MEASUREMENTS OF THE SEA SURFACE IN THE GRAND BANKS FRONTAL REGION, V.E. Delnore, Kentron International, Inc., Hampton, VA 23666, and R.F. Harrington, W.L. Jones, C.T. Swift, NASA Langley Research Center, Hampton, VA 23665.	241
10. MICROWAVE RADIOMETRIC AIRCRAFT OBSERVATIONS OF THE FABRY-PEROT INTER-FERENCE FRINGES OF AN ICE-WATER SYSTEM, R.F. Harrington, C.T. Swift and J.C. Fedors, NASA Langley Research Center, Hampton, VA 23665.	242

TUESDAY AFTERNOON
June 3, 1:30 - 5:00

REMOTE SENSING - PASSIVE

DKN 2C

Session F.2

Chairman: D.C. Hogg
Wave Propagation Laboratory
NOAA
Boulder, Co.

	<u>Page</u>
1. MICROWAVE REMOTE SENSING FOR THE WEATHER SERVICES, D.C. Hogg, M.T. Decker and C. Strauch, Wave Propagation Laboratory, NOAA/Environmental Research Laboratories, Boulder, Co. 80303.	244
2. SEA-SURFACE TEMPERATURE, WIND SPEED AND ATMOSPHERIC WATER VAPOR: A COMPARISON OF CONVENTIONALLY MEASURED DATA WITH DATA RETRIEVED FROM SATELLITE-BORNE MICROWAVE RADIOMETRY, R. Hofer and E.G. Njoku, Jet. Propulsion Laboratory, 4800 Oak Grove Drive, Pasadena, CA. 91103.	245
3. LARGE ANTENNA MULTIFREQUENCY MICROWAVE RADIOMETER (LAMMR) SYSTEM DESIGN, J.L. King, NASA Goddard Space Flight Center, Greenbelt, MD. 20771.	246
4. ANTENNA DESIGN FOR LARGE ANTENNA MULTIFREQUENCY RADIOMETER (LAMMR) L.R. Dod, NASA Goddard Space Flight Center, Greenbelt, MD. 20771, and Ramon Miezi, Sigma Data Systems,	247
5. DERIVATIONS OF VARIOUS GEOPHYSICAL PARAMETERS FROM A SEVEN-CHANNEL SATELLITE-BORNE PASSIVE MICROWAVE SENSOR, H.K. Burke and K.R. Hardy, Environmental Research and Technology, Inc., 696 Virginia Road, Concord, Mass. 01742, and A.T. Edgerton, Hughes Aircraft Company, P.O.Box 92912, Los Angeles, CA. 90009.	248
6. DERIVATION OF SEA ICE CONDITIONS UTILIZING SATELLITE-BORNE PASSIVE MICROWAVE SENSORS, H.K. Burke and J.H. Ho, Environmental Research and Technology, Inc., 696 Virginia Road, Concord, Mass. 01742, and A.T. Edgerton and G. Poe, Hughes Aircraft Company, P.O.Box 92919, Los Angeles, CA. 90009.	249
7. STUDIES OF VEGETATION EFFECTS ON SOIL MOISTURE DETERMINATION, J. Eckerman, G. Orr, M. Dombrowski, M. Doyle, J. Schutt and J. Wang, NASA, Goddard Space Flight Center, Greenbelt, MD 20771.	250
8. PASSIVE MICROWAVE REMOTE SENSING, L.U. Martin and C.T. Beard, Naval Research Laboratory, Washington, D.C. 20375.	251

	<u>Page</u>
9. MARKOVIAN MODELS OF THE SPATIAL COHERENCE OF ATMOSPHERIC FIELDS: THEIR IMPACT AND AVAILABILITY FOR REMOTE SENSING STUDIES, P.M. Tol-dalagi, Research Laboratory of Electronics, M.I.T. 77 Massachusetts Avenue, Cambridge, Mass. 02139.	252
10. INVERSION OF DATA FROM DIFFRACTION-LIMITED MULTIWAVELENGTH REMOTE SENSORS WITH NONLINEAR DEPENDENCE OF OBSERVABLES ON THE GEOPHYSICAL PARAMETERS, P.W. Rosenkranz, Research Laboratory of Electronics, M.I.T., 77 Massachusetts Avenue, Cambridge, Mass. 02139.	253
11. MULTIPARAMETRIC INVERSE PROBLEMS IN MICROWAVE RADIOMETRY OF OCEAN AND ATMOSPHERE, A.M. Shutko and A.G. Grankov, Institute of Radio-engineering and Electronics, Marx Avenue 18, Academy of Sciences of the USSR, Moscow K-9, GSP-3, USSR 103907.	254

WEDNESDAY MORNING
June 4, 8:30 - 12:00

RADIATIVE TRANSFER THEORY AND
REMOTE SENSING OF LIGHTNING

DKN 2C

Session F.3

Chairman: J. Goldhirsh
Applied Physics Laboratory
Laurel, MD.

	<u>Page</u>
1. EFFECT OF CHANNEL DETAILS ON THE FIELDS INDUCED BY A LIGHTNING RETURN STROKE, R.L. Gardner, Department of Physics and Cooperative Institute of Research in Environmental Sciences, University of Colorado, Boulder, Co. 80309.	257
2. RADIATIVE TRANSFER THEORY FOR A TWO-LAYER RANDOM MEDIUM WITH CYLINDRICAL STRUCTURE, S.L. Chuang, J.A. Kong, Department of Electrical Engineering and Computer Sciences and Research Laboratory of Electronics, M.I.T., Cambridge, Mass. 02139, and L. Tsang, Department of Electrical Engineering, Texas A and M University, College Station, TX 77843.	258
3. RADIATIVE TRANSFER THEORY APPLIED TO REMOTE SENSING OF HOMOGENEOUS MEDIA CONTAINING DISCRETE SCATTERERS, M.E. McGillan, Department of Electrical Engineering, Computer Science and Research Laboratory of Electronics, M.I.T., Cambridge, Mass. 02139.	259
4. RADIATIVE TRANSFER THEORY FOR ACTIVE AND PASSIVE MICROWAVE REMOTE SENSING OF HOMOGENEOUS LAYER CONTAINING SPHERICAL SCATTERERS, R. Shin, J.A. Kong, Department of Electrical Engineering, Computer Science and Research Laboratory of Electronics, M.I.T., Cambridge, Mass. 02139, and L. Tsang, Department of Electrical Engineering, Texas A and M University, College Station, TX 77843.	260
5. RADIATIVE TRANSFER THEORY FOR ACTIVE REMOTE SENSING OF HOMOGENEOUS LAYER CONTAINING ELLIPSOIDAL SCATTERERS, M. Kubacsi, R. Shin, Department of Electrical Engineering, Computer Science and Research Laboratory of Electronics, M.I.T., Cambridge, Mass. 02139.	261
6. ACTIVE MICROWAVE REMOTE SENSING OF AN ANISOTROPIC TWO-LAYER RANDOM MEDIUM, M.A. Zuniga, S.L. Chuang, J.A. Kong, J.K. Lee, Department of Electrical Engineering, Computer Science and Research Laboratory of Electronics, M.I.T., Cambridge, Mass. 02139.	262
7. MODIFIED RADIATIVE TRANSFER THEORY FOR ACTIVE REMOTE SENSING OF A TWO-LAYER RANDOM MEDIUM, M.A. Zuniga, J.A. Kong, Department of Electrical Engineering and Computer Science and Research Laboratory of Electronics, M.I.T., Cambridge, Mass. 02139.	263

WEDNESDAY AFTERNOON

June 4, 1:30 - 5:00

SURFACE/UNDERGROUND PROPAGATION

DKN 2C

Combined Session F.4/AP-5

Chairman: R.J. King
University of Wisconsin
Madison, WI

	<u>Page</u>
1. EARTH CONDUCTIVITY EFFECT ON THE FIELD OF A LONG HORIZONTAL ANTENNA, A. Mohsen, Department of Electrical Engineering, University of Manitoba, Winnipeg, Canada.	264
2. MONOPOLE ANTENNAS OVER LOSSY GROUND, H.K. Schuman and T.E. Baldwin, Atlantic Research Corporation, 5390 Cherokee Avenue, Alexandria, Virginia 22314.	264
3. EXPERIMENTAL AND THEORETICAL STUDIES OF LATERAL-WAVE PROPAGATION, M.F. Brown, R.W.P. King, L.C. Shen, and T.T. Wu, Gordon McKay Laboratory, Harvard University, Cambridge, Massachusetts 02138.	265
4. DIFFRACTION AT A SURFACE IMPEDANCE DISCONTINUITY APPLICATION TO SEA-LAND RADIO WAVE PROPAGATION, G. Franceschetti and V. G. Vaccaro, Istituto Elettrotecnico, Università di Napoli, Italy.	266
5. COUPLED MODELS ANALYSIS FOR A NON-UNIFORM TROPOSPHERIC WAVEGUIDE, J. R. Wait, ERL/NOAA/CIRES, U.S. Department of Commerce, Boulder, Colorado 80303.	267
6. UHF LONG DISTANCE DUCT PROPAGATION, Mauro S. Assis, Centro de Tecnologia Promon, Praia do Flamengo 154, 22210 Rio de Janeiro - RJ, Brazil.	268
7. FIELDS OF A HORIZONTAL LOOP OF ARBITRARY SHAPE BURIED IN A TWO LAYER EARTH, J.R. Wait and D.A. Hill, ERL/NOAA and ITS/NTIA, U.S. Department of Commerce, Boulder, Colorado 80303.	269
8. PROCÉDES ELECTROMAGNETIQUES DE DETECTION DE FILONS METALLIFERES: ETUDE NUMERIQUE DE L'INFLUENCE DU PENDAGE DU GISEMENT POUR DIFFERENTS DISPOSITIFS D'EXCITATION, M. Caeterman, P. Degauque, B. Demoulin et R. Gabillard, Université des Sciences et Techniques de Lille, Département Electronique, 59 655 Villeneuve d'Ascq, Cedex, France.	270
9. SCATTERING OF RADIO WAVES FROM AN EARTH MODEL WITH A PERIODIC ROUGH SUBSURFACE, M.S. El Tanany, M. El Said, S.F. Mahmoud, Electronic and Communications Department, Cairo University, Giza, Egypt.	264

THURSDAY MORNING

June 5, 8:30 - 12:00

LINE-OF-SIGHT PROPAGATION
DKN 2C

Combined Session F.5/AP-S

Chairman: R.K. Crane
Environmental Technology Res.Lab.
Concord, MA

	<u>Page</u>
1. RESULTS OF RAIN ATTENUATION MEASUREMENTS AT 13 GHz, Y. Kumar and DPS Seth, Telecommunication Research Center, Khurshid Lal Bhavan, Janpath, New Delhi - 110001, India.	272
2. REMOTE SENSING OF RAINDROP SIZE DISTRIBUTING FROM MICROWAVE SCATTERING MEASUREMENTS-II, Y. Furuham, T. Ihara and Tohma, Radio Research Laboratories, Ministry of Posts and Telecommunications, Koganei-shi, Tokyo 184, Japan.	271
3. COMPLEX PERMITTIVITY OF SAND-STORM MODELS AT 9 GHz, A. Kumar, The Higher Institute of Electronics, Beni Walid, Socialist People's Libyan Arab Jamahiriya.	273
4. PROPAGATION OF MICROWAVES UNDER ADVERSE SAND-STORM CONDITIONS OF IRAQ, H.T. Al Hafid, S.C. Gupta and M. Ibrahim, Department of Electrical Engineering, Mosul University, Mosul, Iraq.	274
5. DIRECTION FINDING OF MULTIPATH PROPAGATION, Kazuaki Takao, Department of Electrical Engineering, Kyoto University, Sakyo, Kyoto 606, Japan.	275
6. THE PREDICTION OF CLEAR-AIR FADING FOR TERRESTRIAL LINE-OF-SIGHT AND LOW-ANGLE SATELLITE RADIO PATHS, Claus Fengler, Department of Electrical Engineering, McGill University, Montreal, Quebec H3A 2A7.	271
7. A NEW METHOD FOR EVALUATING REFRACTIVITY PROFILES FROM SURFACE MEASUREMENT, M.T. Badr, Telecommunication Research Center, Dokki Exchange Building, Dokki, Cairo, Egypt.	276
8. MODELING THE INCREASE IN LOSS CAUSED BY PROPAGATION THROUGH A GROVE OF TREES, Mark Weissberger and Juergen Hauber, IIT Research Institute Staff at the Department of Defense, Electromagnetic Compatibility Analysis Center, Annapolis, Maryland, 21402.	277

THURSDAY AFTERNOON
June 5, 1:30 - 5:00

PRECIPITATION ATTENUATION AND DEPOLARIZATION

DKN 2C

Combined Session F.6/AP-5

Chairman: K.S. McCormick
Communications Research Center
Ottawa, Ontario

	<u>Page</u>
1. MODELING RAIN ATTENUATION OF EARTH-SPACE MICROWAVE LINKS, M.A. Weissberg and R.H. Meidenbauer, IIT Research Institute Staff of the Department of Defense, Electromagnetic Compatibility Analysis Center, Annapolis, MD. 21402.	278
2. SPATIAL RAIN RATE DISTRIBUTION MODELING FOR EARTH-SPACE LINK PROPAGATION CALCULATIONS, S.O. Lane and W.L. Stutzman, Virginia Polytechnic Institute and State University, Department of Electrical Engineering, Blacksburg, VA. 24061.	279
3. WAVELENGTH DEPENDENCE OF SLANT PATH RAIN ATTENUATIONS AT MILLIMETER WAVELENGTHS, E.E. Altshuler and L.E. Telford, Rome Air Development Center, Electromagnetic Sciences Division, Hanscom AFB, Mass. 01731.	280
4. SIMPLIFICATION OF CALCULATIONS OF RAIN-INDUCED DIFFERENTIAL ATTENUATION AND CROSS POLARIZATION AT MILLIMETER WAVES PROPAGATION, A.M. Ghuniem, I.E. Salm, Ahd El-Samie Mostapha, Telecommunication Research Centre, Dokki Exchange Building, Dokki, Cairo, Egypt.	281
5. THE ANALYSIS ABOUT THREE TYPES OF POLARIZATION CORRECTORS FOR SATELLITE COMMUNICATION WITH FREQUENCY REUSE SYSTEMS, Zhang Ri-rong, Shijiazhuang Communication Laboratories, Shijiazhuang, Hebei, China.	278
6. TAMPA TRIAD 19 GHz RAINY SEASON DIVERSITY RESULTS FOR 1978-1979, D.D. Tang and D. Davidson, GTE Laboratories Inc., Waltham, Mass. 02154, and S.C. Bloch, University of South Florida, Tampa, Fl. 33620.	282
7. CHARACTERIZING THE RAIN MEDIUM, P.H. Wiley and S.C. Ahalt, Virginia Polytechnic Institute and State University, Department of Electrical Engineering, Blacksburg, VA. 24061.	283
8. DEPOLARIZATION OF THE 28.56 GHz COMSTAR BEACON SIGNAL BY ICE PARTICLES AT WALLOPS ISLAND, VIRGINIA, J. Goldhirsh, Applied Physics Laboratory, The Johns Hopkins University, Laurel, MD. 20810.	284

9. SUMMARY OF 1979 ATTENUATION AND DEPOLARIZATION MEASUREMENTS MADE WITH THE CTS (11.7 GHz) AND COMSTAR (19.04 and 28.56 GHz) BEACONS, E.A. Manus, P.H. Wiley, C.W. Bostian, W.L. Stutzman, J.R. Dent, R.E. Marshall and P. Santago, Electrical Engineering Department, Virginia Polytechnic Institute and State University, Blacksburg, VA. 24061. 285
10. SIMULTANEOUS EARTH-SPACE PROPAGATION MEASUREMENTS USING THE 28.5 GHz COMSTAR BEACON AND A 16.5 GHz POLARIZATION DIVERSITY RADAR, Y.M.M. Antar, A. Hendry, Division of Electrical Engineering, National Research Council of Canada, Ottawa, Ontario K1A 0R8, and J.J. Schlesak, R.L. Olsen, R.C. Bérubé, Communications Research Center, Department of Communications, Ottawa, Ontario K2H 8S2. 286

TUESDAY AFTERNOON
June 3, 1:30 - 5:00

IONOSPHERIC MODIFICATION AND IRREGULARITIES

DKN 2A

Session G.1

Chairman: G. Lyon
University of Western Ontario
London, Ontario

	<u>Page</u>
1. PLASMAPAUSE AND AURORAL OVAL IRREGULARITIES DURING MAGNETIC STORMS, Zvi Houminer and Jules Aarons, Air Force Geophysics Laboratory, Hanscom AFB, Mass. 01731, and Eileen MacKenzie, Emmanuel College, Boston, Mass. 02115.	288
2. A CASE STUDY OF MULTI-FREQUENCY IONOSPHERIC SCINTILLATIONS, C.H. Liu and K.C. Yeh, Department of Electrical Engineering, University of Illinois at Urbana-Champaign, 155 Electrical Engineering Building, Urbana, Illinois 61801.	289
3. PRELIMINARY RESULTS FROM THE NRL MADRE HF RADAR FOR THE HEAO-C LAUNCH, D.R. Uffelmann and J.R. Davis, Naval Research Laboratory, Washington, D.C. 20375.	290
4. INTERPRETATION OF BERMUDA POLARIMETRY DATA FOR THE HEAO-C IONOSPHERIC HOLE, M.H. Reilly, Naval Research Laboratory, Washington, D.C. 20375.	291
5. ANALYSIS OF UNUSUAL SIGNAL STRENGTH VARIATIONS OBSERVED IN THE 14 AND 21 MHz BANDS FOLLOWING AN ATLAS-CENTAUR ROCKET LAUNCH, D.B. Odom, N.P. Viens, Raytheon Company, Wayland, Mass. 01778, and J.A. Klobuchar, AFCL (PHP), Hanscom AFB, Mass. 01731.	292
6. RECENT IONOSPHERIC MODIFICATION EXPERIMENTS CONDUCTED AT PLATTEVILLE-COLORADO, C.M. Rush, E.J. Violette, J.C. Carroll and R.H. Epselnd, U.S. Department of Commerce, Institute for Telecommunication Sciences, Boulder, Co. 80303.	293
7. DETERMINATION OF ELECTRON DENSITY PROFILE FROM THE RESONANCE SCATTER OF RADIO WAVES AND THE VERTICAL-INCIDENCE IONOGRAMS, V.V. Belikovitch, E.A. Benediktov, G.I. Tyorina, Radio Research Institute, Gorky, USSR, and T.L. Gulyaeva, Institute of Terrestrial Magnetism, Ionosphere and Radio Wave Propagation, USSR Academy of Sciences, Troitsk, Moscow Region, USSR.	294

WEDNESDAY MORNING
June 4, 8:30 - 12:00

M. LINDEMAN PHILLIPS MEMORIAL SESSION
ON IONOSONDE TECHNIQUES

DKN 2E

Session G.2

Chairman: K. Toman
NOAA
Boulder, CO

	<u>Page</u>
1. AUTOMATIC PROCESSING OF DIGITAL IONOGRAMS, Bodo W. Reinisch, University of Lowell, Center for Atmospheric Research, 450 Aiken Street, Lowell, Massachusetts 01854.	296
2. METHODS FOR DISPLAY AND ANALYSIS OF DIGITAL IONOSONDE DATA, THE DOP-PLIONOGRAM, J.W. Wright and M.L.V. Pitteway, U.S. Department of Commerce, NOAA/Environmental Research Laboratory, Boulder, Colorado 80303.	297
3. NEW DATA PROCESSING ROUTINES FOR THE DIGITAL NOAA IONOSONDE, A.K. Paul, U.S. Department of Commerce, NOAA/Environmental Research Laboratory, Boulder, Colorado 80303.	298
4. FIRST RESULTS FROM THE NOAA HF RADAR, F.T. Berkey, J.R. Doupnik and G.S. Stiles, Center for Atmospheric and Space Sciences, Utah State University, Logan, Utah 84322.	299
5. IONOGRAM SCALING ALGORITHM, H. Waldman, RCA Laboratory, David Sarnoff Research Center, Princeton, New Jersey 08540.	300
6. A COMPUTER BASED IONOSPHERIC SOUNDING AND H.F. NOISE MEASURING SYSTEM, G.F. Earl, Defence Research Center, Salisbury, South Australia, Australia 5091.	301
7. PERFORMANCE MEASURES FOR AN AUTOMATED SOUNDER SYSTEM, R.L. Merk, Naval Ocean Systems Center, Code 8142, San Diego, California 92152.	302

WEDNESDAY AFTERNOON

June 4, 1:30 - 5:00

IONOGRAM INTERPRETATIONS, IONOSPHERIC
DRIFTS, AND DISPERSION

DKN 2A

Session G.3

Chairman: K. Davies
NOAA
Boulder, CO

	<u>Page</u>
1. GRAVITY WAVE EFFECTS OBSERVABLE WITH MODERN IONOSONDE, J.E. Titheridge, NOAA-SEL, Boulder, Colorado 80303.	304
2. LEAST SQUARE CALCULATION OF N(h) PROFILES, J.E. Titheridge, NOAA-SEL, Boulder, Colorado 80303.	305
3. DYNASONDE STUDIES OF CHEMICAL DEPLETION OF THE IONOSPHERE, J.W. Wright and M.L.V. Pitteway, U.S. Department of Commerce, NOAA/Environmental Research Laboratory, Boulder, Colorado 80303.	306
4. GRAVITY WAVES PROPAGATION AT E-REGION, A.E. Giraldez, LIARA, avenida Libertador 327, Vte Lopez (Bs As) Argentina.	307
5. MILLSTONE HILL INCOHERENT SCATTER OBSERVATIONS OF THE AURORAL IONOSPHERE, J.V. Evans, J.M. Holt, W.L. Oliver and R.H. Wand, Lincoln Laboratory, M.I.T., Lexington, Michigan 02173.	308
6. TIME SPREADING OF TRANSIENT PULSES BY THE IONOSPHERE, R.E. McIntosh, Department of Electrical and Computer Engineering, University of Massachusetts, Amherst, Massachusetts 01003	309

WEDNESDAY MORNING
June 4, 8:30 - 12:00

MEASUREMENTS OF MAGNETOSPHERIC AND SPACE PLASMAS:
PROBES, VLF AND HF

DKN IE

Session H.1

Chairman: R.W. Fredricks
TRW
Redondo Beach, CA.

	<u>Page</u>
1. THE WISP/HF SYSTEM FOR SPACELAB, H.G. James, Communications Research Center, Department of Communications, Ottawa, Ontario K2H 8S2.	311
2. IONOSPHERIC WAVE MEASUREMENTS WITH SATELLITE-BORNE CROSS-POWER SPECTRUM ANALYZERS, K.J. Harker and F.W. Crawford, Institute for Plasma Research, Stanford University, Stanford, CA. 94305.	312
3. RADIATION EFFICIENCY AND PATTERN OF A VLF ELECTRIC DIPOLE ANTENNA IN THE MAGNETOSPHERE, U.S. Inan and T.F. Bell, RadioScience Laboratory, Stanford University, Stanford, CA. 94305.	313
4. A NUMERICAL STUDY OF SATELLITE RECEPTION OF VLF SIGNALS USING WAVEGUIDE CONCEPTS, R.A. Pappert, W.F. Moler and J.A. Ferguson, EM Propagation Division, Naval Ocean Systems Center, San Diego, CA. 92152.	314
5. THE METROLOGY OF LINEAR RANDOM WAVE FIELDS IN SPACE PLASMA, (Invited), L.R.O. Storey, Centre National de la Recherche Scientifique, Centre de Recherche en Physique de l'Environnement, 45045 Orléans, France.	315
6. PRELIMINARY RESULTS FROM CONTROLLED VLF EXPERIMENTS IN THE MAGNETOSPHERE USING THE NEW TRANSMITTER AT SIPLE STATION, ANTARCTICA, R.A. Helliwell, J.P. Katsufraakis, D.L. Carpenter, U.S. Inan, T.F. Bell and T.R. Miller, RadioScience Laboratory, Stanford University, Stanford, CA. 94305.	316
7. WHISTLER-MODE SIDEBAND GENERATION IN THE MAGNETOSPHERE, C.G. Park, RadioScience Laboratory, Stanford University, Stanford, CA. 94305.	317
8. VLF ELECTROMAGNETIC WAVE DISTRIBUTION FUNCTIONS IN THE MAGNETOSPHERE, F. Lefevre, RadioScience Laboratory, Stanford University, Stanford, CA. 94305.	318
9. OBSERVATION OF POLAR VLF EMISSION OBSERVED BY SEMI-POLAR ORBITAL SATELLITE "KYOKKO", Takeo Yoshino, Takashi Shibata and Kazuyuki Nakagawa, University of Electro-Communications, Chofu-shi, Tokyo 182, Japan.	319

WEDNESDAY AFTERNOON

June 4, 1:30 - 5:00

PLASMA RELATED THEORETICAL STUDIES

DKN 2D

Session H.2

Chairman: R. Gagné
Université Laval
Québec, Québec

Page

1. BOUNDARY CONDITIONS AND ANTENNA MODELS IN A WARM ISOTROPIC PLASMA, 321
N. Singh, Physics Department, Utah State University, Logan, Utah
84321.
2. ELECTRON TEMPERATURE DERIVED FROM INCOHERENT SCATTER RADAR OBSER- 322
VATIONS OF THE PLASMA LINE FREQUENCY, Tor Hagfors, Department of
Electrical Engineering, Norwegian Institute of Technology, N-7034
Trondheim-NTH, Norway, and M. Lehtinen, EISCAT Scientific Asso-
ciation, Geophysical Observatory, SF-99600 Sodankyla, Finland.
3. PROPAGATION IN A GYROMAGNETOELECTRIC MEDIUM, P.R. McIsaac. School 323
of Electrical Engineering, P. Hall, Cornell University
Itaca, New York 14853.
4. COVARIANT FORMULATION OF WAVE-PARTICLE INTERACTION FOR RELATIVISTIC 324
PLASMAS, A.K. Sinha, COMSAT, Communications Satellite Corporation,
950 L'Enfant Plaza, SW, Washington, D.C. 20024.
5. HEATING OF A PLASMA BY A DOUBLE LAYER, N. Singh, Physics Department, 325
Utah State University, Logan, Utah 84322, U.S.A., and H. Thiemann,
IPW, Freiburg, West Germany.

MONDAY MORNING

June 2, 8:30 - 12:00

VERY LONG BASELINE INTERFEROMETRY

DKN 2D

Combined Session J-1/AP-S

Chairman: N.W. Broten
Herzberg Institute of Astrophysics
National Research Council
Ottawa, Ontario

	<u>Page</u>
1. CANADIAN LONG BASELINE INTERFEROMETER, D.N. Fort, National Research Council, Ottawa, Ontario K1A 0R6.	327
2. THE PROPOSED CANADIAN VLB ARRAY, T.H. Legg, National Research Council, Ottawa, Ontario K1A 0R6.	328
3. VLBI ARRAY STUDIES, Mashall H. Cohen, California Institute of Technology, Pasadena, CA 91125, U.S.A., and K.J. Kellerman, National Radio Astronomy Observatory, Green Bank, West Virginia, U.S.A.	329
4. THE MARK-III VLBI SYSTEM - A WIDEBAND DATA RECORDING AND PROCESSING SYSTEM FOR VERY-LONG-BASELINE INTERFEROMETRY, A.R. Whitney, Haystack Observatory, Westford, Mass. 01886, U.S.A.	330
5. THE MARK-III DATA ANALYSIS SYSTEM. A COMPLETE SYSTEM FOR THE RECOVERY OF GEODETIC AND ASTROMETRIC INFORMATION FROM VLBI OBSERVATIONS, J.M. Ryan for the East Coast VLBI Group Goddard Space Flight Center, Greenbelt, MD 20771, U.S.A.	331
6. PHASE SCINTILLATION MEASUREMENT SYSTEM USING REAL TIME VLBI, N. Kawano, F. Takahashi, T. Yoshino, and N. Kawajiri, Kashima Branch, Radio Research Laboratories, Kashimamachi Ibaraki 314, Japan.	326
7. RADIOMETRIC SYSTEM FOR MEASUREMENT OF INTEGRATED WATER VAPOR AND LIQUID ON EARTH-SPACE PATHS, D.C. Hogg and F.O. Guiraud, Environmental Radiometry, Wave Propagation Laboratory, NOAA/Environmental Research Laboratories, Boulder, Co. 80303, U.S.A.	332
8. TWO YEARS ON BASELINE AND EARTH ROTATION PARAMETERS OBTAINED FROM ANALYSIS OF 35-km INTERFEROMETER OBSERVATIONS, D. MacCartney, G. Kaplan, J. Josties, W.K. Klepczynski, M. Lamsakis, T. Angersofer, U.S. Naval Observatory, Washington, D.C. and K. Johnston, J. Spencer, U.S. Naval Research Laboratory, Washington, D.C.	333

MONDAY AFTERNOON
June 2, 1:30 - 5:00

RADAR ASTRONOMY

DKN 2D

Session J.2

Chairman: T.W. Thompson
Planetary Science Institute
Pasadena, CA.

	<u>Page</u>
1. PIONEER VENUS RADAR RESULTS: ALTIMETRY AND IMAGING, P.G. Ford and G.H. Pettengill, Department of Earth and Planetary Sciences, M.I.T., Cambridge, MA. 02139, and H. Masursky, Branch of Astrogeologic Studies, U.S. Geological Survey, Flagstaff, Arizona 86001.	335
2. THREE-STATION RADAR IMAGES OF VENUS: RESOLUTION LIMITS AND A PROPOSED 1-km RESOLUTION MAPPING SYSTEM, R.F. Jurgens, G. Morris and R.M. Goldstein, Jet Propulsion Laboratory, California Institute of Technology, 4800 Oak Grove Drive, Pasadena, CA. 91103.	336
3. RADAR MAPPING OF MARS AT JPL: PLANS AND PROGRESS, G.S. Downs, Jet Propulsion Laboratory, California Institute of Technology, 4800 Oak Grove Drive, Pasadena, CA. 91103.	337
4. BISTATIC RADAR STUDIES OF PLANETARY SURFACES, R.A. Simpson and G.L. Tyler, Center for Radar Astronomy, Stanford University, Durand Building, Stanford, CA. 94305.	338
5. OUTER-SOLAR-SYSTEM RADAR ASTRONOMY: 1979 RESULTS, S.J. Ostro, National Astronomy and Ionosphere Center, Cornell University, Ithaca, N.Y. 14853.	339
6. VOYAGER I RADIO OCCULTATION EXPERIMENT OF SATURN'S RINGS, E.A. Marouf, G.L. Tyler and V.R. Eshleman, Center for Radar Astronomy, Stanford University, Stanford, CA. 94305.	340
7. CORONAL OCCULTATIONS OF SPACECRAFT RADIO SIGNALS, D. Routledge, Electrical Engineering Department, University of Alberta, Edmonton, Alberta T6C 2E1, and H.M. Bradford, Canadian Coast Guard College, Sydney, Nova Scotia.	341

TUESDAY AFTERNOON
June 3, 1:30 - 5:00

SPECTROMETRY AND TECHNICAL DEVELOPMENT

DKN 2D

Session J.3

Chairman: A.T. Moffet
California Institute of Technology
Pasadena, CA.

	<u>Page</u>
1. SPECTROMETRY WITH THE VLA, L.F. D'Addario, P.J. Napier and A. Rots, National Radio Astronomy Observatory, Edgemont Road, Charlottesville, Virginia 22901.	343
2. JPL 2 ¹⁶ CHANNEL 20 MHZ BANDWIDTH DIGITAL SPECTRUM ANALYZER, George A. Morris, Jr. and Helmut C. Wilck, Jet Propulsion Laboratory, California Institute of Technology, 4800 Oak Grove Drive, Pasadena, CA. 91103.	344
3. A WIDEBAND DIGITAL AUTOCORRELATOR FOR SPECTRAL ANALYSIS, P.A. Ekstrom, Staff Scientist, Battelle-Northwest Laboratories, P.O.Box 999, Richland, Washington 99352.	345
4. THE DESIGN OF ACOUSTO-OPTICAL SPECTROMETERS FOR RADIO ASTRONOMY, C.R. Masson, George W. Downs Laboratory of Physics, California Institute of Technology, Pasadena, CA. 91125.	346
5. A LOW NOISE S-BAND RADIOMETER, K.F. Tapping, J.M. Bastien, E.J. Stevens and C.S. Philipson, National Research Council, Ottawa, Ontario K1A 0R6.	347
6. THE HAYSTACK OBSERVATORY COMPUTER SYSTEM: A MODULAR APPROACH TO TELESCOPE CONTROL, B.G. Leslie, Haystack Observatory, Westford, Mass. 01886.	348

WEDNESDAY MORNING

June 4, 8:30 - 10:00

RADIO STARS

DKN 2D

Session J.4

Chairman: J.L. Yen
University of Toronto
Toronto, Ontario

	<u>Page</u>
1. NON-THERMAL VARIABLE RADIO EMISSION FROM GALACTIC STARS, (Invited), P.A. Feldman, Herzberg Institute of Astrophysics, National Research Council of Canada, 100 Sussex Drive, Ottawa, Ontario K1A 0R6.	350
2. THERMALLY EMITTING RADIO STARS, (Invited), C.R. Purton, CRESS, York University, Toronto, Ontario.	351

WEDNESDAY AFTERNOON

June 4, 1:30 - 5:00

RADIO ASTRONOMY ANTENNAS

DKN 2E

Session J.6

Chairman: T.H. Legg
Herzberg Institute of Astrophysics
National Research Council
Ottawa, Ontario

	<u>Page</u>
1. DEVELOPMENTS IN HIGH PRECISION LARGE SPACE TELESCOPE DESIGN, T.B.H. Kuiper, P.N. Swanson, P.D. Batelaan, Jet Propulsion Labo- ratory, California Institute of Technology, 4800 Oak Grove Drive, Pasadena, California 91103, U.S.A., and M.K. Kiya, J.P. Murphy and M.W. Werner, NASA Ames Research Center.	353
2. ELECTROSTATICALLY-CONTROLLED ANTENNAS, D.H. Staelin and J.H. Lang, Massachusetts Institute of Technology, Cambridge, Massachusetts 02139.	354
3. A 30 METER HOOP/COLUMN EARTH ORBITING VERY LONG BASELINE INTER- FEROMETER, L.D. Sikes, Harris Government Electronic Systems Division, Melbourne, Florida 32901.	355
4. AN INTERFEROMETER FOR MILLIMETER WAVELENGTHS, W.J. Welch, D.D. Thornton, W. Hoffman, M.C.H. Wright, D.R.W. Williams, R.L. Plambeck, J.H. Bieging, Radio Astronomy Laboratory, University of California, Berkeley, California 94720.	356
5. A SIMPLE AND ACCURATE ANTENNA THEODOLITE Chuang-Jy Wu and S. Geryl Herzberg Institute of Astrophysics, National Research of Canada, Ottawa, Ontario K1A 0R6.	357
6. OBSERVING RADIO STARS WITH THE ARECIBO INTERFEROMETER, K.C. Turner, Arecibo Observatory, P.O. Box 995, Arecibo, Puerto Rico 00612.	358
7. AN IMPROVED RADIO SOURCE CATALOG BASED UPON 35 km INTERFEROMETER OBSERVATIONS, G. Kaplan, J. Josties, W.K. Klepczynski, M. Lamsakis, T. Angersofer, U.S. Naval Observatory, Washington, D.C., and K. Johnston, J. Spencer, U.S. Naval Research Laboratory, Washington, D.C.	359

TUESDAY MORNING

June 3, 9:00 - 12:00

RADIO SCIENCE IN CANADA
DEVELOPPEMENTS RADIO - SCIENTIFIQUES AU CANADA

Théâtre de la Cité Universitaire

Session Plénière / URSI/AP-S Plenary Session

A la mémoire de / Dedicated to the Memory of
J.H. Chapman

Président / Chairman: J.R. Wait
U.S. Department of Commerce
NOAA, ERL
Boulder, Co.

Introduction / Opening remarks: J.A. Cummins
Président, Comité directeur
Steering Committee chairman
Université Laval
Québec, P.Q.

Mot de bienvenue / Welcome: J.-G. Paquet
Recteur
Université Laval

CANADIAN SATELLITES FOR
IONOSPHERIC STUDIES AND DOMESTIC
COMMUNICATIONS

C.A. Franklin
Department of Communications, Ottawa, Canada

SUMMARY

The Canadian scientific satellite program, which is now over twenty years old, began with the development of the topside sounder, Alouette-I, early in 1959 at the Defence Research Telecommunications Establishment, Ottawa. This satellite, which was the first to be designed and built outside the United States and the Soviet Union, was launched from the NASA Western Test Range in September, 1962. It was followed by the launching of three more scientific satellites of increasing complexity; Alouette-II in 1965, ISIS-I in 1969 and ISIS-II in 1971. The Alouette/ISIS program has been an immense scientific and technological success; Alouette-I and II each operated for approximately ten years, ISIS-I and II are still functioning well and over 1,158 papers and reports have been published to date. However, after eighteen years of data collection and analysis it is likely that changing priorities will result in operations terminating during 1980. With no further scientific satellites planned, Canadian activities in ionospheric space research are expected to become increasingly directed towards participation in the space programs of other countries. Planned experiments for the space shuttle include a Wave Injection Facility - based on Alouette/ISIS technology, and a Wide Angle, Michelson Interferometer for auroral studies.

In 1967, government activities in space were redirected from scientific to communications satellites. This led to the establishment of Telesat in 1969, and with the launching of the first ANIK-A 4/6 GHz satellite in November, 1972, Canada became the first country to establish a domestic geostationary communications satellite system.

Recognizing, at the outset, the advantages of operating in a band with no flux density limits, attention was turned to the use of the 12/14 GHz band for satellite communications. This led in 1970, to an agreement between Canada and NASA to develop a high-powered communications technology satellite (HERMES) operating in the 12/14 GHz band. HERMES was launched in January 1976 and subsequently demonstrated a wide variety of new communications services, including direct-to-home television broadcasting. Further trials of direct broadcasting are now underway, using 12/14 GHz transponders on the ANIK-B satellite, which may lead to commercial service on ANIK-C in 1982. The paper concludes with an outline of the next generation of broadcast satellites and a description of a multipurpose UHF satellite which is being planned to provide mobile communications services in Canada.

IONOSPHERIC PROPAGATION

R.E. Barrington
Communications Research Centre, Department of Communications
Ottawa, Canada

The Alouette satellite made possible the study of radio wave propagation in unexplored regions of the ionosphere in addition to the observations of new types of waves that could not be detected by ground based facilities. Solutions to several outstanding problems in ionospheric propagation were found as well as a host of new questions. A striking feature of the space observation was the response of the ionosphere when it is excited at a characteristic frequency or resonance. The responses at several of the characteristic frequencies have been explained in terms of the propagation of electrostatic waves while the responses at other such frequencies are still unexplained. Although the Alouette and ISIS satellites were not able to excite the ionosphere at VLF frequencies they were capable of observing naturally occurring noise, and whistlers in this frequency band. Such observations resulted in a much better understanding of the effects of positive ions on ionospheric propagation particularly near resonant frequencies.

A number of propagation experiments have been carried out to determine the nature of ionospheric inhomogeneities, with particular emphasis on the dynamic, high latitude ionosphere. Satellite beacons radiating at several harmonically related frequencies have been a prime tool for such studies. Canadians have also done considerable pioneering work on the characteristics of waves partially reflected from irregularities embedded in the lowest levels of the ionosphere. A large array of HF antennas and receivers coupled to an extensive processing facility has been used to investigate the characteristics of signals reflected obliquely from the ionosphere. This facility makes possible the separation of modes by means of time delay or doppler frequency, the determination of angle of arrival, as well as extensive analysis of the wavefronts of such signals.

New initiatives in the study of ionospheric propagation are based on the wave injection facility, planned for flights in the NASA Spacelab. This facility will permit much more extensive investigations of propagation in the vicinity of resonant frequencies. It will also open new and exciting opportunities to study ionospheric propagation in the non-linear region, where the wave is capable of significant perturbation of the medium. Since the facility will be part of a payload capable of generating ion and electron beams, studies of wave particle interactions and their importance to ionospheric dynamics will be possible.

ADVANCES IN VLBI

J.L. Yen
Department of Electrical Engineering
University of Toronto
Toronto, Ontario M5S 1A4

The very long baseline interferometer is a well established instrument in astronomy for the study of cores of galaxies and quasars which are the seats of enormous energy, and for the study of molecular masers in regions where stars are born. In addition, the capability for precise positional determination has led to the use of VLBI in precision geophysical measurements. Advances in high density magnetic tape recording, in high precision maser oscillators, and the use of a communication satellites as a data link or a phase link to synchronize distant oscillators have led to instruments of greater sensitivity and precision. The development of methods of image reconstruction using undersampled data has revealed intricate structures of compact sources. However, for more extensive studies dedicated instruments are required. A proposed Canadian Very Long Baseline Array will be described.

Plénière/Plenary 4

EM METHODS OF ORE PROSPECTING: - A STATUS REPORT

G. F. West, Geophysics Lab, Department of Physics,
University of Toronto, Toronto.

Inductive electromagnetic sensing systems operating in the audio frequency band are widely used in exploration for base metal ores. Such ores frequently occur as a connected network of semi-conducting sulphide minerals (bulk conductivity $10\text{-}10^2 \text{ S m}^{-1}$) situated in a poorly conductive host rock ($10^{-2}\text{-}10^{-5} \text{ S m}^{-1}$) underneath a layer of moderately conductive weathered rock or overburden (0-100m of $10^0\text{-}10^{-2} \text{ S m}^{-1}$).

The geophysicist wishes to: a) maximize the instrumental sensitivity so as to find small deep conductors; b) accommodate the wide range of target and host media conductivities that arise in nature; c) obtain data with a high geometrical information content from which to deduce the size, attitude and shape the conductors; d) have the maximum possible spatial resolution so nearby conductors may be separated; e) obtain information from which the conductivity of the detected bodies can be estimated. All this should be provided by highly portable, rugged, simple and cheap apparatus.

Naturally, the geophysicist's dream cannot be achieved. The design of a practical EM system involves making trade-offs between various desirable characteristics while pushing the limits of current commercial electronic technology. Consequently, a large variety of different systems exist to fulfill different exploration needs. New airborne and ground EM systems are being developed which have improved performance without incurring too great a penalty in cost and complexity. The main development trends are the following: 1) use of a wide frequency spectrum to handle a broad range of target and host conductivities, and enable discrimination between moderate and highly conductive bodies; 2) measurement of the ground's response in the time domain rather than frequency domain; 3) increased instrumental sensitivity by better filtering methods and higher moment transmitters; 4) multi-sensor systems to improve geometrical interpretation. Examples of the foregoing will be presented.

Apparatus is not the only area where improvements are being achieved or are on the horizon. Data interpretation is being improved by better modelling of hypothetical geological situations, (mainly by numerical modelling), by automated data handling and pattern recognition, and by direct inversion techniques for determining the conductivity structure of the host bedrock and overburden. Navigation is another area where better electronic systems could contribute greatly to improved airborne prospecting systems. At present, doppler velocimeters and radar altimeters are the only common methods of supplementing manual flight path control and recovery by photography. Systems usable by a low flying, rapidly manoeuvring aircraft are what is required.

MONDAY MORNING

June 2, 08:30 - 12:00

BIO ELECTROMAGNETICS

DKN 2A

Session A

Chairman: D. Morris
Division of Physics
National Research Council, Ottawa

DEVELOPMENTAL ANOMALIES INDUCED BY PULSED MICROWAVE RADIATION

G. d'Ambrosio, F. A. Di Meglio, G. Ferrara

Istituto Elettrotecnico, University of Naples, Italy

A. Tranfaglia

Istituto di Entomologia Agraria, University of Naples, Italy

Many experimental data were collected, especially in recent years, about biological effects of electromagnetic waves, but the attention of researchers was devoted mainly to unmodulated radiation: this paper deals with a number of experiments at entomological level, and pulse modulated microwaves were used. Developmental abnormalities (teratogenic effects) induced by exposure to electromagnetic fields of pupae of the yellow mealworm (*Tenebrio molitor* L., Coleoptera: Tenebrionidae) have been extensively studied since 1967 so that the behaviour of such effects when microwave CW exposure parameters are varied, is rather well known. Working at a fixed energy dosage and increasing power, were observed:

- a) a low power, sub-threshold and non-thermal weak effects region,
- b) a medium power, constant (still non thermal) effects region,
- c) a high power, strong (thermal) effects region.

Our new pulsed radiation experiments revealed a different picture: the onset of teratogenic phenomena occurred at mean power levels very higher than in previous CW treatments and, when the threshold was reached, a rapid transition to strong (thermal) effects was observed. In other words, at low and medium power levels, pulsed exposures seem to be less teratologically effective, so that one can suppose that, between pulses, some rapid recovery mechanism occurs. But when thermal power levels are reached, suddenly strong destructive effects take place. These results are important essentially for two kinds of reasons. From one hand, given the wide use of pulsed microwaves (radar) for civil and military purposes, any knowledge about biological actions of such fields may be useful for setting safety criteria and hazard protection regulations. From the other hand, the differential behaviour of biological systems, under CW and pulsed radiation, and the hypothesis of a rapid recovery aptitude may be an useful hint in delineating an interaction model, both at a biophysical and at a systemic level, for a better understanding of observed phenomena.

IRRADIATION OF PROLATE SPHEROIDAL MODELS OF HUMANS AND ANIMALS
IN THE NEAR FIELD OF A SMALL LOOP ANTENNA

A. Lakhtakia, M. F. Iskander, C. H. Durney, and H. Massoudi
Department of Electrical Engineering
University of Utah
Salt Lake City, Utah 84112

With the growing interest in calculating the near-field absorption characteristics of biological models, it became apparent that general conclusions cannot be obtained from studying the exposure to realistic sources of complicated near fields. This is because the near fields are strongly dependent on the specific parameters of their sources, and hence it is very difficult to categorize them or classify their absorption characteristics. What is possible, however, is to study the absorption due to several elementary sources of sufficiently different, but exactly known, near fields, and to use them as building blocks in studying the hazardous effects of realistic exposure conditions. In an attempt to follow this procedure, we describe in this paper the absorption characteristics of the prolate spheroidal models of humans and animals exposed to the near field of a current loop placed coaxially along the z-axis. The electric field of the current loop is zero along its axis, and hence is significantly different from that of a plane wave.

The problem is formulated in terms of an integral equation using the transverse dyadic Green's function. The fields radiated by a current loop are expanded in terms of the vector spherical harmonics and the extended boundary condition method (EBCM) is employed to solve the problem. A SAR distribution in the spheroid model will be presented graphically as a function of the frequency as well as the distance between the spheroid and the loop. Special emphasis will be placed on the difference between the absorption characteristics of the spheroid model when exposed to the plane waves, and the near fields of electric dipoles and current loops. Results for heating patterns in the spheroid models, when surrounded by the current loop, will also be presented and the validity of the depth-of-penetration concept in the near-field heating process will be discussed.

RAYONNEMENT DE GUIDES RECTANGULAIRES EN PRESENCE DE MILIEUX STRATIFIES - APPLICATION AUX SONDES BIOMEDICALES.

J. AUDET, J.Ch. BOLOMEY, Ch. PICHOT*
M. ROBILLARD, M. CHIVE, Y. LEROY**

*Laboratoire des Signaux et Systèmes
Groupe d'Electromagnétisme - C.N.R.S. - E.S.E.
Plateau du Moulon - 91190 GIF-sur-YVETTE - France

**Centre Hyperfréquences et Semi-conducteurs
L.A. au C.N.R.S. n° 287, Université de Lille I
B.P. 36 - 59650 VILLENEUVE D'ASCQ - France

Ces dernières années de récents développements dans le domaine de la radiométrie médicale (D.D. N'Guyen, M. Chive, Y. Leroy, J.Ch. Bolomey, Ch. Pichot et J. Audet, IMPI - Monaco - 11-15 Juin 1979; A. Mamouni, D.D. N'Guyen, Y. Leroy, E. Constant, RGE, 9, 697-702, 1979) nous ont conduit à étudier le rayonnement de guides rectangulaires en présence de milieux biologiques (J. Audet, J.Ch. Bolomey, Ch. Pichot, Bioelectromagnetics Symposium, URSI, Seattle 501, June 1979). Ces guides modélisent les sondes-applicateurs destinés à être mis en contact avec la peau. Les milieux étudiés peuvent généralement être représentés par un empilement de lames homogènes dissipatives (A. Guy, IEEE MTT, 19, 214-223, 1971) telles que la peau, tissu adipeux et tissu musculaire. La connaissance du coefficient de réflexion du mode fondamental excité dans le guide et celle du champ proche est fondamentale pour la conception de ces sondes.

Le problème a été abordé numériquement de deux manières : dans la première, il s'agit de l'étude de la discontinuité entre deux guides rectangulaires dont l'un est largement surdimensionné pour simuler l'espace libre. Les milieux étant dissipatifs, l'influence des parois sera rendu négligeable en prenant une discontinuité suffisamment grande. Une seconde méthode a consisté à considérer le rayonnement d'un guide à lames parallèles. Une vérification entre les deux méthodes est alors possible en prenant la discontinuité sur une seule dimension.

L'étude de la discontinuité entre deux guides rectangulaires en présence de milieux stratifiés a été séparée en deux problèmes indépendants : d'abord celui d'une discontinuité entre guides dans le vide et ensuite celui d'un empilement de lames dans un guide, en associant à chaque mode (m, n) une onde plane d'incidence θ_c telle que :

$$\sin \theta_c = \frac{\sqrt{\left(\frac{m\pi}{a}\right)^2 + \left(\frac{n\pi}{b}\right)^2}}{\omega \epsilon_0 \mu_0} \quad \left(\begin{array}{l} a = \text{largeur du guide} \\ b = \text{hauteur du guide} \end{array} \right)$$

Le problème a ainsi été ramené dans le plan de la discontinuité par la méthode bien connue de la matrice caractéristique (M. Born et E. Wolf, Principles of Optics, Pergamon Press, 58-59, 1964). Une comparaison faite avec le calcul du coefficient de réflexion du mode fondamental par la loi de Fresnel a permis de dégager certaines zones de validité de ce dernier ainsi que dans le cas du guide à lames parallèles. Ces méthodes ont été exploitées dans un certain nombre de cas d'intérêt pratique.

EDGE-TRACKING OF CARDIAC STRUCTURES
A METHOD FOR TRACKING
OF THE
EDGES OF CARDIAC STRUCTURES

J. Kuhfeld, L. Roemer, and G. Malindzak*
Electrical Engineering Department
The University of Akron
Akron, Ohio 44325

*Northeastern Ohio Universities
College of Medicine
Rootstown, Ohio 44272

Edge-tracking moving cardiac structures is achieved by

- (1) generating a pseudo-random digital noise pattern to drive a broadband ultrasonic transducer,
- (2) correlating the return echo with the original noise sequence, and
- (3) adjusting the signal processing circuits to keep the signal of interest at a uniform illumination level. In this context, uniform illumination means the processing circuits' gain will be adjusted so that an equal number of 0's and 1's of the detected digital signal occur in the region where the cardiac structure is believed to be present.

This method of processing was chosen to reduce, (a) the peak ultrasonic power for patient safety in future clinical applications; the cardiac structures of interest change slowly with respect to the signal duration over which the correlation is performed, and (b) the effects of irregular endocardial surfaces; endocardial tissue rises out of the nominal interface surface creating echoes appearing and disappearing as the surface texture fluctuates. The angle of this tissue (with respect to the signal beam) will change, i.e., its aspect ratio will change, resulting in a variable reflection cross-section causing large variations in reflected energy.

Application of these methods allows identification of a single point as the cardiac structure edge intercepted by the beam. Tracking is not easily lost due to minor variations in cardiac surface texture.

FREQUENCY DOMAIN PROFILE RECONSTRUCTION
FOR TISSUE CHARACTERIZATION

C.Q. Lee and L.F. Sio
Communications Laboratory
Department of Information Engineering
University of Illinois at Chicago Circle
Box 4348, Chicago, IL 60680

Recently a time domain method of profile reconstruction which permits simultaneous determination of the attenuation and the impedance profiles for tissue characterization by ultrasound was discussed (Lee, C.Q., Ninth International Symposium on Acoustical Imaging, Houston, Texas, December 3-6, 1979). However, this method is valid only for narrow frequency band signals in which the tissue region may be modeled by sections of ordinary lossy transmission lines.

In this paper we present a more general approach by using a frequency domain analysis. We consider a one dimensional problem in which the constitutive parameters of a tissue medium vary only along the path of the interrogating ultrasonic pulse. Furthermore, we assume that the acoustic properties of the medium can be approximated by a finite number of piecewise uniform layers which are modeled by sections of generalized transmission lines having series impedance and shunt admittance $Z_k(\omega)$ and $Y_k(\omega)$, respectively, for each section. The specific details of $Z_k(\omega)$ and $Y_k(\omega)$ depend on the parameters to be considered.

By solving the coupled equations for each section by means of the Lagrangian approach, the constitutive parameters of each layer may be expressed in terms of the input reflection coefficient at the sending end. Thus, given the steady state reflected waves at the source terminal, which may be obtained by the Fourier transform of the time signal in a pulse-echo measurement, the profile reconstruction can be achieved by successive calculations of parameters in each section.

Using the method presented, experimental and computer simulated results for some known cases are presented, taking into account the absorption of sound due to medium viscosity.

WEDNESDAY MORNING

June 4, 10:30 - 12:00

MEASUREMENTS OF LARGE ANTENNAS

DKN 2D

Combined Session A/J.5

Chairman: W.J. English
Intelsat
Washington, D.C.

MEASUREMENT METHOD OF EARTH STATION
ANTENNA POLARIZATION CHARACTERISTICS

T.Satoh and F.Makita
Kokusai Denshin Denwa Co., Ltd.
Tokyo, Japan

An accurate method was newly developed to measure the axial ratio of less than 0.2 dB over the 500 MHz bandwidth at 6 GHz and 4 GHz bands, respectively, of the Yamaguchi TTC&M/IOT antenna of a 32-m diameter. Different from the conventional measurement method (D.DiFonzo, W.J. English and W.S. Trachtman, 1976 AP-S Symp.) which replaces the feed assembly of the measured antenna with a polarization matching network and rotates it to obtain null point, the developed method features the phase-amplitude detection of the co- and cross-polarization signals through the fixed feed assembly. The measurement will be made by use of a satellite of good axial ratio and a small polarization reference antenna.

Figure 1 illustrates the transmit axial ratio measurement configuration. A carrier signal f_1 and the bi-phase modulated signal $f_1 + \Delta f$ are transmitted from the earth station in two orthogonal circular polarizations. The cross-polarization component caused by the up-link depolarization appears in the looped-back co-polarization signal received. The cross-polarization signal can be separated from the co-polarization signal by the phase-amplitude detection, since the signals of f_1 and $f_1 + \Delta f$ are correlated, and the overall up-link depolarization is obtained. The depolarization of the antenna concerned can be derived from the measured overall link depolarization by subtracting the satellite depolarization vector through the measurement by use of the polarization reference antenna of which feed assembly is rotated by 90° . By this method, a satisfactory measurement of 32-m antenna depolarization characteristics has been made.

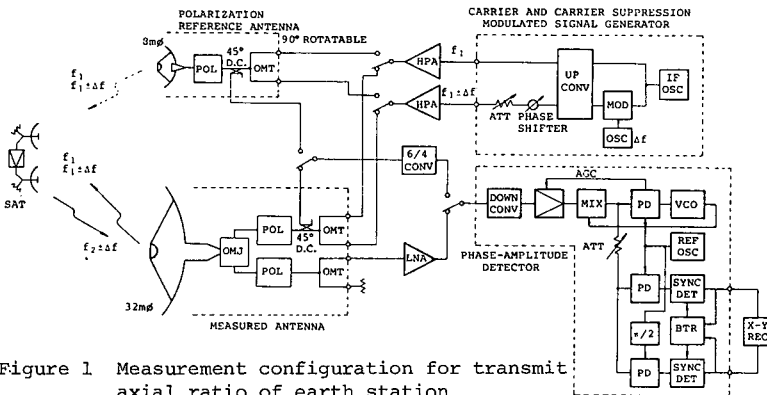


Figure 1 Measurement configuration for transmit axial ratio of earth station

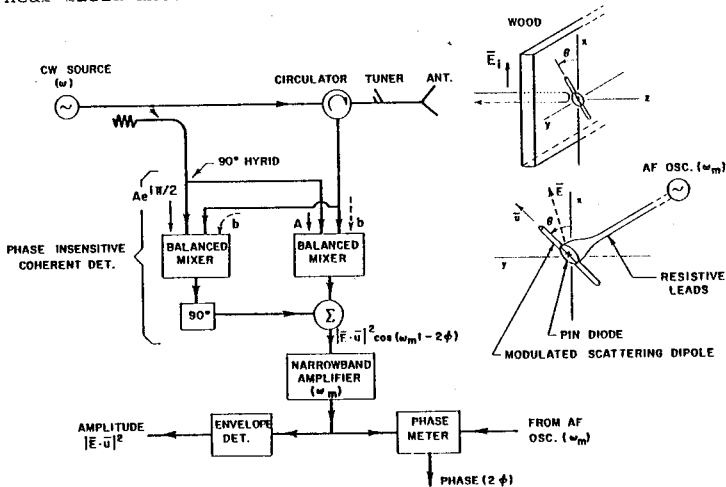
PROBING AMPLITUDE, PHASE AND POLARIZATION OF MICROWAVE
FIELD DISTRIBUTIONS IN REAL-TIME

R. J. King and Y. H. Yen

Dept. of Electrical & Computer Eng., Univ. of WI, Madison, WI 53706

The homodyne system shown is being used to map field distributions and to nondestructively test wood at 4.8 GHz. A key feature is the use of a dipole scatterer which is modulated by switching a PIN diode at an audio frequency ($f_m = 10$ kHz) via resistive leads. The modulated backscattered signal is coherently detected using an image rejection mixer. Its AF output at f_m has an amplitude proportional to square of the electric field component along the dipole $|\vec{E} \cdot \vec{u}|^2$ and a phase angle equal to the round-trip RF phase, 2ϕ [King, Microwave Homodyne Systems, Pergin Press, 1978]. Thus, the amplitude is easily measured using an envelope detector, and the RF phase is easily measured by an AF phase meter, using the modulating voltage for the reference. By positioning the dipole in the field and orienting it in the desired direction, the amplitude and phase of any component of the electric field can be mapped in real-time. Being a homodyne system, it has great sensitivity (~ -125 dBm) and is linear over a wide dynamic range.

In testing wood, of particular interest is the attenuation, polarization and phase of the field after transmission through the wood. These can be used to find the complex dielectric tensor, and/or the moisture content, grain direction and density. To accomplish this, the dipole is scanned near dimension lumber, and spun in the x-y plane at 11,000 RPM to give amplitude, phase and polarization data simultaneously and independently. Typical data for wood will be shown and discussed. These techniques should also be of value in mapping field distributions over large regions in real-time, e.g., near-field antenna measurements.



NEAR FIELD ANTENNA MEASUREMENTS AT TEXAS INSTRUMENTS

J. P. Montgomery and S. Sanzgiri
Texas Instruments Incorporated
Dallas, Texas 75266

Modern near field scanning techniques are emerging from the basic research environments of universities and government laboratories into industrial surroundings. This paper details the involvement and describes the facilities for planar, cylindrical, and spherical scanning at Texas Instruments Antenna Laboratory. The motivation and history of TI's involvement in near field scanning is discussed.

TI has a 6' x 6' automated planar scanner. The scanner allows computer control of the x and y axes as well as the z axis. This scanner has been modified by an azimuth table to accommodate cylindrical scanning. Spherical measurements are made in an automated anechoic chamber with a model mount.

Software for planar, cylindrical, and spherical scanning has been verified by measurement and comparison to the far field of a planar slotted waveguide array. The diagnostic capabilities of planar scanning have been realized by using digital image processing techniques and displays. High quality shades of gray displays are shown using enhancement techniques.

Real time computing is a reality with the recent acquisition of a TI990/12 minicomputer and an array processor. Other research efforts include multiprobe systems, high speed I/Q receivers and mechanical tolerance studies.

MEASUREMENT OF LARGE ANTENNA SURFACE DISTORTION

Dr. R. S. Neiswander, TRW, Defense and Space Systems Group
Redondo Beach, California

Large, high performance microwave antenna in space are demanded in many near-future operational scenarios including those of communication, passive radiometry and radio astronomy. Typically, after achieving orbit, the antenna unfurls to a hundred meters or so in diameter, and establishes a surface geometry accurate to a fraction of a millimeter. Rather than relying upon passive rigidity of the supporting structure, the cost effective way of obtaining and retaining the precision surface may be by active control, dynamically counteracting the flexing of a lightweight structure by a network of deformation sensors and responsive actuators. We describe here one approach to a deformation measurement sensor system.

In addition to providing a measurement accuracy of a fraction of a millimeter at the antenna surface, the sensor must have these capabilities:

- Measurements must be made relative to a central, common coordinate reference, and therefore measurement ranges may be 50 meters or larger.
- The sensor system must not interfere with either the microwave or mechanical characteristics of the active antenna.
- Sensor measurements must be made in real time with outputs compatible with microprocessing and control loop requirements.
- Measurement accuracy must be totally immune to spurious background effects such as sunlight glints, earthshine, and radio frequency interference.

The proposed sensor system is optical. It consists of a set of centrally sited (e.g., at the antenna apex-hub) staring receivers, each dedicated to observing the displacements of a group of light emitting diode targets located at critical points at the antenna surface. For discrimination, the diodes are synchronously modulated. Target positions are measured at the receivers by lateral effect planar diffuse silicon photodiodes.

Currently, under contract to NASA Langley Research Center, a bread-board sensor has been fabricated and tested. Results of laboratory evaluations indicate that for a 100 meter diameter deployable mesh antenna, measurement accuracies of 0.25 millimeters should be achievable. Receivers are to be mounted to a common ring at the antenna hub. Target sampling points are both at the periphery (e.g., at the structural hoop) and intermediate (e.g., at the ribs or at mesh tie-points). Although a response of 1 Hz is adequate for this application, response rates up to 100 Hz could be made available.

MONDAY MORNING

June 2, 08:30 - 12:00

SCATTERING I

DKN 1A

Session B.1

Chairman: R.E. Collin
Case Western Reserve University
Cleveland, Ohio.

ELECTROMAGNETIC SCATTERING BY TWO PARALLEL PROLATE SPHEROIDS

B.P. Sinha and R.H. MacPhie
 Department of Electrical Engineering
 University of Waterloo
 Waterloo, Ontario, Canada.

The multipole expansion technique applied by the authors (B.P. Sinha and R.H. MacPhie, Radio Sc., 12, 171-184, 1977) to the scattering from a single prolate spheroid of a plane electromagnetic wave with arbitrary polarization and angle of incidence using only the $\underline{M}^{(a)}$ vectors [$\underline{M}^{(a)} = \nabla\psi(h;\xi,\eta,\phi)\hat{x}\hat{a}$, $\hat{a} = (\hat{x},\hat{y},\hat{z})$] has been used in the present problem together with the translation addition theorems for spheroidal vector wave functions (B.P. Sinha and R.H. MacPhie, Quart. Appl. Math., to be published). The translational addition theorems which transform the outgoing wave from one spheroid into the incoming wave at the other spheroid assume the simplest form for $\underline{M}^{(a)}$ vectors because they translate like a scalar wave function $\psi(h;\xi;\eta;\phi)$. Thus the problem is drastically simplified as compared to the choice of Mie vector wave functions [$\underline{M}^{(r)} = \nabla\psi(h;\xi,\eta,\phi) \times \hat{r}$ and $\underline{N}^{(r)} = \frac{1}{k} \nabla \times \underline{M}^{(r)}$] which has been used by Bruning and Lo (IEEE Trans. AP, 19, 378-390, 1971) for the problem of scattering by two spheres.

The general solution for an N-body system is obtained in the form $\underline{S} = \underline{G}^{-1} \underline{I}$, when \underline{S} and \underline{I} are respectively the column vectors of coefficients of the series expansions of the scattered and incident fields and \underline{G} is the transformation matrix which depends only upon the geometries and spacing of the scatterers. Numerical computations for mono and bi-static cross-sections are given only for the two body system of parallel prolate spheroids.

The practical applications of N-body systems are quite numerous. One example is that of the grating of very thin parallel prolate spheroids with large axial ratios ($a/b \geq 100$) which represents a grating of parallel thin wires of finite length. Another typical problem is the scattering from rain drops modelled as prolate spheroids.

SCATTERING BY A FINITE RESISTIVE PLATE

Thomas B.A. Senior
 Radiation Laboratory
 The University of Michigan
 Ann Arbor, Michigan 48109

A widely used method for the solution of scattering problems is to formulate an integral equation for the current or some appropriate component of the field at the surface of the body and to solve the equation numerically. In some instances, however, even the formulation of a valid and effective integral equation is a non-trivial task, and this is so for a resistive plate of infinitesimal thickness and finite transverse dimensions illuminated by an electromagnetic wave.

A number of integral equation formulations are considered, based either on the standard boundary conditions

$$\hat{n} \wedge \underline{E}|_{-}^{+} = 0, \quad \underline{J} = \hat{n} \wedge \underline{H}|_{-}^{+} = -\frac{1}{R} \hat{n} \wedge (\hat{n} \wedge \underline{E})$$

where \hat{n} is the unit outward normal to the upper face (+ sign), R is the resistivity of the plate in ohms per square, and \underline{J} is the total induced electric current, or on the alternative conditions

$$\begin{aligned} \frac{\partial E_n}{\partial n} \Big|_{-}^{+} = 0, \quad \frac{\partial E_n}{\partial n} + ik \frac{R}{Z} E_n \Big|_{-}^{+} = 0 \\ H_n \Big|_{-}^{+} = 0, \quad \frac{\partial H_n}{\partial n} \Big|_{-}^{+} + ik \frac{Z}{R} H_n = 0 \end{aligned}$$

valid for a planar sheet, where Z is the intrinsic impedance of free space. We remark that

$$\hat{n} \cdot \nabla \wedge \underline{J} = ik \frac{Z}{R} H_n, \quad \nabla \cdot \underline{J} = -\frac{1}{R} \frac{\partial E_n}{\partial n}$$

The case $R = 0$ corresponds to perfect conductivity, but the simplified approach that Y. Rahmat-Samii and R. Mittra (IEEE Trans. AP-22, 608-610, 1974) have developed for a perfectly conducting plate has no analogue when $R \neq 0$. Various integral equations resulting from the application of the above conditions are presented, and their properties discussed.

SCATTERING FROM "INTERNALLY THICK" RESISTIVE STRIPS

K. M. Mitzner, Aircraft Group, Northrop Corp., Hawthorne, CA

In recent years, there has been considerable study of scattering, especially at or near grazing incidence, from resistive strips which are thin compared both to the free space wavelength and to the wavelength and attenuation length in the resistive medium. (See, for example, T.B.A. Senior, IEEE Trans. Antennas Propagat., AP-27, 808-813, 1979.)

In this paper we consider the more general case in which the thickness of the resistive medium may be significant compared to the wavelength or attenuation length in the medium itself and, in addition, the medium may be layered.

If the medium is sufficiently lossy, then such an internally thick strip can be characterized by three parameters. One convenient choice is the two driving point impedances Z_+ and Z_- and the transfer impedance Z_x derived by using a two-port transmission line analogy for scattering by the medium at normal incidence. Another choice is the corresponding admittance parameters Y_+ , Y_- , Y_x .

For a strip with internal thickness large compared to the relevant attenuation lengths, we have $Z_x = 0$, and $Z_+ = 1/Y_+$ and $Z_- = 1/Y_-$ then represent two uncoupled surface impedances.

For a single layer resistive medium or a symmetrical layering, we have $Z_+ = Z_-$, $Y_+ = Y_-$, so only two parameters are needed. In this case there is a useful equivalent formulation in terms of a shunt impedance

$$Z_e = (Z_+ + Z_x)/2 = 1/[2(Y_+ + Y_x)]$$

and a series impedance

$$Z_m = 2(Z_+ - Z_x) = 2/(Y_+ - Y_x)$$

which characterize the jumps in tangential \underline{H} and \underline{E} respectively across the strip.

It can then be shown that, for grazing incidence with \underline{E} parallel to the edge of an infinitely long strip, the scattering is the same as from a thin resistive strip with impedance Z_e . (This impedance is designated as R by Senior because it is always real for an internally thin strip.) For \underline{H} parallel, the scattering at grazing incidence is the same as from a thin "magnetic" strip characterized by Z_m .

COMBINED INTEGRAL EQUATION--FINITE ELEMENT SOLUTION
TO ELECTROMAGNETIC SCATTERING BY A MISSILE WITH PLUME

M.A. Morgan and K.G. Gray
Department of Electrical Engineering
Naval Postgraduate School, Monterey, CA 93940

A hybrid finite element method (FEM) and surface integral equation (SIE) technique is applied to the problem of plane-wave electromagnetic interaction with a missile having an inhomogeneous plasma exhaust plume. Previous approaches to this class of problems have relied upon SIE solution techniques for both missile and plume substructures. Approximate techniques such as impedance type boundary conditions (T.K. Wu and D.R. Wilton, URSI Meeting, Boulder, Co, Nov. 1978) and homogeneous layer modeling have been necessary to utilize the SIE method for the complex inhomogeneous plume.

The combined approach presented here incorporates the SIE method for the conducting body of the missile, while using the FEM (M.A. Morgan and K.K. Mei, IEEE AP-27, 212-214, March 1979) to compute EM interaction with an axisymmetric inhomogeneous lossy plasma model. A theoretically exact method is employed to both couple the scattering solutions from the missile and plume, as well as to ensure induced current continuity at the exhaust nozzle missile-plume interface. Results are presented comparing calculations based on this technique with those of previous SIE efforts.

RESONANCES OF THIN-WALLED PENETRABLE SCATTERERS

E. M. Kennaugh
The Ohio State University ElectroScience Laboratory
Department of Electrical Engineering
Columbus, Ohio 43212

A linear operator approach permits one to distinguish two types of resonance for lossless thin-walled scatterers. In one type of resonance, the interior field is an amplified replica of the incident field. In the second, the scattered field is a multiple of the free-space outgoing field or a characteristic mode. Generally distinct, these resonances may coincide for special cases.

The design of thin-walled scatterers which exhibit each type of resonance are discussed. Examples of resonant gains for spherical and cylindrical geometries are presented. Walls of dielectric and of wire grid type are considered and the effect of small wall losses estimated.

PROPERTIES OF PLANAR MULTILAYER DIELECTRIC STRUCTURES

Herbert Feldman and Benjamin Rulf
The MITRE Corporation, Bedford, MA, 01730

Planar multilayer dielectric structures are widely used both in electromagnetics (radomes, windows, etc.) and in optics (spatial filters, interferometers). The frequencies or angles of incidence at which transmission resonances occur, i.e., at which the reflection vanishes, are the characteristics of the structure. An electrically symmetrical structure of $2n + 1$ layers ($n = 1, 2, \dots$), has the same number of parameters as a general structure of $n + 1$ layers. We can show however, that the symmetrical structure has advantages that make it vastly superior. They emerge from the following observation: The condition for transmission resonance for a general $n + 1$ layer structure is found by equating to zero a complex quantity, $F + jG$ say, yielding two simultaneous nonlinear equations.

$$F(\omega, \theta, d_1, d_2, \dots, d_{n+1}) = 0, \quad (1a)$$

$$G(\omega, \theta, d_1, d_2, \dots, d_{n+1}) = 0. \quad (1b)$$

Here ω is the frequency, θ the angle of incidence, and d_1, d_2, \dots the electrical thicknesses of the $n + 1$ layers.

To have n equations with n unknowns, we can choose some of the unknowns arbitrarily, giving us a number of "degrees of freedom." Usually, we would pick a number of points (ω_i, θ_i) in the (ω, θ) plane, and one thickness, d_1 say (or a quantity related to d_1), and solve eqs. (1a, 1b) for the remaining unknowns d_2, d_3, \dots, d_{n+1} .

In the case of a symmetrical $2n + 1$ structure, we show in a general way that the condition for transmission resonance reduces to a single nonlinear equation of the form (1a). We can choose n arbitrary points (ω_i, θ_i) , and one electrical thickness d_1 (or a related quantity, such as the transmission phase at some angle), and solve the resulting equations

$$F(\omega_i, \theta_i, d_1, d_2, d_3, \dots, d_{n+1}) = 0 \quad (i = 1, \dots, n), \quad (2)$$

for d_2, d_3, \dots, d_{n+1} . The number of "degrees of freedom" (i.e., frequencies or angles of incidence we can choose at which (1a, 1b) holds) is at least double in the case of the symmetric structure. Moreover: once d_1, d_2, \dots have been determined, eq. (1a) is a continuous curve in the (ω, θ) plane, relating how the angle of incidence has to change with frequency to keep the transmission resonance. On the other hand, eqs. (1a), (1b) represent two curves in the (ω, θ) plane, whose intersection points (which are isolated) represent the only points at which the resonances occur, for the nonsymmetrical structure.

WAVE REFLECTION FROM AN ANISOTROPIC MEDIUM:
A COORDINATE-FREE APPROACH

by

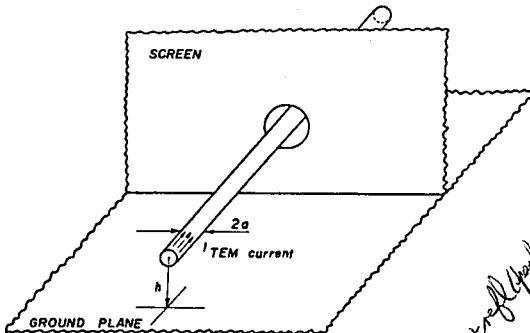
Hollis C. Chen
Department of Electrical Engineering
Ohio University
Athens, Ohio 45701 U.S.A.

Based on the eigenvectors of a wave matrix of an anisotropic medium, a coordinate-free method is presented in this paper. The purpose is to unify and systematize the analysis of wave reflection from the anisotropic medium. The incident wave may have any polarization. The new results, all in coordinate-free forms, include: (1) the dispersion equation of an anisotropic medium, (2) the laws of reflection and refraction, (3) the directions of field vectors, (4) the Booker Quartic equation, and (5) the transmission and reflection coefficient matrices.

COMPUTATION OF THE EQUIVALENT CAPACITANCE FOR A
WIRE PASSING THROUGH AN APERTURE IN A CONDUCTING SCREEN

D. Kajfez, C. M. Butler, T. Zbontar
University of Mississippi, University, MS 38677

A uniform transmission line consisting of a single wire above a ground plane extends through a small aperture in a metal screen oriented perpendicularly to the ground plane and to the wire as shown in the figure below. With a TEM wave incident along the wire, the reflected and transmitted waves on the wire are to be evaluated. Equations for the dynamic electromagnetic field problem are formulated (D. B. Seidel, C. M. Butler, USNC/URSI 1976 Annual Meeting, p. 24) and are solved by the moment method. The unknown electric surface current consists of both entire domain functions (TEM guided waves) and subdomain functions (evanescent waves). Due to the fact that the circular aperture size is only slightly larger than the wire radius, the exact kernel is used throughout the formulation. The system of equations resulting from the moment method is of the mixed type, which in this case resulted in an ill-conditioned numerical system of equations. A change of variables was performed such that all the unknowns in the numerical system of equations were rendered equal in physical units and the condition number of the system was greatly improved. The numerical results indicate, that as long as the aperture dimensions are small in comparison with the wavelength, the equivalent circuit consists of a shunt capacitance which is virtually independent of frequency.

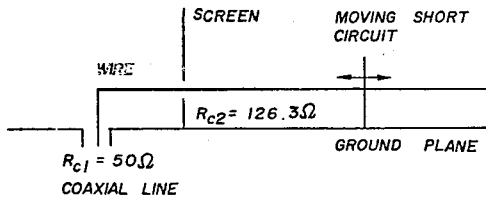


*Quasi (infinite) plane
TEM diffraction
 $i = (a) - \text{high order eff.}$*

EXPERIMENTAL DETERMINATION OF THE EQUIVALENT CAPACITANCE FOR A WIRE PASSING THROUGH AN APERTURE IN A CONDUCTING SCREEN

D. Kajfez, T. Zbontar, C. M. Butler
The University of Mississippi, University, MS 38677

A uniform TEM transmission line consists of a wire (of circular cross section) placed above a metal ground plane. A discontinuity is introduced in the form of a vertical screen which contains a hole for the passage of the wire. In order to characterize the equivalent circuit of the discontinuity it is necessary to measure the complex reflection coefficient on the wire under various loading conditions (moving short). Precision measurements of reflection coefficient are made with a network analyzer, which requires the use of a 50 ohm coaxial transmission line (see figure). The transition from the coaxial to the single wire configuration is calibrated by the fractional linear curve-fitting procedure (D. Kajfez, IEEE Trans. IM-24, pp. 4-11, 1975). This curve-fitting procedure is used also to determine the equivalent circuit of the discontinuity. Data processing by computer provides also a standard deviation of the measured results. A check of the reliability of the procedure is provided by computing the efficiency of the equivalent two-port. The measured results in the frequency range from 220 to 2000 MHz indicate that the equivalent circuit consists of a single shunt capacitance and that the additional line length and dissipation both can be neglected.



Calibration
Signature

MONDAY MORNING

June 2, 8:30 - 12:00

SPECIAL SESSION ON OPTICAL COMMUNICATIONS 1

FIBER AND GUIDED WAVE OPTICS 1

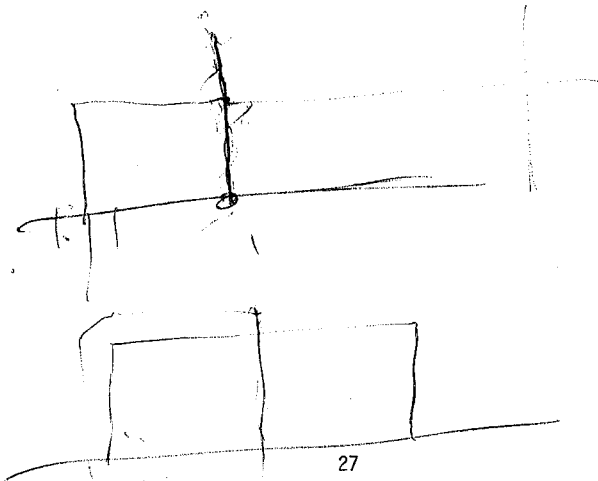
DKN 2B

Combined Session B.2 / AP-S

Chairman and Organizer: G.L. Yip
McGill University
Montréal, Québec

The following paper belongs to the IEEE AP-S Symposium and the summary is included in the IEEE AP-S Digest under Combined Session B.2/AP-S.

9. EFFECTS OF A CENTRAL DIP ON THE TIME DISPERSION CHARACTERISTICS OF GRADED-INDEX OPTICAL FIBERS, G. Cancellieri, P. Fantini, M. Mezzetti, Fondazione G. Marconi, Villa Griffone, Pontecchio Marconi, Bologna, Italy.



MULTIMODE OPTICAL FIBERS - PROFILE CONTROL AND ANALYSIS

Herman M. Presby
Bell Laboratories
Crawford Hill Laboratory
Holmdel, New Jersey 07733

The information carrying capacity of multimode optical fibers is mainly determined by the quality of the refractive index distributions of their cores. With ideal refractive index distributions these fibers can, in principle, have signal bandwidths on the order of ten GHz·km. However, extremely careful control of the index profile is required to achieve this theoretical goal. Slight departures from the optimum index distribution lead to a dramatic decrease of the fiber bandwidth. This is true not only for departures of the optimum exponent value of a pure power law profile, the value of which is determined by the dopant materials introduced into the fiber, but it happens whenever the ideal profile is distorted in any way. Sinusoidal ripples, a central dip and various "bulge" deformations can reduce the bandwidth by nearly two orders of magnitude, to several hundred MHz·km.

It is the purpose of this paper to provide a current overview of the effects on fiber bandwidth of fiber material properties and profile perturbations. Some attention will also be given to profile measurement and analysis.

NEW WAVE PHENOMENA IN OPTICAL
WAVEGUIDES AND GENERALIZED
RULES OF REFRACTIVE INDEX

by T.K. Tien

Bell Telephone Laboratories
Holmdel, N.J. 07733

A large number of wave phenomena in optical waveguides has been discovered since the advent of integrated optics. We will review "Zig-zag waves and waveguide modes, m-line spectroscopy, concept of mode-index, tapered-film couplers, two dimensional, optics and two layered construction of optical circuits". All these wave phenomena may be explained by two simple rules known as rules of refractive index. The first rule concerns light wave propagation in a multi-layer waveguide structure. It states: "In a multi-layer structure parallel to the wave propagation such as the slab waveguide, light wave tends to propagate in the region where the refractive is a largest, or, the wave velocity is a slowest". The second rule involves optics in the plane of the waveguide: "So far as the wave motion in the plane of the waveguide is considered, refraction and total reflection may be computed by Snell's low and the critical angle, provided that mode-index is used for the refractive index in the calculation". These rules were generalized from experimental observation and have never been rigorously proved. We will discuss them in depth based on a potential-well model of the waveguides.

Propagation in Graded-Index Waveguides: A Review of Techniques*

Leopold B. Felsen
Polytechnic Institute of New York
Department of Electrical Engineering
Route 110, Farmingdale, N. Y. 11735

Graded index waveguides play an important role as propagation channels for optical signals. In the multimode regime, the accurate determination of the modal group velocities is essential for prediction of signal distortion. This paper reviews various methods of analysis for slab and circular, uncladded and cladded waveguides. Emphasis is placed on the interpretation of the mathematical techniques in terms of rays, beams, and evanescent waves, which provide a physical understanding of the associated propagation mechanisms and of their limitations. Numerical results are presented to illustrate accuracy and computational complexity. Also discussed are extensions of the techniques for axially uniform graded index guides to accommodate longitudinal and inhomogeneities such as tapers and bends.

* Invited paper.

ANALYSIS OF INHOMOGENEOUS OPTICAL WAVEGUIDES
USING COLLOCATION METHOD

T.H. Nguyen and G.L. Yip
Department of Electrical Engineering
McGill University
Montreal, Quebec, Canada.

In the optimum design of the refractive index profile of multi-mode fibers, it is preferable to have an effective and simple method with a high accuracy for computing the propagation characteristics in fibers. There has been a wide variety of numerical techniques developed for this purpose. In this paper, we propose a new modified collocation method which, besides its simplicity, has the advantage of being a global approximation method.

The fiber under consideration consists of a radially inhomogeneous core imbedded in a homogeneous finite cladding region with a lower refractive index than that of the core axis. The transverse field components in the core region are expressed by a system of differential equations and are approximated by piecewise polynomial functions. The coefficients of these polynomials are then calculated from continuity conditions and collocation conditions which require the differential equation system to be satisfied exactly at certain points (i.e. collocation points) within the core. The dispersion relation for various modes can be found by matching the fields at boundaries. As a first try, we have used this method for the case of symmetric slab waveguide studied previously with the step approximation (G.L. Yip and E. Colombini, *Optical and Quantum Electronics*, 10, 353-360, 1978). Results are very encouraging and a comparison with the conventional Runge-Kutta method showed that the new technique saved about half the computing time. We are now applying this method to the problem of cylindrical fibers with various proposed refractive index profiles and are trying to study their dispersion characteristics. Detailed results will be presented at the meeting. Comparisons will also be made to results of an earlier study on inhomogeneous optical fibers, using the Runge-Kutta method (G.L. Yip and Y.H. Ahn, *Electronics Letters*, 10, No. 4, 37-38, 1974).

PULSE PERFORMANCE OF GRADED-INDEX OPTICAL WAVEGUIDES
UNDER EQUAL AND DIFFERENTIAL EXCITATION

G.A.E. Crone ¹, Ph.D and J.M. Arnold ², Ph.D

- 1) RF Technology Centre, ERA Technology Ltd., Leatherhead, Surrey, UK.
- 2) Dept. of Electrical Engineering, University of Nottingham, Nottingham, NG7 2ND, UK.

It is shown that pulse broadening in multimode graded-index optical waveguides is significantly affected by the levels of excitation of the higher order modes.

The propagation characteristics and fields of all the propagating modes are calculated using a scalar wave optics formulation by numerical solution of the scalar wave equation; the relative times of flight being assessed using the Hellmann-Feynmann theorem.

Pulse widths are calculated as functions of the profile parameter α under conditions of equal excitation, high order mode suppression and GaAs laser excitation. Under equal excitation, the results show the pulse broadening to be larger than that predicted by zero-order WKB methods where the near cut-off modes are not included in the impulse response calculation. Artificially reducing the mode volume by suppressing the high order modes reduces the pulse width and a characteristic comparable with WKB methods is obtained if enough modes are suppressed.

Finally it is shown that the differential excitation produced by a GaAs source model causes a reduction in pulse broadening, compared with the equal excitation case, due to little power being launched into the high order modes. The excitation coefficients of the modes being assessed using the modal matching techniques.

ASYMPTOTIC ANALYSIS OF INHOMOGENEOUS PLANAR AND
CYLINDRICAL DIELECTRIC WAVEGUIDES

J. M. Arnold, Dept. of Electrical Engineering,
University of Nottingham, UK.

The fundamental theoretical problem in constructing a description of propagation of optical waveguides consists of the determination of modal field distributions and propagation constants, usually formulated as a linear eigenvalue problem. When the number of modes supported by the waveguide is large, asymptotic methods are appropriate. However, in realistic models, difficulties arise at interfaces between different media (core and cladding, for instance), particularly when caustics are sufficiently close to them to interact significantly. In such cases, conventional WKB theory cannot be applied, and various types of uniform approximation must be devised. Since such cases arise in practice, there is a need for effective analytical and numerical procedures.

The method to be described involves mapping the original linear eigenvalue problem into a similar one whose solution is known. This is achieved by a transformation between variables, expressible as a non-linear differential equation whose asymptotic properties are much more tractable than those of the original linear problem. In particular, its solution varies on the slow scale of refractive index variations, and not on the rapid scale of transverse modal variations, leading also to highly efficient numerical procedures.

By these means, a fully systematic, uniform approximation scheme to all orders can be constructed, and exhibited in the form of explicit corrections to WKB theory in cases where the latter fails.

PROPAGATION CONSTANT AND GROUP DELAY OF GUIDED MODES
IN GRADED INDEX FIBERS: EVANESCENT WAVE THEORY (EWT)
COMBINED WITH NON LINEAR TRANSFORMATION TECHNIQUES

G. Jacobsen
Electromagnetics Institute
Technical University of Denmark
DK-2800 Lyngby, Denmark

Evanescent Wave Theory (S. Choudhary, L.B. Felsen J.O. S.A. (67) 1977 pp 1192-1196) provides a systematic scheme for evaluation of modal propagation constants and group delays given as asymptotic series in $1/k$ where k (the free space wave number) is the large parameter of the problem. The systematic calculation scheme has been applied for analytical determination of terms in the asymptotic series to include $O(1/k^8)$ and it has been demonstrated that very accurate numerical results are obtained for low order modes of a near parabolic profile (G. Jacobsen, J.J. Ramskov Hansen, Appl. Opt. (18)1979 pp 2837-2842) using the error estimate that is implicitly given in the asymptotic calculation method. For higher order modes of the near parabolic profile accurate results were obtained using a simple linear transform (G. Jacobsen, J.J. Ramskov Hansen, Appl. Opt. (18)1979 No. 22). For profiles far from parabolic shape neither of the methods mentioned before gave accurate results.

Using the non-linear transformation schemes developed by D.Shanks (J. of Math. and Phys. 1955 pp 2-42) it will be demonstrated how very accurate results for both propagation constants and group delays are obtained for all modes of near parabolic profiles as well as profiles that are far from parabolic shape. It should be emphasized that these transformations extract information from all terms of the asymptotic series both when the series is converging and diverging. This makes it possible to give more accurate results by calculating more terms beyond $O(1/k^8)$ analytically, and thus the systematic calculation scheme that is built into EWT turns out to be of importance.

Numerical results will be given for a profile of near parabolic shape and one that is far from parabolic shape and the results will be compared to a simple WKB technique that gives results to including $O(1/k^2)$. The application of non-linear transformation schemes of different order will be demonstrated.

Paolo GALEATI, Vittorio RIZZOLI and Carlo G. SOMEDA
Istituto di Elettronica , University of Bologna,
Villa Griffone, Pontecchio Marconi, Bologna - ITALY

Pulse compression effects in cascaded graded-index fibers have drawn substantial attention in recent years. By now, it is well understood that suitable combinations of "under-compensated" and "over-compensated" index profiles are beneficial to the fiber band width. Most of the theoretical work in this area concentrated on approaches to long-route predictions drawn from measurements on individual fibers. In these cases splicing plays an essential role.

In this paper, on the other hand, we present some results that refer to the case where two graded-index fibers are cascaded without mode mixing effects. In practice, this assumption could correspond to two fibers which are carefully jointed in the factory, or even to a fiber which is drawn from a preform that has a step discontinuity in its profile along its axis. The main purpose is to see whether in this way one can relax the tolerances on the "optimum profile", which are well known to be very tight for axially uniform α -type fibers.

In order to obtain realistic results, we consider germania-doped silica fibers with a pure silica cladding having a graded-index core with α -type profile. For this kind of fibers, extensive data concerning material dispersion are available from the literature (F.M.E. Sladen et. al., *Electronics Letters* 15, 19th July 1979). The results are extremely encouraging. For instance, it is found that for a given α of one fiber, the useful range of α values for the other one, yielding a prescribed bandwidth \times length ($B \times L$) product is two to three times as large as the corresponding acceptable range for the uniform fiber case. Furthermore, an α -type fiber having a profile parameter considerably different from the optimum for uniform fiber operation can be effectively equalized by the tandem connection with little penalty on the maximum attainable $B \times L$ product. This means that a fabrication process yielding a wide spread of profile parameters can still be useful for building broad band links, provided that fibers with different profiles be suitably allocated.

Finally it is shown that the above conclusions are not restricted to the case of a profile dispersion parameter independent of dopant concentration, but still hold even for strongly nonlinear dispersion characteristics (J.A. Arnaud and J.W. Fleming, *Electronics Letters* 12, 1st April 1977).

MONDAY AFTERNOON
June 2, 1:30 - 5:00

HIGH FREQUENCY SCATTERING

DKN 1A

Session B.3

Chairman: T.B.A. Senior
University of Michigan
Ann Arbor, MI.

A RADAR CROSS SECTION STUDY OF SIMPLE SHAPES BY UTD METHOD

J. Huang & C. L. Yu, Code 3313
Naval Weapons Center, China Lake, CA 93555

The radar backscatter characteristics of both hostile and friendly surface and airborne vehicles are an important factor in their detectability and survivability. Development of accurate analytical models of the Radar Cross Section (RCS) of these vehicles is an important part of weapon system development and evaluation. Simple shapes such as flat plates, corner reflectors, and elliptical cylinders are important building blocks in the development of these analytical models. An accurate way of predicting the RCS of these components has been developed using the Uniform Geometrical Theory of Diffraction (UTD). The inclusion of the improved UTD's diffraction coefficient, higher order diffraction terms, the effective and efficient search techniques for locating reflection points on complex curved surfaces and diffraction points on edge discontinuities offers better accuracy over previous work. The theoretical RCS calculations obtained by this approach compare very well with experimental data and are shown to be an improvement over that of Ross and others.

A HIGH FREQUENCY ANALYSIS OF THE BACKSCATTER
FROM FINNED CYLINDERS OF FINITE LENGTH

T. Jirapunth, P.H. Pathak and R. G. Kouyoumjian
The ElectroScience Laboratory, The Ohio State University
1320 Kinnear Road, Columbus, Ohio 43212

A high-frequency analysis is presented for the backscatter from a perfectly-conducting finite length circular cylinder with three identical planar fins placed 120° apart near one of its ends. This configuration is illuminated by an arbitrarily polarized electromagnetic plane wave which is obliquely incident on the cylinder. Away from the nose-on and tail aspects, an approximate solution to this problem is synthesized from the uniform GTD (UTD) solutions to two related problems; namely, the backscatter from a finite length circular cylinder without fins, and the backscatter from a two-dimensional circular cylinder with a single fin. The solution to the first problem employs the uniform edge diffraction coefficients given in (Kouyoumjian & Pathak, Proc. IEEE, pp. 1448-1461, Nov. 1974). This solution remains valid even within the caustic regions (near nose-on and tail aspects) for the finite cylinder; also, the diffraction from the two ends of the cylinder properly combine to yield a bounded and continuous field for aspects at and near broadside. The other solution for the two-dimensional circular cylinder with a fin also employs the uniform edge diffraction coefficient together with a recently developed uniform solution for the diffraction by a convex cylinder given in (Pathak, J. Radio Science, pp. 419-435, May-June 1979). The total backscattered field then consists of the UTD fields backscattered by the finite cylinder alone and a modified physical optics result for the fields backscattered from each of the visible fins. In the latter case, the fin contribution essentially consists of the UTD fin scatter result pertaining to an effective 2-D cylinder with a fin, but modified by a factor that accounts for the 3-D nature of the fin. Thus, the important field interactions between the fins and the cylinder are taken into account in contrast with the previous high frequency treatment of this problem. Calculations of the echo area based on this solution are compared with measured values.

AN EXTENSION OF THE UNIFORM GTD TO THE
DIFFRACTION BY A WEDGE ILLUMINATED
BY A DIPOLE CLOSE TO ITS EDGE

R. Tiberio and G. Pelosi
Istituto di Elettronica
University of Florence
Florence, Italy

R.G. Kouyoumjian
The Ohio State University ElectroScience Laboratory
Department of Electrical Engineering
Columbus, Ohio 43212

In calculating the field diffracted by a perfectly-conducting wedge illuminated by a dipole placed close to its edge, the near field of the dipole may be important. An approximate ray solution for this problem is interesting in itself and also may be useful when combining the moment method with the GTD. Although an asymptotic solution is not expected to be valid in the near zone, the uniform GTD (UTD) has been found to be surprisingly accurate in such cases. In this paper it is shown that the method can be extended to significantly reduce the distance between the source and the edge normally required by the UTD.

This result is achieved by including higher order terms in the asymptotic expansion of the diffracted field which are obtained via the modified Pauli-Clemmow method of the steepest descent. Although a double pole close to the saddle point may occur, the same method can be applied and uniform, closed form expressions for the scattered far field are obtained. By introducing a ray fixed coordinate system and taking into account transverse and radial components of the incident field, the diffraction coefficient for the far-zone field due to an arbitrarily directed dipole can be expressed in terms of a 2×3 matrix. The elements of this matrix are the scalar diffraction coefficients which include higher-order terms, for the TE (hard b.c.) and TM (soft b.c.) cases. This solution is compared with an approximate solution based on the UTD augmented by slope diffraction.

Calculations of the diffracted field for various locations and orientations of the dipole are shown and compared with numerical results based on an eigenfunction solution.

PREDICTION OF CAVITY AND NATURAL RESONANCE FREQUENCIES BY G.T.D.

E. M. Kennaugh
The Ohio State University ElectroScience Laboratory
Department of Electrical Engineering
Columbus, Ohio 43212

Using formulas derived by the Geometrical Theory of Diffraction for surface ray attenuation and phase shift (R. G. Kouyoumjian and P. H. Pathak, Proc. IEEE, 62, 1438-1447, 1974), all TE and TM interior (real) and exterior (complex) resonance frequencies are predicted for conducting spherical and cylindrical boundaries. Results obtained using this technique for other boundary shapes are compared with available data.

The concept of a unique kill-pulse, or K-Pulse, excitation which effectively terminates oscillations of a resonant antenna or scatterer is introduced. Determination of the K-Pulse for a thin wire and use for predicting natural resonances is discussed.

DETERMINATION OF RADIATION PATTERN OF CONICAL ANTENNAS
BY THE GEOMETRICAL THEORY OF DIFFRACTION

J.Ch. BOLOMEY, J. CASHMAN, S. EL HABIBY

Laboratoire des Signaux et Systèmes

Groupe d'Electromagnétisme

C.N.R.S. - E.S.E.

Plateau du Moulon - 91190 GIF-sur-YVETTE - France

This study has been motivated by the coupling improvement of detectors and mixers in the infrared region (Matarrese L.M. and Evenson K.M., Applied Physics Letters, vol. 17, n° 1, July 1970), but the method can be used in many other applications. For point contact devices (MIM, Schottky, Josephson, W-Ni,...), the coupling factor can be deduced from the radiation pattern of conical structure (J.Ch. Bolomey et al., Int. Conf. on Infrared and Millimeter Waves. Miami, December 10-15, 1979).

Because of the high frequencies of interest, the problem lends itself to analysis by the G.T.D.. By means of diffracted rays generated at the antenna discontinuities, it is possible to calculate the radiation pattern.

Two particular coupling structures have been considered: the bi-conical antenna surmounted by infinite cylinder, and the conical antenna alone.

The results obtained by G.T.D. are valid unless the half-angle of the tip of the cone is too small.

The GTD results have been compared with those calculated by integrating the surface currents measured by modulated scattering method in the vicinity of the near field in anechoic chamber or approximated by a travelling wave distribution. In all cases the agreement is well, demonstrating the usefulness of G.T.D. for calculating radiation patterns of conical structures. The calculation is very fast, compared to the other methods, and is compatible with extensive use in view of coupling optimisation.

HIGH FREQUENCY SCATTERING FROM AIRCRAFT MODELED
BY FLAT PLATES AND CONE FRUSTA

Earl C. Burt
Gregor A. Dike
Robert F. Wallenberg
Syracuse Research Corporation
Merrill Lane
Syracuse, New York 13210

Scattering from perfectly conducting polygonal flat plates and circular cone frusta has been analyzed in connection with the bistatic inverse scattering problem for aircraft. Both physical optics and the geometrical theory of diffraction (GTD) have been employed on these basic target shapes. The formulas obtained for the measured scattered field can be given by easily evaluated closed-form expressions which are valid for a wide range of bistatic angles and arbitrary polarizations.

The physical optics approximation applied to a polygonal flat plate gives the scattered field in terms of an integral taken over the surface of the plate. This surface integral can be reduced to the sum of easily evaluated line integrals through the use of Green's Theorem.

In the case of a (right and nonright) circular cone frustum the scattered field predicted by physical optics can be given in terms a surface integral taken over the illuminated portion of the frustum. To evaluate this integral a cylindrical type coordinate system can be set up to describe the surface parametrically, and the appropriate surface area differential introduced. The resulting double integral can be evaluated in two steps. The integral corresponding to the circumferential direction can be approximated using the method of stationary phase. The remaining integral can be evaluated exactly in the case of a cylindrical frustum. For a proper cone frustum the integral can be written in terms of the function

$$F(x) = \int_0^1 s^{1/2} e^{-jxs} ds.$$

This function can be evaluated by use of its Taylor series for small values of x . For large arguments a useful asymptotic expansion is available. $F(x)$ can therefore be computed easily and accurately for any value of x .

Using the diffraction coefficients for a finite wedge, the GTD can be used to account for diffraction effects for both the edges of flat plates and the "endcap" discontinuities of cone frusta. For the case where the transmitter and receiver polarizations are both right circular the singularities which usually occur in the diffraction coefficients are shown to cancel.

MASLOV METHOD AND ASYMPTOTIC FOURIER TRANSFORM

R. W. Ziolkowski and G. A. Deschamps
 Department of Electrical Engineering
 University of Illinois
 Urbana, Illinois 61801

It is well-known that the representation of a high frequency field by geometrical optics fails in the vicinity of a caustic. Among several solutions to this problem (boundary layer expansions, integral expressions derived from an ansatz, etc.), a systematic approach due to Maslov consists essentially of operating in the phase-space M (position-wavevector) instead of the space X (position). A flow, which characterizes the system, is defined in M by Hamilton's equations. The flow lines, or phase-space rays, are projected on X along the rays of geometrical optics. If the field is given on some surface S in X by an expression of the form $\exp[ik\phi(x)] \Sigma (ik)^{-p} A_p(x)$, it can be continued in the vicinity of S by well-known methods of geometrical optics (GO). The phase $\phi(x)$ on S in conjunction with the eikonal equation can be used to construct the wavevector k at every point x on S . The locus of the pair (x, k) is a surface Σ in M which, carried by the flow, generates a subspace Λ called a Lagrangian manifold. The caustics are the projections on space X of the apparent contour Γ of Λ . Rays that come together at a caustic point are projections of distinct phase-space rays on Λ which, in general, remain distinct when projected on the wavevector space K or on a mixed space Y defined by p components of the position vector and the $(n-p)$ components of the wavevector corresponding to different directions. It has been shown that for any caustic point there is a space Y such that the phase-space rays projected on it do not coalesce.

To the field $u(x)$ over x corresponds a field $v(y)$ on Y related to it by a Fourier transformation F involving the variables that have been changed in going from X to Y . Thus, $v = Fu$. The partial differential equation for v is easily deduced from that for u through the Fourier transformation F . An important observation of Maslov is that when the geometric optic expansion for u fails, near to a caustic point, there is always a space Y such that geometrical optics applies to the corresponding wavefunction v . If v_0 is the zero-th order GO expression for v , Maslov takes $F^{-1}v_0$ as the expression for u . This is an integral representation that may be evaluated numerically, analytically, or by applying known techniques to obtain a uniform asymptotic expression.

A generalization of this procedure is considered where v is first replaced by an $n+1$ terms expansion v_n and then Fourier transformed: $F^{-1}v_n$. Furthermore, in regions where u and v can be represented by $(n+1)$ terms asymptotic expansions (u_n, v_n) it can be shown that those are related through an asymptotic Fourier transformation F_n of range $n+1$, i.e., one resulting from an asymptotic evaluation carried out up to $(n+1)$ terms. Thus, $v_n = F_n u_n$.

This expression may be used in lieu of the GO expansion and the generalized Maslov solution will be expressed by $U = F_n^{-1} F_n u_n$. In contrast to F , the transformation F_n is local but otherwise it has properties similar to F . Two simple examples will illustrate Maslov's method and a comparison with other methods for computing the field near to a caustic will be briefly discussed.

ON THE EVALUATION OF CERTAIN HALF-PLANE
DIFFRACTION INTEGRALS NEAR SHADOW BOUNDARIES

Ronald J. Pogorzelski
TRW Defense and Space Systems Group
One Space Park, Redondo Beach, California 90278

The so-called Spectral Theory of Diffraction (STD) has been applied in obtaining asymptotic expansions for the fields diffracted by a perfectly conducting half plane illuminated by an arbitrary incident wave (R. Mittra and Y. Rahmat-Samii, Radio Sci. 13,31-48,1978). This analysis led to expansions valid outside the vicinities of the shadow boundaries known as the transition regions as well as expansions valid on the shadow boundaries. Calculation of the diffracted fields off the shadow boundaries but within the transition regions was relegated to numerical integration along the steepest descent path. While such integration yields correct and useful results, it does not provide them in a form consistent with those in the other regions. That is, the results thus obtained are not arranged according to the order of their dependence on the wave number k . In the present work expansions are obtained for the diffracted fields within the transition regions in powers of the deviation of the field point from the corresponding shadow boundary. The results are easily arranged according to the order of their wave number dependence and are thus made consistent with the previously obtained asymptotic expansions valid on and away from the shadow boundaries.

In the case of plane wave diffraction by a pair of staggered half-planes, also treated via STD (R. Mittra and Y. Rahmat-Samii, Radio Sci. 12, 659-670, 1977), one is faced additionally with the presence of a pole in the integrand of the spectral integral. Using standard techniques (L. Feisen and N. Marcuvitz, Radiation and Scattering of Waves, Prentice-Hall, 1973, Ch. 4), the pole contribution has been handled appropriately to yield asymptotic expansions valid outside the transition regions and on the shadow boundaries. Again, however, the expansions fail in the transition regions. Upon preliminary investigation it appears that the reasoning applied in obtaining expansions for the transition region fields in the single half-plane case can be applied to the staggered pair case as well. It would thus be possible to evaluate the diffracted field in all regions and for all angles of plane wave incidence and arrange the results according to the order of their wave number dependence.

MONDAY AFTERNOON
June 2, 1:30 - 5:00

WIRE ANTENNAS 1

DKN 1B

Session B.4

Chairman: W. Tilston
Til-Tek
Richmond Hill, Ontario

CURRENT DISTRIBUTIONS, INPUT IMPEDANCES, AND
RADIATION PATTERNS OF WIRE ANTENNAS

James D. Lilly, Constantine A. Balanis
Department of Electrical Engineering
West Virginia University
Morgantown, W. Va. 26506

The Moment Method has been used extensively in the past (by R.F. Harrington, C.M. Butler, G.A. Thiele, D.R. Wilton, and others) to evaluate the radiation characteristics of linear wire structures, especially when used in the scattering mode. In this paper, the method has been applied to the problem of determining current distributions, input impedances, and field patterns for linear thin-wire dipoles of various lengths and diameters when used as antennas.

The results produced by the moment method are compared to the dipole characteristics established by the classic technique of assuming a sinusoidal current distribution. As reported by others (e.g. T.K. Sarker, Dig. URSI Meet., 68, Nov. 1979) input impedances do not agree closely between the two methods. Greater similarity is observed between the field pattern results, especially when the dipole has a small diameter (the classic method assumes an infinitely thin wire). As the dipole diameter is increased, considerable changes occur in the low-intensity regions of the pattern, where nulls and minor lobe details become less distinct.

NETWORK ANALOGS OF WIRE ANTENNAS-FORMULATION: T. H. Lehman and E. L. Coffey, The BDM Corporation, Albuquerque, NM

In the past, network analogs of antennas have been formulated using either bootstrap or network synthesis approaches. The first method is not self-consistent and results in ad hoc circuit values for parameters such as radiation resistance and higher order coupling terms. For the second method, circuit parameters are calculated from known antenna responses, and therefore at least a subset of the problem must be solved beforehand using a different solution technique. In this paper, we develop network analogs for wire antennas that are not only self-consistent and direct but that also provide a framework for obtaining approximate solutions to scattering problems.

The network analogs are formulated from the integral form of Maxwell's equations in the time domain. First, the time-dependent Pocklington's equation is discretized via the finite element technique using piecewise continuous expansion functions for the vector potential with approximate boundary conditions. Next the vector potential is evaluated in terms of the antenna currents using pulse expansion functions for the current where spatial integrations over the retarded time are accomplished using local Taylor series expansions. Combining the two expressions yields approximate coupled third-order (in time) differential equations with time retarded antenna currents as the dependent variables. By partitioning the equations into discrete intervals along the time-space characteristic, the equations reduce to a form in which only the currents as functions of proper time are the dependent variables. Higher order coupling terms can now be represented as linear combinations of the antenna sources. The network analogs of the antennas follow immediately from these equations.

The details of this method will be presented using simple examples to illustrate the fundamental concepts of the technique.

NETWORK ANALOGS OF WIRE ANTENNAS - APPLICATIONS: E. B. Mann, W. R. Zimmerman and T. H. Lehman, The BDM Corporation, Albuquerque, NM

In a previous paper, a self-consistent technique for representing wire antennas as network analogs was presented. Application of the technique to single-wire antennas results in a very simple circuit equivalent of the antenna with sources that are linear combinations of the excitation at discrete points along the antenna. In this paper, it will be demonstrated that when the technique is applied to more complex antennas (Yagi, etc.) similar simple circuit equivalents are obtained.

The extension of the network analog technique to more complex antennas is straight forward. Briefly, the antenna response equations are separated into self terms and coupling terms. The self term for an individual wire is exactly the same as for the case of a single wire in free space. The coupling terms are obtained by calculating the contribution of the vector potential due to a neighboring wire within one space-time interval. Adding these terms to the self terms results in a coupled third-order (in time) differential equation for each wire with the retarded currents as the dependent variable. Again, from space-time interval characteristics, the equations are reduced to a set of differential equations where the dependent variables depend only on the proper time. The circuit equivalent for each wire is the same as for the case of an individual wire in free space however now the equivalent sources are linear combinations of the excitations at discrete points on all the wires.

The details of the technique will be presented and the technique will be applied to several antenna configurations. Emphasis will be directed towards approximate but practical results for antennas with both linear and non-linear loads.

THE INSULATED CONDUCTOR IN A RELATIVELY DENSE MEDIUM
AS A TRANSMISSION LINE AND RADIATOR

R. W. P. King

Gordon McKay Laboratory, Harvard University, Cambridge, MA 02138

When a transmitting antenna or heating element has to be embedded at a considerable depth in electrically dense matter such as a living body or the ocean or earth, it is usually necessary to supply power by means of a transmission line that extends from the air outside to the element in question. Simple expedients such as coaxial lines with extended short sections of the inner conductor are not generally useful owing to the currents on the outside of the entire feeding line. A superior alternative can be constructed from a single insulated conductor. With proper design this can serve in sequence as a transmission line, matching section, and localized power radiating and transferring device. A combination of several coupled and properly phased elements of this type can be used to further localize the irradiation or heating. With the proper choice of frequency, structures can be designed that are very small in size and suitable for insertion into tumors or that are very large for use in bore holes in the earth. The theory of single and 2, 3 and 4 variously phased coupled elements will be outlined.

ANALYTICAL SOLUTIONS FOR THE CURRENTS ON AN
ELECTRICALLY THICK TUBULAR RECEIVING ANTENNA

Lawrence W. Rispin and David C. Chang
Electromagnetics Laboratory
Department of Electrical Engineering
University of Colorado
Boulder, Colorado 80309

In our earlier work (USNC/URSI Int'l. Symp., Seattle, Wash., 1979) we pointed out how the Wiener-Hopf technique can be utilized to find the currents induced on a semi-infinite tubular cylinder by a uniform plane wave at arbitrary incidence and arbitrary polarization. These currents can be identified as being associated with scattered fields which are either TM_m or TE_m with respect to the antenna axis, where the subscript, m , refers to the m^{th} order variation of a current component with respect to the azimuthal measure, ϕ . In the case of a finite-length antenna, this approach yields the initial current reflections from each end. In this work we show that further application of the Wiener-Hopf technique to find the subsequent reflections of the initially reflected currents from the ends, leads to a summable infinite series of reflected currents for each TM_m and TE_m mode. Also this procedure to sum the multiply reflected currents fully takes into account the conversions between the TM_m and TE_m mode currents at the ends. The final solution for each TM_m and TE_m mode current is compact and lends a great deal of physical insight into the redistribution of the currents at the ends as well as into the so-called "shadowing" effects on the back side of the cylinder.

Since many of the terms in the formal solution for the modal currents on the cylinder are in the form of infinite integrals, which must be evaluated numerically, approximate closed-form formulas are developed for these terms, which provide excellent results for antennas a thick as $ka = 1$, provided that the length-to-radius ratio, $2h/a$, is sufficiently large and the incident angle of the uniform plane wave is not too close to grazing. Comparisons are made with numerically obtained data (C.C. Kao, Rad. Sci., 5, 617-624, 1970) for an electrically thick, $ka = 1$, antenna illuminated by a normally incident uniform plane wave, with the resulting agreement being very good.

A FILAMENTARY MULTIPOLE MODEL FOR CYLINDRICAL ANTENNAS

T. Jason Chou

General Electric Co., Electronics Laboratory, Syracuse, NY 13201

Arlon T. Adams

Department of Electrical and Computer Engineering
Syracuse University, Syracuse, NY 13210

The method of moments has proven very useful in solving thin-wire problems in electromagnetic theory. In the thin-wire approach the current flowing on the surface of the wire is modeled by an axial filament, which for thin wires closely approximates the effect of the surface current. If one considers the vector potential due to currents flowing on the surface of cylindrical wire and expands the Green's function into a Taylor series about the wire axis, a series of terms that correspond to electric and magnetic filamentary multipoles along the wire axis are obtained. The leading term of the electric filament series corresponds to the usual thin-wire model and the additional terms represent circumferential variation of the longitudinal (Z-directed) and circumferential (ϕ -directed) electric currents. This expansion method may be applied to expansion of arbitrary currents about a point, axis, or plane, leading to point, filamentary or strip multipoles, respectively.

The above technique is applied to moderately thick (diameter from $.01\lambda$ to 0.1λ) wires and tubes. The zero and first order terms of the filament series are retained to represent the effect of surface current. The method of moments is used. Piecewise sinusoidal expansion and weighting functions are used in a Galerkin formulation.

Various field quantities due to the electric and magnetic filamentary multipoles have been derived. The self and mutual impedances on a single wire and the mutual impedances between the segments on the separate parallel and skewed wires are evaluated. The first order filamentary multipoles representing the circumferential variation of the Z- and ϕ -directed electrical currents are strongly coupled; thus both terms must be included. Special treatment has been derived for the wire ends with open tube and flat cap conditions.

Computer programs in FORTRAN IV have been developed for treating radiation and scattering problems of (1) single wire with flat caps, (2) parallel tube antennas, and (3) skewed tube antennas. Numerous results for the current distribution and the far field patterns are to be presented. A comparison with experimental data shows good agreement. The numerical technique developed here is useful in investigating the effect of first order circumferential variation of the current and in verifying the basic approximation used in the wide spread thin wire model

THE ANALYSIS OF THE FIELD RESPONSE OF SOLID WIRES
EXCITED BY CURRENT FILAMENTS ON THE ENDCAPS

K. R. Demarest
Lafayette College
Department of Electrical Engineering
Easton, Pennsylvania 18042

The precise solution of the current excited on a circular wire of finite length due to an impressed field or voltage has been a much discussed topic in the literature. Most geometries considered to date fall into the categories of either coaxial fed or plane wave excited wires. The impetus for this concentration of effort derives from the fact that wires are usually excited in one of these ways. Although there exist many other ways in which wires can theoretically be excited, most are not of interest since they cannot be physically realized.

A wire/source geometry that has just recently become of interest is that of a solid monopole with flat endcaps, mounted above a large ground plane and excited by a short current filament which is oriented parallel to the wire axis and located at the center of the endcap. The implementation of this unusual source geometry has just recently been attained through the use of a nonlinear surface reaction in which a high power, short pulse laser beam is focused on the surface of a metal target (in this case, the monopole endcap center) to produce a transient, short length current filament within the focal region.

A technique for calculating the current and field response of an end excited monopole is presented. This formulation is a variation of the Fourier transform technique (O. Einarsson, IEEE Trans. Ant. and Prop., 14, 31-37, Jan. 1966) and models the dipole (the monopole and its ground plane image) as a member of an infinite, periodic array (of sufficient spacing to negate coupling effects) of identically excited wires. The array geometry is divided into two distinct regions, and complete field expansions are constructed that satisfy the appropriate boundary and source conditions of each region. Solutions are obtained by requiring these expansions to satisfy the necessary boundary conditions along the extended wire surfaces through the use of a Fourier Galerkin matching technique.

Wire responses as calculated by this technique are presented which demonstrate their basic characteristics as a function of critical wire and source parameters. Special attention is drawn to the current response in the end regions and its dominance by the currents incident from the source filament. Calculated transient responses are also presented and shown to exhibit excellent agreement with measured responses.

TRANSIENT NEAR-FIELDS OF LINEAR ANTENNAS

P. Fellingner, K.J. Langenberg, K.D. Rech
Theoretische Elektrotechnik, Fachrichtung 12.2
Universität des Saarlandes
D-6600 Saarbrücken, FRG

The interest in the transient behavior of antennas has recently turned towards more complicated structures, as for example log-periodic dipole arrays; their EMP and impulse compression properties have widely been under concern. The proposed methods for theoretical investigations are mainly somewhat heuristic or purely numerical. In contrast, an approximate analytical approach based on the Singularity Expansion Method has been developed (K.J. Langenberg, Appl. Phys. 20, 101-118, 1979). It has been shown that coupling effects of adjacent antenna elements must be taken into account for values of the shape parameter $\Omega \leq 14$. Then appropriate expressions for transient near-fields of the single antenna dipoles have to be provided in order to compute the induced transient current in the neighbouring dipoles.

The approximate analytical SE-version of Marin and Liu (L. Marin, T.K. Liu, Rad. Science 11, 149, 1976) as extended to center-loaded or transmission line fed linear antennas (K.J. Langenberg, K.D. Rech, Proc. US National Committee of URSI, Boulder 1978) can easily be extended to their near-field. The resulting expressions in the Laplace domain can be evaluated in two different ways:

- 1) Performing the inverse Laplace transform first, then integrating the modes times the Green function with respect to the source variable taking properly into account the retardation. For the case of approximating the modes analytically, the latter integration is performed in different ways: "exact" numerically using a standard integration routine to investigate the influence of neglecting the retardation of the transient current. It is found that for real step-function excitation that means not too broadband excitation, the retardation can be neglected. Then several approximate procedures are applied to the analytical evaluation of the near-field integrals, including the King-Middleton approximation and moment expansions.
- 2) Interchanging the order of integration yields a formulation which can be treated analytically by Cagniard's method: the source integral with respect to the antenna surface can be changed to an explicit Laplace integral; hence, the corresponding time function can be read off immediately. It remains to perform convolutions with the damped exponentials resulting from the first order poles of the singularity expansion. The same method can be used to compute transient near-fields of prescribed one- or twodimensional aperture distributions. Regarding the acoustic transient radiation problem they can be realized through arrays of piezoelectric piston transducers. Hence, analytical expressions are derived for the transient near-field of widely arbitrary ultrasonic phased-arrays.

The methods described above are illustrated by numerical examples.

A NEW TYPE OF ANTENNA "GAUSS-CURVE DIPOLE"

Zhou Chao-Dong, Zhou Liang-Ming and Yang En-Yao
Northwest Telecommunication Engineering Institute
Xi'an, Shaansi, China

It is well known that when the length L of a straight dipole antenna exceeds $\lambda/2$ (λ : working wave length), it will exhibit sidelobes. When $L > 0.7\lambda$, the main lobe direction will shift from broadside. If L increases continuously, the gain increases slowly due to the appearance of antiphase current in the antenna. With the increase of the length of L , the number of sidelobes increases, the mainlobe splits and changes directions continuously. These factors limit the usable length of a dipole antenna so a dipole with $L < \lambda/2$ is preferable.

If the shape of the dipole changes from a straight line to a plane curve, with the compensation of the time delay of the current phase lag by the path difference, it is possible to keep the main lobe direction broadside and get higher gain. This idea was already reported in reference [1], but the detail design procedures and geometries of antenna structures are not given. This paper introduces a Gauss-curve dipole with a straightened length $L = 0.75\lambda$. Of course, there may be many kinds of curve to be chosen, but the Gauss-curve seems to be a satisfactory one. It will be proved by analysis and experiments. If the shape parameters are properly chosen, the gain of this kind of antenna may reach 7.5 dB. If these antennas are used as elements to form an array, we can use fewer elements to get comparatively high gain and simplify the feeding network. When we use these elements to form a three-element Yagi antenna, its gain may reach 11-12 dB.

This paper gives the geometry of the structure of the Gauss-curve dipole antenna, the principle of selecting geometrical parameters, the analytical and experimental results of radiation patterns, the impedance and gain characteristics, and the parameters of a three-elements Yagi.

[1] F.M. Landstorfer, "New Developments in VHF/UHF Antenna", IEE 169 Antennas and Propagation Part 1 Antenna, 1978.

BACKWARD-WAVE YAGI HYBRID ANTENNA

Walter K. Kahn*
 Naval Research Laboratory
 Washington, D.C.

A novel dipole end-fire array configuration the currents on which inherently tend to taper as required for low sidelobes. In the conventional traveling wave array designed for end-fire, excitation is provided at one end of the array. The currents on a uniform array of elements tend to taper away from that end; other current distributions are obtained by changing the elements themselves or their coupling to the traveling wave structure. In the proposed configuration, Fig. 1, excitation enters at a more medial point of the array, and conceptually the new antenna combines a backward wave segment with a forward-wave Yagi segment. Currents on the medial element and elements adjoining this element (which is excited directly from the source) are enhanced by components usually lumped as (unavoidable) "feed radiation." An array of sixteen dipoles chosen in accordance with this idea was computed to have a sidelobe level better than -20 db at the design frequency and -16 db over an 8% band. A conventional Yagi produces approximately -14 db sidelobes at the design frequency.

*George Washington University, Washington, D.C.

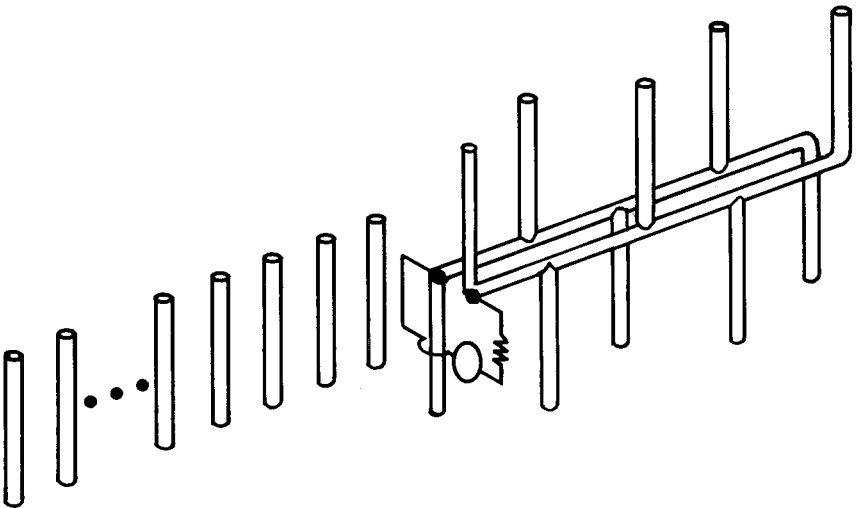


Figure 1

MONDAY AFTERNOON

June 2, 1:30 - 5:00

GUIDED WAVES

DKN 1271

Session B.5

POSTER SESSION

Chairman: R. Gagné
Université Laval
Québec, Qué.

COUPLED-MODE ANALYSIS OF STEEP WAVEGUIDE TRANSITIONS

S. S. Saad, Andrew Corp., Orland Park, Illinois, USA
A. A. Kamal, Cairo University, Cairo, Egypt
S. A. Mashali, National Research Center, Cairo, Egypt

A rigorous coupled-mode analysis is employed to solve steep waveguide tapers for which small-coupling theory fails to be accurate. Two methods of analyzing the taper are introduced.

First, a numerical technique is presented for the case of steep tapers with arbitrarily-shaped cross-sections. The technique requires numerical solution of a set of differential equations describing the longitudinal problem (A. F. Stevenson, J. Appl. Physics, 22, 1447-1460, 1951) for which the coupling coefficients are obtained by numerical solution of the transverse eigenvalue problem (F. L. Ng, IEEE Trans., MTT-22, 322-329, 1974).

Second, closed-form solutions are deduced from Stevenson's differential equations for the cases of linear rectangular and circular steep waveguide transitions. The method is shown to be applicable to almost all transitions that satisfy the following three requirements. The longitudinal variation of geometry must be expressed as an analytical function, the transverse eigenfunctions must be known analytically, and the transition must support only one or two modes. The scattering matrix of the transition is obtained by applying the proper boundary conditions at both ends of the transition using the mode-matching method. Theoretical and experimental results are in good agreement over a frequency band of $\pm 28\%$.

ANALYSIS OF AN ANNULAR SLOT IN A RADIAL WAVEGUIDE
WITH AN INTERIOR TRUNCATED DIELECTRIC

T. L. Keshavamurthy and C. M. Butler
Department of Electrical Engineering
University of Mississippi
University, MS 38677

In this paper the analysis of an annular slot in a radial waveguide is presented. The waveguide is filled inside with a dielectric which is truncated. It is excited in the interior with a radial TEM wave. An integral equation is formulated for the slot electric field (or equivalent magnetic current) and it is solved by moment method. From the slot electric field the scattering parameters and the radiation from the slot are obtained. Data are presented for several waveguide plate separations, slot widths, and for different interior dielectrics.

ANALYSIS OF A COAXIAL TO RADIAL WAVEGUIDE JUNCTION

C. M. Butler and T. L. Keshavamurthy
Department of Electrical Engineering
University of Mississippi
University, MS 38677

In this paper the analysis of the input impedance of a coaxial to radial waveguide junction is presented. An integral equation is formulated for the coaxial electric field (or equivalent magnetic current). The Green's function for the magnetic field is obtained in terms of the appropriate Eigenfunctions. An integral equation is solved numerically for the structure, from which quantities of interest are determined. Also, input reflection coefficient is computed by a variational procedure and compared with results calculated from the more elaborate numerical solution technique. Both yield answers which are in good agreement with approximations found in the literature.

CARACTERISATION ELECTROMAGNETIQUE DE DISCONTINUITES
SIMPLES OU MULTIPLES SUR UN GUIDE DIELECTRIQUE EN BOITIER

M. PETENZI et P. GELIN

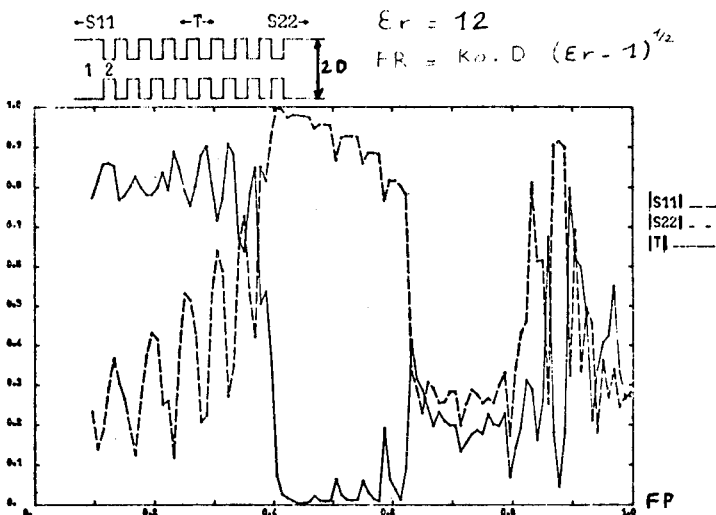
Centre Hyperfréquences et Semiconducteurs
Laboratoire Associé au C.N.R.S. n° 287
Université de Lille I - Bât. P4
59655 VILLENEUVE D'ASCQ CEDEX - FRANCE.

Cette communication a pour objet l'étude des phénomènes électromagnétiques créés par une ou plusieurs discontinuités successives, transversales à l'axe de propagation d'un guide diélectrique, pour la mise au point de structures telles que des filtres, des transformateurs d'impédance, des transitions.

L'utilisation dans cette étude d'un guide diélectrique en boîtier nous permet de travailler avec un spectre discret de modes, et nous donne la possibilité de caractériser des systèmes fermés (boîtier faiblement surdimensionné) aussi bien que des systèmes ouverts (boîtier fortement surdimensionné).

La technique du raccordement de champs (mode matching) dans le plan de la discontinuité ramène la résolution du problème au traitement d'un système matriciel dont la solution est la matrice "S" généralisée de la discontinuité, matrice qui décrit complètement le phénomène de couplage de modes.

La connaissance de cette matrice dans le cas d'une discontinuité simple (localisée en un point de l'axe de propagation) permet ensuite la généralisation à un système constitué par une succession de discontinuités interagissantes, tel celui représenté ci-dessous. Cette généralisation étant obtenue par l'application d'une procédure de chaînage entre les matrices S des différentes discontinuités élémentaires.



Analysis of Leaky Coaxial Cables used in Mine Communications

R.S. Tomar and Alakananda Paul*
Electrical Engineering Department
Indian Institute of Technology, Kanpur, India
*Visiting Assistant Professor
Northeastern University
Boston, Massachusetts

Leaky coaxial cables are extensively used for communications in mines and tunnels. Different types of leaky coaxial cables are in use. Two most important types are loosely braided coaxial cables and coaxial cables with slots. Recently, Wait has suggested methods of rigorous electromagnetic analysis of leaky coaxial cables of the two types mentioned above.

[(1) J.R. Wait IEEE Trans. MTT-24(9) 547-553. Sept. 1976.

(2) J.R. Wait IEEE Trans on Electromagnetic Compatibility vol. EMC-19, No. 1, Feb. 1977 pp. 7-13.] The theory presented by him has not been supported by numerical results so far. One parameter of particular interest in leaky coaxial cable propagation is the surface transfer impedance. The surface transfer impedance of a leaky coaxial cable is defined as the ratio of the axial electric field to the discontinuity in the azimuthal magnetic field at the sheath.

In cases of both loosely braided and slotted coaxial cables, Wait's formulations for the fields have been used to derive and numerically calculate the surface transfer impedance. The calculated values of the surface transfer impedance for various types of cables have been compared with some available measured values as well as with calculated values obtained by approximate methods. Rigorous electromagnetic analysis showed more definite and consistent trends of variation of surface transfer impedance with frequency and physical properties of the cable than other published results. Since Wait's formulation for both loosely braided and slotted coaxial cables are similar, this method can be used for calculation of surface transfer impedance of all leaky coaxial cables.

INTEGRAL EQUATION FORMULATION FOR MODE CONVERSION AND RADIATION FROM DISCONTINUITY IN OPEN-BOUNDARY WAVEGUIDE

S. V. Hsu, E-Systems Inc., Garland, Texas 75042, U.S.A.
 Dennis P. Nyquist, Department of Electrical Engineering and Systems Science, Michigan State University, East Lansing, Michigan 48824, U.S.A.

An integral equation formulation is utilized to describe the phenomenon of mode coupling and radiation due to scattering from obstacles in a cladded dielectric waveguide. Conversion of a single incident surface wave mode to other transmitted and reflected modes is studied.

The region of refractive index contrast produced by the discontinuity is replaced by an equivalent current distribution which maintains a scattered field in the otherwise unperturbed waveguide system. The total electric field in the waveguide consists of the superposition of an impressed excitatory field and the scattered field. Expansion of the scattered field in terms of the normal modes of the unperturbed system results in the following 3-D electric field integral equation (EFIE) for the unknown electric field in the discontinuity region:

$$\vec{E}(\vec{r}) - j\omega\epsilon \int_V [n^2(\vec{r}') - n_b^2(\vec{r}')] \vec{E}(\vec{r}') \cdot \overleftrightarrow{G}(\vec{r}, \vec{r}') dV' = \vec{E}^{inc}(\vec{r})$$

where n and n_b are refractive indices of the discontinuity and the unperturbed waveguide regions, the tensor green's dyadic $\overleftrightarrow{G}(\vec{r}, \vec{r}')$ is equal to $\overleftrightarrow{G}_D(\vec{r}, \vec{r}') + \overleftrightarrow{G}_R(\vec{r}, \vec{r}') + \hat{z}[\delta(\vec{r} - \vec{r}')/j\omega\epsilon_u(\vec{r})]\hat{z}$ with

$$\overleftrightarrow{G}_D(\vec{r}, \vec{r}') = \sum_{n=0}^N -\vec{e}_n(\vec{r}) \vec{e}_n(\vec{r}') \exp(-j\beta_n |z-z'|)$$

and

$$\overleftrightarrow{G}_R(\vec{r}, \vec{r}') = \int_0^{\infty} -\vec{e}(\vec{r}, \rho) \vec{e}(\vec{r}', \rho) \exp[-j\beta(\rho) |z-z'|] d\rho$$

represent the contributions from the discrete and the continuous mode spectrums respectively.

Application of the above EFIE to a dielectric slab waveguide with a slice gap discontinuity is studied and numerical results are obtained by the Method of Moments to determine the modal amplitudes for the scattered fields. This subsequently yields the modal conversion coefficients. The intensity distribution of the radiation field maintained by the discontinuity is also calculated.

B.5 - 7 Poster Session Commission B

FIELD CONFIGURATION OF FUNDAMENTAL AND HIGHER ORDER
MODES IN FIN LINES OBTAINED WITH THE TLM-METHOD

By

WOLFGANG J.R. HOEFER AND YI-CHI SHIH

The Transmission Line Matrix Method is used to compute the cutoff frequency, and the electric and magnetic field components in the cross-section of fin lines. Some field plots for the fundamental and next higher mode are presented. Values for the fundamental cutoff frequency are accurate within one percent.

Department of Electrical Engineering,
University of Ottawa,
Ottawa, Ontario, Canada K1N 6N5
Tel. (613) 231-2493

MODE THEORY OF UNIFORM WAVEGUIDES FILLED
WITH DIELECTRIC INHOMOGENEOUS
ALONG ONE DIRECTION ONLY

Lin Weigan
Chengdu Institute of Radio Engineering
Chengdu, Sichuan
People's Republic of China

Straight waveguides filled with inhomogeneous dielectric whose permittivity varies along one dimension are studied. Emphasis is given to the modes of propagation and to the calculation of the propagation constants. Exact solutions are given for some special cases. In some of these only asymptotic or polynomial solutions have been available previously.

No restriction is placed on the waveguide dimensions so that results developed here apply to the transmission of optical frequency waves as well as to microwave and millimeter waves.

In the waveguide problems of this paper, results obtained cannot be directly drawn on from the existing literature and have been worked out from fundamental theory of differential equations. The problem of elliptical waveguides filled with dielectric whose permittivity varies along the direction of propagation is cited as an example.

RECOMMENDATION AND REFERENCE TABLE OF
RIGID ELLIPTICAL WAVEGUIDE DATA

Lin Weigan
Chengdu Institute of Radio Engineering
Chengdu, Sichuan
People's Republic of China

We divide the spectrum from 1.7 GHz to 15.2 GHz into eleven bands (divisions) to cover the wave bands widely used by various countries for straight elliptical waveguides. We then choose the dimensions of the straight elliptical waveguides and of the connecting rectangular waveguides for each wave bands, the attenuation, C.W. power rating and impedance ratio are calculated and tabulated into a table of fifteen columns.

PROPERTIES OF ANISOTROPIC DIELECTRIC TUBE WAVEGUIDES

D.K. Paul* & B.B. Chaudhuri
Electrical Engg. Deptt., I.I.T., Kanpur, INDIA.

The propagation characteristics of an uniaxially anisotropic dielectric tube have been investigated for both symmetrical and hybrid modes of excitation. The tubular structure is considered to be composed of three layers, namely, an anisotropic cladding sandwiched between a core and an outer region, both of which are isotropic. The approach presented here is based on solving Maxwell's equations to find the "characteristic determinant", which is a 8×8 matrix, by matching the axial and azimuthal field components at the respective boundaries. The characteristic equations obtained from this determinant are numerically evaluated for the propagation constants of each waveguide mode. The derivation presented here is quite general. With suitable substitutions for the tube radii and refractive indices, the method is applicable both to rod and hollow waveguide configurations.

Expressions have been derived for the power flow, energy storage and power loss using a perturbation method. The effects of the uniaxial dielectric anisotropy, normalised waveguide parameters, tube thickness and refractive indices on the propagational features have been studied in detail. The modal characteristics show non-zero cut-off for the symmetrical modes. The dominant hybrid mode has a non-zero cut-off only in the asymmetrical configuration of the tube ($n_1 \neq n_2$), provided the tube radii and the refractive indices satisfy certain requirements. Though the TE modes remain unaffected with the present choice of the uniaxial anisotropy, pronounced changes are observed for the TM and hybrid modes. It has also been shown that the present formulation can be reduced to the transcendental equations for two-layered optical waveguide (B.B. Chaudhuri & D.K. Paul, IEEE Trans. MTT-27, 170-172, 1979).

* Presently with Gordon McKay Laboratory, Harvard Univ., Cambridge, Massachusetts 02138, U.S.A.

CALCUL DES COEFFICIENTS DE LA MATRICE SCATTERING D'UNE FOURCHETTE MICROSTRIP APPLICATION AUX COUPLEURS BRANCH-LINES

MM. Citerne J. et Cosnard E.
U. S. T. L. C.H.S. LA n°287 C.N.R.S.
59655 Villeneuve d'Ascq cedex FRANCE

La nécessité de concevoir des systèmes en microélectronique hybride à des fréquences de plus en plus élevées a révélé les carences des théories classiques quant à l'obtention de caractéristiques acceptables pour les multipôles microstrip au delà de la bande X. En 1975, Kompa a proposé une modélisation multimodale de la ligne microstrip dont l'efficacité a été principalement démontrée lors de la conception de quadripôles. Partant de cette même modélisation, nous proposons une étude de la discontinuité présentée en figure 1. Le chaînage de ce type de discontinuités permettant de concevoir des multipôles tels que des diviseurs de puissance ou des jonctions hybrides, l'association avec des éléments actifs (diodes Schottky - transistors à effet de champ) permettra d'optimiser les performances des systèmes de télécommunication en ondes millimétriques.

A partir de la modélisation guide fermé (Kompa-1975 E.L. Vol 11 pp 459-460), on exprime le raccordement multimodal des composantes tangentielles des champs E et H à l'interface des guides 0 et i pour $1 \leq i \leq n$ (figure 1). On obtient donc n+1 équations en fonction des matrices de produit scalaire modal K_{0i} et d'impédance Z_i (formule 1) dont on déduit la matrice scattering $S = Id - 2P$ où P désigne une projection d'un espace de Hilbert.

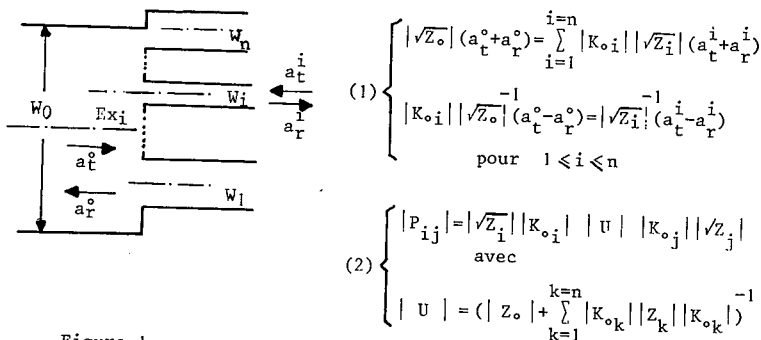


Figure 1

L'intérêt de cette formulation est de ne nécessiter qu'une inversion matricielle; elle garantit donc une bonne stabilité numérique des résultats en traitement sur ordinateur.

Pour étudier des structures complètes, on procède au chaînage et au bouclage de segments élémentaires dont on a une résolution multimodale prenant donc en compte toutes les interactions à l'encontre de la théorie classique. Nous présenterons ce type de résultats appliqué à l'étude d'un coupleur branch-line 3dB.

L'introduction des éléments actifs sous la forme de leur matrice de répartition permettra à terme la conception assistée par ordinateur de structures telles qu'amplificateurs symétriques ou mélangeurs de grandes performances.

TUESDAY AFTERNOON
June 3, 1:30 - 5:00

SPECIAL SESSION ON ELECTROMAGNETIC EARTH
INDUCTION FROM OVERHEAD CONDUCTORS

DKN 1B

Session B.6

Chairman: W.R. Goddard
University of Manitoba
Winnipeg, Manitoba

Organizer: J.R. Wait
U.S. Department of Commerce
NOAA, ERL
Boulder, Co.

INDUCED CURRENT ON AN INFINITE HORIZONTAL WIRE ABOVE EARTH
BY A CLOUD TO GROUND LIGHTENING DISCHARGE

R. G. Olsen, Department of Electrical Engineering
Washington State University, Pullman, WA 99164

Often, undesired currents are induced on transmission lines by lightning discharges. In this paper a technique for calculating the current induced on a single wire transmission line above earth by a distant vertical cloud to ground lightning discharge is given.

To a first approximation, the electromagnetic fields of a vertical cloud to ground lightning discharge can be calculated by assuming that the lightning current constitutes a Hertzian dipole just above the earth's surface. The lightning current can be assumed to be of the form

$$I(t) = \sum_{i=1}^3 c_i e^{-a_i t} \text{ kA} \quad (1)$$

where $c_1 = 27.5$, $c_2 = 30$, $c_3 = 2.5$, $a_1 = 2 \times 10^4$, $a_2 = 2 \times 10^5$, and $a_3 = 10^3$. (Levine and Meneghini, Radio Science, 13, 801-809, 1978).

The Transient induced current is found in three steps. 1) The Fourier transform (in time) of the lightning current is found. 2) An expression for the current induced on a horizontal wire above earth by a distant oscillating Hertzian dipole is found. 3) Using the Fast Fourier Transform (FFT) the inverse Fourier transform of the product of the expressions found in 1) and 2) is found. The result is samples of the transient induced current on the wire.

The Fourier transform of equation 1 can easily be obtained. The solution to the steady state coupling problem is the one given by Olsen and Aburwein which has been modified to be valid over the broad frequency range necessary for computing the transient current (Olsen and Aburwein, USNC/URSI Fall 1978 Proc., p 77). The transient wire current is found by calculating the current due to each exponential current in equation 1 via the FFT and superimposing the results. Each FFT is computed using a sample rate of $1/8$ Hz. A symmetric rectangular window of half width $64 \mu\text{Hz}$ is used to calculate the FFT of the first exponential while a half width of $16 \mu\text{Hz}$ was used for the others. The values of induced current generated by the FFT are valid for times greater than 1.5 microseconds after the arrival time of the lightning pulse.

INDUCED CURRENTS ON AN OVERHEAD TRANSMISSION LINE DUE TO LOCAL ELECTROMAGNETIC SOURCES

David C. Chang, Ahmad Hoorfar and Edward F. Kuester
Electromagnetics Laboratory
Department of Electrical Engineering
University of Colorado
Boulder, Colorado 80309

It is generally accepted that electromagnetic interference on overhead transmission lines due to near-by natural or man-made electromagnetic sources can be one of the important design considerations for high voltage power transmission systems. Since the wire, together with a conducting earth, can form a legitimate wave guiding system, erroneous currents induced by local disturbances indeed can propagate along the wire over large distances. This phenomenon can be particularly pronounced in the frequency range where the height of the overhead wire is not much shorter than a free-space wavelength. In fact, by solving the electromagnetic boundary-value problem involving an overhead wire excited by a delta-function voltage generator, our earlier work (Chang and Olsen, Radio Science, 10, 8,9, 823-831, August-September 1975), demonstrated that in this frequency range, a significant amount of electromagnetic energy is carried away from the generator by a so-called earth-attached mode, arising from the interaction between the wire and the air-earth interface, in addition to those carried by the conventional transmission-line mode, resulting from the interaction of the wire and its imperfect image. Furthermore, because the earth-attached mode usually exhibits a lower attenuation constant in this frequency range, its effect can be stronger than that of the conventional transmission-line mode at great distances.

In this paper, the physical mechanisms for various guiding modes of an overhead transmission line system will be reviewed. Induced current on a single, bare wire as generated by a vertical electric dipole source located on the earth surface away from the wire, is computed for frequencies ranging from 10 KHz to 10 MHz. The total induced current in this case consists of two discrete modes and two continuous spectral components; the significance of each as a function of frequency will be noted. The frequency-domain solution is then used to obtain the approximate real-time current response for impulse sources having the wave form of a double exponential.

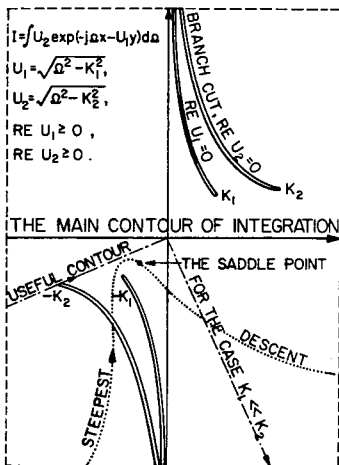
ELECTROMAGNETIC EARTH INDUCTION FROM AN OVERHEAD LINE CURRENT PARALLEL TO THE GROUND

O. A. Aboul-Atta, L. Shafai, and M. Z. Tarnawewky
 Department of Electrical Engineering
 University of Manitoba

The electromagnetic field components of an elevated horizontal line current source of infinite extent and parallel to a flat interface are shown in their exact integral form. Part of the integral solution has been recognized in their cylindrical "Bessel" functions equivalence since (A. N. Sommerfeld, Ann. Physik, 28, 665) 1909. The remaining part of the resulting solution defies analytical equivalence to the known mathematical functions except in some special and limiting cases.

The encountered mathematical difficulty of the Fourier Transform, resulting from the integrand being doubly irrational, is shown and explained. Legitimate analytical approximations (O. A. Aboul-Atta, and E. Tomchuk, J. Inst. Maths Applic 3, 21, 157-163, 1978) for these integrations are derived for both cases of large and small arguments. Their correlation to simple engineering expressions using the image theory and the Struve functions (as given by J. R. Wait, Proc. IRE, 49, No. 10, 1576, 1961, P. R. Bannister, Radio Science, Vol. 3, No. 2, 1968, and others) are illustrated.

All new analytical expansions are given in their suitable form for computer programming with the accentuation of the important and sensitive variables. The techniques used are kept general so as to accommodate all other applications where the interface does not necessarily represent a lossy ground or that the propagation constant in the source's medium is relatively small compared to that below the interface.



THE RIEMANN SHEET OF THE Ω PLANE FOR A RELEVANT DOUBLY IRRATIONAL INTEGRAL

EFFECT OF A BURIED CABLE ON THE FIELDS OF A
VMD ON THE GROUND SURFACE

Adel Z. Botros, and Samir F. Mahmoud
Electronics and Communications Department,
Cairo University, Giza, Egypt.

In active electromagnetic measurements on the ground surface the fields can be appreciably affected by buried conducting objects such as long cables or pipes. In this paper the particular case of a vertical magnetic dipole (VMD) situated on the earth's surface and radiating in the presence of a nearby buried cable, which is parallel to the surface, is considered. At low operating frequencies, the cable diameter is much less than the skin depth in the ground, hence the induced cable current can be assumed totally axial with no azimuthal variation. Furthermore, the dominant part of this induced current is modal currents whose propagation constants are independent of the excitation. The magnitudes of the modal currents are determined by the average electric field of the VMD at the cable surface, the internal cable impedance, and an external impedance depending on the surroundings (J.R.Wait, J.Appl.Phys. 49-2,1978).

The propagation constants of the modal currents are determined from a modal equation which is solved numerically and consequently the magnitude of the dominant modal current is found. The fields radiated by the cable current at the earth's surface are found to produce a characteristic interference pattern when added to the primary fields of the VMD.

The practical case of a cable in poor contact with the surrounding medium is also considered and it is found that the cable currents and their radiated fields are appreciably affected. Several numerical examples relevant to remote sensing applications are presented.

ON THE IMAGE REPRESENTATION OF THE FIELDS OF
A LINE CURRENT SOURCE ABOVE FINITELY CONDUCTING EARTH

A. Mohsen

Department of Electrical Engineering
The University of Manitoba, Winnipeg, Canada

The problem of an electric line source above a conducting earth is treated. The exact solution is in an integral form. Only in particular cases, can the field integrals be evaluated in closed form and it is usually necessary to resort to numerical or approximate methods. Approximations to the integrals appearing in the solution of the problem in terms of complex images are considered. The justification of the image theory technique is investigated. Two extensions of this technique are presented. It is shown that both are legitimate for far field computation. The first extension is, however, more accurate. The field in this case is represented in terms of two images rather than one image as is customarily known (J. R. Wait and K. P. Spies, *Can. J. Phys.*, 47, 2731-2733, 1969). Besides, the effect of the conductivity of earth is easily tractable. The second extension, though less accurate for far field evaluation, has the advantage that it can be extended to the quasi-static range.

An estimate of the neglected terms in both cases is given and their physical interpretation is presented. Contrary to previous works (P. R. Bannister, *IEEE Tr. Antennas & Prop.*, AP-26, 507-508, 1978) the analysis does not restrict the relative magnitudes of the earth and air propagation constants.

The analysis yields simple analytical expressions once the asymptotic values of the Bessel functions involved are used. It also provides a method to improve the efficiency of the numerical solution of the field integrals by incorporating the image contribution.

MEASUREMENT AND ANALYSIS OF CONTROLLED POWERLINE VLF RADIATION
FROM THE HV-DC LINE FROM RADISON TO DORSEY, MANITOBAW-M. Boerner^(1,2), W.R.Goddard⁽¹⁾, J. Cole⁽²⁾, C. Thio⁽³⁾

(1) AEM Laboratory, Electr. Eng. Dept., U. of Manitoba, Winnipeg;
(2) Comm. Lab., Information Eng. Dept., UICC, Chicago; (3) Systems
Planning Division, Manitoba Hydro, Winnipeg

The extensive use of the hydro-electric generating capacity in Northern Manitoba requires long HV-DC/AC transmission lines to serve the Southern part of Manitoba and neighbouring U.S. power companies. The auroral-electroject zone covers three-quarters of the province and consequently, solar storms strongly affect these transmission systems. Harmonics are generated at transformers due to the saturation of their cores by induced currents, and the level of harmonics produced will cause malfunction of control relays, and yield unacceptable distortions in normal AC waveforms leading to the radiation of higher order harmonics from these lines. The hypothesis that powerline radiation of sufficient magnitude penetrates the ionosphere which is responsible for observed stimulation requires further verification. The main need exists to study and measure powerline harmonics radiation up to 10 KHz using ground-based, balloon borne and satellite measurements.

For this purpose we have designed a major experiment to measure the harmonic radiation from the 900 km HV-DC line at distances of up to 600 km away from the line (ground-based), at an altitude of up to 40 km above the line (balloon borne) and at heights from 500 km to 1500 km (satellite observations). In preparation for these experiments a theoretical analysis of PLHR from the MH Radison-Dorsey line taking into consideration the very particular geophysical properties of the Interlake Region and the particular configuration of the line is considered. Extension of the approximate Carson equation, which is valid for these low frequencies, to the particular geophysical environment using a three-layer model is currently carried out. Expanding the model to predict currents as a function of excitations is required to predict PLHR at the various radiation levels in various atmospheric to magnetospheric regions.

We shall present a brief overview of the project and place major emphasis on analytical and experimental results of the specific radiation problem.

Title of the Paper: Electromagnetic Earth Induction from M.T. measurements at Eusebio, a station under equatorial electrojets.

Authors: N.B. Trivedi, E.G. de Souza (Instituto de Pesquisas Espaciais, INPE; Conselho Nacional de Desenvolvimento Científico e Tecnológico, CNPq; C.P. 515, 12200 - S.J. dos Campos, S.P., Brazil).

Magnetotelluric measurements in the period range 100 S to 86400 S were conducted at Eusebio (3.87°S , 321.58°E). Tensor conductivity computations were done and plots were obtained for 6_{xy} and 6_{yx} versus period, T. The conductivity curves 6_{xy} and 6_{yx} show marked dissimilarity. We find from the 6_{xy} curve the depth of intermediate conducting layer in the range of 45-75 Km and the ultimate conducting layer seems to begin at a depth of about 250 Km. We attempt to explain the observed differences between the curves for 6_{xy} and 6_{yx} in terms of peculiar effects from overhead equatorial electrojets.

ANALYSIS OF BURIED PIPELINE VOLTAGES
DUE TO 60 Hz AC INDUCTIVE COUPLING

Allen Taflove
IIT Research Institute
10 West 35th Street
Chicago, IL 60616

The voltages induced on gas transmission pipelines by 60 Hz ac power transmission lines sharing a joint right-of-way are predicted using electrical transmission line theory. Thevenin equivalent circuits for pipeline sections are developed which allow the decomposition of complex pipeline-power line geometries. Programmable hand calculator techniques are used to determine inducing fields, pipeline characteristics, and Thevenin circuits.

The results of field tests on a buried, 34-inch diameter gas pipeline adjacent to a 525 kV ac power transmission line for 54 miles are discussed. Comparison is made between measured inductive coupling data and predictions obtained using the theory developed. An excellent agreement of the predicted and measured results is shown for the location and magnitude of all induced voltage peaks on the pipeline.

TUESDAY AFTERNOON
June 3, 1:30 - 5:00

SPECIAL SESSION ON OPTICAL COMMUNICATIONS III
FIBER AND GUIDED WAVE OPTICS II

DKN 2B

Combined Session B.7/AP-S

Chairman: C. Yeh
U.C.L.A.
Los Angeles, CA.

Organizer: G.L. Yip
McGill University
Montréal, Québec

The following papers belong to the IEEE AP-S Symposium and the summaries are included in the IEEE AP-S Digest under Combined Session B.7/AP-S.

4. BOUNDARY FORMULATION OF PROPAGATION PROBLEMS IN GUIDING STRUCTURES FOR INTEGRATED OPTICS, V. Daniele, I. Montrosset and R. Zich, CESP (CNR) and Istituto Elettronica e Telecomunicazioni, Politecnico di Torino, Corso Duca degli Abruzzi 24, 10129 Torino, Italy.

7. POLARIZATION PROPERTIES OF SINGLE MODE FIBERS, Cynthia P. Smith, Hughes Research Laboratories, Malibu, CA., and Giorgio Franceschetti, University of Naples, Italy.

OPTICAL WAVEGUIDE THEORY

C. YEH

Electrical Sciences and Engineering Department
University of California, Los Angeles
Los Angeles, California 90024

After being nurtured through the critical research and development stage in the early 1970's, optical fiber technology has finally come of age in the late 1970's. It is only a matter of time before the use of optical fiber links as practical communication lines becomes wide-spread. In order to properly design and use an optical fiber link, the propagation characteristics and field distributions of the propagating modes in the optical waveguide must be known. Knowledge of the propagation constants of guided modes as a function of frequency provides information on the bandwidth capability of the fiber guide under consideration while knowledge of the field distributions of guided modes provides information on how to couple efficiently light energy into and out of the fiber guide. Furthermore, this knowledge on the propagating modes also provides the starting point for many treatments on the effects of bending, tapering, surface irregularities, scattering centers or mode conversions.

The purpose of this presentation is to assess several modern analytical and/or numerical techniques which have been used successfully in obtaining the propagation characteristics and field distributions of guided modes in optical waveguides. The pros and cons as well as the limitations of various available analytical/numerical techniques will be discussed. Then, presentation will be given on several selected promising modern techniques (such as the finite-element approach and the scalar wave-FFT method) together with illustrations.

On Weak-Coupling Theory of Optical
Fiber and Film Waveguides

Huang Hung-chia
(Shanghai Univ. of Sci. & Tech.)

The purpose of this paper is to present a self-consistent frame-work for the weak-coupling problems in waveguides. On talking about a coupling as being weak or strong, it is necessary to make definite as to what particular set of modes the said coupling is referred. With reference to a waveguide of varying cross-section, we considered in a recent paper (*Scientia Sinica*, 22, 1147-55, 1979) three different kinds of mode-sets, i.e., the ideal modes, the local modes and the super-local modes, whose coupling strengths depend on the deviation and the variation of the guide cross-section, and on the variation of the slope of the guide profile, respectively.

With proper choice of the mode set, couplings between the modes can be made sufficiently weak and the mathematics required for solving the coupled-mode equations can be greatly reduced by adopting appropriate early approximations. Thus, for an arbitrary mode set C_i , if we assume that the amplitude of the incident mode C_i remains constant, and the incident mode couples to each spurious mode C_j individually, then the original complicated coupling problem is simplified to solving an independent differential equation of the first order: $dC_j/dz = \lambda_j C_j + N_{ji} C_i$, where λ_j is the propagation coefficient of the spurious mode j , and N_{ji} is the coupling coefficient between modes i and j . Using the trial function $C_k = U_k(z) \exp(\int \lambda_k dz)$, $k = i, j$, with $U_i(z) \approx 1$, we immediately obtain the weak-coupling solution: $U_j(z) \approx \{N_{ji} \exp\{\int (\lambda_j - \lambda_i) dz\} dz$.

On the basis of our previous papers on conventional waveguides (*Scientia Sinica*, 9, 142-54, 1960; *Acta Mathematica Sinica*, 11, 238-47, 1961) and the recent paper cited above, it is shown that the coupling coefficients for ideal modes, for local modes and for super-local modes are all related by similar matrices in the sense of Lowey. Formulas are derived so that a single set of coupling coefficients yields all other sets of coupling coefficients. Physical arguments illustrate the reasonableness, under certain restrictions, of extending the applicability of the formulas to cases which also include a continuum of modes.

COUPLED MODES WITH RANDOM PROPAGATION CONSTANTS

Harrison E. Rowe and Iris M. Mack
 Bell Laboratories
 Crawford Hill Laboratory
 Holmdel, N.J. 07733

An exact theory for two coupled modes traveling in the same direction, with white random propagation constants, is developed. Applications include tolerance studies for optical directional couplers. The expected powers in the two modes are determined vs. distance along the coupler, with the ratio of propagation constant spectral density B to coupling C as a parameter. A power divider whose performance is insensitive to geometry may be obtained by proper choice of parameters. Such a device of minimum length is obtained for $B/C = 4$.

The coupled line equations are:

$$\begin{aligned} \dot{I}_0(z) &= -j\beta_0(z) I_0(z) + jC I_1(z), \\ \dot{I}_1(z) &= jC I_0(z) - j\beta_1(z) I_1(z), \end{aligned}$$

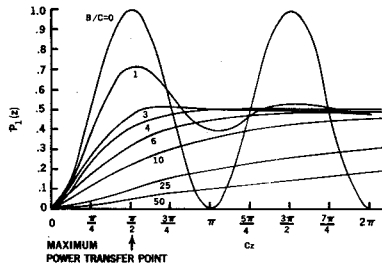
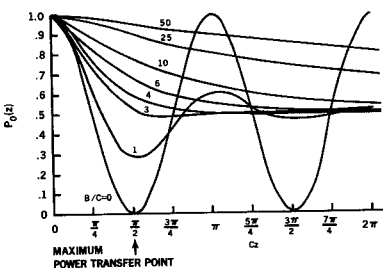
where C is the constant coupling parameter and the phase parameters $\beta_0(z)$, $\beta_1(z)$ are random and independent, having the same mean value β and spectral density B. We take as initial conditions unit input to mode 0, zero input to mode 1:

$$I_0(0) = 1, \quad I_1(0) = 0.$$

We seek the average powers in the two modes:

$$P_0(z) \equiv \langle |I_0(z)|^2 \rangle; \quad P_1(z) \equiv \langle |I_1(z)|^2 \rangle.$$

These quantities have simple expressions, shown graphically below.



INFLUENCE DE LA CONFIGURATION DES ELECTRODES DE COMMANDE
SUR L'EFFICACITE D'UN COMMUTEUR ELECTROOPTIQUE DU TYPE BOA

F. FAVRE - CENTRE NATIONAL D'ETUDES DES TELECOMMUNICATIONS
LANNION - FRANCE

Nous présentons l'analyse théorique du fonctionnement d'un commutateur électro-optique du type BOA pour l'optique intégrée. Nous montrons qu'il est possible d'améliorer l'efficacité des électrodes en les déposant sur le guide, contrairement à la configuration proposée par PAPUCHON et al (Appl. Phys. Lett. 31, 266, 1977).

Le BOA est schématiquement représenté en Figure 1. Le motif, symétrique par rapport à l'axe z, supporte localement deux modes transverses, l'un symétrique (S), l'autre antisymétrique (AS). Si une seule voie est excitée à l'entrée, le champ électromagnétique peut être considéré comme la somme des champs (S) et (AS) de même amplitude. A la sortie, l'énergie lumineuse est confinée dans une voie lorsque le déphasage $\Delta\phi$ entre les modes est un multiple de π . La commutation s'effectue en faisant varier $\Delta\phi$ de π par effet électrooptique. On montre que, pour un motif donné, la tension $V\pi$ correspondant à cette variation est proportionnelle à $T = (a/b) / (\delta(\Delta\beta/k_0) / \delta n_0)$ où :

$$\delta(\Delta\beta/k_0) / \delta n_0 = \iint f(x, y) (F_S^2(x) - F_{AS}^2(x)) G^2(y) dx dy$$

b est la demi-largeur du guide central, a la demi-distance interélectrodes, β la constante de propagation, k_0 le vecteur d'onde, δn_0 la variation maximum d'indice de réfraction, $f(x, y)$ la répartition de la composante tangentielle du champ électrique et $F(x) G(y)$ une composante normalisée du champ électromagnétique.

La figure 2 représente T en fonction de a/b pour des valeurs de la fréquence normalisée $V_X = 2k_0b(\epsilon_{eff} - \epsilon_s)^{1/2}$ comprises entre π et 2π , limites du cas bimode - (ϵ_{eff} et ϵ_s sont respectivement la constante diélectrique effective de propagation et celle du substrat). En conclusion, nous montrons qu'il est théoriquement possible d'approcher la valeur minimum de la tension de commutation quelque soit V_X en réduisant la distance inter électrodes à la moitié de la largeur du guide central.

Nous espérons présenter une confirmation expérimentale de cette théorie lors de la conférence.

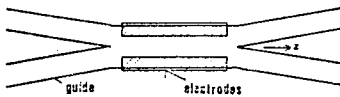


FIGURE 1

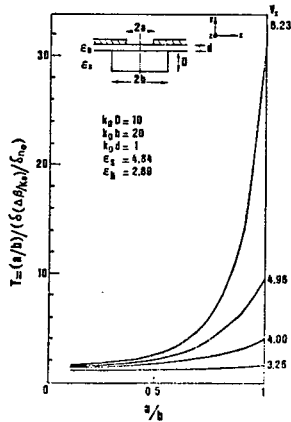


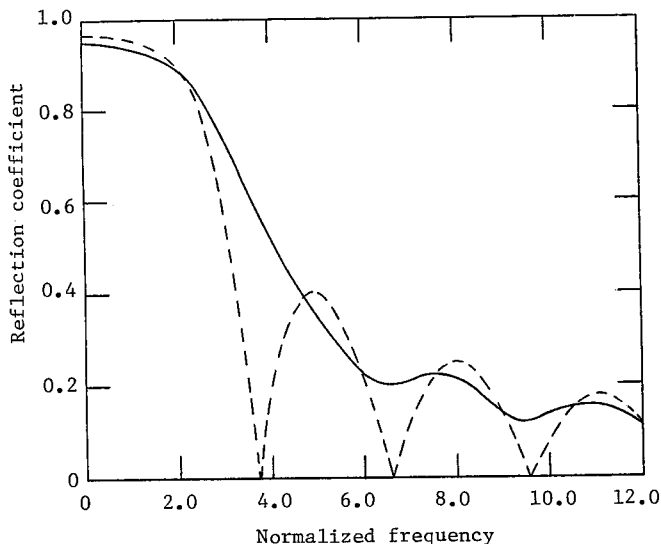
FIGURE 2

FILTER CHARACTERISTICS OF IMPERFECT PERIODIC STRUCTURES

D. L. Jaggard and G. T. Warhola
 Department of Electrical Engineering
 University of Utah
 Salt Lake City, Utah 84112

Periodic structures have played an important role in optics and electromagnetics since the late nineteenth century. Of recent interest is the use of periodic structures as filters, couplers, and distributed feedback elements in integrated optical circuits. Here we investigate the filter characteristics of passive, imperfect periodic structures. In particular, we examine the reflection of light (or other electromagnetic energy) from structures characterized by a modulated periodic dielectric permittivity. The propagation characteristics and the reflection coefficient of such structures are predicted by use of the theory of almost periodic media [see A. R. Mickelson and D. L. Jaggard, *IEEE Trans. AP-27*, 34 (1979), and D. L. Jaggard and A. R. Mickelson, *Appl. Phys.* 19, 405 (1979)].

We compare below the reflection from a perfect (periodic) structure with that from an imperfect (almost periodic) structure. The latter is modeled by 100 percent amplitude modulation of a periodic permittivity and a relatively small modulation frequency. The periodic structure displays the usual Bragg reflection characteristics (dashed line) whereas the almost periodic structure shown here exhibits a relatively smooth reflectance (solid line).



ELLIPTICAL OPTICAL FIBERS

S.R. Rengarajan and J.E. Lewis
Department of Electrical Engineering
University of New Brunswick
Fredericton, NB, Canada E3B 5A3

Three-layer step index optical fibers of circular cross-section have been studied by several workers to realize a sufficiently enlarged core for single mode propagation. A two-layer step index elliptical fiber recently has been shown to preserve polarization (Dyott, et al., Electronics Letters, 15, 380-382, 1979). Three-layer elliptical fibers combine these two features and are studied in this work.

The characteristic equations of the elliptical dielectric tube waveguide recently have been presented (Lewis, et al., IEE J. Microwaves, Optics and Acoustics, 3, 147-155, 1979). These equations are modified to study cladde, W-type and tube-type fibers. Using accurate algorithms for Mathieu functions, the characteristic equations are solved numerically to obtain phase velocity and cut-off characteristics of dominant and some higher-order modes for different eccentricities, refractive indices and thicknesses. Group velocity and power flow characteristics also are presented. A two-layer step index elliptical fiber is presented as a special case.

MULTIMODE OPTICAL FIBERS WITH NON CIRCULAR
CROSS SECTION

M.Brenici, P.F.Checcacci, R.Falciai, A.M.Scheggi
Istituto di Ricerca sulle Onde Elettromagnetiche of C.N.R.
Firenze, Italy

Optical fibers with cross section deviating from circularity can be encountered in practice due to fabrication defects.

In a previous work (P.F.Checcacci, R.Falciai, A.M.Scheggi, J.Opt.Soc.Am. 69, 1255-1259, 1979), we showed the existence in elliptical step index fibers of two distinct classes of rays: *whispering* and *bouncing* rays which represent respectively a generalization of the skew and meridional rays of the circular fiber.

The object of the present contribution is an experimental investigation of the two classes of modes corresponding to the above mentioned classes of rays, in fibers with different degree of ellipticity. To this purpose, by utilizing a technology already developed for fabricating step index (silica-plastic) fibers, we realized fibers with non circular cross section. As preforms commercial pure silica rods were used which we treated with CO₂ laser under different working conditions for obtaining preforms with variable quasi elliptical cross sections. The measurements were carried out by illuminating the fiber at an end face with a HeNe laser followed by a system of lenses which gives a light spot very small with respect to the fiber cross section and scanning the major axis of the fibers so to excite modes belonging either to the whispering or bouncing class. The near field pattern observed after a few tens of centimeters of fiber length was interpreted on the basis of the analytical ray theory developed by the authors. The prevailing existence of bouncing modes in strongly elliptical fibers was also proved, thus confirming the interest of such fibers for a better matching with injection laser and edge emitting LED's.

Non-Circular Optical Waveguides and Modal Choice

Yang Shuwen

Chengdu Institute of Radio Engineering,

Chengdu, Sichuan, P. R. C.

In this paper we investigate the propagation characteristics of light in non-circular dielectric optical waveguides based on the micro-wave-modal experiments. It is found that the attenuation of non-circular waveguides is smaller than that of circular guides and the attenuation of the odd modes is smaller than that of the even modes in non-circular dielectric waveguides. Hence it is profitable to use non-circular optical fibers. Furthermore, it is profitable to choose the odd mode. By using the non-circular guides, we can stabilize the polarization for single mode optical fiber, and the better propagation characteristic is obtained.

WEDNESDAY MORNING

June 4, 8:30 - 12:00

ANALYTICAL AND NUMERICAL TECHNIQUES

DKN 1A

Session B.8

Chairman: P. Silvester
McGill University
Montréal, Québec

FINITE ELEMENT METHOD FOR SOLVING THREE-DIMENSIONAL
ELECTROMAGNETIC DISCONTINUITY PROBLEMS

G. L. Maile

RF Technology Centre, ERA Technology Ltd.
Cleeve Road, Leatherhead, Surrey, England. KT22 7SA

R. L. Ferrari

Cambridge University Engineering Department
Trumpington Street, Cambridge, England. CB2 1PZ

A finite element method that determines the vector fields within a closed electromagnetic structure such as a waveguide or cavity is described. The programmed method is applicable to problems where the presence of arbitrary discontinuities makes the analytical solution of Maxwell's equations impracticable and previous finite element methods inappropriate.

A functional is expressed in terms of either the electric or magnetic field vector variable. The boundary conditions are shown to be vector generalisations of the Dirichlet and Neumann conditions that occur in scalar finite element analysis. The functional is recast in algorithmic form assuming a linear variation of field within a general tetrahedral sub-domain. Global matrices are constructed for an assemblage of tetrahedra filling the volume of interest. The assembled global matrix problem can be solved either as a deterministic problem representing a waveguide with a known modal excitation or as an eigenvalue problem. General user orientated computer programs have been written and applied initially to test problems for which exact values are available for comparison and then to some three-dimensional discontinuity problems that are only soluble by the few existing three-dimensional vector numerical methods.

Equivalent circuit parameters have been determined for an H-plane waveguide junction discontinuity. The results are compared with published theoretical and experimental values and data obtained by further experimental measurements. Reflection and transmission coefficients for the waveguide discontinuity formed by a slant interface between dielectric media of different permittivities are presented. Dominant mode resonance frequencies of a cavity partially loaded with dielectric are compared with those obtained by a three-dimensional numerical method formulated by Albani and Bernardi based on the discretisation of Maxwell's equations in integral form and a three-dimensional transmission-line matrix method (S.Akhtarzad and P.B.Johns, Proc.IEE, Vol.122, No.12,1975, pp.1344-1348). The results indicate that the new finite element method can be applied to a wide range of electromagnetic problems, accuracy being a monotonic function of the number of elements employed in the sub-division.

NUMERICAL MODELING OF ARBITRARY BODIES
WITH TRILATERAL SURFACE PATCHES USING
THE ELECTRICAL FIELD INTEGRAL EQUATION

J.J.H. Wang
Engineering Experiment Station
Georgia Institute of Technology
Atlanta, Georgia

Arbitrary Surfaces can be conveniently modeled to any desired degree of accuracy by planar Trilateral patches. Numerical modeling with trilateral surface patches using the magnetic field integral equation was conducted by Wang (J.J.H. Wang, Radio Science, 13, 947-952, 1978). Trilateral patch modeling using the electric field integral equation was investigated by Wilton, et al. (D.R. Wilton, S.S.M. Rao, A.W. Glisson, 1979 AP-S International Symposium, 151-154, 1979).

In this presentation a surface-patch modeling technique using the electric field integral equation is discussed. The present algorithm differs from that of Wilton, et al. in the basis functions and the moment generating process. Numerical examples will be presented in comparison with known data for several types of geometries.

SOLVING A CLASS OF OPEN AND CLOSED
DISCONTINUITY PROBLEMS WITHOUT MATRIX INVERSION

R. Mittra and C. H. Tsao
Department of Electrical Engineering
University of Illinois
Urbana, Illinois 61801

The purpose of this paper is to show how the spectral domain approach can be applied in conjunction with the FFT algorithm to solve a wide class of discontinuity problems in open and closed regions. Previously, the spectral approach had been successfully employed for solving a class of scattering problems, e.g., an iris discontinuity in a rectangular waveguide, a periodic grating comprising an infinite array of strips, and a perforated screen. It has been shown that these problems can be solved without resorting to matrix methods that are conventionally employed for solving problems of this type. Three important attributes of the spectral approach are: (i) it is numerically efficient, (ii) it has a built-in accuracy check; hence, the solution is reliable, and (iii) it is capable of handling electrically large structures (e.g., gratings with cell sizes on the order of several wavelengths), which would require generation and inversion of a prohibitively large and costly matrix if formulated in a conventional manner.

In this paper, we present the generalization of the spectral approach where the geometry of the region on two sides of the interface is dissimilar. Some examples of such structures are a step discontinuity in a waveguide and a corrugated surface. Clearly, the waveguides on the two sides of the junction plane are different for the step discontinuity problem. Similarly, for the corrugated structure, the region above the interface is an infinite half-space whereas the one below is a short-circuited waveguide of finite length.

We show in this paper how the original integral equation for the problems of the type described above can be embedded into one which is valid over an extended range that encompasses the entire cell. (This procedure is similar to the one used previously for symmetric structures.) Next, the solution of the extended-range integral equation is derived via an iteration procedure which makes express use of the FFT algorithm at each step of the iteration. Satisfaction of the boundary condition is verified at each step and provides a means for checking the accuracy of the solution. Numerical results illustrating the application of the method to both open and closed region problems are included in the paper. The examples serve to demonstrate the relative numerical efficiency and accuracy of the spectral domain approach vis-a-vis the conventional methods.

NUMERICAL ASPECTS OF AN EFFICIENT SCHEME
FOR COMPUTING THE REFLECTED FIELD FROM A
SMOOTH ARBITRARY SURFACE

A. M. Rushdi and R. Mittra
Department of Electrical Engineering
University of Illinois
Urbana, Illinois 61801

This paper considers the problem of electromagnetic reflection from a smooth surface that is specified only numerically at a set of grid points. A conventional solution to this problem entails a numerical interpolation of the surface followed by a search for the specular point. The reflected field is obtained next via the geometrical optics formula, which, however, is accurate only to the order of k^0 . Furthermore, no convenient means is available in this approach for obtaining the higher-order term. In contrast, the present method is both efficient and accurate because it bypasses the surface interpolation and yields an expression for the field that is accurate to the order k^{-1} .

The theory of the method has been discussed by us in an earlier paper (Rushdi and Mittra, URSI Meeting, Boulder, 1979) and we emphasize only some aspects of the numerical computation in this paper. Basically, the method begins by computing the reflected rays off the surface at the numerically specified points. Next, the observation point P is associated with the pencil composed of the reflected rays nearest to P. Finally, the field at P is computed via the Generalized Geometrical Optics (GGO) Formula (Mittra and Rushdi, URSI Meeting, Seattle, Washington, June 1979), which allows for a paraxial transverse variation of the field and is accurate paraxially to within the k^{-1} term. One of the basic differences between the present method and its earlier version (Mittra and Rushdi, AP-S Trans., November 1979) is the use of the more accurate GGO formula. Another important difference is that the efficiency of the method has been improved by eliminating the step required to obtain the "mean ray."

The accuracy and efficiency of the method have been verified by applying it to the computation of the H-plane field scattered from a hyperboloid with a feed located at its external focus. Only a numerical description of the hyperboloid surface was supplied to the computer. The k^0 part of the field has been found to have excellent agreement with the exact solution of Keller, et al. (Comm. on Pure and Appl. Math., 1956), while the total field has been compared with that obtained by the time-consuming PO integration method. Accurate results were obtained at a nominal cost, approximately 0.04¢ per observation point.

ON THE EVALUATION OF SOMMERFELD INTEGRALS BY A
MODIFIED FILON'S METHOD

H.J. Price and T. C. Kalahdar Rao

In the numerical evaluation of many complex integrals in which the integrand contains a complex exponential, the oscillations of the exponential require closely spaced steps. This is the case in the numerical evaluation of Sommerfeld integrals which occur, for example, in the analysis of electromagnetic propagation conducting grounds.

In the past, Newton's iterative method has been used. This paper presents an alternative method which has a number of advantages over other schemes. A change of variable is made so that the integrand can be expressed as a function of the imaginary part of the exponent of the exponential term. The integral can then be expressed as a sum of two integrals which involve multiplicative sine and cosine terms. Filon's method can be applied to the resulting integrals, allowing larger integration steps with a resulting reduced computation time.

Numerical results are presented.

A NUMERICAL TECHNIQUE FOR CALCULATING INTERACTIONS
BETWEEN WIRES AND SURFACES

W. A. Imbriale*
Jet Propulsion Laboratory
California Institute of Technology
Pasadena, California 91103

and
R. J. Pogorzelski
TRW Defense and Space Systems Group
Redondo Beach, California 90278

Thin wire structures are typically solved by using the method of moments. This method of solution works well when the structure is relatively small in terms of wavelengths. Accurate solutions for scattering from large surfaces can be obtained by the use of physical optics as the method of moments solution is generally impractical due to the large size matrix required. This paper describes a method for computing the interactions between thin wire structures and surfaces utilizing a combination of a method of moments solution for the wires and a physical optics solution for the surfaces.

The method of solution is as follows: the currents on the wires due to a set of impressed voltages V_0 , in the absence of the surface scatterers, is determined by the method of moments and is denoted the zeroth order current $I_0 = Z^{-1}V_0$ where Z is the impedance matrix of the wire structure in free space. The wire structure is assumed to radiate and the physical optics currents induced on the surfaces are calculated, $J_0 = R_{WS} I_0$ where J_0 is the physical optics current and R_{WS} is a matrix which operates on the wire currents to give J_0 . Physical optics is then used to determine the fields radiated by the surfaces which in turn induce voltages on the wires; thus $V_1 = R_{SW} J_0$ where R_{SW} is a matrix which transforms the physical optics current to wire voltages. The currents on the wires due to these voltages are $I_1 = Z^{-1}V_1$. The process is then repeated for each successive scattering computation. The total wire current I_T due to the components of wire and surface scattering is computed by adding up the currents due to the infinite number of scattering interactions, thus $I_T = [U - Z^{-1}R_{WS}R_{SW}]^{-1}Z^{-1}V_0$ where U is the unit matrix. Once the total wire currents are known, the total physical optics currents and the far field radiation patterns can be computed.

The technique is applied to the problem of a dipole above a finite ground plane and computational results are presented.

*Formerly of TRW Defense and Space Systems Group

THE UNIMOMENT-MONTE CARLO METHOD
APPLIED TO TWO-DIMENSIONAL INTERIOR BOUNDARY-VALUE PROBLEMS

R.W.Campbell
Martin Marietta Corporation
Aerospace Division
Denver, Colorado

The Unimoment-Monte Carlo method, originally developed as a solution approach to electromagnetic exterior scattering problems (E.L. Coffey, "An Analog/Hybrid Computer Solution of Electromagnetic Scattering Problems," :PhD dissertation, Virginia Polytechnic Institute and State University, 1976), has been applied to the solution of two-dimensional interior boundary-value problems. This technique relies upon a combination analytical/probabilistic formulation and results in an overall solution approach with distinct advantages over standard numerical methods. For example, in addition to being able to handle arbitrary problem domains and boundary conditions, the Unimoment-Monte Carlo method allows for an approximate closed-form solution over the greater part of the domain as opposed to a point-by-point numerical solution generated by other techniques. Results at selected points within the domain can also be obtained without having to solve the entire problem; thus a quick 'coarse' look at critical points within a complex problem can be obtained before attempting a more rigorous solution.

Results will be presented for simple two-dimensional geometries considering the special cases of Laplace's equation and the scalar Helmholtz equation. Although suffering more in accuracy than other conventional numerical approaches due to the probabilistic side of the technique, satisfactory results have been obtained. Extension of the method to more general two and three-dimensional boundaries will be briefly discussed.

A HYBRID FD-TD/MOM APPROACH TO THE ELECTROMAGNETIC
COUPLING AND APERTURE PENETRATION

Allen Taflove and Korada Umashankar
IIT Research Institute
10 West 35th Street
Chicago, IL 60616

General electromagnetic coupling and shielding problems have been difficult to treat with analytical and/or numerical methods because of the complicating effects of apertures, curvatures, corners, and complex internal contents of structures. Only canonical structures and simple aperture shapes have been studied previously in an attempt to gain insight into coupling mechanisms using analytical and method of moment (MOM) numerical approaches. A powerful alternate approach is the (FD-TD) Finite Difference-Time Domain method (A. Taflove, "Time Domain Solutions for Electromagnetic Coupling", IIT Research Institute Final Technical Report, RADC-TR-78-142, June 1978) which allows computation of the penetrated internal EM fields by direct modeling of realistic structures, apertures, and internal contents.

In order to treat coupling problems more effectively, new hybrid techniques have been developed which involve combining the FD-TD method either with the MOM or some other appropriate technique. The hybrid FD-TD/MOM approach which will be presented, is based on a novel use of the so-called, "field equivalence theorem" due to Scheikunoff. In the hybrid FD-TD/MOM method, the coupling problem is analyzed in two steps by treating the relatively simple external and the relatively complex internal regions separately. The method involves first, determination of an equivalent short-circuit current excitation in the aperture region of the structure which is obtained by solving an exterior problem (using MOM) with the aperture being closed for a given external illumination. The computed equivalent current excitation in the aperture region is next utilized to illuminate the interior region and the penetrated interior fields are computed by the FD-TD method. The computed interior fields for an aluminum cylinder with one open end are compared with available experimental and numerical results to demonstrate validity of the technique.

The hybrid method based on Scheikunoff's "field equivalence theorem" is also applicable when coupled wires or material bodies are present and coupled strongly to the aperture. The results of the application of the hybrid MOM/MOM approach to "a finite wire scatterer behind a narrow slot perforated conducting screen" are also compared with available data.

DFNA - THE DIRECT FORM OF NETWORK ANALOGS: E. L. Coffey and T. H. Lehman, The BDM Corporation, Albuquerque, NM

Electromagnetic scattering from objects immersed in time-varying, non-linear, or dielectric media must include the effects of the medium in the mathematical and numerical formulations of the problem. This is difficult using integral equation or method of moments techniques except for the simplest of objects. The Direct Form of Network Analogs (DFNA) is amenable to this task as well as many others.

Briefly, all space is divided into a family of cells, the geometry of which maybe arbitrary or conform to the scatterer and volume of space to be considered. Maxwell's equations can be solved in each cell (subject to the boundary conditions imposed at intercell boundaries) for circuit components (R's, L's, and C's) and an interconnection diagram (network). The resulting circuit, which may contain time-varying or non-linear components, is solved by using a large-scale network analysis code such as NET-2 or SCEPTRE. Any dielectric non-uniformity is absorbed into the capacitance components. This method has three advantages over some other techniques: (1) the problem can be worked "in the small" at first, then reconnected using the derived circuit components; (2) all network variables represent integrated field variables, hence there is gained immediate physical insight into the problem; and (3) no new computer codes need be developed.

The details of the DFNA method will be presented, after which several examples from various practical electromagnetics problems will be needed to illustrate how the method is used, the method's advantages and disadvantages, and what computational problems must be overcome.

MATRIX SIZE REDUCTION FOR MICROSTRIP CIRCUITS

Y.L. Chow and M. Tutt, Department of Electrical Engineering, University of Waterloo, Waterloo, Ontario, Canada. N2L 3G1

The spatial Green's function for finite microstriplines has recently been obtained by Chow (URSI Meeting, Boulder, Co., November 5-9, 1979, accepted for publication in MTT). As a result it is possible to calculate the input impedance of most circuits of microstriplines by the moment method. For a long and complicated microstripline, however, the matrix in the moment method solution may become uneconomically large. Therefore, it is desirable to seek a scheme to reduce the matrix size.

The scheme in fact is readily available from R.F. Harrington ("Field Computation by Moment Method", The MacMillan Co., New York, 1968, pp. 47-48). There he approximates a triangle basis function by three step functions and effectively reduces two matrix elements to one. Carrying this approximation to both the basis and testing functions for a Galerkin solution, he reduces effectively four elements to one and thus reduces the matrix size by a factor of two.

Such reduction can be repeated to reduce the matrix size by multiples of 2, without undue loss of accuracy. The reason is that while the repeated reduction decreases the accuracy, it is partially compensated by the increase in accuracy in approximating the triangle basis and testing functions.

For such reduction for microstriplines, the formulas given by Harrington have to be multiplied by a factor of two.

This paper ends the above studies with two numerical examples.

WEDNESDAY MORNING
June 4, 8:30 - 12:00

RANDOM MEDIA

DKN 1B

Session B.9

Chairman: A. Ishimaru
University of Washington
Seattle, WA.

BEAM WAVE INTENSITY FLUCTUATIONS IN WEAK AND
STRONG ATMOSPHERIC TURBULENCE

J. Carl Leader
McDonnell Douglas Research Laboratories
P.O. Box 516, St. Louis, MO 63166

The analyses of the mutual intensity function (J. C. Leader, J. Opt. Soc. Am. 68, 175-185, 1978) and intensity covariance (J. C. Leader, J. Opt. Soc. Am. 69, 73-84, 1979) of a spatially partially-coherent wave propagating through atmospheric turbulence have been extended to provide solutions for the case of a beam wave of arbitrary focus. Although the explicit expressions for the coherence length, intensity, radius, and phase front curvature resulting from the second order analyses are shown to be valid regardless of the strength of turbulence, the intensity covariance expression becomes invalid when the plane-wave log-intensity deviation $[\sigma_p = (1.23 k^{7/6} C_n^2 R^{11/6})^{1/2}]$ exceeds unity. The intensity covariance analysis fails to predict observed strong-turbulence intensity-fluctuations because the expressions for the log-amplitude and phase log-amplitude structure functions used in the analysis become invalid under strongly turbulent conditions. The physical reason why the structure functions and attendant analyses fail in strong turbulence is the onset of multiple scattering which is reflected in a reduced spatial coherence of the propagating wave. However, because the extended analyses treat the propagation of partially coherent waves it is possible to calculate the intensity fluctuations resulting from propagation over a strongly turbulent path as a succession of weakly turbulent intervals if the coherence parameters of the beam along the path may be estimated. This iterative procedure has been performed using coherence parameter values obtained from the second-order analyses and phase variance values obtained from the self-consistent (iterated) calculations of the intensity variance. The functional variation of the log-amplitude variance (employed in the computations) was calculated by the extended Tatarskii method (S. F. Clifford, et al. J. Opt. Soc. Am. 64, 148-154, 1974) using the quadratic approximation for the complex-phase structure function (for calculational self-consistency) without an arbitrary frequency cutoff parameter. This iterative technique for calculating intensity statistics yields normalized values of the intensity variance that are in good agreement with measured data and saturate to a value of unity in extremely strong turbulence as required. Limitations and extensions of this calculational technique will be discussed.

RADIO SCINTILLATIONS DURING OCCULTATIONS
BY TURBULENT PLANETARY ATMOSPHERES

Richard Woo

Jet Propulsion Laboratory, California Institute of Technology
Pasadena, CA 91103

Akira Ishimaru

Department of Electrical Engineering, University of Washington
Seattle, WA 98195

Fang-Chou Yang

Dikewood Corporation, Los Angeles, CA 90024

The radio occultation experiment which uses the radio link between the earth and spacecraft passing behind planets has proven to be a useful method for remote sensing turbulence in planetary atmospheres. In this paper we examine the effects of defocusing and anisotropic irregularities on the turbulence-induced fluctuations of the radio occultation signal when the fluctuations are weak (variance of log-amplitude fluctuations less than unity) and the outer scale is larger than the Fresnel size. We employ Rytov's method along with geometrical optics to study the frequency spectra and coherences of the log-amplitude and phase fluctuations of spherical waves operating at one as well as two frequencies. The turbulence is assumed to be described by a spatial wavenumber spectrum that is power-law. Examples of numerically computed spectra and coherences are given to show their dependence on defocusing and anisotropy. The theory is demonstrated by comparison with measurements of the Venus atmosphere made by Pioneer Venus in 1979 at 2.3 and 8.4 GHz.

EFFECTIVE PROPAGATION CHARACTERISTICS OF DISCRETE RANDOM MEDIA

V. N. Bringi, H. Direskeneli, V. K. Varadan,
V. V. Varadan, and T. A. Seliga
Wave Propagation Group
Department of Electrical Engineering,
Department of Engineering Mechanics,
and the Atmospheric Sciences Program
The Ohio State University
Columbus, Ohio 43210

The propagation of coherent electromagnetic waves in a discrete random medium has been previously analyzed using the T-matrix of a single scatterer together with configurational averaging procedures. This paper presents sample computational results of the effective propagation constant of coherent waves in random media (such as attenuation and phase shift) as a function of scatterer concentration and electrical size. The scatterers are considered to be spheroidal in shape with either parallel or random orientation and randomly distributed in a supporting or matrix medium of infinite extent. Both perfectly conducting and dielectric scatterers are considered with the matrix medium being a lossless dielectric. Applications of such "effective" properties of random media are considered in the light of artificial dielectrics, echo reduction, etc.

DIFFUSION OF A BEAM WAVE IN RANDOM DISCRETE SCATTERERS

Akira Ishimaru, Rudolf Cheung, and Yasuo Kuga
Department of Electrical Engineering
University of Washington
Seattle, Washington 98195

The study of wave propagation and scattering in a random distribution of scatterers has attracted considerable attention in recent years because of the increasing interest in optical communication through fog and millimeter wave propagation in rain.

Plane wave solutions for a slab of discrete scatterers have been obtained by solving the equation of transfer using the matrix eigenvalue technique and the Monte Carlo method. In this paper, the solution using the diffusion approximation is presented and compared with the exact solution. It is shown that except for a thin slab case, the agreements between the diffusion solution and the exact solutions are excellent.

The beam wave solution, however, is quite different from the plane wave solution. This is in contrast with the forward scatter solution for turbulent media with large scale sizes. In this case, there is hardly any difference between the beam wave and the plane wave solutions. For discrete scatterers with sizes comparable to a wavelength, the scattering takes place in all directions and therefore, there is a considerable beam spread and backscattering, and these scattered waves for a beam wave are quite different from those of plane wave.

This paper presents a detailed theoretical and experimental study of the diffusion of a beam wave for a slab of discrete scatterers. The theoretical solutions are obtained in the form of Fourier Bessel integrals which satisfy the boundary conditions at the front and the back sides of the slab. The coherent and incoherent transmitted fluxes are calculated.

The experiments are conducted using an optical beam with the beam diameter of 0.544 mm and $\lambda = 0.632 \mu\text{m}$ and latex spheres with $D = 0.481 \mu\text{m}$. The average scattering cross section of $0.126 \mu\text{m}^2$, and the mean cosine of the scattering pattern $\bar{\mu} = 0.809$ are calculated using the Mie solution. The volume densities range from 10^{-4} to 10% corresponding to the optical depth of 2.16×10^{-2} to 2.16×10^3 for a 50 mm long glass container. The measured intensities using the detector with a small finite receiving area show close agreement with the theoretical predictions. Because of the large beam spread, the received intensity is found to be close to the coherent intensity.

COHERENT WAVE PROPAGATION THROUGH A SPARSE
CONCENTRATION OF PARTICLES

G. S. Brown
Applied Science Associates, Inc.
Apex, NC 27502

The Foldy-Twersky integral equation (FTIE) for the average or coherent field propagating through a sparsely populated, random, uncorrelated distribution of particles is solved to show that the average field inside any particle is a plane wave. This result is in conflict with the average single particle integral equation which dictates that the average internal field cannot, in general, be a plane wave. The conflict is a consequence of the approximate nature of the FTIE and it can be resolved by examining the conditions under which the average single particle scattering amplitudes resulting from the two integral equations are nearly equal. The major implications of this analysis are that (1) the classical Foldy result for the propagation constant of the average or coherent field [L. L. Foldy, Phys. Rev., 67(2), 107-119, 1945] follows directly from the FTIE and its implicit assumptions regardless of the electrical or physical properties of the particles, and (2) the FTIE only applies to situations where the effects of multiple scattering upon the coherent field are negligible.

MULTIPLE PHASE-SCREEN CALCULATION OF THE
TEMPORAL BEHAVIOR OF STOCHASTIC WAVES

D. L. Knepp
Mission Research Corporation
P.O. Drawer 719
Santa Barbara, California 93102

A numerical solution of the parabolic wave equation for plane-wave propagation through a finite random slab is obtained. The random slab is composed of electron density fluctuations characterized by a Bessel function power spectral density (Shkarofsky, Can. J. Physics, 46, 2133-2153, 1968) which is essentially a power-law with an explicit inner scale cutoff. In the solution technique, the random slab is divided into a finite number of slices. The field fluctuation through each slice is calculated by replacing the slice by a phase-changing screen located at its center, whose statistical properties are determined from the statistics of the electron density fluctuations. At each phase-screen, the statistical phase is added to the electric field phase and the wave is then propagated to the next phase screen or to the observer. After obtaining the numerical solution at a number of discrete frequencies centered about a carrier frequency, a time domain solution can be obtained by the use of Fourier transform techniques.

Results for the mean time delay and the time delay spread of a modulated waveform are compared to the analytical results of Yeh and Liu (Radio Science, 12, 671-680, 1977) using temporal moment methods. Intermediate numerical results for the two-frequency mutual coherence function are compared to the analytical results of Sreenivasiah, et al (Radio Science, 11, 775-778, 1976) valid in the strong-scattering regime.

Time domain results after propagation through a strong, dispersive gaussian lens are presented and shown to be identical to analytical results. Also shown are the expected dispersive and scattering effects due to propagation of a pseudo-noise phase-shift keyed modulated waveform through a finite sized random barium cloud at a carrier frequency of 100 MHz.

FULL-WAVE SOLUTIONS FOR THE DEPOLARIZATION OF THE
SCATTERED RADIATION FIELDS BY ROUGH SURFACES OF ARBITRARY SLOPE

Ezekiel Bahar
Electrical Engineering Department
University of Nebraska, Lincoln, Nebraska 68588

Employing a variable coordinate system associated with the local features of two-dimensionally rough surfaces with arbitrary slope, full-wave solutions are derived for the depolarization of the scattered radiation fields. These full-wave solutions are compared with the quasi-optics solution and the iterative or perturbational solutions for slightly rough surfaces and they are shown to bridge the wide gap that exists between them.

The full-wave solutions are consistent with energy conservation, duality and reciprocity relationships in electromagnetic theory. These solutions account for upward and downward scattering of the incident waves with respect to the horizontal reference plane, thus shadowing and multiple scattering are considered. Applications to two-dimensionally periodic structures and random rough surfaces are also presented. The full-wave solutions are examined for Brewster, grazing and specular angles and backscatter. Special consideration is also given to good conducting boundaries.

ELECTROMAGNETIC SCATTERING FROM ROUGH SURFACES
BASED ON STATISTICAL CHARACTERIZATION OF THE TERRAIN

Robert J. Papa and John F. Lennon
Deputy for Electronic Technology
Rome Air Development Center
Electromagnetic Sciences Division
Hanscom AFB, MA 01731

This paper will present two aspects of a program to calculate electromagnetic scattering from rough terrain: the use of statistical estimation techniques to determine topographic parameters and the results of a single-roughness-scale scattering calculation based on those parameters, including comparison with experimental data. The literature contains well established formulas for the normalized bistatic cross section of terrain which is gently undulating, with surface height variations that are large compared to a wave length. In addition, there are several theoretical models for surfaces characterized by two scales of roughness. All these formulations require the terrain to be described by statistical quantities such as the type of distribution appropriate to the surface heights, their mean value and variance, and the degree of correlation among points in the region. For the present calculation, digitized topographic maps are used to generate data bases for the required scattering cells. The application of estimation theory to the data leads to the specification of statistical parameters for each cell. The estimated parameters are then used in an hypothesis test to decide on a probability density function (PDF) that represents the height distribution in the cell. The accuracy of the analysis depends on the selection of appropriate PDFs, the available data, and the estimators employed. For the applications of interest, large numbers of cells are involved; this factor, along with the digitized measurement structure, and the complexity of the multivariate height distributions resulted in the first estimation being based on a single observation of the multivariate data. A subsequent approach involves multiple observations of the heights on a bivariate basis, and further refinements are being considered. In the second part of this presentation the results of applying the statistical analysis to a site in eastern Massachusetts will be used in a single-roughness-scale electromagnetic scattering analysis. This allows comparison with experimental forward scatter data available at that site. The computer program calculates the amount of specular and diffuse multipath power reaching a monopulse receiver from a pulsed beacon positioned over a rough earth. The program allows spatial inhomogeneities and multiple specular reflection points. The calculated loss of boresight pointing accuracy attributable to diffuse multipath is then compared with the experimental results. The model is now being extended to include the case of two scales of roughness and improved parameter estimation.

WEDNESDAY MORNING

June 4, 8:30 - 12:00

HF - TO - UHF ARRAYS

DKN ID

Combined Session AP-S/B.10

Chairman: H.V. Cottony
5204 Wilson Lane
Bethesda, MD.

The following papers belong to the IEEE AP-S Symposium and the summaries are included in the IEEE AP-S Digest under Combined Session AP-S/B.10.

1. A BROADBAND CAVITY ANTENNA WITH A STEERABLE CARDIROID PATTERN, B.A. Munk and C.J. Larson, Ohio State University, Columbus, Ohio.
2. THE TERMINATED RADIAL ARRAY AS A HIGH FREQUENCY SCANNING BEAM ANTENNA, D.W. Griffin, University of Adelaide, South Australia.
3. OPTIMUM PATTERN SHAPE OF SHORTWAVE ANTENNAS FROM RADIO-LINK COMPUTATIONS, A. Stark, Rohde & Schwarz, Munich, Germany.
4. A NEW COMBINED ANTENNA AND PROPAGATION MODEL, S. Chang, IIT Research Institute, ECAC, Annapolis, MD.
5. A COMPACT REACTIVELY STEERED ANTENNA ARRAY, R.J. Dinger, W.D. Meyers, Naval Research Laboratory, Washington, D.C.
6. MINIATURIZATION TECHNIQUES FOR HF LOG-PERIODIC DIPOLE ARRAYS, H. Shnitkin, Norden Systems, Norwalk, Connecticut.
7. A WIDEBAND CORNER-REFLECTOR ANTENNA FOR 240 TO 400 MHz, J.L. Wong and H.E. King, The Aerospace Corporation, Los Angeles, CA.

THE DIRECTIVITY OF ANTENNA ARRAY EXCITED
BY WEIGHTED WALSH CURRENT

Xie Chu-Fang

Chengdu Institute of Radio Eng.
Chengdu, Sichuan
People's Republic of China

Although Walsh functions and their applications have been receiving much attention recently, there are only a few papers concerning the problem of radiation. The subject of this paper is to calculate the directivity of a dipole array when excited by Walsh current. It is indicated that, when excited uniformly or weighted sinusoidally, the directivity of a dipole array for $\rho = L/ct = 100$ is 21.7 or 16.7 respectively.

PHASE-FREQUENCY SCANNABLE TRAVELING WAVE ARRAYS

Henry J. Stalzer, Jr., Manhattan College, Riverdale, NY; and
Alexander Hessel and Jerry Shmoys, Polytechnic Institute
of New York, Farmingdale, NY.

Arrays of periodically loaded line sources can produce electronic beam steering with phase-frequency control. These structures require fewer phase shifters than do their phase-phase counterparts.

An example of a structure of this type is a dielectrically loaded corrugated surface excited with a constant phase gradient across its rectangular grooves. Such a structure supports a spectrum of surface waves of both polarizations. By introducing periodic discontinuities along the grooves, the surface waves become leaky and radiate at an angle dependent on the signal frequency, the periodicity of the discontinuities and the phase gradient. The structure thus provides for phase scan in one plane and frequency scan in the orthogonal plane.

In order to design such an array, it is necessary to determine the surface wave propagation constants, prior to imposing of periodic loading, as a function not only of frequency, but also of phase gradient, and to ascertain the regions of possible single mode operation in the desired polarization. It is found that as the phase scan from broadside is increased, the frequency range over which a single surface mode will propagate is decreased and the purity of the polarization is diminished. Curves for several designs are presented which take into account the scan and polarization limitations imposed by the interaction of phase and frequency scanning.

USE OF A QUAD ARRAY TO GENERATE AN
APPARENT TARGET POSITION

D. C. WU AND R. E. SURRETT
NAVAL RESEARCH LABORATORY
WASHINGTON, D. C.

The Naval Research Laboratory has developed a state-of-the-art Simulation facility (from 8 to 18 GHz) to enable test and evaluation of electronic warfare systems and techniques for countering the missile threat to the Navy. In this facility, a matrix antenna array is located on a spherical surface at one end of a large shielded anechoic chamber. This array directs and radiates modulated RF energy to simulate target cross-section, location and motion as would be encountered by a missile seeker in a "real world" electromagnetic environment. The missile seeker under test is mounted on a three-axis flight simulator at the other end of the chamber, a distance of 22.86 m from the array. This location is also the focal point for the matrix antenna array. As seen from the focal point, the array provides a nominal field-of-view of 20° in azimuth and 10° in elevation, while spacing between antennas is 1.25° . This paper summarizes the work performed in the study of target position generation via a quad array.

The matrix antenna array is subdivided into basic building blocks known as "quads". A quad consists of four adjacent antennas located at the corners of the square. Signals are routed to the selected quad through a switch matrix. Attenuators and phase shifters are used to control the amplitude and phase of the excitation for each of the four antennas. This controlled excitation permits target positions within the quad to be generated with a high degree of accuracy.

The apparent target position generated by the quad array was measured by a phase-type interferometer system mounted on the flight simulator. The phase interferometer consisted of two pairs of antennas, one vertically displaced and the other horizontally displaced. Antenna spacing was 38.1 cm. The target position in azimuth and elevation is directly computed from the measured electrical phase of each antenna pair.

The required excitation for each quad array antenna is obtained from an exact expression which assumes equal phase excitation and is a function of interferometer geometry, quad array geometry, target position, and frequency. This expression shows that the simulated target position always lies within the physical area bounded by the four antennas. In addition, it provides for a constant radiated power from the quad independent of the simulated target position. When the quad array is excited as required, an overall measured target position accuracy of one milliradian is obtained in the 8 to 18 GHz region.

WEDNESDAY MORNING
June 4, 8:30 - 12:00

SPECIAL SESSION ON OPTICAL COMMUNICATIONS IV
FIBER AND GUIDED WAVE OPTICS III

DKN 2B

Combined Session B.11/AP-S

Chairman: L.B. Felsen
Polytechnic Institute of New York
Farmingdale, N.Y.

Organizer: G.L. Yip
McGill University
Montréal, Québec

The following papers belong to the IEEE AP-S Symposium and the summaries are included in the IEEE AP-S Digest under Combined Session B.11/AP-S.

4. CALCULATION OF DISPERSION FOR TWO OPTICAL FIBER PROFILES BY THE PROPAGATING BEAM TECHNIQUE, M.D. Feit and J.A. Fleck, Jr., Lawrence Laboratory, University of California, Livermore, CA. 94550.

9. SIGNAL PROPAGATION IN THE MULTIMODE OPTICAL WAVEGUIDE AS A RANDOM MEDIUM, K. Itoh, K. Tatekura and H. Itoh, Department of Electronic Engineering, Hokkaido University, Sapporo, 060 Japan.

FLAT DISC, RADIALY NON-HOMOGENEOUS, LENS

S. Cornbleet
Department of Physics, University of Surrey
Guildford, England

Radially variable media, with a refractive index law $n = \text{sech } \rho$, are known to focus rays from an axial source at points on the axis of symmetry. If the system is limited by a plane surface perpendicular to the axis, mid-way between the source and the first of these foci, at which point the rays are all parallel to the axis, a lens is created with the exit rays remaining parallel to the axis. This is the "short focus horn" of Brown (Microwave Lenses, Methuen p89, 1953). A considerable portion of the material of such a lens is superfluous in that the necessary outward spread of rays need not be contained within a dielectric medium. A thin flat lens is proposed in which the radial gradient of refractive index is sufficient to collimate the rays within the thickness of the medium. An optical lens of this kind has been discussed but only in the paraxial approximation $f/D = 20$ (E.W. Marchand, Gradient-Index Optics, Academic Press, 1978, p87). A wide angle, $f/D = 1$ is considered here.

Rays from an axial source are incident on the plane front face, at which the assumption is made that locally the rays obey Snell's law as for an infinite uniform medium. Such an assumption is common in physical optics and its validity is discussed. The rays are then required to curve so that they all become horizontal on reaching a plane perpendicular to the axis within the medium, thus giving a plane exit surface. The integral representing the ray path in a radially non-uniform medium is, however, no longer complete as in the short focus horn. Trial functions have to be inserted until a close enough approximation to the plane exit surface is obtained. This is shown to be possible for the proposed geometry and a refractive index law is thereby derived.

The symmetry of the resulting design is such as to allow the insertion of a central reflecting surface converting the lens into a plane coated reflector.

ELECTROMAGNETIC WAVE PROPAGATING IN
UNIFORM WAVEGUIDES CONTAINING
INHOMOGENEOUS DIELECTRIC

Lin Weigan
Chengdu Institute of Radio Engineering
Chengdu, Szechuan
People's Republic of China

Uniform waveguides filled with inhomogeneous dielectric whose permittivity varies along one dimension are studied. Emphasis is given to the modes of propagation and to the calculation of the propagation constants. Exact solutions are given for some special cases. In some of these only asymptotic or polynomial solutions have been available previously. No restriction is placed on the waveguide dimensions so that results developed here apply to the transmission on optical frequency waves as well as to microwave and millimeter waves.

In the waveguide problems of this paper, results obtained cannot be directly found in the existing literature and have been worked out from fundamental theory of differential equations. The theory of the confluent hypergeometric function has been of great help in our treatment of these problems.

FIRST-ORDER CORRECTIONS TO EXPRESSIONS
FOR PARAXIAL BEAM PROPAGATION IN MULTIMODE
PARALLEL-PLATE OR DIELECTRIC-SLAB WAVEGUIDES

Edward F. Kuester and David C. Chang
Electromagnetics Laboratory
Dept. of Electrical Engineering
University of Colorado
Boulder, Colorado 80309

The authors have previously developed a numerically efficient hybrid method for evaluating the fields of a beam propagating in a multimode parallel-plate or dielectric slab waveguide. This method is based on the self-imaging properties of these waveguides, by which Fourier or Fresnel images are periodically reproduced at certain positions along the guide, in the paraxial approximation of the wave equation. In this paper we will discuss the first-order corrections to the paraxial expressions for both types of waveguide. In the case of the parallel-plate guide, the corrections are due only to small changes in the propagation constants of the modes, while for the dielectric slab, there are slight corrections to the field patterns of the modes themselves. These correction terms are then used to find the shift in the focal points of the beams from those predicted by the paraxial expressions. Numerical comparisons will be made with computations based on the exact mode expansions. These show that with the correction terms, a typical optical waveguide may be calculated for propagation lengths of up to 1 km or more, as opposed to only about 1 m or so for the paraxial expression.

MULTIMODE PROPAGATION IN ANISOTROPIC OPTICAL WAVEGUIDES

D.K. Paul* & R.K. Shevgaonkar
Electrical Engg. Deptt., I.I.T., Kanpur, INDIA.

Using far from cut-off approximation ($d/\lambda_0 \gg 1$) we have derived elegant expressions for the characteristic equations and their relevant solutions to determine the guided wave features of an optical waveguide having an axial dielectric anisotropy. The approximation as used in the general analysis of anisotropic dielectric waveguide is valid for the modes which are far removed from cut-off. However, most optical fibers meet this condition and the analysis is applicable for all excited modes.

First, the characteristics are found for a guide of infinite size and then, using a first order perturbation technique, the approximate characteristics are obtained for a guide of large but finite dimensions. Also, the attenuation constant has been calculated following the concept of a complex permittivity in a lossy medium. Symmetrical TE and TM as well as hybrid modes have been investigated. The variable waveguide parameters, such as normalised diameter, refractive indices, dielectric anisotropy, etc., have been included in the generalised expressions. For each mode studied here, the results computed by the approximate method show very good agreement with those of the time-consuming exact analytical solutions. The dependence of the power carrying capacity and attenuation on the waveguide parameters highlights the usefulness of the dielectric anisotropy in optical waveguides.

* Presently with Gordon McKay Laboratory, Harvard Univ., Cambridge, Massachusetts 02138, U.S.A.

BANDWIDTH PREDICTION OF AN OPTICAL ROUTE

by

G S Gupta (1) and P J B Clarricoats (2)

- (1) RF Technology Centre, ERA Technology Ltd., Leatherhead, Surrey, UK
- (2) Elect.Eng.Dept., Queen Mary College, London, E.1 UK

The bandwidth of an optical system depends on the number of factors such as dispersion of refractive index profile in the fibre, the excitation strength of various modes by the source and upon the extent of intermodal coupling caused, for example, by microbending. When a number of fibres are joined together to form an optical link, the bandwidth of the route may increase with link distance because of compensation between the fibre profiles. Using modal matching techniques, the bandwidth of a system similar to the British post office Ipswich-Kesgrave link was predicted.

The technique essentially involves expanding the transverse electric and magnetic fields of the two fibre guides on either side of the discontinuity in terms of the normal modes of the respective guides. The power excited in each mode after the discontinuity was assessed by the application of the orthogonality condition, and the discontinuity was represented by a junction matrix.

The relative time of propagation for each mode in a single fibre was obtained by direct numerical method and with the assumption that no intermodal coupling occurs within the fibre the relationship between the input power at one end of the fibre to the output power at the other end was expressed as a delay matrix. Then by cascading the delay and junction matrices for each fibre and joint, the overall response has been calculated.

The results obtained were compared with experimental data, showing good qualitative agreement.

MODAL INTERFERENCE OF LASER LIGHT EMITTED FROM AN OPTICAL FIBER

Masaaki IMAI

Department of Engineering Science, Hokkaido University, Sapporo
060 Japan

The far-field radiation pattern of coherent light from an end face of multimode optical fiber shows a speckling phenomenon. The appearance of speckle patterns is a result of modal interference of guided modes with random phases. The speckled feature may occur due to the fact that laser light transmitted through an optical fiber suffers random phase changes after many reflections at an irregular boundary of the core and cladding interfaces or through the passages of light in the relatively large core having random fluctuations of the refractive index. It is well known that the visibility of speckle patterns depends not only on the coherence time (or the spectral bandwidth) of a light source but also on the mode dispersion of optical waveguides.

Using a statistical approach of speckled intensity distribution, we have studied the dependence of the average contrast of speckle patterns on the guide length for different types of optical fibers such as a graded-index fiber, a step-index fiber, and a Selfoc fiber (M. Imai et al., *Optik* 48, 335-340, 1977; *ibid.* 51, 429-434, 1978). It has been found experimentally for the speckle contrast that the interference effect could be reduced when mode conversion takes place extensively due to sinusoidally serpentine bends of optical fibers (M. Imai et al., *Opt. Commun.* 30, 299-303, 1979).

In this paper, the theoretical study is conducted for far-field radiation patterns occurring from modal interference of far-guided modes. The average intensity distribution of far-field patterns is analyzed by assuming a Gaussian autocorrelation function for refractive-index inhomogeneities in an optical fiber. The results show that the on-axis maximum intensity decreases as the correlation length of refractive-index inhomogeneities becomes small compared with the wavelength of light, whereas the off-axis average intensity decays with increasing the distance from the axis. The average intensity distributions obtained are found to be nearly Gaussian for both types of an optical fiber with step-index and graded-index profiles of the refractive index.

The average contrast of speckle patterns is defined as a normalized standard deviation of speckled intensity signal, i.e.,

$$V = \frac{\langle \Delta I^2 \rangle^{1/2}}{\langle I \rangle} = \frac{(\langle I^2 \rangle - \langle I \rangle^2)^{1/2}}{\langle I \rangle}$$

is used as a measure of statistical contrast of speckle patterns. Here, $\langle I \rangle$ and $\langle I^2 \rangle$ denote the mean value and the mean square value of the speckle radiation intensity, and the bracket $\langle \dots \rangle$ stands for an ensemble average. Therefore, by determining the average squared intensity as well as the average intensity of the far-field patterns, the average contrast can be also calculated under the assumptions of a Gaussian statistics for the refractive-index inhomogeneities and will be shown as a function of lateral position in the far-field plane.

ANALYSE ET MESURE DU BRUIT MODAL DANS UNE LIAISON
PAR FIBRE OPTIQUE MULTIMODE COMPRENANT UN CONNECTEUR OU UN COUPLEUR

Y. Tremblay, K.O. Hill et B.S. Kawasaki
Centre de Recherches sur les Communications,
Ministère des Communications,
Ottawa, Canada K2H 8S2

Le bruit modal est produit par les composantes dont les performances dépendent des modes de propagation de la lumière dans la fibre optique. Les épissures, les connecteurs et les coupleurs ont de telles performances. Comme ces éléments font partie des liens de communication par fibre optique, la présence de bruit modal est jusqu'à une certaine limite inévitable et peut réduire sensiblement la qualité de la transmission. Il est donc important de prévoir le niveau de ce bruit afin de le considérer lors de la conception des systèmes.

Dans cette étude nous présentons une analyse théorique simple qui explique la nature du bruit modal selon les caractéristiques de la fibre et le type d'élément qui le produit. La caractéristique principale de la fibre influençant le bruit modal est le nombre de modes de propagation qu'elle supporter. En règle générale, plus le nombre de modes est élevé plus le niveau du bruit modal est faible. Dans le cas où ce bruit est le résultat d'une atténuation sélective ou d'un filtrage des modes de propagation de la lumière, nous avons dérivé une expression qui en prévoit le niveau. Des résultats expérimentaux obtenus par des mesures de bruit effectuées sur des configurations optiques comprenant un connecteur confirment l'expression théorique. Nous présentons ces résultats ainsi que d'autres portant sur la production de bruit modal par un coupleur à structure biconique.

Combined Microbend and Wavelength Dependant Loss Evaluation
for Single and Multi Mode Fibers.

Santanu Das
Department of Electrical Engineering
University of Alberta
Edmonton, Alberta Canada

The microbending loss and the wavelength dependant propagation loss for single and multi mode fibers is calculated at different wavelengths. These losses are then combined for the respective fibers to gain an insight to their overall performance. For operating wavelengths in the 0.8-0.85 μm and 1.1-1.2 μm spectral regions, it is predicted that multimode fibers are more suited for statistical power spectrum exponent 'p' very near zero. For long distance communication where actual cable configuration may lead to power spectra 'p' \approx 2 or greater, singlemode fibers suffer much lower losses than multimode fibers.

WEDNESDAY AFTERNOON

June 4, 1:30 - 5:00

TRANSIENTS

DKN 1A

Combined Session AP-S/B.12

Chairman: D.L. Moffatt
The Ohio State University
Columbus, Ohio

The following papers belong to the IEEE AP-S Symposium and the summaries are included in the IEEE AP-S Digest under Combined Session AP-S/B.12.

3. TRANSIENT SCATTERING FROM CURVED THIN WIRES BY THE FINITE ELEMENT METHOD, T.C. Tong and A. Sankar, TRW Defense and Space Systems Group, Redondo Beach, California.
4. TIME-DOMAIN INTEGRAL EQUATION APPROACH TO EM SCATTERING BY DIELECTRIC SOLIDS, H. Mieras and C.L. Bennett, Sperry Research Center, Sudbury, Massachusetts, and R. Lyons, University of Michigan, Ann Arbor, Michigan.
5. DIFFRACTION EN REGIME TRANSITOIRE PAR DES OBSTACLES CONDUCTEURS OU DIELECTRIQUES, B. Jecko and A. Papiernik, Université de Limoges, Limoges, France.
6. ON DEMONSTRATING BASIC ELECTROMAGNETIC PHENOMENA USING TIME-DOMAIN SOLUTIONS, E.K. Miller, University of California, Livermore, California, J.A. Landt, University of California, Los Alamos, New Mexico, F.J. Deadrick and G.J. Burke, University of California, Livermore, California.

7. TIME-DOMAIN SEM, W.A. Davis, Virginia Polytechnic Institute and State University, Blacksburg, Virginia and J.T. Cordaro, University of New Mexico, Albuquerque, New Mexico.

8. THE DIFFERENTIAL FORM OF NETWORK ANALOGS: APPLICATIONS TO EMP AND SGEMP EXTERNAL RESPONSE PROBLEMS, W.R. Zimmerman, T.H. Lehman, E.L. Coffey and R.L. Hutchins, The BDM Corporation, Albuquerque, New Mexico.

9. TRANSIENT RESPONSE OF MULTICONDUCTOR TRANSMISSION LINES EXCITED BY A NONUNIFORM ELECTROMAGNETIC FIELD, A.K. Agarwal and H.J. Price, Mission Research Corporation, Albuquerque, New Mexico and S.H. Gurbaxani, University of New Mexico, Albuquerque, New Mexico.

10. NUMERICAL REPRESENTATION OF TRANSMISSION LINE EQUATIONS BY INTEGRATION ALONG CHARACTERISTICS IN THE PRESENCE OF A REALISTIC GROUND PLANE, H.J. Price and T.C. Kalahdar Rao, Mission Research Corporation, Albuquerque, New Mexico.

TIME-DOMAIN ELECTRIC FIELD INTEGRAL EQUATION
 APPROACH TO THE SOLUTION OF TRANSIENT SCATTERING
 BY ARBITRARILY-SHAPED OBJECTS

S. M. Rao, D. R. Wilton, and A. W. Glisson
 University of Mississippi
 University, MS 38677

Previous approaches to the problem of computing transient scattering by arbitrarily-shaped conducting scatterers have utilized the time-domain form of the magnetic field integral equation (MFIE) because of its relative simplicity. However, the MFIE applies only to closed bodies; for the capability to treat both open and closed bodies, the electric field integral equation (EFIE) formulation is required. In this paper we develop a numerical procedure for use with the time-domain EFIE

$$- \left[\frac{\partial^2 \bar{A}(\bar{r}, t)}{\partial t^2} + \nabla \frac{\partial \Phi(\bar{r}, t)}{\partial t} \right]_{\text{tan}} = - \bar{E}_{\text{tan}}^i$$

where \bar{A} is the usual vector potential, Φ is the scalar potential, and \bar{E}^i is the incident field.

The scatterer is modeled by triangular patches which offer greater flexibility in modeling complicated geometries and in changing patch densities than does the use of quadrilateral patches. Because of the spatial derivatives appearing in the EFIE, however, a special set of subdomain basis functions, developed earlier for use with the frequency domain EFIE, must be used with the triangular patch model. With these basis functions, application of the method of moments yields a set of linear equations for the current basis coefficients which may be solved by the usual marching-on-in-time procedure.

The time-domain EFIE formulation is applied to the problems of scattering by a square plate and by a sphere. Both objects are illuminated by a Gaussian pulse and currents and back-scattered far-field are computed. The results compare well with those computed by alternate methods.

TIME DOMAIN CALCULATION OF AIRCRAFT MODEL RESPONSE

C.L. Bennett and H. Mieras
 Sperry Research Center, Sudbury, MA 01776

A time domain formulation has been implemented for the calculation of scattering from complex conducting bodies in the resonance region. On the fuselage, modeled as a cylinder, an \vec{H} -type space-time integral equation is used:

$$\vec{J}(\vec{r}, t) = 2 \hat{n} \times \vec{H}^{\text{inc}}(\vec{r}, t) + \frac{1}{2\pi} \int_S \mathcal{L}(\vec{J}(\vec{r}', \tau) \times \hat{R}) dS'$$

where $\tau = t - R/c$, $\vec{R} = \vec{r} - \vec{r}'$, $\mathcal{L} = \frac{1}{R} + \frac{1}{Rc} \frac{\partial}{\partial \tau}$

On the wings, modeled as flat plates, an \vec{E} -type formulation results in

$$\nabla(\nabla \cdot \vec{A}(\vec{r}, t)) - \frac{\partial^2 \vec{A}(\vec{r}, t)}{c^2 \partial t^2} = -\epsilon \frac{\partial \vec{E}_{\text{tan}}^{\text{inc}}(\vec{r}, t)}{\partial t}$$

where

$$\vec{A}(\vec{r}, t) = \frac{1}{4\pi} \int_S \frac{\vec{J}(\vec{r}', \tau)}{R} dS'$$

These equations are solved simultaneously by marching in time. Computational results were verified by measurement on a time domain scattering range for a number of aircraft models, missile models, and other cylinders with fins at various aspects.

WEDNESDAY AFTERNOON

June 4, 1:30 - 5:00

SPECIAL SESSION ON INVERSE SCATTERING - I
THEORETICAL APPROACHES

DKN 1B

Session B.13

Chairman: C.L. Bennett
Sperry Research Center
Sudbury, MA

Organizer: W.M. Boerner
U.I.C.C.
Chicago, IL

THE NONEXISTENCE OF NON-RADIATING SOURCES AND THE UNIQUENESS OF
THE SOLUTION TO THE INVERSE SCATTERING PROBLEM

W. Ross Stone
MEGATAK Corporation
1055 Shafter Street
San Diego, California 92106

The Bojarski Exact Inverse Scattering Theory provides a solution to the general inverse scattering problem. Bleistein and Cohen (J. of Math. Physics 18, 194-201, 1977) have shown that this solution is unique providing the source term in the problem is of compact support and there are no nonradiating sources present. Nonradiating sources are sources which produce a field that is identically zero outside a finite volume. A simpler, independent proof of uniqueness (subject to the same conditions) was presented by Stone.

Although of significant theoretical importance, the non-uniqueness associated with nonradiating sources is of little practical consequence, since, for example, a medium inhomogeneity which constitutes a nonradiating source cannot interact with the probing wave in a remote probing problem. In spite of this, controversy has surrounded the implications and consequences of nonradiating sources for over 20 years. Much of this has resulted from misunderstandings of the physical meaning of a nonradiating source. Indeed, the author has yet to present or attend the presentation of a paper in which the uniqueness of the solution to the inverse scattering problem was discussed without at least one comment from the audience being made which was based on a physically inconsistent model of a nonradiating source.

This paper presents a simple, rigorous proof that nonradiating sources, which are of compact support and which are proper source terms for the inhomogeneous wave equation (i.e., which produce fields that are solutions of the wave equation), do not exist. This nonexistence is shown to be a direct consequence of the basic uniqueness of the solution to Maxwell's equations and the wave equation. In short, this removes the restriction concerning nonradiating sources from the uniqueness proof for the inverse scattering problem. The very significant consequences of this result are examined, as well as the correct physical picture of nonradiating sources. It is shown why several often-cited "counterexamples" to the nonexistence of nonradiating sources are incorrect. Nonradiating sources are shown to be primarily a mathematical construct. The relationship between this result and such well known problems as the nonscattering potential is also discussed.

A WELL-POSED ANALYTIC CLOSED FORM SOLUTION OF
THE EXACT INVERSE SCATTERING INTEGRAL EQUATION

Norbert N. Bojarski
16 Pine Valley Lane
Newport Beach, California 92660
Telephone: (714) 640 7900

The exact inverse scattering integral equation of this author (1973) is rederived. This integral equation consists of a Fredholm integral equation of the first kind, relating the unknown sources to an effectual field (introduced by this author), which is computable by a modified Kirchhoff integral for all points in space from knowledge of the incident and scattered (remotely sensed) fields on a surface enclosing the unknown sources. The kernel of this integral equation consists of the imaginary part of the free space Green's function, with an arbitrarily chosen free space reference velocity.

The concepts of an arbitrary reference slowness (reciprocal of velocity) space, and an associated reference slowness free space Green's function, are introduced, yielding an infinite set of simultaneous Fredholm integral equations of the first kind. Since the unknown fields do not depend on the arbitrarily chosen reference slownesses, a well-posed analytic closed form solution of the set of simultaneous integral equations is obtained by integration over all slownesses. The uniqueness and well-posedness of this solution is discussed.

Multi-dimensional Inverse Scattering

For The Reduced Wave Equation

V. H. Weston
Purdue University
West Lafayette, Indiana 47907

In general the multi-dimensional inverse problem with incomplete or sparse data is inherently a non-linear problem. In particular, the inverse problem for the reduced wave equation $\Delta u + k^2 n^2(x)u = 0$ where the data set consists of a finite set of measurements of the scattered field produced by a fixed incident field requires the solution of a system of non-linear functional equations.

The usual approach is to linearize the problem by retaining only the first order perturbation term in a formal expansion obtained by expanding $n(x)$ about a known or assumed value $n_*(x)$. Apart from questions on the non-uniqueness of the problem, the validity of such an approximation is never questioned, nor is the required degree of closeness of the measured data to the calculated data corresponding to $n_*(x)$ considered. Recently the complete non-linear problem has been rigorously treated, and it has been shown that with certain restrictions, a unique solution can be obtained that minimizes $\int_D (n_*^2 - n^2)^2 w dx$, where w is a suitably chosen weight factor. The solution can be obtained by an iteration process starting from the linearized approximation. Conditions restricting the size of the difference of the measured data to the data corresponding to $n_*(x)$, have been obtained that validates the convergence of the iteration process.

An Example of Resolving the Nonuniqueness in an
Inverse Scattering Problem

Robert J. Krueger
Dept. of Mathematics and Statistics
University of Nebraska
Lincoln, NE 68588

A general condition is established which guarantees the uniqueness of the solution of a particular type of inverse problem for wave propagation in an absorbing medium. It is then shown by means of an example that while this condition may be satisfied, the generalized Gelfand-Levitan equation used to solve the inverse problem may have a nonunique solution. Finally, it is shown how to augment the generalized Gelfand-Levitan equation so as to uniquely construct the solution of the inverse problem.

Inverse Scattering and the Born Approximation

Ralph E. Kleinman
Applied Mathematics Institute
University of Delaware
Newark, DE 19711

Brian D. Sleeman
Department of Mathematics
University of Dundee
Dundee, Scotland DD1 4HN

The inverse scattering problem of inferring geometric and constitutive features of an object from a discrete set of measurements of the far field scattered by the unknown target when illuminated by a known incident plane wave is considered. Through the Born approximation the far field and refractive index are shown to be a Fourier transform pair. An approximate far field may be interpolated from the measured values in a limited frequency band using characteristic functions on subintervals. An approximate inversion is carried out to obtain a first approximation for the index of refraction. Methods of improving the approximation including optimal choices of characteristic functions are discussed.

THE APPLICABILITY OF AN INVERSE METHOD FOR RECONSTRUCTION OF
ELECTRON DENSITY PROFILES

M. H. Reilly and A. K. Jordan
Naval Research Laboratory
Washington, DC 20375

Inverse scattering theory is used to reconstruct profiles of electron density from the analytic representation of the reflection coefficient. The complex reflection coefficient, $r(k)$, is represented as a rational function of the wavenumber k . Using a three-pole approximation for $r(k)$, one-dimensional inverse scattering theory is applied to obtain a closed-form expression for the electron-density profile function $q(x)$. The integral equation of inverse scattering theory (Gelfand-Levitan equation) is solved by a differential-operator technique and several numerical examples are given. Three-pole reflection coefficients are found to be applicable to the reconstruction of relatively thin electron layers which might be generated in the laboratory. Rational reflection coefficients with an increased number of poles are found to be necessary to simulate other electron layers of physical interest. This is demonstrated by comparison of multipole reflection coefficients in the Butterworth approximation with reflection coefficients calculated from Epstein's direct scattering theory for electron layers. A parameter in the Epstein theory, which characterizes the total electron content of the layer, is related to the number of poles needed to reconstruct that layer. Estimates are thus obtained of the number of poles needed to reconstruct ionospheric layers and other plasmas of physical interest.

RESONANCES OF A DIELECTRICALLY COATED CONDUCTING SPHERE:
SURFACE WAVES AND THE INVERSE SCATTERING PROBLEM.

Philip J. Moser, J. Diarmuid Murphy, Anton Nagl, and
Herbert Überall
Department of Physics, Catholic University
Washington, DC 20064
Guillermo C. Gaunard, Naval Surface Weapons Center
White Oak, Silver Spring, MD 20910

The theory of resonance scattering, developed by some of the present authors in the context of the scattering of acoustic waves from elastic obstacles, or of elastic waves from fluid-filled cavities or solid inclusions, is here applied to the problem of radar scattering from dielectrically-coated, perfectly conducting spherical targets. The numerous, sharp and narrow resonances obtained in previous calculations of the corresponding radar cross sections (see, e.g., Ruck et al, Radar Cross Section Handbook, Plenum New York, 1970) are shown here to correspond to the real resonance frequencies of the target, which can be calculated from a real characteristic equation and agree approximately with the real part of the natural frequencies. A surface-wave interpretation of these resonances is made entirely on the basis of real analysis, thus avoiding the complexities of the Watson transformation. The dispersion curves for these surface waves are obtained, which show (for the TM mode) a discontinuous transition from conductor-type at low frequencies to dielectric-type at high frequencies. The inverse problem is also solved (see, e.g., G. C. Gaunard, H. Überall, and L. R. Dragonette, IEEE Trans. Antennas Propag., Special Issue on Inverse Methods in Electromagnetics, W. M. Boerner, ed., to be published) by showing how from the spacing and the widths of the resonances, the dielectric constant and the thickness of the coating may be obtained. Finally, the relationship between the present resonance theory, and the singularity expansion method or SEM (see, C. E. Baum, Interaction Note 88, December 1971) is briefly sketched.

Commission B

A theoretical and numerical method
for inverse scattering problems in electromagnetics

A. ROGER, *Laboratoire d'Optique Electromagnétique, E.R.A. au CNRS n° 597, Faculté des Sciences et Techniques, Centre de St-Jérôme, 13397 MARSEILLE CEDEX 4, France.*

We deal with profile reconstruction problems. The scattering body is described by a function or profile F of one variable (Body Profile or B.P.) and the far scattered field is characterized by a function E of one variable (Scattering Profile or S.P.).

1. The method. It is based on the Newton Kantorovitch algorithm (generalization of the well known Newton algorithm for finding the zero of a real function). It is a step by step procedure, which if converging, yields the exact solution. At the beginning of a step, one starts from the estimated B.P. F_n computed at the preceding step (for the first step, a special method of evaluation is needed), and one computes the corresponding S.P. E_n with the help of the program devoted to the direct problem. By the same time, one calculates the functional derivative of E with respect to F (analogous to the tangent in the Newton method). It is the generalization of the concept of gradient to the case of functions. Finally, one must invert a linear functional equation to find a new better estimate F_{n+1} , which will be used in the next step.

2. Advantages and disadvantages : This algorithm gives no information about existence and uniqueness of the solution. On the other hand, it is very adaptable to practical problems : in particular, one can choose as S.P. the intensity of the far scattered field, and thus avoid the phase problems. By comparison with classical gradient methods, this procedure presents two advantages. Firstly a practical one : the functional derivative can be computed directly with very little increase of the computation time, because it can be expressed analytically and rigorously. Thus the direct program is used only one time per step instead of the $(n+1)$ times required by the numerical computation of n partial derivatives. Secondly a more fundamental advantage : one does not choose a priori n parameters which could be redundant or useless. The problem is analyzed directly in terms of operators and functions. The "instability" can be theoretically studied and one can apply adequate techniques (Tikhonov Miller regularization). Also, the expression of the functional derivative is very useful for the problem of synthesis.

3. Examples : This algorithm has been successfully applied in the TE polarization and perfectly conducting case, to cylinders (the B.P. is the cross section and the S.P. is either the bistatic scattering or the back scattered cross section) and to gratings (A. ROGER and D. MAYSTRE, *Optica Acta*, 26, 447-460, 1979. The B.P. is the profile of the grooves and the S.P. the efficiency as a function of the angle of incidence). We will present several profile reconstructions from simulated scattering data, and some results concerning the problems of synthesis.

THURSDAY MORNING

June 5, 8:30 - 12:00

SCATTERING II

DKN IA

Session B.14

Chairman: Y.L. Chow
University of Waterloo
Waterloo, Ontario

Small Aperture Coupling Between Dis-Similar Regions

R. E. Collin

Electrical Engineering and Applied Physics Department
Case Institute of Technology
Case Western Reserve University
Cleveland, Ohio 44106

The usual small aperture coupling theory is based on the use of a field equivalence theorem and a multipole expansion of the equivalent aperture sources along with image theory. This theory has two shortcomings: it does not result in power conservation and is not applicable to coupling between dis-similar regions. In this paper it is shown that power conservation can be achieved by including the radiation reaction field as part of the field that determines the equivalent dipole moments of the aperture. The reciprocity principle is applied to determine the effective dipole strengths for radiation into the separate dis-similar regions. The problem of small aperture coupling between dis-similar regions is thus readily solved.

This new theory of small aperture coupling is a simple extension of the older theory and permits problems such as waveguide to free space and waveguide to cavity coupling to be easily treated. The theory is illustrated with the above as examples.

APPROXIMATE SOLUTIONS FOR TRANSMISSION THROUGH
ELECTRICALLY SMALL APERTURES

Roger F. Harrington
Department of Electrical Engineering
Syracuse University
Syracuse, New York 13210

The problem of computing the electromagnetic coupling through an aperture between two regions is in general a mathematically difficult one. For plane conducting screens, analytical solutions exist for slits, circular apertures, and elliptic apertures. Numerical and experimental solutions have been found for other shapes. Few solutions exist for apertures between regions of more general shape.

In this paper the formulas obtained from a one-term or several-term moment method solution are evaluated using simple trial functions. In many cases the resulting approximate solutions differ from exact solutions by only a few percent. The frequency dependence of the transmission coefficient of the approximate solution is identical to that of the exact solution. The problems of apertures in thick conductors, waveguide-fed apertures, and cavity-backed apertures will also be discussed in terms of approximate solutions.

APERTURE-COUPLED FIELDS IN ASYMMETRIC BODIES

L. N. Medgyesi-Mitschang
McDonnell Douglas Research Laboratories
St. Louis, Missouri 63166

The problem of electromagnetic fields penetrating through small apertures has been treated previously using the Bethe small-hole theory. Recently, the method of moments (MM) has been applied to symmetric and asymmetric apertures in a body of revolution (BOR) (H. K. Schuman and D. E. Warren, IEEE Trans. AP-26, 778, 1978). In the present case, the MM technique is applied to the case of an asymmetric aperture embedded anywhere on an asymmetric surface (a body of translation, BOT). The aperture orientation is such that its edges lie parallel to the coordinates of the BOT. The analysis uses the Scheikunoff equivalence theorem, which replaces the external sources (\vec{E}_1, \vec{H}_1) illuminating a body with apertures with an equivalent problem having only aperture current sources. From the aperture currents, the near fields inside the body (\vec{E}_2, \vec{H}_2) are computed.

The salient steps of the analysis are as follows. The aperture voltage is expanded in a set of triangle and pulse functions. Computer implementable expressions are obtained for the aperture admittance in terms of the BOT surface impedance. The aperture-coupled fields \vec{E}_2 and \vec{H}_2 are computed from the voltage induced in the aperture as a result of the illuminating fields. This voltage is the equivalent aperture excitation voltage which can be obtained from the aperture admittance and the currents in the aperture region. Knowing the equivalent aperture excitation voltage, the currents on the BOT surface in the presence of the aperture are obtained. Then all three components of \vec{E}_2 and \vec{H}_2 are determined using a near-field formalism to be described. Representative calculations show the computed fields to be in good agreement with published data.

LOW FREQUENCY SCATTERING FROM A CIRCULAR TUBE OF FINITE LENGTH

P. Parhami, and S. Govind
TRW DEFENSE AND SPACE SYSTEMS GROUP
One Space Park . Redondo Beach . California 90278

A pair of exact integral equations for the three-dimensional Electromagnetic Scattering from a finite tube has been derived by C. C. Kao [J. Applied Physics, November 1969]. These equations are decoupled in the sense that enables one to compute the transverse and the axial currents in separate steps, thus saving considerable amount of core and computer time when the method of moments is employed.

Low frequency scattering currents and near fields for a finite tube (radius \ll length \ll wavelength), as encountered in many EMP applications, introduces several numerical problems for the method of moments procedure. In this paper, a low frequency asymptotic solution is found for the aforementioned integral equations, and the results have been analytically reduced to a form such that the currents and the near fields (both inside and outside the tube) are computed directly without the aid of complicated numerical techniques such as the method of moments. Several numerical examples are included to verify the validity of the derivations and to demonstrate the low frequency shielding properties of finite length tubes.

SCATTERING BY ROTATING OSCILLATING TARGETS

R. E. Kleinman and R. B. Mack
Applied Mathematics Institute
University of Delaware
Newark, Delaware 19711

A theoretical and experimental treatment is presented of the problem of scattering of a plane electromagnetic wave from a perfectly conducting object which is undergoing small rotational oscillations about an axis through the body colinear with the direction of incidence. This extends to small rotational oscillations in the plane transverse to the incident direction the previous theoretical and experimental analysis of scattering by linearly oscillating targets (R. E. Kleinman and R. B. Mack, IEEE Trans. AP-S, AP-27, 344-352, 1979).

A theoretical analysis based on the quasi stationary approximation is developed which expresses the scattered field of the oscillating object in terms of parallel and cross polarized scattered fields for the stationary object which includes terms up through δ^2 where δ is the oscillation angle. The average power is found to this order of accuracy. The linear term in S is absent if the oscillation is symmetric but present otherwise.

The experiment consisted of rotating a right circular cylinder about a line perpendicular to the cylinder axis at the cylinder's mid-length. Both symmetric and asymmetric sinusoidal motion were achieved with good accuracy in frequency and amplitude of the oscillation. Measurements were carried out at 10 GHz with a CW system using separate antennas for transmitting and receiving. Phase and amplitude of the scattered field were measured for transmitter and receiver polarizations both parallel and orthogonal to each other and for transmitter polarization parallel, orthogonal, and at 45° to the cylinder axis.

The theoretical and experimental results are compared. Results indicate that even small transverse oscillations of the scatterer produce measurable modulations of the back scattered field that are more easily detected with orthogonal rather than parallel transmitter-receiver polarizations and that these effects are predicted by the theoretical model.

SIMPLE INTERPRETATIONS OF SCATTERED FIELD
OF SPHERES BY OPTIMIZED SIMULATED IMAGES

by Y.L. Chow and M. Tutt, Department of
Electrical Engineering, University of
Waterloo, Waterloo, Ontario, Canada.
N2L 3G1

Chow et al. recently studied the scattering of EM field from a conducting sphere (Chow, Tutt and Charalambous; URSI Meeting, Boulder, Co., November 6-9, 1978). The method they used was the optimized simulated images. The basic idea was to place a few 'simulated' images of electric and magnetic dipoles inside the sphere and optimize their locations and strength for minimum error in the boundary conditions.

This approach is simple in concept and programming. Also at low and intermediate frequencies, only a small number of images are required to reduce the boundary errors to a few percent. The reason for such simplicities may be that, unlike regular scattering methods, the optimized method uses nonlinear operations.

As the results are simple, physical interpretations of them are easy. For example, when an exciting dipole approaches a conducting sphere to a distance r , the strength of the electric and magnetic dipole images in the sphere increases as $1/r$, i.e. the sphere is in the radiation zone of the exciting dipole. When r is reduced beyond $k_0 r = 1$, the image strength abruptly increases as $1/r^3$, i.e. the sphere is now effectively in the induction zone. It is interesting to note that there is practically no range of distance that the strength increases as $1/r^2$. Similarly simple interpretations are found for the image locations.

Based on the simple interpretations, the graphs of r vs. image strength and locations can in fact be constructed without computation.

Following the simple construction for one sphere and one exciting dipole, one can easily construct the images for multiple spheres under different excitations. The resulted field from the latter construction is found to satisfy the boundary conditions, still within a few percent of error.

NATURAL MODE RESONANCES OF DIELECTRIC OBJECTS

P.W. Barber, Department of Electrical Engineering,
University of Utah, Salt Lake City, UT 84112.

R.K. Chang, Department of Engineering and Applied
Science, Yale University, New Haven, CT 06520.

The fields in and around a dielectric sphere can become very large when the sphere is illuminated at a frequency corresponding to one of its natural modes of oscillation. The modes consist of an infinite set of TE_{ns} and TM_{ns} types which are related to the s^{th} zero of the eigenvalue equation for the n^{th} spherical harmonic. The amplitude of the fields at resonance can be very large for high permittivity dielectrics (P. Affolter and B. Eliasson, *Trans. MTT*, 21, 573-578, 1973). A recent series of papers (J. Van Bladel, *Trans. MTT*, 23, 199-208, 208-217, 1975) have used an expansion in inverse refractive index to investigate some of the theoretical aspects of the problem, including mode orthogonality properties and the nature of the induced electric and magnetic dipoles.

In the present investigation, the extended boundary condition method is used to determine the resonance characteristics of nonspherical dielectric objects. The resonance structure is found to be a function of the orientation and polarization of the incident wave. Figure 1 shows the polarization dependence for a 2:1 prolate spheroid at broadside incidence. Consideration of these resonances as well as angular scattering patterns on and off resonance provide insight into the nature of the induced electric and magnetic dipoles.

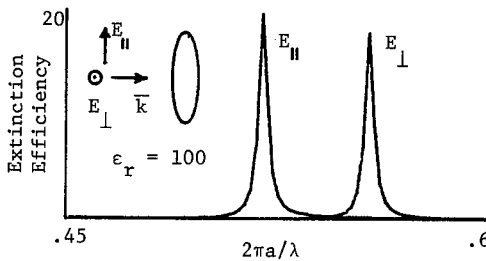


Fig. 1: Resonances of a dielectric prolate spheroid. Major semi-axis = \underline{a} .
Minor semi-axis = \underline{b} .

SEM ANALYSIS OF SCATTERING FROM AN INFINITE PERIODIC ARRAY

D. H. Herndon, E. W. Smith and E. J. Dombroski
Harris Corporation
Melbourne, Florida

Scattering from an infinite periodic array of metallic scatterers has been treated by several authors. These papers use Moment Method to solve the vector integral equations for the scattered field. Since these arrays find uses as frequency selective surfaces in broadband antenna systems the Moment Method solution requires that the problem be solved at many frequencies to obtain a wideband frequency response. The arrays are effectively filters when used in this application, and it would seem more efficient to specify the response with poles.

The poles of each array are calculated using the Singularity Expansion Method (SEM). How the poles vary with changing geometrical parameters are calculated and plotted. The expansion functions used allow a variety of elements to be evaluated. Once the poles are located an equivalent circuit is calculated and compared with previous circuit models such as capacitive plate arrays. The SEM analysis also leads to the location of branch cuts in the complex plane and an explanation of their physical significance.

A SINGULARITY EXPANSION METHOD ANALYSIS OF TWO FINITE LENGTH THIN CYLINDERS OF ARBITRARY ORIENTATION

D. Maynard Schmale, Lloyd S. Riggs and T. H. Shumpert
Electrical Engineering Department
Auburn University
Auburn, Alabama 36830

The scattering characteristics of two variable length arbitrarily oriented, perfectly conducting, right circular cylinders are investigated. Pocklington type integrodifferential equations with thin wire kernels are formulated in terms of a complex frequency variable for the currents induced on scatterers. The system equations are reduced to matrix form by application of the Method of Moments.

Results will be cast in terms of the Singularity Expansion Method. Specifically, trajectories of the natural resonances of the scattering system will be presented. Comparison to work done by previous investigators, (Shumpert, T. H., K. R. Umashankar, and D. R. Wilson, IEEE Trans. Ant. Prop., 23, 2, 1975), will afford some interesting results with respect to the fundamental scattering characteristics of cylinders.

SEM EQUIVALENT CIRCUIT SYNTHESIS FOR THE SPHERICAL ANTENNA

K. A. Michalski
L. W. Pearson
Department of Electrical Engineering
University of Kentucky
Lexington, KY 40506

The authors, as well as other workers, have presented broadband equivalent circuits derived by way of the Singularity Expansion description for various high-Q antennas: namely, the straight wire, the wire loop and a Yagi-Uda array structure. A similar study for a spherical structure serves as a complement to earlier work since the spherical radiator represents the low-Q extreme. The present paper reports the more significant results from a study of the spherical antenna.

The "dominant pole-pair approximation" reported by Streable and Pearson [G. W. Streable and L. W. Pearson, University of Kentucky Electromagnetics Research Report 79-1, May 1979; also submitted to IEEE Trans. Ant. & Prop.] is shown to lead to a less accurate approximation in the case of the sphere than it does in the thin structures reported earlier. Where the wire results involved negative excursions in the real part of admittance of order 1% or less of the peak admittance, this excursion is of order 20% for the sphere.

The "capacitive deficiency" of truncated SEM circuits reported by Streable et al. [G. W. Streable, L. W. Pearson, and K. A. Michalski, 1979 Radio Science Meeting, Seattle, Washington, June 1979] appears, as expected, in the sphere results. However, the low-Q character of the sphere causes the principal energy transfer to or from the structure to occur in a single oscillation during the forced response part of the time history--the time during which the capacitive deficiency comes to play. Therefore, the capacitive correction suggested by Streable et al. is likely to be important for low-Q structures.

The SEM circuit responses are observed to converge at a rate commensurate with the Mie series as higher order modes are added to the circuit. While not surprising, this insight may prove useful in understanding the convergence phenomena for SEM circuits modeling more complex structures.

Results are presented to stand with the wire results in bounding the circuit response accuracies attainable with SEM equivalent circuits for radiating structures.

THURSDAY MORNING

June 5, 8:30 - 12:00

SPECIAL SESSION ON INVERSE SCATTERING - II
TRANSIENT SIGNATURE INTERPRETATION

DKN 1B

Combined Session B.15/AP-S

Chairman and Organizer.: W.M. Boerner
U.I.C.C.
Chicago, IL

The following papers belong to the IEEE AP-S Symposium and the summaries are included in the IEEE AP-S Digest under Combined Session B.15/AP-S.

2. INTERACTIVE SOLUTION OF THE TIME-DOMAIN INVERSE SCATTERING PROBLEM FOR AN INHOMOGENEOUS, LOSSY DIELECTRIC SLAB, A.G. Tijhuis, Department of Electrical Engineering, Delft University of Technology, P.O.Box 5031, 2600 GA Delft, The Netherlands.
3. SEM APPROACH TO THE TRANSIENT SCATTERING BY AN INHOMOGENEOUS, LOSSY DIELECTRIC SLAB, A.G. Tijhuis and H. Block, Department of Electrical Engineering, Delft University of Technology, P.O. Box 5031, 2600 GA Delft, The Netherlands.
5. RADAR WAVEFORM SYNTHESIS METHOD - A NEW RADAR DETECTION SCHEME, Kun-Mu Chen, Department of Electrical Engineering and System Science, Michigan State University, East Lansing, Michigan 48824.
6. DECISION THEORETIC TARGET CLASSIFICATION, J.P. Toomey and C.L. Bennett, Sperry Research Center, 100 North Road, Sudbury, Massachusetts 01776.

PROBING OF PLANE AND CYLINDRICALLY STRATIFIED MEDIUM.
BIOMEDICAL AND GEOPHYSICAL APPLICATIONS.

J. AUDET, J.Ch. BOLOMEY, B. DUCHENE, D. LESSELIER, Ch. PICHOT, W. TABBARA

Laboratoire des Signaux et Systèmes - Groupe d'Electromagnétisme
C.N.R.S. - E.S.E., Plateau du Moulon - 91190 GIF-sur-YVETTE, FRANCE

Three different problems have been investigated, they have in common the use of rigorous representation of the fields based either on integral equations or modal expansions. All these problems are oriented toward biomedical or geophysical applications.

In the first problem, a plane stratified medium is illuminated by an arbitrary pulse. Optimization techniques are used to determine the unknown parameters of the medium from the measurement of the reflection coefficient. Different minimization algorithms have been used and their results compared in order to determine the most suitable one in terms of stability and speed of convergence. The approach has been applied to the reconstruction of conductivity profiles and shows substantial improvement when compared to previous exact ones developed in our group. Further developpements will be oriented to acoustic probing of ocean water.

The second problem deals with the diagnostics of a plane stratified medium, modelizing a stack of human tissues and muscle, illuminated by a plane parallel flanged waveguide or a rectangular flanged one at a given frequency. The reflection coefficient of the exciting mode is computed rigorously and its dependance on the frequency and on the parameters of the medium is investigated. The results are also compared to those given by an approximate theory based on geometrical optics approximation. We show that in some cases it is easy to deduce the unknown parameters from the reflection coefficient.

In the third problem a cylindrically stratified medium modelizing a blood vessel is illuminated by an acoustic plane wave or a gaussian beam. The scattered field at various frequencies is determined and its dependance on the parameters of the medium is studied in order to characterize as accurately as possible the blood vessel. In a time domain approach the blood vessel is approximated by a plane stratified medium and the acoustical impedance profile is seeked, comparison with experimental results shows a good agreement.

ELIMINATION OF UNDESIRED NATURAL RESONANCES
FOR IMPROVED TARGET IDENTIFICATION

J. Volakis and L. Peters, Jr.
The Ohio State University ElectroScience Laboratory
Department of Electrical Engineering
Columbus, Ohio 43212

Natural resonances exist in the data obtained using video pulse radar systems for detecting buried targets. Some of these resonances are caused by the antenna and other sources of clutter. Certain processing steps can be performed to eliminate undesired resonances. The procedure is illustrated on data obtained over a tunnel at Gold Hill, Colorado. The processing steps include:

1. Pole Extraction Process

This is in reality a digital or time domain filtering process where a natural resonance or a complex conjugate pole pair and its associated residue are removed from the waveform. The reader is cautioned that this is not done by evaluating the residue and then subtracting it from the waveform, but instead it is done in the time domain via a difference equation approach. This process could indeed be referred to as time domain filtering. The approach has an advantage in that the natural resonances that are energized at different times can be accounted for properly.

2. Correction Process

In the process of extracting a natural resonance, the remainder of the waveform is modified by this filtering process. This step simply takes out the distortions introduced by the filtering process.

3. Reconstruction Process

The late time portion of the signals can be used to generate the early time signal of a given pole pair. This makes it possible to reduce the effects of clutter in the early time region of the signal and to better evaluate the initial part of the signal reflected from the target.

The time at which a given resonance has been "turned on" can be estimated from the waveforms obtained at step 3. Time domain waveforms as obtained using the video pulse radar will be presented to illustrate cases before and after processing. Particular attention will be focussed on detecting the time at which the signal scattered by the tunnel is observed. Grey level maps prepared from data with and without processing will be shown. The map obtained from the processed data clearly shows the tunnel at the known depth.

DECISION THEORETIC TARGET CLASSIFICATION

J.P. Toomey and C.L. Bennett
(Sperry Research Center, Sudbury, MA 01776)

Target classification may be viewed as a crude form of inverse scattering that determines which of M prespecified body shapes is most consistent with the scattered field measurements. Since all real-world measurements are corrupted by error or noise, practical target classification problems must deal with statistical uncertainty. Statistical decision theory is a mathematical discipline which provides rules for choosing between alternative hypothesized states of nature based on data describing the actual state of nature. This paper describes a method, founded on statistical decision theory, for discriminating between different target shapes by appropriately processing the backscattered waveform or target signature as observed in radar receivers. It is shown how the target classification processor structure can be deduced or synthesized from an appropriate mathematical model of the problem. The utility of the approach is illustrated by the results of an analysis of a target classification problem using currently operational radars.

CLASSIFICATION TECHNIQUES IN INVERSE SCATTERING

A. A. Ksienski and Heng-Cheng Lin*

The Ohio State University ElectroScience Laboratory
Department of Electrical Engineering
Columbus, Ohio 43212

The inverse scattering problem is approached from a hypothesis testing point of view. Any a priori information available combined with object characteristics of interest provide the base for forming the alternative hypotheses. These hypotheses are then tested with respect to the received scattering data. The nature and range of the hypotheses will be discussed and shown to accommodate various levels of a priori information.

Often in practice considerable information is available for some expected objects, but very little may be known for others. An appropriate technique to handle such situations will be discussed and results utilizing the technique will be presented.

The classification performance for a set of eight airplane types will be presented and the use of various features and their affect on performance will be discussed. The feature choices and classification performance will be shown to be directly related to the targets' scattering properties. The classification performance will be shown to be also strongly dependent on the choice of the radar illumination frequencies, particularly so when the number of frequencies utilized is very limited.

The present status and future prospects for the classification approach to target identification will be discussed.

*Presently with Harris Corporation, Melbourne, Florida 32901.

THE USE OF NEAREST NEIGHBOR AND LINEAR DISCRIMINANT TECHNIQUES
FOR SHIP IDENTIFICATION USING HF RADAR

Eric K. Walton
The Ohio State University
ElectroScience Laboratory
Department of Electrical Engineering
Columbus, Ohio 43212

The identification of ships from the radar returns of an HF radar system is discussed. The data base used here consists of measurements made on eight different ship models. The models used were available as either 1/500 scale or 1/700 scale or both, and were located on a ground plane. Measurements were made at ten harmonically related frequencies from 1.085 ghz. This is equivalent to a scaled frequency range from 2.17 to 21.7 mhz (1/500) or from 1.55 to 15.5 mhz (1/700) and resulted in L/λ_0 ranging from 0.61 to 2.12 (L = vessel length; λ_0 = wavelength of first harmonic). Both the amplitude and the absolute phase were recorded at each of the ten harmonics for several 5° increments about bow, stern and broadside (elevation angle = 61°).

Processing for target identification included the application of the nearest neighbor and linear discriminant techniques to particular subsets of the available harmonic data. The feature sets used included amplitude alone; amplitude with absolute phase; and amplitude with relative phase. Results and comparisons are discussed.

THURSDAY AFTERNOON
June 5, 1:30 - 5:00

SPECIAL TOPICS

DKN 1B

Session B.16

Chairman: R. MacPhie
University of Waterloo
Waterloo, Ontario

ELECTROMAGNETIC FIELDS OF A DIPOLE SUBMERGED
IN A TWO-LAYER CONDUCTING MEDIUM IN THE ELF REGIME

T. M. Habashy, J. A. Kong, W. C. Chew
Department of Electrical Engineering and
Computer Science and Research Laboratory
of Electronics
Massachusetts Institute of Technology
Cambridge, Massachusetts 02139

For communication in sea water with dipole antennas in the extremely low frequency regime, the well known far field asymptotic methods used for high frequency applications are no more applicable and the brute force numerical integration is limited by the excessive computation time.

To attack such problems we first formulate the solutions for the electromagnetic fields due to a horizontal or vertical electric dipole buried in a two layered stratified medium in integral forms.

In the low frequency limit we make use of four different approaches to solve the problem and compare their results. First, a brute force numerical integration is carried out along the Sommerfeld integration path and results are obtained for some typical cases for comparison with the other more time saving methods. In these time saving methods we deform the Sommerfeld integration path to the steepest descent paths found by setting the phase term equal to that at the two branch points. In carrying out the deformation we account for the singularity contributions other than the branch points by three different approaches: (1) the normal mode approach where residues of the poles of the integrand are computed; (2) the multiple image expansion approach in which the contributions from the different images are calculated after the integrand is expanded in power series; and (3) the hybrid approach where combinations of both modes and images are utilized.

It is shown that the deformation methods greatly reduce computational time and permits physical interpretation. Numerical results for all four methods are illustrated, compared, and discussed.

A New Quasistatic Representation for
Horizontal Magnetic Dipoles Near a Lossy Half-Space

James N. Brittingham

Lawrence Livermore Laboratory
Livermore, California 94550

In a previous paper ["New Quasistatic Representation for Sommerfeld Integrals," J. N. Brittingham and G. J. Burke, URSI, National Meeting, June 18-22, 1979], a method was developed to find a more exact representation for the field from electric dipole near lossy half-spaces. This method consisted of separating the original Sommerfeld integrals into two separate parts. Near the interface, one part can be shown to dominate the other. This dominating term can be written analytically.

This paper will present the magnetic field from a horizontal magnetic dipole near a lossy half-space found from this new approach. The new results will be compared with work presented previously.

"Work performed under the auspices of the
U.S. Department of Energy by the Lawrence
Livermore Laboratory under contract number
W-7405-ENG-48."

ANTENNES EPAISSES DE REVOLUTION : APPLICATION AU COUPLAGE
DES COMPOSANTS ET AUX CAPTEURS LARGE BANDE.

J.Ch. BOLOMEY, S. EL HABIBY, F. HILLAIRE, D. LESSELIER

Laboratoire des Signaux et Systèmes

Groupe d'Electromagnétisme

C.N.R.S. - E.S.E.

Plateau du Moulon - 91190 GIF-sur-YVETTE - France

Les antennes épaisses de révolution de dimensions voisines de la longueur d'onde font l'objet d'un intérêt croissant. Leur utilisation au titre du couplage de composants actifs ou passifs des ondes millimétriques jusqu'à l'infrarouge, la recherche de capteurs électromagnétiques large-bande justifient pleinement cet intérêt.

La détermination du courant superficiel sur une telle structure en régime d'émission peut se faire numériquement par résolution de l'équation intégrale d'Albert et Synge; cette équation est de 1^è espèce et à noyau régulier, et permet en outre de s'abstraire des résonances du problème intérieur complémentaire. Elle s'est avérée (Bolomey et al, IEEE - AP/S Symposium and URSI Meeting, Seattle, U.S.A., Juin 1979, pp 663-666) particulièrement intéressante, après que l'on eu surmonté son mauvais conditionnement numérique, dans le cas d'antennes cylindriques d'arêtes vives ou arrondies. Or cette équation s'applique rigoureusement à une structure de méridienne de forme quelconque, et de champ d'excitation arbitraire, à condition que soit respectée la symétrie de révolution. Ainsi, ont été calculées des structures à pointes (cônes et troncs de cônes) particulièrement destinées au couplage infrarouge et des structures bulbes pour la détection large bande; une grande attention a été portée à l'influence des arêtes (charges localisées) et de la forme de la méridienne au voisinage de la source sur les propriétés de telles antennes. Le cas de structures de conductivité finie, mais élevée, a été envisagé simplement par l'intermédiaire d'une impédance superficielle. Un contrôle expérimental tout à fait satisfaisant a été obtenu par la mesure en chambre anéchoïde des champs proches, et du champ à grande distance.

MAPPING THE ELECTRIC FIELD INSIDE A FINITE DIELECTRIC CYLINDER

R. Bansal, R. W. P. King, and T. T. Wu

Gordon McKay Laboratory, Harvard University, Cambridge, MA 02138

This paper describes the experimental setup and measurement techniques for determining the standing-wave patterns inside a circular cylinder of water, excited by the time-harmonic electromagnetic field from an external source. The experimental results are examined in the light of the available numerical data, and the possibility of internal axial and transverse resonances is explored. The "effective" water-column used in our study was 50 cm in height and had a radius of 8.65 cm. The measurements were carried out at 100, 300, and 600 MHz. The conductivity of the water was varied from approximately zero to 3.5 Si/m by adding different amounts of salt to distilled water. Both the amplitude and the phase of the induced electric field were measured in the experiment.

RELATIONS BETWEEN THE ANTENNA AND SCATTERING CHARACTERISTICS
IN TERMS OF MEASURABLE PARAMETERS

C.W. Choi and J.J.H. Wang
Engineering Experiment Station
Georgia Institute of Technology

The scattering characteristics of antenna, or the antenna characteristics of a scatterer, was formulated by Green (Ohio State Univ. Report 1223-17, Nov. 1963) and Garbacz (Proc. IEE, Vol. 111, No. 10, Oct. 1964). However, their expressions involve parameters, such as the current in the antenna terminal and the structural scattering coefficient C , which are difficult to measure or compute. J. Appel-Hansen (IEEE Trans. Ant. Prop., Vol. 27, No. 5, Sept. 1979) developed a new technique to determine the gain and radiation pattern of an antenna through simple measurements of its maximum and minimum scattering cross sections when terminated in a reactive load.

In this paper, Appel-Hansen's equation is re-examined from the viewpoint of the basic antenna scattering equation of Green. In the new formula some restrictions and ambiguities in Appel-Hansen's equation were removed. In a similar manner, the structural scattering characteristics of an antenna can be entirely expressed in terms of measurable parameters such as its gains and its maximum and minimum scattering cross section when loaded reactively. Theoretical derivations of the new formulas and some experimental results utilizing these simple formulas will be discussed in the presentation.

LASER INDUCED EXCITATION OF THE CHARACTERISTIC MODES OF METAL OBJECTS

W.H. Peake and J.G. Meadors
The Ohio State University ElectroScience Laboratory
Department of Electrical Engineering
Columbus, Ohio 43212

When short pulse laser radiation of appropriate intensity strikes a metallic object, a localized transient current pulse is created on the metallic surface. This current pulse excites the modal surface currents, which then radiate an electromagnetic field with a temporal structure characteristic of the size and shape of the illuminated object. A number of targets were illuminated with laser pulses of 1 ns duration, 30 mJ energy, and a $1.06\mu\text{m}$ wavelength to optically generate this transient excitation, and the radiated electromagnetic fields were observed.

The properties of the localized current pulse were studied by illuminating a set of discs and posts on a ground plane, using a short monopole antenna as the receiving element. By analyzing the received electromagnetic pulse shape as a function of range, the static, induction and radiation field of the current pulse can be separated and used to infer the properties of the pulse itself. The results indicate that the current pulse is normal to the surface, with a moment of magnitude $M(t) \approx M \exp(-t^2/t_0^2)$ where $t_0 \approx 0.4$ ns and $M = -7 \times 10^{-4}$ ampere-meter in vacuum. We have also illuminated several targets (wires, cones) which had resonances within the bandwidth of the receiving system. For thin wires the first two poles of the received signature were extracted, and found to be in good agreement with calculations of Richmond, Marin and others.

Although the physical mechanism which transforms the incident optical energy into an electrical current pulse is not yet entirely clear, it is believed to be due to thermionic emission from the locally heated surface. Calculations based on this mechanism are used to discuss the observed dependence of the strength and time history of the induced current moment on the incident laser energy density, polarization, rise time, and on the ambient air pressure. Limitations imposed by the thermal time constant of typical metals to such applications as the identification of metallic targets, and the patterns of monopole antennas on aircraft or other vehicles are discussed.

SATURATION EFFECTS IN COHERENT ANTI-STOKES RAMAN SPECTROSCOPY (CARS)

Herschel Weil, The University of Michigan, Department of Electrical and Computer Engineering, Ann Arbor, MI 48109; Paul W. Schrieber, U.S. Air Force, Aero Propulsion Laboratory, Wright Patterson AFB, 45433

In CARS a medium such as a molecular gas mixture whose temperature and molecular concentrations are to be investigated is irradiated by two intense laser beams, the pump and Stokes beams, whose frequency difference matches a vibrational frequency characteristic of the molecular species of interest. A non-linear wave-wave-particle interaction (scattering) then generates radiation, which may be quite intense, at the corresponding anti-Stokes frequency.

Equations are presented to describe the generation of CARS spectra under physical assumptions corresponding to an experimental set-up for the remote probing of combustion processes. The analysis takes into account a number of competing physical effects such as other non-linear scattering processes and saturation due to depletion of the vibrational ground state population. Threshold and saturation levels are explored numerically.

TRANSIENT CORONA EFFECTS ON WIRE OVER THE GROUND

K. C. CHEN
Air Force Weapons Laboratory
Kirtland AFB, NM 87117

Military aircraft, such as TACAMO and Airborne Command Post, employ long VLF trailing wire antennas. These antennas are required to survive exposure to nuclear electromagnetic pulse environment. During such an exposure the electric field on the trailing wire antenna can be considerably greater than the breakdown electric field of the air, which results in corona around the wire. As a first step in understanding wires with corona, the Air Force Weapons Laboratory set up a wire over a copper wire mesh ground plane facility at Kaman Sciences Corporation. A high voltage pulser is used to drive this transmission line up to 90 Kv. Baum's electric and magnetic field sensors are situated on the ground plane to measure the corona effect. The recorded signals clearly show the onset of the corona which is characterized by a dip in the measured data. Corona data for different wire types, e.g., Aluminum, Copper; for a range of voltage levels; and for both polarities; have been collected.

A nonlinear corona model based on a transmission line equation with a nonlinear capacitance per meter is developed. First, a general solution for the nonlinear transmission line equations is obtained. Second, the pulse velocity is deduced from the measured data as a function of pulse magnitude. Relationship between line current and voltage is studied. Townsend's electron avalanche theory is also applied to interpret the test data.

ELECTROMAGNETIC THEORY OF MULTI-LAYERED SHIELDS WITH
PARTICULAR REFERENCE TO ELECTRICAL BONDING BETWEEN SHIELDS

K.S.H. Lee, Dikewood Corporation, Santa Monica, California, U.S.A.

Recently, the theory of inductive shielding (R.W. Latham and K.S.H. Lee, Canad. J. Phys., 46, 1745 - 1752, 1968) has been applied to derive simple engineering formulas to describe the magnetic field that penetrates into a single-layered shielded enclosure of arbitrary shape (K.S.H. Lee and G. Bedrosian, IEEE Trans. on Ant. and Propag., AP-27, No. 2, 194 - 198, March 1979). In this paper we extend the previous work to enclosures of multi-layered shields and investigate the effect of electrical bonding between the shields on the shielding effectiveness of the enclosure.

We will first solve the boundary-value problem of two concentric spherical shields using the theory of inductive shielding, and then generalize the results to a multi-layered shielded enclosure of arbitrary shape. The results will be interpreted in terms of equivalent circuits by means of which we introduce the concept of bonding between the shields. The effect of bonding will be evaluated by solving simple circuit problems. Finally, we will show the corresponding results for a multi-layered cylindrical shield.

THURSDAY AFTERNOON

June 5, 1:30 - 5:00

SPECIAL SESSION ON INVERSE SCATTERING III

DKN 1271

Combined Session B.17/AP-S

POSTER SESSION on ELECTROMAGNETIC IMAGING

Chairman: N.N. Bojarski
Newport Beach, CA.

Organizer: W.M. Boerner
UICC
Chicago, Ill.

The following papers belong to the IEEE AP-S Symposium and the summaries are included in the IEEE AP-S Digest under Combined Session B.17/AP-S.

4. A TIME-DOMAIN MONOSTATIC INVERSE SCATTERING SCHEME, S.K. Chaudhuri and P.A. Lenz, Department of Electrical Engineering, University of Waterloo, Waterloo, Ontario N2L 3G1.
5. AN APPLICATION OF GEOMETRICAL THEORY OF DIFFRACTION (GTD) AND PHYSICAL OPTICS TO OBJECT IDENTIFICATION THROUGH INVERSE SCATTERING ANALYSIS, G.A. Dike, E.C. Burt and R.F. Wallenberg, Syracuse Research Corporation, Merrill Lane, Syracuse, N.Y. 13210.
9. EXTENSION OF PHYSICAL OPTICS INVERSE SCATTERING USING POLARIZATION UTILIZATION, W.M. Boerner, AEM Laboratory, Department of Electrical Engineering, University of Manitoba, Winnipeg, Manitoba R3T 2N2, and C.M. Ho, Communications Laboratory, Information Engineering Department, SE0-1104, UICC, P.O.Box 4348, Chicago, Ill. 60680.
10. NONCONVERGENCE RESULTS FOR THE APPLICATION OF THE MOMENT METHOD (GALLERKIN'S METHOD) FOR SOME SIMPLE PROBLEMS, T.K. Sarkar, Department of Electrical Engineering, Rochester Institute of Technology, Rochester, N.Y. 14623.

THE PHASE RETRIEVAL PROBLEM

Leonard S. Taylor

Electrical Engineering Department, University of Maryland
College Park, Maryland 20742

The phase retrieval problem arises in applications of electromagnetic theory in which wave phase is apparently lost or impractical to measure and only intensity data is available. The mathematics of the problem provides unusual insights into the nature of electromagnetic fields. In this paper the theory will be reviewed and illustrated and some new results discussed. The basic issue of the phase retrieval problem, stated for a one-dimensional field, is that although a unique Fourier transform relation exists between the field, $F(x)$, in the Fraunhofer plane and the field, $u(x')$, in the object plane, the process of conjugation of a zero, z_k , of $F(z)$, $z = x + jy$, to its mirror position, z_k^* , produces no change in the intensity, $I(x)$, but does yield a different phase. The infinite fold phase ambiguity which appears as the result of the zero conjugation possibilities in the Fraunhofer plane implies that additional information or processing of the object wave must be available to obtain the phase. Among the possible solutions which have been studied are reference beam addition, apodization and the use of multiple intensity distributions. The latter is possible in many applications and permits use of an iterative computational procedure (the Gerchberg-Saxton algorithm, for example) in which the Fourier transform and its inverse are calculated and the measured modulus replaces the computed modulus at each step. Recently we have asked whether relations between the intensities in the object plane which correspond to fields in the Fraunhofer plane with different zero conjugations would provide useful information. We have been able to demonstrate that a surprisingly simple relation exists for fields, $u_k(x')$, $u(x')$, which differ because of conjugation of the zero at z_k . This relation leads to a hierarchical ordering of the corresponding powers in the Fraunhofer plane and also provides insights into the nature of the phase ambiguity. The relation can be used to supplement the Gerchberg-Saxton algorithm. Our computer tests of the Gerchberg-Saxton algorithm against real laser phase profile data will be described.

Coded Aperture Imaging with Spatial Frequency Redundancy

S. C. Som
Applied Physics Department
Calcutta University
92 Acharya Prafullachandra Road
Calcutta 700009, INDIA.

Coded aperture imaging techniques are useful when electromagnetic and other radiations can not be focussed in the optical sense. Some of the application areas of this technique include γ -emission imaging of radionuclides, emission and transmission imaging of x-rays and γ -rays, x-ray and ultrasonic tomography etc. In principle, this technique can be used in any region of the spectrum, but practical considerations of implementation may restrict its use to the shorter wavelength region. The image decoding methods that are usually considered are of two types: correlation and deconvolution. In correlation techniques, the main problem is to find a suitable decoding aperture so that its cross-correlation with the coding aperture is approximately a delta function. On the other hand, the main problem in the deconvolution method is that the Fourier transform of the coding aperture may be very small or zero for some frequencies.

In this paper, a new deconvolution technique is described which makes use of spatial frequency redundancy to control the Fourier transform of the effective coding aperture. The basic drawback of the deconvolution processing is thus removed. It is shown that the new concept of spatial frequency redundancy in conjunction with the sampling theorem may provide a useful solution to the problem of image retrieval in coded aperture imaging. The basic theory, a convenient method of realizing spatial frequency redundancy and some results of simulation will be presented.

DETERMINATION OF PROPERTIES OF AN OBJECT
FROM ITS TRANSIENT EDDY CURRENT RESPONSE

by

Y. Das and J.E. McFee

Defence Research Establishment Suffield
Ralston Alberta

Detectors based on the principle of electromagnetic induction are routinely used to detect metallic objects buried near the ground surface. Addition to these detectors of the capability of determining depth, size and other parameters of the detected objects will be highly desirable in some applications including the detection of buried unexploded artillery shells. After a brief background to the above application, the paper will discuss the problem of determination of parameters of a permeable, conducting object from its transient eddy-current response. The model used for the shells is a sphere of arbitrary electrical parameters and the sensor is a coaxial system of coils. The step response of a sphere is represented by a sum of decaying exponential terms and the first step involved in the explicit determination of parameters is to extract amplitude and decay factors from a measured set of samples of the response. The scope and limitations of potential methods of achieving this objective will be discussed. In light of the limitations of these methods, a few feature selection schemes potentially useful for object classification (as opposed to explicit determination of parameters) will also be introduced.

SYNTHETIC IMAGING FROM COHERENT BACKSCATTERING

Jiunn S. Yu

Applied Physics Division 2353
Sandia Laboratories, Albuquerque, N.M. 87185

A radar is capable of synthetic imaging through coherent processing of object backscatterings. The completeness of image depends on the extent of object-aspect angles from which backscatterings are processed, and the image sharpness (resolution) depends on the sampling schemes of a receiver designed in consistence with a predetermined transmitter waveform. This paper applies the Woodward's method of 1946 to synthesize the scattering intensities across the widths of an object from different aspect angles. Scattering intensities along the depths of an object are resolved by compressed short-pulses of linearly or logarithmically chirped waveforms using the Hamming's weighting. A brief review of general principles and a comparison with synthetic-aperture radars for terrain mapping are made before a repetitive waveform is specified for radar transmitter to illuminate several axially symmetric objects. Backscattered pulse-trains from the targets are then analytically formulated for a coherent receiver whose outputs may either be in the time or frequency domain. Transformations of the receiver outputs are subsequently performed to synthesize the images of these objects. Data processing algorithms that avoid the slant-range and cross-range ambiguities are developed by specifying the maximum object sizes and the resolution limits of a radar system. Actual applications to imaging earth satellites are discussed with practical constraints imposed by orbital parameters. The need and the technique for image enhancement are demonstrated with emphasis on scattering-center concepts and for occasions when objects are imaged only through a limited range of aspect angles. Limits of applicability and potentials for extension are finally outlined for the synthetic imaging techniques using coherent backscatterings of monostatic or multistatic radars. Polarization sensitivities and three-dimensional imaging possibilities will also be discussed.

THREE METHODS FOR MICROWAVE IMAGING OF BURIED, DIELECTRIC ANOMALIES

G. Tricoles, E. L. Rope, R. A. Hayward
General Dynamics Electronics Division
P. O. Box 81127, San Diego, CA 92138 USA

Several applications of electromagnetic wave scattering aim at acquiring information about remote or inaccessible objects from measured data. Examples include radar, direction finding, and laboratory diagnostics of dielectric or metallic objects. These applications can be described as forms of inverse scattering. The imaging of inaccessible or remote objects is a somewhat special inverse process and so is the synthesis of computer-generated holograms for imaging. Although objects can be identified without imaging, say from the spectral responses in wideband measurements, imaging can be useful when little information about the object is known before the measurement or when the dielectric between the object and sensor is inhomogeneous.

This paper describes three methods for imaging with microwaves. The methods were applied to imaging anomalies in a dielectric half-space, such as soil, with antennas above the air-soil interface.

One method is holographic.¹ Phase and intensity measured over planar area, were encoded in binary, detour phase holograms, and images were formed in reconstructions with laser light. Another method was based on the angular spectrum. (See Ref. 1.) It produced images by numerically backward propagating the Fourier transform of the measured phase and intensity. For both of these methods a single frequency was adequate for determining object size and shape. The objects were flat and had simple structure and measurements were made in the nearfield. Both measured data and images are given to show the effects of wave polarization, antenna spacing from the interface, object depth, surface roughness, and soil moisture.

The third method utilized two frequencies, one being twice the other. The complex reflectance was modelled as a polynomial with one polynomial for each frequency. The polynomial has exponential functions as variables so it was solved by a mathematical method due to Prony. This method gave both object depth and thickness, at least for flat objects. Experiments utilized 2 GHz and 4 GHz and bistatic antennas. Images are synthesized by plotting the computed depth and thickness as a function of position in a raster scan.

REFERENCE

1. O.-C. Yue, E. L. Rope, and G. Tricoles, "Two Reconstruction Methods for Imaging Buried Dielectric Anomalies", IEEE Trans., Vol. C-24, pp 381-390 (1975).

A TARGET DERIVED REFERENCE TECHNIQUE FOR FREQUENCY DIVERSITY IMAGING

N.H. Farhat, C.K. Chan* and T.H. Chu
University of Pennsylvania
The Moore School of Electrical Engineering
Philadelphia, PA 19104

*Massachusetts Institute of Technology
Lincoln Laboratory
Lexington, Mass.

The use of frequency diversity or frequency swept technique in achieving super-resolution in imaging three dimensional perfectly conducting objects is described and demonstrated by computer simulations. It is found to be a multi-static generalization of the inverse scattering theory; namely that the shape of a 3-D perfectly conducting object and its scattered far field recorded by a set of coherent receivers forms a 3-D Fourier transform pair. By invoking Fourier projection theorems, slices of the object can be imaged separately thus establishing the feasibility of a tomographic radar. However, in order to generate an undistorted image of the object, an unwanted carrier signal recorded by each receiver that depends on the distance of the receiver from the object has to be first removed. In particular a target derived reference (TDR) technique that can achieve this goal is described. The advantages of using this approach are enumerated. This technique utilizes the illumination of the object by a high frequency imaging signal and a harmonically related low frequency reference waveform at which the object behaves as a point scatterer. It is found that in order to have negligible distortion in the image, the smallest wavelength of the reference signal has to be at least 40 times the maximum dimension of the object. An example demonstrating this effect for a perfectly conducting sphere is presented. A microwave circuit configuration employing the TDR technique presently under study will be described.

FRIDAY MORNING

June 6, 8:30 - 12:00

REFLECTOR ANTENNAS II

DKN 1A

Session B.18

Chairman: G.Y. Delisle
Université Laval
Québec, P.Q.

IMPROVING SCAN CAPABILITY OF PARABOLIC REFLECTORS BY USING
CLUSTER FEEDS

S.W. Lee*, P. Cramer, Jr., and K. Woo
Jet Propulsion Laboratory
California Institute of Technology
Pasadena, California 91103

In modern multibeam reflector antennas, the feed is usually made of a periodic array of identical elements. The radiation from each element produces an independent beam in space. For feed elements located away from the focus of the reflector, the corresponding beams have undesirable characteristics such as low gain and high sidelobes. An effective way to reduce this deficiency is to employ a cluster of feed elements, instead of a single element, to control each and every beam. With proper excitations (both magnitude and phase), the cluster can significantly improve the scan capability of the reflector antenna, because of the following effects: (A) The cluster produces more amplitude taper over the reflector's aperture than a single feed element does, and (B) the cluster reduces the phase error over the reflector's aperture. In the present paper, we concentrate on effect (B), the reduction of phase error by a properly designed cluster feed.

As an example, consider an offset parabolic reflector with aperture diameter 100λ , offset height 20λ , and focal length 96λ (the f-number of the parent reflector is 0.4). The feed is a periodic array with an exact triangular lattice. Each cluster consists of seven elements, namely, a center element surrounded by six auxiliary elements on a circular ring of radius 1.5λ . In order to demonstrate effect (B), not (A), we compare our cluster with a single feed element which produces the same amplitude taper (about 15 db) over the reflector's aperture. The comparison is listed below.

Scan in beamwidth	Lateral feed dis- placement	Feed type	Beam- width	Sidelobe level (db)	Gain (db)	Efficiency (%)
0	0λ	single	0.69°	-30.5	48.8	76
		cluster	0.71°	-32.5	48.4	69
7.25	10λ	single	0.80°	-13.0	46.8	49
		cluster	0.71°	-23.5	47.8	60
11.00	15λ	single	0.90°	-7.0	45.5	36
		cluster	0.74°	-15.0	46.6	47

We note that, for scanned beams, the use of a cluster feed significantly improves the sidelobe level, gain, and efficiency.

*Lee is with the University of Illinois, and is a consultant to JPL.

DUAL OFFSET REFLECTOR ANTENNAS --
GO VERSUS GTD

Y. Rahmat-Samii and C. Coyle
Jet Propulsion Laboratory
California Institute of Technology
Pasadena, California 91103

Dual offset reflector antennas have potential applications both as spacecraft multiple beam antennas and also earth terminals. Due to the more stringent requirements on reflector antenna performance, it is necessary that their far-field characteristics be predicted accurately and efficiently. In order to simplify the complexity of the analysis, attempts have been made to employ the concept of the equivalent parabola. While this concept provides a reasonable result for a very limited scan, it has been found that it is not accurate for predicting the scan loss for large scan angles.

In this paper, the dual offset reflector analysis is made by application of the Geometrical Theory of Diffraction (GTD) to the subreflector and physical optics (PO) to the main reflector. The evaluation of the PO integral is performed using the Bessel-Jacobi series method. This combined method results in an efficient and accurate computational analysis of the two-reflector system. Both offset Cassegrainian and Gregorian antennas are studied with their sub-reflectors constructed by intersecting a cone or a cylinder with the hyperboloid (ellipsoid) surface. An in-depth study is then performed to illustrate the significance of the edge diffracted field as an improvement to Geometrical Optics (GO). This study is important as it demonstrates the range of applicability of GO which takes considerably less computer time than GTD. Both on-focus and off-focus feeds are considered. A comparison is also conducted between the dual reflectors and their single reflector counterpart. Extensive numerical results are presented for scan loss, sidelobe levels, cross-polarization, etc. After examining different magnifications, it is concluded that the gain loss versus beam scanning is more severe than that which would result from the equivalent offset paraboloid.

SIMPLE FORMULAS FOR DESIGNING
AN OFFSET MULTIBEAM PARABOLIC REFLECTOR

S. W. Lee[†] and Y. Rahmat-Samii
Jet Propulsion Laboratory
California Institute of Technology
Pasadena, California 91103

Offset parabolic reflectors are widely used in today's multibeam antenna systems [Proc. IEEE, Vol. 66, pp. 1592-1618, 1978]. Many theoretical methods (computer programs) are available for analyzing the reflector performance [example, IEEE Trans. Antennas Propagat. Vol. 27, pp. 294-304, 1979]. These methods are the "forward" type in the sense that performance parameters (gain loss, sidelobe, scan, cross-over, etc.) can be calculated only after the configuration of the reflector (and feed) is given. In many practical applications, however, the problem often is the "inverse" type, namely, given a specification of performance parameters, the reflector configuration is designed.

In this paper, a systematic procedure based on simple formulas for solving such an inverse problem is presented. Two types of feed element patterns are considered for deriving the simple formulas. When the feed element is at the focal point, the first type gives an aperture distribution over the projected aperture described by a quadratic function. In the second type, instead of specifying aperture distribution, it is assumed that the on-focus element is a point source and has a radiation pattern described by a cosine function to the power q . For the first type, the simple formulas are derived using Silver's integral [Microwave Antenna Theory and Design, Dover Publication, 1965, p. 194] by evaluating it in a closed form. For the second type, numerical results for many different cases are obtained using the computer program developed at JPL and then properly fitted polynomials are introduced to represent the numerical data. These simple formulas are constructed for sidelobe levels, gain loss due to scan, beam deviation factor, etc. Numerous numerical results are presented for many different cases of practical interest to demonstrate the accuracy and applicability of the formulas.

[†]S. W. Lee is with the University of Illinois, Urbana, and is a consultant to JPL.

BACK-HEMISPHERE PATTERN COMPUTATION FOR REFLECTOR
ANTENNAS USING SPECTRAL THEORY OF DIFFRACTION

W. L. Ko and R. Mittra
Department of Electrical Engineering
University of Illinois
Urbana, IL 61801

The back-hemisphere pattern of a reflector antenna is of practical interest because of the need for an accurate estimate of the antenna noise temperature. Conventionally, the geometrical theory of diffraction (GTD) and its uniform versions are employed for the computation of wide-angle pattern of reflectors, including the radiation in the back-hemisphere. However, modifications of GTD, e.g., the equivalent current method must be used in the caustic region, for instance, the rear-axial direction of a focal-fed paraboloid, where the conventional GTD methods break down. In this paper, we present an alternative approach to the problem described above, one that is based on the spectral theory of diffraction (STD). This technique is an extension of the method that was presented in an earlier URSI paper (Ko and Mittra, "High Frequency Scattering From Smooth Surfaces with Edges -- a Spectral Domain Approach," National Radio Science Meeting, November, 1978, Boulder, Colorado), which dealt with the cylindrical shell problem. The starting point of this method is still the half-plane edge-diffraction coefficient á la Keller; however, in the STD framework the Keller coefficient is interpreted as one part of the kernel of the STD integral expression for the far field. The other part of the kernel is derived by using the argument that the contribution due to the physical optics current on a semi-infinite half plane -- an integral part of the GTD edge-diffraction coefficient -- should be replaced with another expression which is more appropriate for the curved surface under consideration. The STD integral representation with such a kernel is valid not only in the GTD trouble regions, e.g., the shadow and reflection boundaries, but in the caustic regions as well. Numerical results illustrating the application of the present method to reflector antennas presented in the paper and comparison with other approaches are included.

THE ELECTROMAGNETIC EFFECTS OF ELECTRICALLY
SMALL CONDUCTING WIRES LOCATED IN THE APERTURE
OF THE MAYPOLE REFLECTING ANTENNA

Jerry C. Brand, E. W. Smith, R. T. Hower
Harris Government Systems Group
Melbourne, Florida

Various electromagnetic scattering effects are produced when the feed support wires of a reflector antenna are located in the antenna's aperture. This is the case for the Harris space-deployable Maypole concept currently being studied under the sponsorship of NASA's Langley Research Center. This concept, which is being considered for antennas with reflector diameters in the range of 30-200m, will have missions which include as requirements low sidelobes and high efficiency. Since these support wires, which may be as thick as 0.6cm in diameter, are in the aperture then their contribution to the far-field pattern and the subsequent impact on the efficiency budget must be computed.

Each wire is many wavelengths long and is separated from other wires by a large number of wavelengths (except possibly at the attachment area). This allows the problem to be solved with a high-frequency technique. The solution to the field scattered from an infinitely long, uniform wire immersed in a plane wave is well known [1]. After the electric and magnetic fields from the wire are found, the equivalent current concept can be used to find fictitious currents which will produce the same fields. By integrating these equivalent currents on each wire in the aperture, the superposition of these scattered fields provides the far-field radiation pattern of the antenna with the support wires.

[1] J.B. Keller and D.S. Ahluwalia, "Diffraction By A Curved Wire", *SIAM J. Appl. Math.*, Vol. 20, No. 3, May 1971, pp. 390-405.

RF CONSIDERATIONS OF SUBREFLECTOR SUPPORTS
FOR CASSEGRAIN ANTENNA SYSTEMSJerry C. Brand and Edward W. Smith
Harris Government Systems Group
Melbourne, Florida

The subreflector support for a Cassegrain antenna can be provided by a radome or spar configuration. This support ideally should not detract from the RF performance of the antenna system, but, since this ideal support cannot be realized, a suitable support can be obtained and optimized to yield the best performance possible.

The modeling of the interaction of a radome or spar support structure with electromagnetic energy is complex. To directly apply Maxwell's equations to the interaction of EM energy with matter would be a very time consuming task. Therefore, certain simplifying assumptions must be made and justified before passing an accurate judgment on radome or spar performance.

An electromagnetic wave striking a dielectric interface contains three traveling wave components. These components are an incident wave, a reflected wave, and a transmitted wave. If the magnitude of the reflected wave is not zero, multiple reflections occur within the radome and radome wall [1]. By assuming only one reflection, a single reflection (or transmission) coefficient is obtained for a localized point on the radome. This assumption greatly simplifies the problem.

An electromagnetic wave striking a conducting surface is almost totally reflected. Thus, the reflected energy from a spar never reaches the main reflector, and causes a shadow on the reflector. The effects of this blockage on the overall system performance and the calculation of such effects have been reported in several papers [2], [3]. Polarization effects are averaged to yield a composite effect on the antenna's performance. Any scatterin and/or diffraction effects are included by applying GTD (Geometrical Theory of Diffraction) methods to the appropriate geometry.

References

- [1] M.V. Klein, Optics, John Wiley and Sons, New York, 1970, pp. 205-215.
- [2] John Ruze, "Feed Support Blockage Loss in Parabolic Antennas" CAMROC Technical Memo, No. 19, February 1967.
- [3] P.D. Potter, "The Design of a Very High Power, Very Low Noise Cassegrain Feed System for a Planetary Radar", TR No. 32-653, Jet Propulsion Laboratory, Pasadena, CA August 1964.

ANALYSIS OF CURVED RADOMES BY RAY TECHNIQUES*

S. W. Lee, R. Mittra, V. Jamnejad and M. Sheshadri
Department of Electrical Engineering
University of Illinois
Urbana, Illinois 61801

Many practical antennas are covered by radomes, whose effects on the antenna radiation is of considerable importance, especially in today's high-performance radar communication systems. In the past quarter of a century, several standard analyses have been devised for analyzing radome effects. None of them are exact and improvements are always needed.

In the present paper, we try to improve the standard radome analyses in the two aspects: the description of the incident field, and the curvature of the radome surface. More specifically, there are two new features in our approach:

- (a) The radome is normally situated in the near-field zone of the antenna, which may be a horn, a slot, or an array. Taking into consideration the finite antenna size, we approximately replace it by an array of discrete point sources, each of which radiates a spherical wave. Note that this approximation is different from that used in conventional techniques in which the incident field from the antenna is approximately represented by a spectrum of plane waves, instead of spherical waves.
- (b) In calculating the wave transmission through the radome, the curvature of the radome is invariably ignored in the conventional analyses. Our approach, however, does treat the radome as a curved surface by calculating the transmission of a spherical wave via ray techniques.

*This work was supported by Naval Air Systems Command under Contract N000 1979C-0281.

BOUNDARY VALUE PROBLEMS OF ANTENNAS
IN THE METALLIC CYLINDRICAL WEDGE REGIONSMao Kang-hou
P.O. Box 3923
Peking, People's Republic of China

This paper studies the boundary value problems of electromagnetic wave excited by electric source on the metallic cylindrically tipped wedges. This paper tackles the solution of Maxwell's equations for electric dipole excitation. We obtain three components of the far fields and the radiation resistances for the conducting infinite metallic cylindrical wedge.

In order to justify our theory, we have taken two components of elementary dipoles on the metallic cylindrically tipped wedges and compared the results with the radiation resistances of the same dipoles placed on the metallic parabolic cylinder. In this special case, they coincide completely.

The field components in the far zone, when the dipole is placed perpendicular to the ridge of the cylindrically tipped wedges are given by Wait and Okashimo.*

The radiation resistances of the dipoles placed on the metallic parabolic cylinder are given by Chen Jing-xiong and Mao Kang-hou.**

* Wait, J.R. and Okashimo, K. : Can. J. Phys., Vol. 34

** Chen Jing-xiong and Mao Kang-hou : Scientia Sinica.,
2, (1978), 173-192.

DESIGN AND ANALYSIS OF A MEANDERLINE POLARIZER

James P. Montgomery
Texas Instruments Incorporated
Dallas, Texas 75226

This paper presents the results of an investigation into computer aided design and analysis of meanderline polarizers. This effort is specifically directed at achieving an optimum polarizer (defined by the user) over a specified bandwidth.

The design technique is based on the meanderline equivalent circuit suggested by SRI. A gradient optimization procedure is used. The transmission line effects of all dielectric layers has been included. Realization of the meanderline geometry is accomplished using a numerical scattering solution. Particular importance is placed on including the capacitance increase of the geometry due to adjacent dielectrics. The scattering solution is based on a Galerkin solution of the infinite geometry (J.P. Montgomery, IEEE Trans. Antennas Propagat., 23, pp. 70-75, 1975). A pulse basis with proper current edge singularities is utilized. Specific modes are utilized for corner geometries.

The validity of the design and analysis is illustrated by comparison with several simulator measurements. Additionally, a four layer polarizer utilizing identical sheets has been built and tested which achieves a maximum axial ratio of 1.6 dB over the bandwidth 7-18 GHz. Additional experiments in the band 18-50 GHz and at C band will also be presented.

RADIATION CHARACTERISTICS OF DIELECTRIC SPHERE

LOADED CORRUGATED CONICAL HORN

R. A. Nair and S. C. Gupta
Department of Electrical Engg.,
College of Engineering, University
of Mosul, IRAQ.

Results of the experimental and theoretical study of the effects of placing a dielectric sphere in front of, but displaced from, the aperture of a corrugated conical horn are included. The analytical treatment of the radiation characteristics of the device is based on the scattering theory. Calculations based on this formulation show good overall agreement with experimental data of radiation patterns. It is concluded that:

(i) the dielectric sphere mounted (off-set) corrugated conical horn carrying HE_{11} mode has greater pattern directivity with low secondary lobes as compared with that of conventional corrugated conical horns of the same dimensions.

(ii) the $-3dB$ beamwidth of corrugated conical horn can be reduced by dielectric spheres placed off-set in front of its aperture and $-3dB$ beamwidth is found to be dependent on the dielectric sphere diameter.

(iii) the on-axis gain of the corrugated conical horn is improved due to dielectric sphere loading.

(iv) the feed system with a two dimensional variable pattern control is attractive as a high directivity multiple beam paraboloidal reflector feed for many space applications.

FRIDAY MORNING

June 6, 8:30 - 12:00

SPECIAL SESSION ON INVERSE SCATTERING IV
GEOPHYSICAL SOUNDING

DKN 1B

Session B.19

Chairman: Leon Peters, Jr.
The Ohio State University
Columbus, Ohio

Organizer: W.M. Boerner
U I C C
Chicago, Ill.

MAXIMUM ENTROPY INVERSION
OF UNDERGROUND ELECTROMAGNETIC AND SEISMIC DATA

R. M. Bevenssee

Lawrence Livermore Laboratory, Livermore, CA.

Solutions of undetermined problems of data inversion to obtain underground parameter profiles of dielectric constant, wave velocity, or conductivity are discussed in the context of the "First Principle of Data Reduction" [J. G. Ables, Astron. Astrophys. Suppl. Series, 15, 383-393, 1974]:

"The result of any transformation imposed on experimental data shall incorporate and be consistent with all relevant data and be maximally noncommittal with regard to unavailable data."

The Maximum Entropy (ME) Spectral Analysis method is first briefly reviewed, as applied to the extrapolation of the autocorrelation of a process. This is equivalent to the least squares fitting of an autoregressive model to the process.

The ME solution to the problem of determining a subsurface dielectric constant profile via high-frequency cross borehole measurements is discussed. To simplify the problem, while retaining its essence, straight rays are assumed through the region divided into cells. The most probable distribution of dielectric constant is obtained, subject to the constraints of fixed total amount and the observed total phase shift along each ray. Some numerical solutions are presented.

The ME determination of a seismic velocity profile from transit time measurements of longitudinal waves is discussed. The rays are assumed initially straight but become curved in accord with Snell's law in successive iterations of the ME algorithm. A numerical solution is presented to illustrate the rate of convergence to a reasonable velocity profile.

The more difficult problem of converging on a two-dimensional layered underground conductivity distribution from low-frequency surface potential measurements is treated. The algorithm used to compute surface potentials from an assumed profile is one using probabilistic potential theory. The procedure of iterating back and forth between a conductivity profile and a computed potential distribution by the ME principle, so as to converge on a reasonable profile, is illustrated by example(s).

EXACT INVERSE SCATTERING FOR
PIECE-WISE CONTINUOUS MEDIA

Norbert N. Bojarski
16 Pine Valley Lane
Newport Beach, California 92660
Telephone: (714) 640 7900

The exact inverse scattering integral equation of this author (1973) is rederived. This integral equation consists of a Fredholm integral equation of the first kind, relating the unknown sources to an effectual field (introduced by this author), which is computable by a modified Kirchhoff integral for all points in space from knowledge of the incident and scattered (remotely sensed) fields on a surface enclosing the unknown sources. The kernel of this integral equation consists of the imaginary part of the free space Green's function, with an arbitrarily chosen free space reference velocity.

It is shown that the effectual field is an imaginary field, consisting of the destructive interference between the real physical causal field and an artificial anti-causal field, all emanating from the sources induced by the incident field, and propagating at the arbitrarily chosen reference velocity.

For piece-wise continuous media, the vast predominance of the sources induced by the incident field are on the surfaces delineating the piece-wise continuous segments of the medium. Thus, a graphic time-space display of the effectual field yields the spatial and temporal locations of the discontinuity interfaces, and consequently, the average segment wave propagation velocity. A solution of the integral equation is thus unnecessary for such media.

This graphic solution is well suited for seismic geophysical exploration, non-destructive testing, radar and sonar scattering by perfect reflectors, etc.

Numerico-experimental results for a two dimensional layered medium with a plane impulsive incident field, as well as an unknown point source in an arbitrary medium (the passive artillery location problem), are presented.

INTERPRETATION OF DATA FROM THE UTEM
EM PROSPECTING SYSTEM

G. F. West, Geophysics Lab, Department of Physics,
University of Toronto, Toronto,
Y. Lamontagne, Lamontagne Geophysics Ltd.,
740 Spadina Avenue, Toronto.

A wide-band time-domain ground electromagnetic prospecting system has been developed for ore exploration where the target bodies are so deep or situated in such conductive rocks or under such conductive overburden as would be difficult for a classical EM system to handle. The receiver maps the H (and sometimes E) field in the vicinity of a fixed transmitter antenna consisting of a horizontal single turn loop up to a kilometer square. The receiver utilizes a coil as H field sensor. The transmitter current has a precise current controlled triangular current waveform in the frequency range 10-30 Hz. Thus, the received signal waveform is a square wave in the case of a highly resistive ground (rise time $\approx 15\mu\text{s}$). Distortion of the square wave by eddy currents induced in the ground is determined in 10 logarithmically-spaced time intervals to an accuracy of 1-2 ppk in the later time intervals. Receiver and transmitter waveforms are synchronized by stable local crystal oscillator clocks.

Data from the UTEM system is well suited to quantitative and semi-quantitative interpretation by model fitting, and in rare cases by inversion methods. In ore prospecting, one is generally trying to identify and locate target conductors in the bedrock, and distinguish such features from locally more conductive or thicker parts of the overburden. Scale model and numerical model studies show that there are two distinct processes by which a local conductor can generate a magnetic field anomaly: 1) by direct induction of a current vortex locally within the conductor; 2) by local concentration of the regional current flow induced in the host rock or overburden. The first of these mechanisms is generally of more diagnostic value in ore prospecting, but it may not be possible to arrange the survey parameters so that a response by local induction is observed. However, there are many cases where the two responses can be identified and separated, and interpretation facilitated.

Examples of field and model data for a variety of geological situations will be presented.

GEOTOMOGRAPHY APPLIED TO NUCLEAR WASTE
REPOSITORY SITE ASSESSMENT

R. J. Lytle, J. T. Okada, E. F. Laine
Lawrence Livermore Laboratory
Livermore, California 94550

Electromagnetic borehole-to-borehole transmissions were made in the Stripa Mine near Buldshmedshyttan, Sweden in April 1979. Transmission loss measurements were made between five sets of 76 mm boreholes 30 meters long located at the end of a drift. Spacings of the boreholes varied from 2 meters to 20 meters. Greater than 25,000 data points were taken. A geotomography was constructed to show the variation of attenuation between boreholes. The observed spatial variation of electromagnetic attenuation appears to be consistent with the expected stress relief created by the mine. Transmission loss measurements were also made between two boreholes drilled from the surface to near the mine. Data taken at 21 MHz shows the nearly uniform attenuation character of this sampled region. These experiments demonstrated that geotomographic data collection/interpretation provides high resolution images of the underground environment. These experiments have indicated that geotomographic remote probing procedures can provide useful input to those charged with providing the detailed site characterizations needed for both short and long term monitoring of underground nuclear waste repositories.

DETECTION AND IDENTIFICATION OF BURIED FERROUS OBJECTS
BY MEASUREMENT OF THEIR ASSOCIATED MAGNETOSTATIC FIELDS

by

J.E. McFee and Y. Das

Defence Research Establishment Suffield
Ralston Alberta

The physical and magnetic properties of a ferrous object in a magnetostatic field, such as the earth's field, may be related to the parameters (dipole moment, orientation and location) of the dipole moment associated with the object. This is discussed for the special case of a permeable spheroid and generalizations to arbitrary shapes are made.

A novel method to determine the dipole parameters is outlined. It consists of measuring one or more components of the magnetic field of the dipole in a two dimensional grid and performing a two dimensional multiparameter nonlinear least squares fit to the data. Unlike many other methods no previous knowledge of the parameters is required.

Results of computer simulation are presented to show that reliable and consistent parameter estimation is obtained and that pseudo-realtime operation is achievable on a fast minicomputer. Effects of electronic and sensor noise and motion of sensors are included for all major classes of magnetometer sensors. Examples are included of application of the method to experimentally obtained data.

SELF-CONSISTENT EVALUATIONS OF COMPLEX CONSTITUTIVE PARAMETERS

Jiunn S. Yu

Applied Physics Division 2353
Sandia Laboratories, Albuquerque, N.M. 87185

Postulating the constitutive relations is known as an essential step in the formulation and solution of the Maxwell's equations. Physically, the complex constitutive parameters serve as a mean of relating charge motions to applied forces. Macroscopic properties of a linear medium are thus commonly characterized by these parameters, and their evaluations are based on certain measurements relatable to analytically-solved field vectors. Evaluation techniques using bounded and unbounded waveguides are first reviewed with brief discussions on inherent assumptions and approximations. This paper emphasizes the self-consistent evaluations in which the modal coefficients of a complete set of orthogonal modes are known to be recursively related. The techniques are self-consistent in that N sets of modal coefficients can be determined within various bounds of uncertainties from measured data, and that the resulting N sets of constitutive parameters are consistent to within quantifiable inaccuracies and imprecisions. A lossy sphere of undetermined medium is used as the first example where multipole coefficients are determined from multistatic scattering measurements. Actually measured data from a scattering range are used with a refractive index chart to evaluate the constitutive parameters of several specimens. A pair of coaxially coupled coils serves as the second example where the self and transfer impedances can be measured to consistently evaluate the desired parameters for an unbounded medium such as an earth formation or a large volume of liquid. The first is useful when $f > 500$ MHz and when a specimen can be tumbled into a small sphere. For geophysical explorations with in-situ measurements, the second example is suitable for $f < 500$ MHz. Relative usefulness compared with other techniques will be summarized in conjunction with the homogeneous and isotropic assumptions. Also, the postulates for conduction, displacement, and tortuous currents will be discussed for a medium with complex mixes of many substances.

ANTENNA DESIGN FOR GEOPHYSICAL APPLICATIONS*

H. M. Buettner
Lawrence Livermore Laboratory
Livermore, California 94550

Electrically short, highly directional antennas can be very useful for down-hole, electromagnetic probing of geophysical features. The electrical shortness of the antennas enables one to resolve fine subsurface features, while the directionality improves system signal to noise ratio and enables one to locate subsurface anomalies from a single borehole. This presentation outlines the results of work which has produced electrically short, directional antennas operating in the 10 to 200 MHz region for use in a borehole environment.

Shortening our antennas is accomplished by surrounding the antenna elements with a sheath material having an electromagnetic wave velocity much less than that of free space. Two classes of materials suitable for this purpose are ferrites and ferroelectrics. We have produced a ferrite-sheath antenna in this manner which exhibits a shortening of 4.6 at an operating frequency of 190 MHz. This quarter-wave, resonant monopole has an input impedance of 75 Ohms and a diameter of 3.0 cm. The experimental value for shortening of 4.6 agrees well with that obtained by computer simulation.

Azimuthal directionality in the antenna radiation pattern results when the antenna conductors are moved away from the axis of symmetry of the sheath. As a rough rule of thumb, radiated power will be maximized in a given direction whenever the wave travels an odd number of quarter-wavelengths in that direction, and minimized whenever it travels an even number of quarter-wavelengths or zero (R. J. Lytle and E. F. Laine, IEEE Transactions on Geoscience Electronics, Vol. GE-16, No. 4, 304-307, 1978). This technique has been employed with a ferrite sheath to produce an antenna having a front-to-back ratio of 3 db at an operating frequency of 200 MHz.

Antenna shortening, directionality, and other characteristics such as input impedance, usable frequency range, efficiency, and sheath diameter depend upon judicious material selection. An assessment of conventional sheath materials has been performed which indicates that for down-hole applications ferrite-sheath materials produce the most desirable combination of antenna characteristics in the low frequency regime (10 to 50 MHz). Ferroelectric sheath materials are generally more appropriate for the high frequency regime (> 50 MHz).

*Work performed under the auspices of the U. S. Department of Energy by the Lawrence Livermore Laboratory under contract number W-7405-ENG-48.

THE DESIGN OF A RADIO FREQUENCY PROBE FOR USE IN
HYDROCARBON EXPLORATION

by G. S. Huchital
Schlumberger-Doll Research
P. O. Box 307
Ridgefield, CT 06877

Most of the oil and gas produced today is found in porous reservoir rocks. Two basic parameters necessary to the oil and gas industry in order to estimate the in situ reserves are the porosity of the host rock (ϕ) and the percentage of the fluid that is water (S_w). One minus the water saturation is the percentage of fluid that is hydrocarbon.

Well logs provide the industry with measurements of the porosity, water saturation, type of rock (lithology) thickness of deposited beds etc. These parameters are determined by measuring acoustic, nuclear and electrical properties of the sedimentary rocks. Porosity measurements are provided by both acoustic and nuclear techniques.

Electric properties of materials can be described by three basic quantities: resistivity, magnetic permeability and dielectric constant. The measurement of resistivity has been successfully used to locate hydrocarbons for many decades. The magnetic permeability of most sedimentary rocks appears to have little relation with formation evaluation parameters. As for the dielectric constant it represents a new and significant measurement to the well logging industry.

This paper will discuss the design of a radio frequency probe. This probe will be used to measure both resistivity and dielectric constant. Particular attention will be given to the response of the device in the radially cylindrical, vertically layered medium present in the drill hole. Numerical simulation results will be presented detailing the effect of the drill hole and other radial inhomogeneities on the response of the device. In addition the numerical simulation of the response of the device to the vertical layered medium presented by drilling through the earth will also be discussed.

FRIDAY MORNING

June 6, 8:30 - 12:00

MICROSTRIP ANTENNAS AND ARRAYS

DKN 1271

Combined Session AP-S/B.20

POSTER SESSION

Chairman: R.E. Munson
Ball Aerospace
Boulder, Co.

The following papers belong to the IEEE AP-S Symposium and the summaries are included in the IEEE AP-S Digest under Combined Poster Session AP-S/B.20.

1. CALCULATED AND MEASURED PERIMETER FIELD DISTRIBUTIONS FOR MICROSTRIP ANTENNAS, K.R. Carver, New Mexico State University, Las Cruces, N.M.
2. THE CIRCULARLY POLARIZED ELLIPTICAL PRINTED-CIRCUIT ANTENNA, S.A. Long and L.C. Shen, University of Houston, Houston, Texas,
3. CHARACTERISTICS OF A CAVITY BACKED ANNULAR SLOT ARRAY, A. Shoamaneh, F. Rahman and L. Shafai, University of Manitoba, Winnipeg, Manitoba.
4. CALCULATION OF H-PLANE MUTUAL COUPLING BETWEEN RECTANGULAR MICROSTRIP ANTENNAS, A.R. Sindoris, Harry Diamond Laboratories, Adelphi, MD., C.M. Krowne, North Carolina State University, Raleigh, N.C.
5. A 7.5 GHz MICROSTRIP PHASED ARRAY FOR AIRCRAFT TO SATELLITE COMMUNICATION, F.W. Cipolla, Ball Aerospace Systems Division, Boulder, Co., and L.P. Trapani, Griffiss Air Force Base, N.Y.
6. ANALYTICAL AND EXPERIMENTAL INVESTIGATION OF XP-FILM MATERIAL FOR HARDENED PRINTED DIPOLE ARRAY DESIGN, R.S. Chu, S.Y. Peng, R. Tang and N.S. Wong, Hughes Aircraft Company, Fullerton, California.
7. MUTUAL COUPLING BETWEEN RECTANGULAR AND CIRCULAR MICROSTRIP ELEMENTS, R.P. Jedlicka, M.T. Poe and K.R. Carver, New Mexico State University, Las Cruces, N.M.

8. DESIGN OF COLLINEAR LONGITUDINAL SLOT ARRAYS FED BY BOXED STRIPLINE, P.K. Park, Hughes Missile Systems, Canoga Park, CA., and R.S. Elliott, UCLA, Los Angeles, CA.
9. REDUCING BACKLOBES FROM MICROSTRIP ARRAYS, M. Shields, Ball Aerospace Systems, Division, Boulder, Co.

APPROXIMATIVE COMPUTATION OF MUTUAL COUPLING
BETWEEN MICROSTRIP RESONATORS

E. VAN LIL, A. VAN DE CAPELLE
K.U. Leuven, Afd. Microgolven en Lasers
Kardinaal Mercierlaan 94
B - 3030 Heverlee, Belgium

From a spectral analysis point of view (decomposition of the field in plane waves), the mutual admittances between apertures can be found, by an analogue raisonnement as in (Harrington : "Antenna theory I", pp. 61-92), to be :

$$Y_{12} \doteq \frac{\left\{ \text{Re} \left[(\bar{\epsilon}_{a1} \cdot \bar{k}_T) (\bar{\epsilon}_{a2}^* \cdot \bar{k}_T^*) e^{-j\Delta\varphi} \right] + (k_z^*)^2 \cdot \text{Re} (\bar{\epsilon}_{a1} \cdot \bar{\epsilon}_{a2} e^{-j\Delta\varphi}) \right\}}{k_z^*} d\xi d\eta$$

when the aperture fields $\bar{\epsilon}_{a1}$ and $\bar{\epsilon}_{a2}$ are known, and where $\Delta\varphi = \xi \Delta x + \eta \Delta y$ is the phase factor due to the position differences between the reference axis of both apertures.

So, when we insert those values in the models for the rectangular resonators, (E. Van Lil, et al. : "Design models for rectangular microstrip resonator antennas" 1978 I.E.E.E. Symp. on AP, pp. 264-267), we are not only obtaining better models for the resonator itself, but are able to calculate the coupling between arbitrary spaced resonators. Approximations, agreeing with the theoretical values within 1% have been derived for the fundamental mode.

(°) The authors are respectively research assistant and qualified researcher of the Belgian National Science Foundation.

IMPEDANCE-MATCHING OF MICROSTRIP RESONATOR ANTENNAS

H.F. Pues and A.R. Van de Capelle, K.U. Leuven,
 Dept. Elektrotechniek - M.I.L., B-3030 Heverlee,
 Belgium.

The limiting factor on the bandwidth of microstrip resonator antennas is the impedance. Consequently it must be possible to increase the bandwidth of these antennas by means of an impedance-matching network. Such a network can be realized on the same substrate as the radiator and will occupy about the same area (or less).

The frequency dependence of a microstrip resonator antenna can be characterized by its quality factor Q . An approximate expression for the Q -factor of a rectangular microstrip resonator antenna has recently been published (J. Vandensande, H. Pues and A. Van de Capelle : "Calculation of the bandwidth of microstrip resonator antennas", Proceedings of the 9th European Microwave Conference, Brighton, Sept. 1979, pp. 116-119). From the knowledge of the Q -factor one can easily deduce the relative bandwidth (for an input voltage standing wave ratio less than, say, S) which can be achieved without an impedance-matching network (BW_1) and with such a network (BW_2).

One finds :

$$BW_1 = \frac{1}{Q} \cdot \sqrt{S + 1/S - 2} \quad (\text{antenna supposed to be matched at resonance})$$

$$BW_2 = \frac{1}{Q} \cdot \frac{\pi}{\ln((S+1)/(S-1))} \quad (\text{matching network supposed to be ideal})$$

From these formulas it follows that for usual values of S the bandwidth can be increased by a factor of about 4.

Several S- and X-band antennas with a matching network have been designed. It concerns rectangular patch antennas with a network consisting of stubs and lines on the same substrate. In these designs the antenna and the network form a Tchebyscheff bandpass filter. Detailed measurement results of "impedance bandwidth" and "radiation pattern bandwidth" will be presented.

INPUT IMPEDANCE AND RADIATION CHARACTERISTICS OF
A CIRCULAR MICROSTRIP ANTENNA

W. C. Chew, J. A. Kong
Department of Electrical Engineering and
Computer Science and Research Laboratory
of Electronics
Massachusetts Institute of Technology
Cambridge, Massachusetts 02139

In the past, the problem of radiation due to a circular microstrip antenna has been attacked by solving for the fields with the assumed current distributions corresponding to a resonant cavity bounded by magnetic walls. To compute the input impedance and the radiation patterns, the dyadic Green's functions for a two-layer stratified medium has to be used. We compare the calculated results with previous results using free-space Green's function and find that the previous assumptions are valid only when the microstrip thickness is very thin. Furthermore, for actual excitation with a probe, the current distribution is a superposition of more than just the fundamental TE_{11} mode. To account for this deviation, we use the vector Hankel transform method to formulate the microstrip antenna problem in terms of vector dual integral equations, incorporating the dielectric effect with the dyadic Green's function for stratified media. From the formulation, we derive the current distribution under a probe excitation. The radiation pattern is computed for each individual mode as well as for the superposition of all modes corresponding to the actual current distribution. The actual current distribution is compared with the assumed current distribution. Also, the input impedance computed using such a technique is compared with the mode-expansion technique that is commonly used. The theoretical results are compared with experimental data and their differences discussed under the context of these different approaches.

Hankel Transform Domain Analysis of Open
Circular Microstrip Radiating Structures

K. Araki^{*}, T. Itoh^{*}, and Y. Naito^{**}

^{*} Dept. of Electrical Engineering, University of Texas
Austin, TX 78712, USA

^{**} Tokyo Institute of Technology, Tokyo, Japan

A circular disc conductor printed on a dielectric substrate backed by a ground plane has been widely employed as a resonator or an antenna element and investigated extensively (S. Mao et al, IEEE, MTT-16, pp. 455-462, 1968; J. R. Jones et al., IEE MOA, 2, pp. 157-164, 1977). Most of these analyses are based on the quasi-static cavity model where magnetic side wall is assumed at the edge to derive resonant frequencies. Radiation patterns are calculated from the magnetic current flowing along this magnetic wall. When the substrate is thin compared to the wavelength or dielectric constant of substrate is high enough, these approximate treatments will provide satisfactory results. At higher frequencies, however, the cavity model method may not be accurate and a more rigorous full wave analysis such as the one in this paper is needed.

The present method is an extension of the spectral domain approach (T. Itoh et al., Proc. WPCAT, 1979) and is based on the formulation in the Hankel transform domain. The method has a number of attractive features: (1) Instead of formulating the problem in the space domain in terms of coupled integral equations, we obtain simple algebraic equations in the transform domain. (2) Green's functions are given in a closed form. (3) No time-consuming inverse-transforms are needed to obtain the complex resonant frequency and the radiation pattern. (4) Numerical processing is quite simple since we only need to deal with a small size matrix eigenvalue problem due to the fact that a certain physical nature of the unknown current on the disk may be incorporated in the formulation. (5) Fields associated with orthogonal circular polarizations are incorporated in the process.

Several numerical examples are presented in the paper and compared with available experimental data where feasible.

AP/B.20 - 14

ANALYSIS OF CONDUCTING STRIPS AND PATCHES
PRINTED ON A GROUNDED DIELECTRIC

M. C. Bailey
NASA Langley Research Center
Hampton, Virginia 23665

CANCELLED - ANNULÉ

MONDAY AFTERNOON

June 2, 1:30 - 5:00

SPECIAL SESSION ON OPTICAL COMMUNICATIONS II

DEVICES AND SYSTEMS

DKN 2B

Combined Session C.1/D

Chairman: A.R. Boothroyd
Carleton University
Ottawa, Ontario

Organizers: A.R. Boothroyd P.H. Wittke
Carleton University Queen's University
Ottawa, Ontario Kingston, Ontario

OPTICAL FIBER SYSTEMS: PROGRESS AND PROSPECTS

C. Kao

ITT Electro-Optical Products Division, Roanoke, Virginia

Major systems involving thousands of kilometers of optical fiber cables have been scheduled for installation in the 1981-83 time period and many more are under planning. Does this mean that optical fiber systems technology has matured? Are we witnessing the applications where optical fiber systems are found to be economically attractive? Can we identify the *raison d'etre* of using optical fiber systems in new applications? What prospects hold for optical fiber systems? The answers to these questions are attempted in this review of the progress and prospects of optical fiber systems.

The number of countries around the world with optical fiber system installations has grown to over 20. While most of the installed systems are trial installations, they are paving the way for further installations. The majority of the systems are sponsored by the PTT's and are for carrying fairly large traffic between central offices. Some installations are for carrying relatively small traffic into and out of areas with high electromagnetic interference, such as at an electricity generating plant. Several installations connect the satellite ground station to a distribution hub. These are known as entrance links and carry TV or telephone signals. A few are specialized systems, such as those with improved privacy of transmission, and those designed for trunking of TV signals, and those to demonstrate wired city concepts. Apart from the specialized system, these systems can demonstrate economic competitiveness against other solutions.

Much system work is in the planning phase. These include many military applications, undersea telecom systems, and systems with fiber being used as sensors. These systems generally explore the special features of the fiber properties to achieve unique solutions to particular problems or system performance improvements in areas of need.

The scheduled installations of major systems demonstrate the maturity of the technology for producing the first generation products. It is just the beginning of an era when as a result of technology progress and more pertinently, lower fiber system cost, many future systems will become economically attractive and affordable for a host of new and currently identified applications.

RECENT ADVANCES IN LIGHT SOURCES FOR
OPTICAL COMMUNICATIONS

Henry Kressel
RCA Laboratories
Princeton, NJ 08540

Laser diodes and light-emitting diodes incorporating heterojunctions are well established as practical devices. The majority of the diodes currently in use consist of AlGaAs devices emitting in the vicinity of $0.85 \mu\text{m}$. However, rapid advances are being made in double-heterojunction diodes (lasers and LEDs) fabricated using InGaAsP epitaxially deposited on InP substrates. These emit in the 1.2 to $1.5 \mu\text{m}$ region where the fiber attenuation is very low. Major areas of concentration are in: (1) reliability improvement in order to extend the mean time to failure estimated values to consistent values in the 10^6 hr. range; (2) laser structures which consistently operate in a single spatial mode over a useful power emission range; (3) improved understanding of the modulation properties of laser diodes at high frequencies.

PHOTODETECTORS FOR FIBRE OPTICAL COMMUNICATIONS

by J. Conradi

Bell-Northern Research
P.O. Box 3511, Station C
Ottawa, Ontario
Canada

The operating characteristics and the state-of-the-art of PIN and avalanche photodiodes for fibre optical communications over the 0.8 - 1.6 μm range will be reviewed. The joint influence of detector and receiver circuit element parameters on digital and analog receiver sensitivity will be discussed.

NARROW STRIPE LASERS FOR LINEAR APPLICATIONS

C. Lindström and P. Tihanyi
Institute of Microwave Technology
Stockholm, Sweden

Very narrow stripe (2-3 μm) proton isolated GaAlAs/GaAs injection lasers have been developed. The fabrication technique is straight forward with high yields and suitable for large scale production. These lasers delivers continuous output light power up to 20 mW free from unregularities ("kinks") in the input current to light output conversion. They are multimode lasers with low harmonic distortion. Furthermore these narrow stripe lasers exhibit a linear fast pulse response without the "light-spike" usually observed for broad stripe lasers. Accelerated ageing of these lasers at 80°C ambient temperature predicts a lifetime over one million hours at room temperature.

These characteristics and the ease of fabrication makes the narrow stripe proton isolated injection laser suitable for commercial use. Especially where analog applications and/or high pulse modulation are needed.

The fabrication method and the characteristics for these lasers will be presented.

The financial support was supplied by the L M Ericsson Telephone Company and the Swedish Board of Technical Development.

A COMBINATION OF ORGANOMETALLIC PYROLYSIS

AND

LIQUID PHASE EPITAXY

J.P. Noad, C.M. Look and A.J. SpringThorpe
Bell-Northern Research
Ottawa, Ontario

Conventional channeled substrate laser (CSL) structures have been shown to produce GaAlAs injection laser diodes for optoelectronic applications with significantly improved linearity. By further incorporating the channel within a p-type blocking layer current confinement can be enhanced, leading to reductions in laser thresholds.

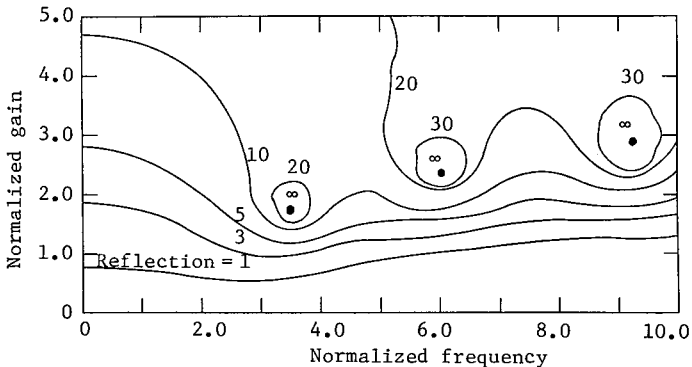
In this paper, a new technique is described in which channels are grown in a p-type GaAs blocking layer by using the technique of organometallic pyrolysis (OMP). The conventional 4 layer double heterostructure is then grown using standard LPE techniques. With the use of this new procedure, lasers have been produced which show good linearity to outputs greater than 14 mW. This method offers several advantages over alternate growth techniques for preparing CSL's. Device preparation and performance will be examined in terms of linearity and threshold. The effect of parameters such as the carrier concentration of the blocking layer, the channel width and the layer thickness on device performance will also be discussed, and compared to CSL's produced by more conventional techniques.

OSCILLATION CHARACTERISTICS OF ACTIVE ALMOST PERIODIC STRUCTURES

G. T. Warhola and D. L. Jaggard
 Department of Electrical Engineering
 University of Utah
 Salt Lake City, Utah 84112

Interest in the oscillation properties (i.e., threshold gain and resonant frequency) of active periodic structures was stimulated by the design and operation of distributed feedback (DFB) lasers for use in optical communications [see, e.g., H. Kogelnik and C. V. Shank, *J. Appl. Phys.* 43, 2327 (1972)]. Here we investigate the oscillation characteristics of active DFB structures in which the feedback is supplied by an almost periodic longitudinal variation of the permittivity or gain. The deviation from a perfectly periodic variation may be intentional or may be the result of fabrication errors.

The analysis of these active almost periodic structures is based on the vector coupled-mode equations which describe the structure [see, e.g., Bellman and Wing, *An Introduction to Invariant Imbedding*, John Wiley, New York (1975), or D. L. Jaggard and A. R. Mickelson, *Appl. Phys.* 19, 405 (1979)]. A typical plot of threshold gain as a function of frequency, with reflection as a parameter, is shown below for an almost periodic structure. As expected, oscillation (shown by infinite reflection) only occurs for discrete frequencies, three of which appear on this plot. We compare and contrast the threshold characteristics for active almost periodic structures with their periodic counterparts.



BANDWIDTH CHARACTERIZATION OF FIBER LINKS

R. IYER & A. JAVED

Dispersion characteristics of a fiber link that consists of several nominal lengths of fibers jointed together, cannot be related deterministically to the (nominally) specified bandwidth values of the individual sections because of the random effects introduced at the fiber joints and statistical differences between the specified and actual bandwidth values of the sections. In this paper, the fiber link bandwidth is modelled as a statistical quantity and some preliminary results that relate the link dispersion to the first and second order moments of the r.m.s. dispersion of each section are obtained. Such characterizations of fiber links are expected to be of interest in fiber system specification and planning studies.

OPTICAL WAVELENGTH INTERSATELLITE COMMUNICATIONS SYSTEM

A. K. Sinha

Communications Satellite Corporation; Washington, D.C.

High capacity (> 1 Gbps) intersatellite communication is feasible with the help of a laser transmitter and optical detector system. In this paper, application of a high capacity, wideband laser communication system for intersatellite communication is considered. Results of a parametric study of the system parameters, including the aperture size, power, capacity, bit error rate, range, etc. are presented. Some general implications for a global satellite communications systems are briefly discussed.

More specifically, the transmission characteristics of laser intersatellite links between geosynchronous satellites are modeled analytically. Several types of laser transmitters are considered for this purpose. Assuming Poisson distribution for photon arrival rate, and quantum statistical laws of black body radiation for the background solar input acting as a source of noise, the basic trade-off analyses of the link are performed. In particular, the bit error rate for a binary pulse gate transmission system is calculated under various operating conditions. Finally, the relevance of intersatellite links for advanced system concepts of satellite communications, such as antenna farms and satellite clusters, is briefly discussed.

A BASEBAND VIDEO AND FM AUDIO FIBER OPTICAL
COMMUNICATION SYSTEM FOR EDUCATIONAL AND
DEMONSTRATION PURPOSES

K.J. Clowes and G.L. Yip
Department of Electrical Engineering
McGill University
Montreal, Quebec

A complete fiber optical communication system developed at McGill is described. Baseband colour video signals and an FM-modulated audio signal at 10 MHz are sent through a fiber bundle which connect to the receiver and transmitter through low-cost plastic connectors. The electrical signal intensity modulates an LED in the transmitter and a silicon avalanche photodiode is used in the receiver for low-noise optical detection. The input and output audio and video signal levels and impedances are at the standard broadcast values, thus allowing the system to be easily inserted at any point in a standard network. This makes the system easy to demonstrate and no adjustments are required. A modular approach was used in building the system so as to clearly separate the various system blocks (LED driver, power supply, etc.). The electronics were simplified as much as possible to facilitate explanation of all aspects of system design. The system will be demonstrated and the terminal electronics will be discussed. Noise and distortion factors will be discussed as well as the performance specifications of the system. The use of this relatively low-cost optical communication system as an education tool will also be presented. Finally, possible practical applications of such a system will be pointed out.

TRANSMISSION OF 18 TV CHANNELS OVER A 1-km
ANALOG FIBER OPTICAL COMMUNICATION SYSTEM

K.J. Clowes and G.L. Yip
Department of Electrical Engineering
McGill University
Montreal, Quebec

J.C. Dagenais
Télécabre Vidéotron
St-Hubert, Quebec

H. Stephenne
Service de la recherche
Ministère des Communications, Quebec

An analog optical communication system has been developed at McGill which is capable of transmitting 18 TV channels and the entire commercial FM band over 1 km of optical fiber. The work has been done as part of a project sponsored by "Action concertée sur la câblodistribution" to find applications for fiber optical communication systems in Quebec's CATV industry. A highly linear stripe-geometry GaAs - GaAlAs double heterostructure laser operating at 830 nm is used in the transmitter. The receiver employs a fast silicon avalanche photodiode for best noise performance. The input and output signals are the 12 standard VHF TV channels, the commercial FM band and six mid-band TV channels. The power levels are compatible with standard CATV equipment and the interfaces are at 75 ohms. The system will be demonstrated and the interface circuits will be discussed. Noise and distortion considerations and the system performance will be presented. Methods for further improving the performance, including pre-distortion, feedback and feed-forward, will also be discussed. Practical system considerations will be presented and the merits of analog modulation over digital modulation for this application will be discussed. Finally, proposed collaborative work with Télécabre Vidéotron on a field trial of the system will be presented.

WEDNESDAY MORNING
June 4, 8:30 - 12:00

SATELLITE AND RADIO TRANSMISSION
DKN 2A

Session C.2

Chairman: J.F. Hayes
McGill University
Montréal, Québec

Optimum Satellite Frequency Estimates for Canada and U.S.

Paul F. Christopher
The MITRE Corporation
Bedford, Massachusetts 01730

Five rain regions of North America are treated, using a promising new model by R. K. Crane. This model is modified to include an f^2 dependence for rain attenuation, and total attenuation vs. frequency (2-90 GHz) is generated. These attenuation plots are used as inputs to a frequency selection process, and antenna system costs as a function of required surface tolerance are assumed to vary slowly (for diameter < 2m.) across the entire frequency band.

With fixed antenna sizes at the spacecraft and ground terminal, frequency is then varied until maximum received signal is found. (LOSS-GAIN) plots are especially useful for frequency selection, and characteristic local minima occur on these plots at interesting frequencies. The most severe rain attenuation region (Florida Gulf Coast) is singled out for special attention. At 30° ground elevation angle, 27 GHz is found to be the frequency required for maximum signal strength at .99 availability and the corresponding frequency at .999 availability is 12 GHz. (LOSS-DIFFERENTIAL GAIN) is also generated to find frequency which best combat uplink interference sources. 35 GHz at 30° elevation and .99 availability is favored, dropping to 15 GHz at .99 availability.

Optimum frequencies are seen to be region, required availability, and orbit-dependent. The advantages of an inclined, elliptic 12-hour orbit (Molniya orbit) for a Quebec ground station are discussed. With aid from both the climate and a typical 41° elevation angle to a Molniya satellite, favored frequencies are greater than 30 GHz at .99 availability.

VIDEO COCHANNEL INTERFERENCE INTO DIGITAL
COMMUNICATION SATELLITE SYSTEMS

P. Constantinou, TELESAT CANADA

The growing use of digital modulation schemes in satellite telecommunication systems makes the knowledge of the effect of cochannel interference on digital systems increasingly important. While extensive theoretical work has already been published, few experimental results are available to confirm these theories.

One of the most severe interference cases occurs in the situation where adjacent satellites share the same frequency band, one carrying a high power carrier such as a wide band FM television signal and the other a low power narrow bandwidth digital Single-Channel-Per-Carrier (SCPC) signal.

The purpose of this paper is to present the results of some laboratory measurements on the effect of video cochannel interference on a digital Single-Channel-Per-Carrier (SCPC) signal as employed by Telesat Canada in its Thin Route system.

The experimental set-up on which the interference measurements were carried out consisted of the following:

- A two-phase 40 Kbps SCPC channel unit operating in back-to-back mode.
- A NTSC signal generator and a FM modulator, used as the interference source.

The BER was used as a measure of the effect of the video interference on the SCPC signal for various frequency separations between the SCPC carrier and the interfering video carrier. Measurements were made using a variety of video test patterns. The results are presented as curves relating the BER with the interference level, the SCPC carrier level, the noise level and the frequency separation. The results are compared with the BER curves as predicted by theory.

New Modulation Performance Parameter for
Dual-Polarized Satellite Communication Systems

Lin-Shan Lee

Dept. of Electrical Engineering, National Taiwan University
Taipei, Taiwan.

The orthogonal polarization technique is getting more and more attractive in satellite communication systems because of its efficiency in utilizing the spectrum. Crosspolarization effects are the new problems arising in such systems, because interference induced between the two orthogonal polarizations can degrade the signal quality. The conventional design of such systems requires the crosspolarization discrimination (XPD) in the system to be better than some desired value. In this paper, however, it is proposed that the value of XPD should in fact be used as an additional parameter in evaluating the performance of different modulations for such systems, rather than being used simply as an independent requirement.

Evaluation of modulation performance has been an old problem in communication system design. The traditional performance measures include parameters such as noise sensitivity, bandwidth consumption, information capacity, circuitry complexity, etc., among which the noise sensitivity, which gives signal quality as a function of relative noise density, is one of the most critical measures. However, when crosspolarization effects exist in dual-polarized satellite systems, the noise sensitivity itself actually varies with XPD. In other words, the signal quality becomes a two-dimensional function of both relative noise density and XPD values. Therefore XPD can be used as an additional modulation performance parameter. Digital modulations are used as an example in this paper and different schemes and various design considerations are discussed in details. The results indicate that this additional parameter does help significantly in system design.

SIMULATED IMPULSE RESPONSE OF AIRCRAFT
OBSTRUCTION OF DIGITAL LINKS

PROFESSOR H.S. HAYRE

E.E. DEPT-WAVE PROP. Lab. UNIVERSITY OF HOUSTON, HOUSTON, TX. 77004 (USA)

QPSK digital communication links suffer from multipath signal fading errors. Fading margin of around 20db are usually built in such digital systems, but the duration, repetition frequency, and pdf of fading nulls are other factors often discussed in such studies. Some authors have suggested that an impulse response of such fading scenarios including blockage by intervening Aircraft would suffice for theoretical calculation of associated error rates, although the underlying assumption of linearity may not strictly hold in this non-linear time-varying case of aircraft in different orientations transmitting such beams. Full-scale experiments to obtain such data are both expensive and time consuming, and therefore an ultrasonic simulation of the same is used to obtain their simulated impulse response for field use. Wave-length scaled system models and the percent beam-width coverages are reproduced in water tanks using ultrasonic frequencies. The nonlinearities of the system and the limitations of this approach are included in the quantitative results. F-15, Boeing 747, C-130, and a Huey Helicopter were used for this study. This work shows that this is indeed an inexpensive and rapid simulation method applicable to many practical problems with very reliable results.

BANDLIMITING DISTORTION IN TRANSMITTING VIDEO
AUDIO, AND DIGITAL SIGNALS OVER RADIO
RELAY LINKS

Adel A. Ali

Manitoba Telephone System, Winnipeg, Canada
One Leave at Riyadh University, Saudi Arabia

In recent years digital modulation techniques have been playing an increasingly important role in the transmission of information over terrestrial microwave and satellite systems. This fact, coupled with the ever decreasing available RF spectrum has motivated the common carriers to use the empty lower baseband of existing FDM-FM systems and the available band above the video signal, for transmitting data, TV audio and FM programs. Several methods of modulating and transmitting this hybrid information have been presented in the literature. Most prominent are the data under voice (DAV) and data above voice or video (DAV, DAVID) in which a one T1 stream of 1.544 M bit/s is transmitted simultaneously with the analog voice or video. A critical review of these methods can be found in (Feher, K., et al, IEEE Trans. Com., 23, 1321-1327, 1975 and Feher, K. and Morris, M., IEEE Trans. Com., 23, 1509-1515, 1975). While noise and error rates were treated, the published material does not treat the important problem of bandlimiting distortion that result when the hybrid signal passes through the RF transmitter and receiver filters.

In this study we utilize the known spectral properties of the analog and digital signals to derive an expression for the bandlimiting distortion. We consider the transmission of FM subcarriers and data signal above video. Based on the measured spectrum of the colour bar signal chart we present a model of the video signal amenable to machine computations. While an approximate estimation of the bandwidth can be found using Carson's rule, we show that our results are more meaningful since it relate the used spectrum to system performance. We conclude that the use of this rule to calculate necessary bandwidth for video and one subcarrier will generally lead to a waste of spectrum and result in an over designed system. In the case of data and subcarriers transmission above video, Carson's rule results in a waste of spectrum for low powers and to excess distortion for high subcarrier levels and data loading.

IS ANGLE DIVERSITY BETTER THAN FREQUENCY DIVERSITY?

Dr. P. Monsen
Signatron, Inc.
12 Hartwell Ave.
Lexington, MA 02173
USA

Troposcatter radio communication systems use redundant transmission paths - e.g. frequency, space, angle, to provide protection against multipath fading. Many existing systems use two antennas per terminal and 2 RF carrier frequencies in each direction to achieve quadruple diversity operation. Angle diversity, where a multiple feedhorn structure collect signals with different arrival angles, is an alternative to frequency diversity because it saves a frequency allocation in each direction of a duplex link. With angle diversity, one must cope with correlation between diversity channels, additional loss in a received beam squinted away from the main beam, and delay fluctuations between angle of arrival signals. On the positive side, angle diversity realizes 3dB more receive power under a fixed transmitter power constraint and, in addition, enjoys an advantage of a long term decorrelation between short term median received signals in each diversity. A program including an extensive analytic and experimental evaluation of these issues has recently been completed. The principal results of this study are:

- (1) Digital troposcatter systems with adaptive receivers can be used to cope with delay fluctuations between diversity channels as well as multipath effects,
- (2) correlation effects in wideband digital systems can in most cases be neglected,
- (3) bit error rate performance for strategic troposcatter systems is about the same for frequency and angle diversity systems.

MAXIMUM LIKELIHOOD SEQUENCE ESTIMATION OVER UNKNOWN
MULTIPATH CHANNELS

Sally Norvell
Naval Ocean Systems Center
San Diego, CA 92152

An algorithm, known as the Maximum Likelihood Sequence Estimator, has been shown to be an effective signal processing technique for use in communicating over multipath channels. This algorithm was developed for use over a known multipath channel. Knowledge of the channel response is needed to specify the metrics for the decoder and to specify the matched filter. In many cases, the channel response is unknown. In this paper a Kalman filter is used to estimate the channel response and is used in conjunction with the Maximum Likelihood Sequence Estimator over unknown multipath channels. Performance curves for the simulation of the Kalman filter - Maximum Likelihood Sequence Estimator are given in this paper.

Theoretical and Experimental Foundations of Microwave YIG $0 - \pi$ Modulator

Xiang Kunxian
(Lecturer, Microwave Remote Sensing
Laboratory, Huazhong Institute of
Technology, China)

A theoretical analysis and experimental foundation of microwave YIG $0 - \pi$ modulator are presented. In order to improve on its carried suppression factors, the transformation function for real, no perfect matching, loss microwave YIG $0 - \pi$ modulator can be supposed to be a quasi-stop function. From its Fourier series, the formulas of carried suppression factors P_{sup} (db) and the modulation loss L_M (db) are obtained. The P_{sup} and the L_M are related to the following factors: the transmission coefficient T_{12} of the YIG $0 - \pi$ modulator, the modulating signal period T , the modulating signal impulse time width τ_u . The phase deflections Δ_+ and Δ_- from phase step function which is related to the YIG hysteresis loop, and the phase deflection δ from the $0 - \pi$ phase modulation. The results obtained show that the longer the T and the smaller the values of δ , Δ_+ and Δ_- , the greater P_{sup} and the less L_M (db).

It has also been proved by experiment that the calculations of P_{sup} (db) and L_M (db) are in fairly good agreement with measurement.

In order to improve the uniformity of the measured P_{sup} (db) and L_M (db) this paper presents the formulas for the error sources of the modulated subcarrier method for measuring P_{sup} (db) and suggests methods for annihilating ΔP_{sup} .

The microwave YIG $0 - \pi$ modulator has two practical constructions, one is the 180° nonreciprocal phase shifter, the other is the form that is obtained by using an appropriately short terminated circulator switching. These devices have a modulated loss of about 1.3db (including transmission loss) and $P_{sup} \geq 30$ db over a more than 3% bandwidth (at C-band and X-band). The modulator is capable of transmitting high power and is already in wide use in the automatic follow-up systems for communication satellite earth stations in this country.

M. Heller
Lehrstuhl für Technische Elektronik
Der Technischen Universität München
West Germany

HARMONIC STABILIZATION - A NOVEL CONCEPT FOR BROADBANDING TRAPATT-AMPLIFIERS

TRAPATTs are high power, high efficiency microwave semiconductors suitable for use as final amplifiers in phased-array-systems. In some cases however there are severe demands for bandwidth and stability, which hardly can be fulfilled by conventional TRAPATT-circuits.

This paper presents design guidelines for TRAPATT-amplifiers to overcome the difficulties mentioned above. The novel concept is based on the high harmonic content of the TRAPATT-oscillation. Diode current as well as voltage show strong harmonic components, which closely interact with the fundamental signal. That is why the stability of the TRAPATT-oscillation depends on circuit tuning at harmonics to a high degree. In contrast to conventional TRAPATT-circuits however, the method of harmonic stabilization calls for lossy terminations at the harmonics. In this way the load impedance at the fundamental can be designed favourable to both stability and bandwidth of the amplifier.

Using this principles, a TRAPATT-amplifier-module has been developed delivering an output power of 50 W at 2.7 GHz. With a modified version of the well known "coupled bar" circuit, a bandwidth of 15 % has been achieved. At the same time, a reduction of the intrapulse phase shift to $7^\circ/\mu\text{sec}$ as well as substantial increase of stability has been observed. It is shown, that harmonic stabilization is a powerful tool for broadbanding TRAPATT-amplifiers.

High Temperature Electronics and Applications
to Balloon Beacons and Long Life Transponders for Venus

¹R. F. Jurgens, ¹A. I. Zygielbaum, and ²J. Blamont
¹Jet Propulsion Laboratory, 4800 Oak Grove Drive, Pasadena, CA
²Service d'Aeronomie du Centre National de la Recherche Scientifique,
91 Verrieres, France

Recent developments in high temperature electronics and associated power sources have reached a level where the design of long-lifetime radio probes operating between 300⁰ to 500⁰ C are possible. The first application might use a simple radio beacon carried by a low altitude balloon in the atmosphere of Venus to chart the atmospheric wind currents.

Simple transponders could be designed to operate for several years on the surface of Venus. These experiments would provide accurate measurements of the spin axis of the planet, a highly refined ephemerides, measurements of atmospheric turbulence, and atmospheric profiles by occultations from the surface. More advanced instruments could be contemplated in a few years as larger scale integration becomes available with ITC's (integrated thermionic circuits) and new thin-film devices.

WEDNESDAY AFTERNOON

June 4, 1:30 - 5:00

SIGNAL PROCESSING

DKN 2B

Session C.3

Chairman: P.H. Wittke
Queen's University
Kingston, Ontario

CORRELATION FUNCTION OF OUTPUT OF BANDPASS NONLINEARITY

Nelson M. Blachman
GTE Sylvania Systems Group, Mountain View, California

For a bandpass nonlinearity such as a TWT amplifier that introduces AM-to-PM conversion, determining the correlation function (and from it the spectrum) of its output is complicated by the fact that a memoryless nonlinearity cannot account for a phase shift. In many cases the input, which may be an FDM signal plus noise, can be regarded as gaussian, as we shall assume, and the output correlation function can be found almost as simply as for a memoryless nonlinearity.

We suppose that the input is $a(t) \cos[2\pi Ft + \phi(t)]$ with correlation function $\sigma^2 r(\tau) \cos[2\pi F\tau + \psi(\tau)]$ and that the output is $g(a) \cos[2m\pi Ft + m\phi(t) + Y(a)]$ for some nonnegative integer m , where $g(a)$ represents the AM-to-AM conversion, and $Y(a)$ the AM-to-PM. If ge^{iY} is expressed as $\sum_{k=0}^K c_k a^k$ with complex (except when $m=0$) coefficients $\{c_k\}$, the output correlation function can be shown to be

$$r^m \cos(2m\pi F\tau + m\psi) \sum_{h,k=0}^{KK} \frac{c_h^* c_k}{\epsilon_m} (\sqrt{2}\sigma)^{h+k} \frac{2^{m+h} 2^{m+k}}{m!} {}_2F_1\left(\frac{m-h}{2}, \frac{m-k}{2}; m+1; r^2\right)$$

where $x!$ denotes $\Gamma(x+1)$, $\epsilon_0=1$, $\epsilon_m=2$ for $m>0$, and ${}_2F_1$ is the hypergeometric function. The latter is a polynomial in r^2 whenever $\frac{1}{2}(h-m)$ or $\frac{1}{2}(k-m)$ is a nonnegative integer, making the corresponding spectral term easy to compute as a sum of autoconvolutions of the input spectrum (N. M. Blachman, IEEE Trans. II-25, 77-79, 1979). For other integer values of h and k the hypergeometric function can be expressed in terms of more familiar functions, but they need not be integers; they must simply exceed -2 .

The foregoing result can be applied to a wide variety of cases. If, for example, we take $m=2$, $c_0=4/\pi$, and $K=0$, we get $(4/\pi^2)r^2 {}_2F_1(1,1;3;r^2) \cos(4\pi F\tau + 2\psi)$ as the correlation function of the output of the standard bandpass hard limiter after this output has been squared to obtain its second harmonic and passed through a filter that eliminates the d-c component. Since a hard limiter has no even-harmonic output, the usual approaches do not yield results like this one. Our general result is obtained from the crosscorrelation function $E\{a^h(t)a^k(t+\tau) \exp[mj\phi(t+\tau)-mj\phi(t)]\}$, which is found to be

$$r^m e^{mj\psi} (\sqrt{2}\sigma)^{h+k} \frac{2^{m+h} 2^{m+k}}{2!} {}_2F_1\left(\frac{m-h}{2}, \frac{m-k}{2}; m+1; r^2\right) / m!$$

TRANSFER FUNCTIONS OF MILDLY NONLINEAR CIRCUITS

Julian J. Bussgang
SIGNATRON, Inc.
12 Hartwell Avenue
Lexington, Mass. 02173

Transfer functions of linear circuits can be modeled conveniently in the frequency domain. Nonlinear circuits pose far more difficult problems. In the case of a mild nonlinearity, where the departure from linearity is not significant, it is possible to take recourse to the Volterra series to generate different frequency domain canonic models. All such models entail expansions whereby the introduction of each additional term compounds the complexity of representation and increases the number of measurements that are needed to specify all the required parameters. Thus, the use of the Volterra series, appears to have an applicability limited to only a narrow class of systems. Nonetheless, these methods have proven so far to be the only ones whereby input and output of a nonlinear system with memory can be related in a deterministic manner. Therefore, the Volterra Series methods deserve attention for both their capabilities and the insight that they offer.

The paper will summarize the earlier canonic models in the narrowband representations (J.S. Bussgang, et al., Proc. IEEE, 62, 1088-1119, 1974) and then outline the more recent elaboration of such models. The number of parameters and the measurement problems will be discussed.

FALSE ALARM PROBABILITIES FOR A LOGARITHMIC DETECTOR

FOLLOWED BY A SUMMER

Joel L. Ekstrom
 HRB-Singer, Inc.
 2100 Reston Avenue
 Reston, Virginia 22091, USA

Logarithmic detectors followed by postdetection integrators are widely used in radar systems, and for the system engineer the false alarm probability (P_{FA}) of this signal processing scheme is of fundamental interest.

In this paper the postdetection integrator is modeled as a device which sums N independent samples of the incoming detected noise and compares the result to a threshold T , so that a false alarm is declared if the sum exceeds T . In order to compute P_{FA} , the probability density function $P(y)$ for the random variable y given by

$$y = \frac{1}{N} \sum_{i=1}^N \ln(x_i) ,$$

where the x_i are independent noise samples each having the Rayleigh distribution

$$P(x_i) = x_i \text{EXP} \left[-\frac{1}{2} x_i^2 \right] ,$$

must first be obtained. $P(y)$ must then be integrated from T to infinity to obtain P_{FA} .

When N is large the classical method of determining $P(y)$ is the Edgeworth series, but the frequently poor convergence of this series on the tails of $P(y)$ makes it of questionable value in computing small values of P_{FA} .

In this paper a modification of the saddle-point approximation technique of DANIELS (Annals of Mathematical Statistics, 1954) is used to derive, for large N , a two-term asymptotic approximation for P_{FA} . The dominant term in the approximation is

$$P_{FA} \approx \left[2\pi N (\theta^2 Y'(1+\theta) + N^{-1}) \right]^{-1/2} \text{EXP} \left[-N(\theta Y(1+\theta) - \ln \Gamma(1+\theta)) \right]$$

where θ is a function of the threshold T , and Y and Y' are logarithmic derivatives of the gamma function.

Results for various values of N and T will be given, with emphasis on P_{FA} values in the range 10^{-4} to 10^{-8} .

AN ADDENDUM TO BAYES' THEOREM

J. S. Avrin

The Aerospace Corporation, El Segundo, CA 90245

Bayes' Theorem is central to much of signal and information processing theory. Its power and generality are widely invoked. However, straightforward application of the Theorem to complex situations can lead to troublesome conceptual difficulties. This paper examines the Theorem's application to the refinement, under measurement uncertainty, of the initial estimate of a parameter that conditions the a priori probability distribution of a set of system states. A dilemma that appears to emerge is identified and then resolved in terms of a certain formalism which features a nonlinear eigenvector equation and which can be viewed as a supplementary Addendum to Bayes' Theorem. Applying the Addendum to the data yields a posteriori estimates for the parameter of interest as well as for the system state distribution. A measure of confidence in the latter is also provided on the basis of a novel interpretation of certain matrix elements appearing in the eigenvector equation.

The Addendum's formalism can also be viewed as an iterative algorithm for deriving the desired estimates. A simple example is treated in some detail in the paper. Known and potential applications include signal source identification, reliability estimation, spectral estimation, tracking and trajectory estimation, and combined detection and parameter estimation.

A noteworthy feature is that the paper is not concerned with least-squares or maximum likelihood estimation, nor is cost or risk an issue.

DESIGN OF SIGNAL SETS WITH
SPECIFIED CORRELATION PROPERTIES

Thomas P. McGree, George R. Cooper
School of Electrical Engineering
Purdue University, W. Lafayette, IN 47907

A new procedure for constructing a set of signals with specified correlation properties is proposed. This procedure, which is algorithmic in nature, creates an arbitrarily sized signal set whose members have the magnitudes of their aperiodic autocorrelation and crosscorrelation functions constrained at all integer shifts of a selected time increment.

The design procedure relies upon the properties of pseudonoise (PN) sequences and the concept of signal expansion via an orthonormal basis set. An important feature of the algorithm is that it is independent of the chosen orthonormal basis set. Hence, relatively simple sets, such as Walsh functions or sinusoids, may be implemented in the construction of the signal set.

The bandwidth occupied by each member of the signal set is of interest in most applications. In general, each signal of this set has the same bandwidth. However, since the design algorithm is independent of the selected orthonormal basis set, the precise bandwidth of the signal set is difficult to specify, although it does depend upon the parameters of the set. Specifically, the bandwidth increases as

- a) The number of signals in the set is increased,
- b) The magnitude constraint on the correlation functions is decreased, and
- c) The number of time shifts at which the correlation functions are constrained is increased.

A simple signal set that illustrates the algorithm and some of the signal set properties is described and possible applications of this class of signals are discussed.

THE APPLICATION OF TSENG-SARKAR WINDOW
TO SPECTRAL ESTIMATION

Fung-I Tseng

Department of Electrical Engineering
Rochester Institute of Technology
Rochester, New York 14623

Tapan K. Sarkar

Several windows (Rectangular, Chebyshev, Hamming, Parzen, Blockman, Blackman-Harris, Kaiser) exist in literature to be used with Fast Fourier Transforms to improve spectral resolution, dynamic range and aliasing in the presence of noise. The unfortunate feature of all these windows is that they cannot be tailored to one's needs. This novel window possesses several attractive features. An user can design the windows in the frequency domain with a specified i) main lobe width, ii) a deep wide null can be placed right by the side of the main lobe to improve spectral resolution, iii) the global slope of the sidelobe levels can be controlled very easily. (This is extremely important when one has broad band noise in the data). iv) Any number of deep wide nulls can be placed in the side-lobe regions to enhance the dynamic range of the spectral estimation (a typical figure would be 60-70 db). It is important to note that all of these four design parameters are interrelated and hence one has to make a design compromise between these four features. v) After one has designed the window completely in the frequency domain, the finite length window in the time domain is obtained simply by FFT of the frequency domain design.

Examples will be presented to illustrate the versatility of this window in spectral estimation of noise contaminated signal. With this window one can "learn" more about the location of the signal with each processing and thereby ultimately could produce an FFT with very little bias. Examples will be presented to support these claims and comparison will be made with other windows with respect to dynamic range and spectral resolution.

SERIAL HF MODEM USING ADAPTIVE ANTENNA TO CANCEL MULTIPATH -
EXPERIMENTAL RESULTS
by

Peder M. Hansen
Naval Ocean Systems Center
Antennas and RF Distribution, Code 8112
San Diego, California, 92152

A serial 3.3 kbit modem using biphase shift keying combined with an adaptive array has been constructed and tested on the air. Normally a serial modem at this rate will not work well at HF because the typical multipath spread exceeds the baud length and intersymbol interference results. In this case a 4 element adaptive array was used to cancel all but one propagation mode eliminating this problem.

In order to determine the effectiveness of the Serial Modem Adaptive Array (SMAA) an on-the-air test was performed using a sophisticated HF Parallel Tone Modem (PTM) with dual space diversity. Testing was done on an over-ocean path of 236 Rm. A sounder was used to select frequencies where severe multipath interference existed, and bit error rates were taken alternately using the SMAA and PTM. Performance for the SMAA exceeded the PTM by more than an order of magnitude in bit error.

THURSDAY MORNING

June 5, 8:30 - 12:00

NOISE AND INTERFERENCE,
CHARACTERIZATION AND MEASUREMENT

DKN 2A

Session E

Chairman: Bhartendu
Environment Canada
Downsview, Ontario

RADIO EMISSION FROM LIGHTNING STEPPED LEADER

John B. Smyth, David C. Smyth and John Durment
Smyth Research Associates, 3555 Aero Court
San Diego, Calif. 92123

There have been a number of experimental observations of the electromagnetic field associated with intracloud lightning discharges (E. P. Krider, et. al: J. Geophys. Res., 80, 2653-2657, 3801-3804, 1975; J. Geophys. Res. 84, 3159-3164, 1979.). A theory has been developed which provides the electromagnetic characteristics necessary for describing the radio emissions from lightning (J. B. Smyth and D. C. Smyth, Radio Science, 11, 977-984, 1976). Theory provides the transfer function of the discharge process. The experimental data are used to evaluate the channel parameters and provide information on the characteristics of the input function, the electrical conduction current.

A comparison of the electric component of the electromagnetic field observed in Florida with the magnetic component of the electromagnetic field observed in Arizona indicates that the physical process of the intracloud lightning discharge is basically the same at both locations. The theory provides a relationship between the electric and magnetic components of the field.

HORIZONTALLY AND VERTICALLY POLARIZED
VLF ATMOSPHERIC RADIO NOISE AT ELEVATED RECEIVERS

F. J. Kelly, J. P. Hauser and F. J. Rhoads
Naval Research Laboratory
Washington, D. C. 20375

A computer program has been developed that is capable of predicting horizontally and vertically polarized atmospheric radio noise at any altitude or location in the earth-ionosphere waveguide for the very low frequency (VLF) range (10-30 kHz). The new program, uses the outputs of two previously written programs, which predict the vertical electric noise field at the ground. The new program computes all the field components at any altitude using the vertical electric field at the earth's surface as a basis. Predicted values from several versions of the new model have been compared with presently available data. The results are encouraging, but more data is needed to test the model.

LIGHTNING AND NUCLEAR ELECTROMAGNETIC
INTERFERENCE ENVIRONMENTS AND SUPPRESSION
TECHNIQUES TO PROTECT ELECTRONIC SYSTEMS

BY

G. H. JOSHI

RAYTHEON - MISSILE SYSTEMS DIVISION, BEDFORD, MASS.
AND

J. DANDO, J. BEILFUSS

HARRY DIAMOND LABORATORIES, WOODBRIDGE, VA.

Military and commercial electronic systems will be exposed to natural interference producing events like lightning inflicting catastrophic damages to the systems. Similarly, they may be exposed to nuclear electromagnetic pulses (NEMP) causing similar and unacceptable permanent damage. The same systems for effective electrical performance have to be made immune to manmade interferences from the cooperative and or non-cooperative emitters in the vicinity. Thus, it is imperative that the electronic systems have to be designed to operate through and/or withstand these interfering environments. This paper presents an approach to suppress the interfering environments. Particular emphasis is placed on the protection techniques against lightning and NEMP. The approach is based on reducing the threat environments to acceptable practical levels, and it consists of identifying adequate shielding, proper grounding, and isolation requirements. Even with these precautions, occasionally additional protection is required. The choice of the terminal protection devices for this is dictated by the characteristics of the threat environments. The key parameters that have to be considered for terminal protection devices are: a) the response time, b) the overshoot, c) the clamping levels of the voltages, d) the insertion loss, and e) the energy dissipation capability of the devices.

The paper provides in addition to these considerations, the current injection test data on a composite terminal protection device chosen to protect a typical electronic system against lightning and NEMP. The characteristics of the injected currents are determined by evaluating the conductive coupling to the devices from the antennas and the cables exposed to lightning and NEMP threat environments.

"Statistics of Electromagnetic Noise due to H.V. Power Lines"

A.U.H. Sheikh Ph.D. M.I.E.E.⁺
J. D. Parsons M.Sc M.I.E.R.E.*

Radio interference due to power lines is a well known phenomenon and it becomes extremely difficult to obtain clear reception while the receiving antenna is in proximity of high voltage power lines. Impulsive noise interference due to 275 KV transmission line has been recorded at frequencies of 80 and 150 MHz.

The noise data available at the output of ACL SR 209-D receiver, in three channels (envelope + two quadrature channels) is recorded on Philips Analog 7 tape-recorder. The band width of the monitoring receiver being 20 KHz.

Noise statistical parameters such as APD, NAD, PWD and PID have been presented here. For the results it is concluded that power line noise mostly occurs in the form of bunched impulses or bursts. It is also shown that noise amplitudes reduce (for the same probability) when the monitoring frequency is increased. A reduction of approximately 8 dB is noted (probability of exceeding the ordinate = 10^{-4}), when the monitoring frequency is increased from 80 to 150 MHz. It is also noted that if the monitoring antenna is moved away from the centre of the power line system the peak noise reduces considerably. A reduction of around 12 dB is observed (probability of exceeding the ordinate = 10^{-6}) when the antenna is placed 4 metres off axis.

+ University of Garyounis, Benghazi, Libya.

* University of Birmingham, Birmingham, England.

AMPLITUDE AND PHASE STRUCTURE OF FIELDS IN "DEGRADED" ANECHOIC ENCLOSURES FOR E.M. INTERFERENCE MEASUREMENTS

S.R. Mishra and T.J.F. Pavlasek
Electrical Engineering, McGill University, Montreal, Canada

Anechoic enclosures for e.m. interference measurements differ from those for antenna pattern measurements in several respects. The size, bandwidth and field uniformity requirements are discussed. The possibilities of utilizing partial wall covering and operating below "rated" frequencies, are examined and the concept of compact enclosures with degraded performance wall material is thus evolved. The relationship of the problem to e.m. wave propagation in the neighbourhood of lossy rough surfaces is considered.

The facility for determining the three dimensional structure within the anechoic room is described. (B. Howarth and T. Pavlasek, *IEEE Trans. MTT*, v20, n9, 1972) Amplitude and phase are measured at various polarizations and frequencies by fully automated equipment. The results are recorded in analog and digital form using a dedicated microprocessor based data acquisition system interfaced to a high speed large scale computer for the processing of data and production of isophot and equiphase maps, or various amplitude and phase profiles. The use of this facility for near-field measurements is also described and selected results are shown.

Results are presented for a frequency-scaled "model" anechoic room intended for e.m. interference studies, measured over a range of 0.6 - 23.5 GHz, representing a full scale room intended for 20 MHz and up, operation.

Isophot and equiphase field maps are shown demonstrating the effects of degradation due to: i) operating below the rated frequencies of the anechoic material ii) partial wall covering. The amplitude and phase structure characteristics in the "degraded" rooms are reminiscent of those encountered in front of a Sommerfeld half-plane (W. Braunbek and G. Laukien, *Optik*, 9, 174, 1952) and particularly in the case of phase, exhibit the behaviour of Airy-ring regions of focussing systems (Y. Lum and T. Pavlasek, *IEEE Trans. AP-12*, 6, 1964) or of multiple scatterers (B. Howarth and T. Pavlasek, *J. Appl. Phys* 44, 3, 1973). The diagnostic use of the phase behaviour is discussed and the design criteria for anechoic rooms intended for e.m. interference studies are considered.

WINDMILL INTERFERENCE TO TELEVISION RECEPTION

Dipak L. Sengupta and Thomas B.A. Senior
Radiation Laboratory, The University of Michigan
Ann Arbor, Michigan 48109

Since 1976 the Radiation Laboratory, under sponsorship from DOE, has been investigating the effects of windmills on the performances of various electromagnetic systems. In particular, electromagnetic effects to television (TV) reception produced by large horizontal axis windmills have been identified and quantified by comprehensive theoretical and experimental (laboratory and on-site) studies.

The present paper describes the significant results obtained from some on-site measurements carried out by receiving commercial TV signals at selected test sites in the vicinity of an operational windmill. At each test site, the total received signal (i.e., direct plus scattered off the rotating blades) were recorded on a strip chart recorder and interference effects were observed on the screen of a TV receiver, and as appropriate, recorded on a video tape.

It has been found that the rotating blades of a windmill can produce pulse amplitude modulation of the total signal received, and that for a receiving antenna so located and oriented as to pick up the specular or forward scattering off the rotating blades, this extraneous modulation can distort the video portion of a TV signal reproduction in the vicinity of the windmill. The measurement procedure, selected results and their implication with regard to proper siting of a windmill having minimal impact on TV reception will be discussed.

SPATIAL FILTERING TECHNIQUES APPLIED TO
NETWORK INTERFERENCE PROBLEMS

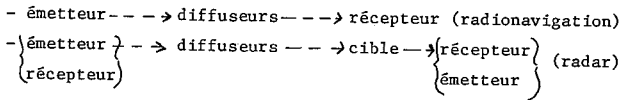
Gary J. Brown
Naval Ocean Systems Center
271 Catalina Blvd.
San Diego, California 92152

High frequency (hf) communication nets suffer from narrow bandwidth limitations, forcing shared frequency techniques to accommodate all net participants. Such techniques usually rely on time/frequency coding to combat common channel interference, however at hf these techniques are inefficient. This study evaluates the application of a simple single null adaptive receiving antenna to provide spatial filtering for the network environment. The characteristics of several net models are analyzed to show the improvement in channel utilization due to the array. The adaptive array techniques are compared to conventional time and frequency coding in terms of channel usage efficiency, and netting protocols compatible with the adaptive array are discussed.

ETUDE EXPERIMENTALE DES TRAJETS MULTIPLES PAR UNE METHODE BISTATIQUE DE
SYNTHESE D'OUVERTURE

par J. Dorey, Y. Blanchard, D. Medynski

En radionavigation aérienne (ILS, VOR, MLS) comme en détection radar, il est indispensable de modéliser l'influence des trajets multiples sur le bilan global de propagation. Ces trajets multiples sont créés par des diffuseurs distribués sur le terrain : végétation, collines, constructions... En première approximation, on caractérise le comportement des diffuseurs par des trajets simples de type :



On peut donc utiliser une méthode expérimentale bistatique dérivée de celle mise en oeuvre dans le radar à ouverture synthétique :

- émetteur cohérent, piloté par horloge atomique, émettant des impulsions récurrents, brèves ($0.1\mu s$), embarqué sur un avion de trajectoire connue par rapport au récepteur ;
- récepteur hétérodyne, au sol, piloté par horloge atomique dont les signaux sont enregistrés et traités sur ordinateur en temps différé.

Le traitement de la localisation et de la mesure de l'amplitude des diffuseurs comporte deux étapes :

- 1°) localisation sur l'ellipsoïde correspondant à l'instant d'arrivée de l'impulsion ;
- 2°) localisation sur cet ellipsoïde par utilisation de l'effet Doppler.

Cette méthode a été utilisée avec succès sur trois sites caractéristiques (aéroport, campagne, bord de mer).

MONDAY AFTERNOON

June 2, 1:30 - 5:00

REMOTE SENSING - ACTIVE

DKN 2C

Session F.1

Chairman: Kenneth Hardy
Environmental Research and Technology Incorp.
Concord, MA.

THE SAR-SEEN SEA: A SPECIAL CASE

Robert O. Harger
Electrical Engineering Department, University
of Maryland, College Park, Md. 20742

An explicit characterization of the synthetic aperture radar (SAR) image of the sea surface is obtained using (i) the two-scale electromagnetic scattering approximation, (ii) a simplified shear-flow model connecting sea surface state and the atmospheric pressure field, and (iii) the SAR image of a time-varying reflectivity density satisfying a dispersion relation. It is assumed that the fine scale structure is of bandpass form, centered near $2k_0$, $k_0 = 2\pi/\lambda_0$, λ_0 the radiated wavelength, and of bandwidth narrow relative to the bandwidth of the large scale structure and that the latter's deviations are small compared to λ_0 : though thus restricted, the resultant model is the first combining elements of all three areas.

The SAR image is then shown to be the result of a concatenation of four linear operations on the atmospheric pressure field at the mean sea surface at (say) $t=0$: the first three are space invariant, the first producing the sea surface height, the second sufficient in itself to characterize the SAR image of a time-invariant scene, and the third present only in the time-variant case; the fourth linear operation is space-variant, embodying the distortion present in any side-looking system - to which all results are in fact applicable - viewing a time-variant scene and interpretable, under a linear approximation to the dispersion relation, as a scaling and skewing.

THE DEPENDENCE OF THE BACKSCATTERED SIGNAL
AUTOCORRELATION FUNCTION ON WATER SURFACE
SCATTERING COEFFICIENT AND ORBITAL VELOCITY
VARIATIONS AND PLATFORM VELOCITY

D.E. Weissman
Hofstra University
Hempstead, New York 11550

J.G. Kim
Old Dominion University
Norfolk, Virginia 23508

A theoretical analysis has been performed to study the relative contributions of ocean surface wave reflectivity variations, water orbital velocity variations and aircraft platform velocity within the Doppler spectrum of a "scatterometer" backscattered signal. This study involves the calculation of the autocorrelation function of the backscattered field when the CW point radar is moving parallel to the surface and is illuminating an area encompassing several of the largest surface waves. The potential of this technique for the remote sensing of surface wavelengths is being assessed. The scattering surface is assumed to consist of incoherent elements whose scattering coefficients and velocity are modulated by the dominant ocean waves. The periodicity of these surface parameters imposes distinct periodic features in the Doppler spectrum of the backscattered electromagnetic field. Envelope detection is shown to cause mixing between Doppler frequencies, yielding distinct features in the autocorrelation of the received field envelope. This is a result of the interaction between the spectral parameters that occurs when the pre-detection spectrum is self-convolved by this detector. The ability to accurately infer surface wavelengths will depend on the resolution of this Doppler information.

The surface is modeled with either monochromatic, multifrequency, or narrowband spatial spectra, and with varying amounts of coherence between the scattering coefficient variations and the scatterer velocity distributions. Also studied was the relative locations in the maxima of these quantities, relative to the wave crest. Numerical calculations using typical aircraft and sea surface parameters show that the added presence of the orbital velocity results in additional features in the signal autocorrelation. These features imply an interference with and some reduction of the resolution and accuracy of the surface wavelength measurements.

This work was supported by the NASA Langley Research Center, Hampton, Virginia under Grant NGR-33-209-002 (Hofstra University and contract NAS1-15648 with O.D.U.)

MULTIFREQUENCY RADAR SEA RETURN

F. B. Dyer, R. N. Trebits, and N. C. Currie
Engineering Experiment Station
Georgia Institute of Technology
Atlanta, Georgia, USA 30332

Simultaneous measurements of radar returns from the sea surface have been made at frequencies of 9.5, 16, 35, and 95 GHz and for various polarizations. These measurements were made for a variety of sea state conditions over a range of grazing angles between 0.5 and 8 degrees and for radar look directions which included upwind, crosswind, and downwind aspects of the sea. The measurements were made from an offshore facility near Panama City, Florida which was instrumented to record local wind speed/direction, significant wave height (highest 1/3 and 1/10), sea wave-front direction, water and atmospheric temperature, barometric pressure, and relative humidity. Special calibration provisions were made to insure accurate measurement of both relative and absolute values of the returns. A total of 146 useful data runs of 3 minutes duration each was obtained over the two month test period. In addition, 46 calibration runs were made.

The primary objective of the investigation was to provide additional insight into scattering at millimeter wave frequencies; however, due to the difficulties associated with relating scattering data from separate experiments, involving different frequencies, sea conditions, and equipments, it was necessary to provide reference measurements at microwave frequencies. These current results appear to provide specific answers to several of the questions raised in earlier attempts to compare results of less comprehensive, two-frequency experiments (F. B. Dyer, 1974 International IEEE/AP-S Symposium, pp 319-322, 10 June 1974). For example, analysis of the new data confirms that radar cross-section per unit area (σ^0) at 95 GHz is essentially no larger than σ^0 at 35 GHz and may be small under some conditions. Perhaps the most interesting new confirmation is that while VV polarized returns are normally larger than those of HH polarization at frequencies up to 35 GHz, at 95 GHz horizontal polarized returns tend to be significantly larger than those which are vertically polarized. While amplitude distributions for both polarizations tend to be skewed toward a log normal-like distribution, the differences between the distributions for horizontally and vertically polarized returns are markedly reduced at 95 GHz. The new data confirm the previously observed trends in frequency spectra for rain and foliage returns, thereby suggesting that similar physical scattering mechanisms may be involved.

Atmospheric Ducting and Clutter Effects on
RF Wave Propagation Over the Ocean Surface

Frank T. Wu
Wai-Mao P. Yu
Alexis Shlanta

Michelson Laboratory
Naval Weapons Center
China Lake, California

Electromagnetic wave propagation in a surface-based tropospheric duct is analyzed with the geometric optics-ray tracing method. In a ducting environment, RF rays are greatly deviated and bent due to the drastic gradient change of atmospheric refractivity (as a function of altitude). For the case of RF rays emerging from a radar transmitter above the duct, the grazing angle associated with each of the rays at the ocean surface is vastly different from that of a non-ducting environment. Since the radar cross-section of sea clutter's is a function of the grazing angle, hence the ray-field of sea clutter echos will be different from that of normal atmospheric condition. In this paper, the sea clutters for both backscattering and bistatic scattering are investigated. The most recent available data of scattering coefficients of sea clutters have been used for the ray-field calculations. Some of the published and unpublished data are examined and compared. It has been found that the sea echos can dominate significantly over the direct radar signals under certain grazing angles and sea surface conditions. A comparison of sea clutter calculations due to ray bending phenomenon in a ducting environment and that of the normal line-of-sight approach will be presented.

CONCEPTUAL PROBLEMS IN LOW-ANGLE SCATTER FROM THE SEA

Lewis B. Wetzel

Naval Research Laboratory, Washington, D.C.

When the sea is illuminated at microwave frequencies at very small grazing angles ($\lesssim 1^\circ$), a physical description of the scattering process becomes complicated by diffractive, atmospheric and real-surface effects which require a reexamination of the conventional concepts of "multipath", "grazing angle", and "shadowing". These concepts are discussed here in terms of simple models for realistic scattering configurations. It is obvious, for example, that in forward scatter the idea of multipath loses its meaning when the receiver lies in the penumbra zone of the source, yet this condition occurs in many practical scattering situations, and implies, moreover, that the behavior of the specular reflection coefficient at very small grazing angles is inaccessible, both conceptually and experimentally, over real sea paths. The presence of the evaporative layer over the sea further complicates this picture by making the local grazing angle a (generally) unknown function of atmospheric conditions above the surface. It is shown, finally, that shadowing may or may not be significant at a given grazing angle, depending on wave heights and slopes and the illuminating wavelength. Here the actual structure of the sea surface becomes important, and the polarization dependence of diffracted fields could affect both forward and backscattered waves.

MEASUREMENTS OF THE VELOCITY CORRELATION FUNCTIONS
IN THE PLANETARY BOUNDARY LAYER WITH A PULSE DOPPLER RADAR

Dusan S. Zrnic' and Glenn Smythe
National Severe Storms Laboratory
1313 Halley Circle, Norman, Oklahoma 73069

A moderate power, 10 cm pulse Doppler radar was used to measure the radial velocities in the optically clear planetary boundary layer. Spatial correlation coefficient of the data field is estimated by correlating small regions (boxes in the polar coordinate system) of data. The correlation coefficient follows reasonably well the $2/3$ power law. Several consecutive scans are used to calculate the temporal correlation function, and it is shown that often a $2/3$ decay in time best fits the data. This is in accordance with Chandrasekhar's theory of turbulence. The space-time correlation is also investigated. Besides implications for turbulence studies, it is demonstrated that the technique can be utilized to retrieve the transverse component of the Doppler wind field.

REMOTE SENSING OF TORNADIC STORMS BASED ON HF RADIO WAVE
FROM IONOSPHERE AND IR IMAGERY FROM GOES SATELLITE

R. J. Hung, The University of Alabama in Huntsville, Huntsville, AL 35807, U.S.A.

R. E. Smith, NASA/Marshall Space Flight Center, AL 35812, U.S.A.

Gravity waves associated with tornado activity have been observed. These observations were made with a high frequency radio wave Doppler array system in which radio receivers located at a central site, NASA/Marshall Space Flight Center, monitored signals transmitted from three independent remote sites on three sets of frequencies and reflected off the ionosphere approximately half way between the transmitter and receiver sites. By using a ray tracing technique, more than twenty case studies have shown that the enhanced convection-initiated gravity waves associated with tornadoes were generated by thunderheads embedded in a squall line, or isolated clouds with intensive convection (R. J. Hung, T. Phan, and R. E. Smith, *J. Atmos. Terr. Phys.*, 40, 831-843, 1978; *J. Geophys. Res.*, 84, 1261-1268, 1979; and R. J. Hung and R. E. Smith, *J. Geomag. Geoelec.*, 31, 183-194, 1979).

Comparison of the computed location of the source of gravity waves from ionospheric observation with radar echo maps indicate that the gravity waves were excited by intense convection associated with tornadic storms, and gravity waves were detected more than one hour before the touchdown of tornadoes which were in the vicinity of the computed location of wave sources.

The study of the GOES IR imagery during the time period between when the gravity waves were being excited and the touchdown of the tornado indicates that clouds associated with tornado activity are characterized by both a very low temperature at the cloud top which is equivalent to a higher penetration of the cloud top, and a very high growth rate of the cold region of the cloud top, the signature of enhanced convections in the cloud.

Comparison between the gravity wave observations and GOES IR digital data analysis shows that the gravity waves were excited when the cold region or high altitude portion of the cloud-top was growing rapidly.

From the data available for these analyses, based on remote sensing from both the ionosphere and the satellite, this provides more than one hour lead time before the touchdown of the tornado.

FREQUENCY VARIATION OF VEGETATION CLUTTER

Fawwaz T. Ulaby
Remote Sensing Laboratory
University of Kansas Center for Research, Inc.
Lawrence, Kansas 66045

A radar clutter model of agricultural targets is developed on the basis of 1-18 GHz backscatter measurements over a wide range of growth conditions. At near-nadir angles of incidence, the histogram of the backscattering coefficient σ^0 (dB) exhibits a non-symmetrical distribution, but at angles above 20° from nadir, the shape of the histogram assumes a log-normal distribution. Empirical expressions for the joint angular and frequency dependence of the mean and median of σ^0 (dB) are provided for each linear polarization configuration. Decorrelation of σ^0 with frequency spacing is also evaluated and modeled.

Combined Active-Passive Microwave Measurements
of the Sea Surface in the Grand Banks Frontal Region

V. E. Delnore, Kentron International, Inc., Hampton, VA 23666
R. F. Harrington, NASA Langley Research Center, Hampton, VA 23665
W. L. Jones, NASA Langley Research Center, Hampton, VA 23665
C. T. Swift, NASA Langley Research Center, Hampton, VA 23665

On October 17, 1979, a NASA research aircraft equipped with a radar scatterometer and a stepped-frequency microwave radiometer overflew the Grand Banks oceanic front region southeast of Newfoundland. The flight was made to coincide with ship observations and with environmental satellite passes.

The scatterometer responds to the radar scattering coefficient of the sea surface, from which low-level wind speeds are inferred, and the radiometer measures the microwave brightness temperature at various frequencies. The data sets are independent; however, analyses of the two are coupled through the second-order dependence of the brightness temperature on the wind speed.

We present here a discussion of the scatterometer and radiometer measurements, with emphasis on the techniques and advantages of a combined active-passive airborne survey.

MICROWAVE RADIOMETRIC AIRCRAFT OBSERVATIONS
OF THE FABRY-PEROT INTERFERENCE FRINGES
OF AN ICE-WATER SYSTEM

R.F. HARRINGTON, C.T. SWIFT, AND J.C. FEDORS
NASA LANGLEY RESEARCH CENTER, HAMPTON, VA 23665

An airborne precision C-Band radiometer has been developed at Langley for participation in a variety of remote sensing field experiments. The unique feature of this radiometer is that four sub-bandwidths and several integration times can be selected within a 4.5-7.2 GHz range for operation at either a fixed frequency or in a frequency scanning mode. This allows the experimenter to adjust the resolution of the particular measurement of interest and to avoid radio frequency interference by tuning the instrument to operate within a clear band. In addition, the frequency scanning capability provides a means to sample layered media, such as ice over water, by observing the characteristic Fabry-Perot interference fringes.

Generally speaking, C-Band is not a desirable choice to measure ice thickness, because random surface height variations of the order of a few centimeters will destroy the coherence within the slab (J.J. Apinis and W.H. Peake, Ohio State Rept 3892-2, 1976). Nevertheless, evidence of the Fabry-Perot fringes were observed on two occasions while the radiometer was set in a frequency scanning mode. The first such response was observed on a flight conducted on March 7, 1978 over Clayton Lake in Western Virginia. During this mission, substantial changes in brightness temperature were observed by collecting data at five frequencies in the band ranging from 5000 to 5288 MHz. The second event occurred on March 20, 1979 on a flight over Prudhoe Bay, north of Alaska. On this mission, a 20K change in brightness temperature was observed with the radiometer scanning from 5.5 to 7.0 GHz over what was believed to be a thin, recently frozen section of sea ice.

TUESDAY AFTERNOON
June 3, 1:30 - 5:00

REMOTE SENSING - PASSIVE

DKN 2C

Session F.2

Chairman: D.C. Hogg
Wave Propagation Laboratory
NOAA
Boulder, Co.

MICROWAVE REMOTE SENSING FOR THE WEATHER SERVICES

D. C. Hogg, M. T. Decker and R. G. Strauch
Wave Propagation Laboratory
NOAA/Environmental Research Laboratories
Boulder, CO 80303

Design of a system for essentially continuously profiling temperature, wind and humidity in the troposphere is given. Precipitable water vapor and cloud liquid integrated in the zenith direction are also provided. The temperature and humidity are sensed by millimeter-wave radiometry, and the wind by Doppler radar. The instruments are all solid state and involve no moving parts to achieve high reliability and unattended operation. Examples of experimental data which influenced the design are presented, and the implications for weather prediction are discussed.

Sea-surface temperature, wind speed and atmospheric water vapor:
A comparison of conventionally measured data with data retrieved
from satellite-borne microwave radiometry

R. Hofer* and E. G. Njoku

Jet Propulsion Laboratory
4800 Oak Grove Drive
Pasadena, California 91103
Mail Stop 168-314

*U.S. National Research Council Resident Research Associate

The SEASAT Scanning Multichannel Microwave Radiometer (SMMR) estimates sea-surface temperature (SST), surface wind speed, integrated water vapor, cloud liquid water content and indicates rain cells. These geophysical outputs are obtained by algorithms operating on measurements of the earth radiation at 6.6, 10.7, 18., 21. and 37. GHz with vertical and horizontal polarizations. Earlier evaluation activities showed the ability to retrieve SST and wind speeds with rms accuracies of 1.5 K and 2 m/sec respectively over a limited range of conditions. The retrievals appear to degrade with increasing weather although the algorithms correct for atmospheric water vapor and liquid water. SMMR data processed with the final calibration and antenna pattern correction algorithms will be available soon. The data should represent the full range of environmental conditions experienced during the SEASAT lifetime.

For the proposed presentation the geophysical parameters will be retrieved by a modified algorithm based on an earlier concept; namely: the statistical relationships between brightness temperatures and geophysical parameters obtained from an ensemble of realistic SST, wind speeds, atmospheric temperature profiles, water vapor profiles and cloud models by multiple linear regression. Non linear features of the problem are treated by relating a suitable function of brightness temperatures to the geophysical parameters and by using different sets of regression coefficients which depend upon values of geophysical parameters determined in an initial calculation. Random noise perturbation of the theoretical brightness temperatures and significance tests provide confidence limits for the regression coefficients. The simulated residual errors of the retrieval algorithms easily meet the design goals of the SMMR. Instrumental biases possibly present may be overcome by regressing actual satellite data versus corresponding geophysical parameters. This procedure provides only an instrument dependent algorithm.

The idea of the algorithm will be briefly described. First results of comparisons of satellite-derived geophysical parameters with data obtained from ships, buoys, aircraft expendable bathythermographs (AXBT's) and radio-sondes will be presented.

Large Antenna Multifrequency Microwave
Radiometer (LAMMR) System Design

J. L. KING
NASA Goddard Space Flight Center
Greenbelt, Maryland 20771, U.S.A.

The LAMMR is a 1.4, 4.3, 10.65, 18.7, 21.3, 36.5, and 91 GHz 4 meter diameter offset reflector mechanically scanned radiometer system. These channels were selected to measure sea surface temperature and wind speed, atmospheric water vapor, liquid water, precipitation, and sea ice parameters from low earth orbiting satellite systems. This system is now included in the National Oceanic Satellite System (NOSS) and Ice Experiment Satellite payloads scheduled for launch in the mid 80's. The LAMMR achieves resolutions from 105 to 7 KM from a 700 KM orbit, which is a factor of 5 better resolutions than were achieved on the Nimbus-7 and Seasat-A Scanning Multichannel Microwave Radiometer (SMMR).

Extensive trade-off studies have been made to select the antenna system designs compatible with a 1 rps rotation which does not perturb the host free-flying satellite which also has to accommodate high resolution optical sensors. The particular antenna offsets and f/D's have to be optimized for dynamic balance to minimize the torque disturbances on the spacecraft as well as meet RF performance requirements. A prime focus offset parabolic reflector fabricated from graphite epoxy (GE) was selected because the low weight and high stiffness of GE which allows the dish to maintain the surface tolerance for 90 percent beam efficiency and .02° knowledge of beam position while scanning. The reflector is under-illuminated at 36.5 and 91 GHz to limit the resolution and the scan rate required for contiguous coverage to 1 rps. One multichannel feed design uses clustered multimode horns to achieve the 3.8 to .26° secondary pattern beamwidths.

The scan mechanism must rotate the antenna and radiometer system at 1 rps and also compensate the angular momentum of the approximately 150 kg spinning system to less than 1 ft. lb. sec. Direct drive brushless DC motors and gear coupled mechanisms have been studied to perform these functions. Standard slip ring and roll-ring data and power coupling systems have also been studied to accommodate the radiometer system on the spinning antenna structure.

The LAMMR radiometers use a variety of designs to cover the 1.4 to 91 GHz frequency range from null balanced tuned radio frequency Dicke at 1.4 GHz to total power super heterodyne at 91 GHz. The radiometer calibration system uses sky horns and ambient temperature microwave loads at 4.3 GHz and above to perform a 2-point calibration. The 1.4 GHz radiometer will probably use a noise injection calibration to eliminate the need for the large 1.4 GHz sky horn. The brightness temperatures from these channels will be digitized into 12 or 14 bit words which are formatted with supporting telemetry data for transmission through the scan mechanism to the spacecraft telemetry system.

Antenna Design for
Large Antenna Multifrequency Radiometer (LAMMR)

L. R. Dod
NASA Goddard Space Flight Center
Greenbelt, Maryland 20771, U.S.A.
Ramons Mieziis
Sigma Data Systems

This LAMMR antenna is a 4 meter diameter offset parabolic reflector with 1.4, 4.3, 10.65, 18.7, 21.3, and 94 GHz radiometer channels. The LAMMR is planned for launch in the 80's in the National Oceanic Satellite System (NOSS) and Ice Experiment Satellite series. The instrument will measure wind speed and sea surface temperature, sea ice parameters, atmospheric water vapor, liquid water, and precipitation.

Tradeoff studies have considered both prime-focus and Cassegrain offset reflectors spinning at 1 rps. A prime-focus antenna made from graphite-epoxy has been selected for good mechanical and r.f. performance. Reflector distortion due to the 1 rps spin has been modeled and r.f. performance of the reflector has been analyzed using a vector-diffraction program with curve fitting of the distorted reflector data points. A design goal of 90% beam efficiency for the 7 radiometric frequency channels requires good mechanical tolerances and careful r.f. design of the reflector/feed system. Computed design data are presented for several feed horn designs that utilize clusters of feed horns to cover the 7 frequency channels. The antenna beamwidth requirements are 3.8° to $.26^\circ$ from the lowest to the highest frequency channels. In order to achieve contiguous coverage at the highest frequencies for the 1 rps spin rate, the reflector must be under-illuminated at 36.5 and 91 GHz. Several feed techniques to achieve under-illumination have been analyzed. In addition, beam pointing errors, feed positional errors, reflector distortions, mechanical tolerances, feed spillover, cross polarization, and beam efficiency are modeled and a summary of the antenna performance is discussed. The results of the analytical study show that the proposed LAMMR antenna system can meet the design goals.

Studies of Vegetation Effects on Soil Moisture Determination

J. Eckerman and

G. Orr, M. Dombrowski
M. Doyle, J. Schutt, J. Wang
Goddard Space Flight Center,
Greenbelt, Maryland 20771, U.S.A.

Experimental observations of microwave brightness temperature variation with soil moisture content were made using L, S and C-band microwave radiometers. Incidence angle, soil density and vegetation were studied parametrically in the Elsinboro sandy loam soil at the Beltsville Agriculture Research Center. For bare fields (fallow), the correlation coefficient for the brightness temperature variation with soil moisture content was .98, .89 and .93 at L, S and C-bands respectively. The data trends at L-band are in agreement with the Newton (1975) data for smooth clay. With vegetation (corn, soybeans, alfalfa, wheat) the correlation coefficients decreased to 0.88, 0.84 and 0.46 at L, S and C-bands respectively. Tilling did change the density, but not the roughness of this sandy loam soil as in the clay observations of Newton. Microwave Brightness temperature was highly dependent on soil density.

PASSIVE MICROWAVE REMOTE SENSING

L. U. Martin and C. I. Beard, Naval Research
Laboratory, Washington, D. C. 20375

Microwave radiometry offers promise as a ground-based passive technique for remotely obtaining information about atmospheric species, structure and processes occurring in the lower atmosphere. Previous experiments by NRL in 1975 and 1976 demonstrated the ability of radiometers, at a frequency of 22 GHz (wavelength $\lambda = 1.35$ cm), to observe dynamic structures by detecting and localizing (in altitude) both short-period ($\approx 1-2$ min) Kelvin-Holmholtz instabilities and longer-period (3-15 min) gravity waves.

In previous experiments, antenna beams from two separated radiometers were pointed to intersect at various angles in the vertical plane between them. One disadvantage of this technique was the restriction on the observed height of the features because of the limited separation between radiometers. To overcome this, an experiment was conducted using a side-looking technique. In this method, the two antennas beams were pointed toward each other in a non-vertical plane.

The experiment was conducted at the National Oceanographic and Atmospheric Administration (NOAA) Test and Evaluation Division site at Sterling, Virginia. Data were taken during September 1979 under a variety of meteorological conditions, including low-level inversions, free convection, clear skies, multi-layered clouds and light precipitation. Analysis indicates that the side-looking technique gives a significant improvement in height capability over the old technique, enabling features as high as 3650 meters to be correlated (with a 670-meter baseline). One example of this height capability was the appearance of features at two separate heights, as evidenced by two distinct delay times, during the same run. These results and others will be discussed during the talk.

MARKOVIAN MODELS OF THE SPATIAL COHERENCE OF
ATMOSPHERIC FIELDS: THEIR IMPACT AND
AVAILABILITY FOR REMOTE SENSING STUDIES

P. M. Toldalagi
Massachusetts Institute of Technology
Research Laboratory of Electronics
Cambridge, Massachusetts 02139

Sensor design characteristics limit theoretically the local retrieval performance of remote sensing instruments. The number and choice of radiometric frequencies, the measurement signal-to-noise ratio observed for each channel introduce limitations on their local vertical resolution and the size of the diffraction apertures, the type of spatial scanning (if any) introduce limits on their local horizontal resolution. Beyond these considerations, however, it is possible in many cases to improve local retrieval results through the use of appropriate spatial smoothing reflecting the spatial correlation structure of the fields being observed. Using the case of TIROS-N/MSU as an example, this paper discusses the improvements obtained while retrieving atmospheric temperature profiles using successively a local statistical retrieval technique, a Kalman filter with stationary dynamics and finally an adaptive filtering technique that relies on the use of a simultaneous General Circulation Model of the atmosphere to identify local markovian structures in the temperature field.

INVERSION OF DATA FROM DIFFRACTION-LIMITED
MULTIWAVELENGTH REMOTE SENSORS WITH NONLINEAR
DEPENDENCE OF OBSERVABLES ON THE GEOPHYSICAL
PARAMETERS

P. W. Rosenkranz
Massachusetts Institute of Technology
Cambridge, Mass. 02139

Linear shift-invariant spatial filtering has been applied to inversion of data from the Scanning Multi-channel Microwave Radiometer on the Nimbus 7 satellite. This instrument measures thermal radiation from the earth in both polarizations at frequencies of 6.6, 10.7, 18, 21, and 37 GHz. The state of the ocean-atmosphere system, for the purpose of radiative transfer calculations at these frequencies, is described by a six-parameter model. The parameters are sea surface temperature, near-surface wind speed, integrated water vapor mass, scale height of water vapor in an exponential distribution, integrated liquid water mass, and characteristic drop radius in a Best drop-size distribution. Nonlinear dependence of brightness temperature on these parameters is approximated by second-order terms in the parameters. The spatial filter deconvolves and inverts the data simultaneously. Residual nonlinearity of the retrieved parameters appears theoretically as crosstalk from the second-order terms to the first-order terms. The criterion of minimum-expected-square-error reduces residual nonlinearity to the lowest value consistent with the signal-to-noise ratio of the measurements and the structure of the filter.

Multiparametric Inverse Problems in Microwave Radiometry
of Ocean and Atmosphere

A.M. Shutko and A.G. Grankov
Institute of Radioengineering
and Electronics, Academy of
Sciences of the USSR, Marx Ave., 18,
USSR, I03907, Moscow K-9, GSP-3

This paper concerns the inverse problem of hydrophysical parameters of ocean surface and meteorological parameters of atmospheric estimations by means of analysing the field of electromagnetic radiation at microwaves. These parameters are: the temperature and salinity of the surface, its state under different wind speeds, integral water vapour content of the atmosphere and liquid water content of the clouds.

For solving this problem, the optimal frequencies are determined in centimeter and decimeter wavelength range. The problem of surface parameter estimations by considering the atmosphere as a transition medium is first discussed. Then, the general problem of estimating the parameters of the "ocean-atmosphere" system is solved.

The accuracy of solution is analysed by considering the main sources of errors inherent in microwave radiometry such as the uncertainty of functional "radiation vs hydrophysical and meteorological parameters" dependences, errors in calibrating the intensity of measured radiation and fluctuation noise of instruments.

The solutions are obtained both for "sufficient" system with the number of wavelengths to be equal to the number of measured parameters and for the system with extra wavelengths.

The worked out methods are tested by means of numerical experiments and examined by suitably processing the experimental data obtained under natural conditions. The obtained results have indicated the high degree of their effectiveness.

WEDNESDAY MORNING

June 4, 8:30 - 12:00

RADIATIVE TRANSFER THEORY AND
REMOTE SENSING OF LIGHTNING

DKN 2C

Session F.3

Chairman: J.Goldhirsh
Applied Physics Laboratory
Laurel, MD.

REMOTE SENSING OF CURRENT IN LIGHTNING RETURN STROKES

D. M. Le Vine and R. Meneghini

Microwave Sensor Branch
Goddard Space Flight Center
Greenbelt, Maryland 20771

CANCELLED - ANNULÉ

EFFECT OF CHANNEL DETAILS ON THE FIELDS INDUCED
BY A LIGHTNING RETURN STROKE

R. L. Gardner
Department of Physics and
Cooperative Institute for Research in Environmental Sciences
University of Colorado
Boulder, CO 80309

A lightning flash is initiated when a stepped leader forms a conducting charged path from cloud to ground. The charged column then discharges, emitting electromagnetic energy at radio frequencies. The discharge column is geometrically complex and the discharge mechanism is not understood.

In this paper we examine, in detail, the relationship between the characteristics of the discharge path and the radiated electromagnetic field. One of the characteristics examined is the tortuosity of the return stroke channel of a cloud to ground discharge. Suppose the discharge channel is constructed of arbitrarily oriented, interconnected, filaments of current. Each filament may be considered as a composite of three dipoles, each directed along a cartesian axis. The vertical component generates electromagnetic fields more efficiently near the earth than the horizontal component. Therefore, one result of tortuosity is that the cloud to ground discharge appears as a vertical column with a current pulse propagation velocity decreased by the cosine of the angle of the filament with the vertical, for each filament. It will be shown that a decrease in the velocity of propagation of the current pulse results in a decrease in the excitation of high frequency components. This decrease must be compared with the similar appearing high frequency attenuation due to propagation in the earth-ionospheric waveguide.

The electric fields for both the tortuous channel geometry and varying velocity of current pulse propagation are calculated in a model that also calculates the effects on the fields of propagation along an imperfectly conducting earth and beneath an anisotropic ionosphere. Levine and Meneghini (J. Geophys. Res., 83, 2377-2384, 1978) derive similar results for a perfectly conducting ground but they ignore the ionosphere. The results presented here agree with Levine and Meneghini up to about 10kHz. Above that frequency the added attenuation due to the more realistic ground model becomes apparent. Reflection from the ionosphere enhances the the ionosphere becomes transparent.

RADIATIVE TRANSFER THEORY FOR A TWO-LAYER
RANDOM MEDIUM WITH CYLINDRICAL STRUCTURE

S. L. Chuang, J. A. Kong
Department of Electrical Engineering and
Computer Science and Research Laboratory
of Electronics
Massachusetts Institute of Technology
Cambridge, Massachusetts 02139

L. Tsang
Department of Electrical Engineering
Texas A and M University
College Station, Texas 77843

In passive microwave remote sensing of earth terrain, the application of the radiative transfer theory to the model of random medium has been proven useful in the interpretation of various experimental data. For laminar structures such as snow-ice field, we can use the model of a random medium with infinite horizontal correlation length which leads to close-form solutions for the brightness temperatures. In the case of vegetation fields with cylindrical structures, we can model the vegetation layer as a two-layer random medium with a small correlation length l_x in the horizontal direction, and a large correlation length l_z in the vertical direction. It is shown that as l_z approaches infinity, the solutions for the brightness temperatures can be obtained in close-form. We then use the Gaussian quadrature method to solve the radiative transfer equations for the two-layer random medium and obtain numerical results in order to compare with our solution for infinite l_z which requires very little computational time in contrast to the numerical method. It is found that as l_x approaches infinity, the kernels in the scattering terms give rise to delta functions, indicating that the forward scattering is dominant over all the other directions. The results obtained with this model are applied to match experimental data collected from corn fields. For the case when l_z is large but not infinity, we find a first order solution with iterative methods. The difference between the zeroth and the first order results is compared for the cases of large albedo.

RADIATIVE TRANSFER THEORY APPLIED TO REMOTE SENSING OF
HOMOGENEOUS MEDIA CONTAINING DISCRETE SCATTERERS

M. E. McGillan
Department of Electrical Engineering and
Computer Science and Research Laboratory
of Electronics
Massachusetts Institute of Technology
Cambridge, Massachusetts 02139

The radiative transfer theory has been found useful in the interpretation of various data collected from microwave remote sensing experiments. For a homogeneous medium containing discrete scatterers, a laboratory model tank can be built to simulate the actual environment and to verify the theoretical predictions. Our model tank is of the size 5' x 8' filled with fine grain silica sand of dielectric constant $(2.97 + i0.0115)\epsilon_0$ where ϵ_0 is the permittivity of free space. Metallic balls with a diameter of 2 mm are buried in the sand to produce scattering effects. The experimental set-up involves the use of an active reflectometer at 15 GHz for measuring the reflectivity of the modelled medium.

In theory we apply the radiative transfer formalism to a two layer homogeneous medium containing metallic Rayleigh scatterers. The resulting integro-differential equations are reduced to a system of linear first order differential equations using Gaussian quadrature. The eigenvalues are then determined and the appropriate boundary conditions are applied to obtain a unique solution for the bistatic scattering coefficients of the system. We then compare the theoretical results with the experimental data collected from the model tank. It is noted that radiative transfer theory is valid only when the coherent effects of wave interactions are negligible. The model tank experiment thus provides a means to explore the limits of radiative transfer theory as we vary the thickness of the sand layer and the number of scatterers inside the layer.

RADIATIVE TRANSFER THEORY FOR ACTIVE AND PASSIVE
MICROWAVE REMOTE SENSING OF HOMOGENEOUS LAYER
CONTAINING SPHERICAL SCATTERERS

R. Shin, J. A. Kong
Department of Electrical Engineering and
Computer Science and Research Laboratory
of Electronics
Massachusetts Institute of Technology
Cambridge, Massachusetts 02139

L. Tsang
Department of Electrical Engineering
Texas A and M University
College Station, Texas 77843

In active and passive microwave remote sensing of low-loss and scattering dominant areas, the effect of volume scattering can be modelled by a homogeneous layer containing spherical scatterers. The radiative transfer theory is used to study the effect of volume scattering by obtaining backscattering cross sections and brightness temperatures. The theoretical results are used to interpret the experimental data collected from snow fields as functions of frequency, incident angle, and snow depth. It is found that when plotted as a function of snow depth the brightness temperature may decrease or increase as snow depth is increased according to whether the subsurface is more or less emissive than the snow layer. The vertically polarized backscattering cross sections σ_{vv} may be lower than the horizontally polarized backscattering cross sections σ_{hh} for shallow snow depth and is always higher for deeper snow depth. The diurnal change, which is exhibited in both the active and passive data, is explained by changing the dielectric properties of a top thin layer to account for the possible melting effects in the afternoon hours compared to the morning hours. In the data matching exercise it is essential to characterize the area with one set of parameters for the model which can match all remote sensing data as functions of frequency, incident angle, and polarization. This is illustrated by matching the active and passive data collected from a snow field on the same day.

RADIATIVE TRANSFER THEORY FOR ACTIVE REMOTE SENSING OF
HOMOGENEOUS LAYER CONTAINING ELLIPSOIDAL SCATTERERS

M. Kubacsi, R. Shin
Department of Electrical Engineering and
Computer Science and Research Laboratory
of Electronics
Massachusetts Institute of Technology
Cambridge, Massachusetts 02139

In the active remote sensing of low-loss and scattering dominant areas, the effect of volume scattering can be modeled by a homogeneous layer containing discrete ellipsoidal scatterers. The low frequency solution of the ellipsoidal scattering model is used with the radiative transfer theory to calculate backscattering cross sections. The closed form solution is obtained through an iterative approach. The radiative transfer equations and the boundary conditions are cast into the form of integral equations using albedo as an iteration parameter. Then an iterative process is applied to solve the integral equations. Unlike the case of spherical scatterers, where the depolarization of the backscattered intensities are of the higher order effect than the like-like polarization, the depolarized and like-like polarized backscattering cross sections are of the same order in albedo for the case of ellipsoidal scatterers. Comparing the results with the solutions for the spherical scatterers we find that the depolarized backscattering cross sections are much higher for the ellipsoidal scatterers. This model is thus used to interpret experimental data which exhibit high depolarization returns.

ACTIVE MICROWAVE REMOTE SENSING OF AN ANISOTROPIC
TWO-LAYER RANDOM MEDIUM

M. A. Zuniga, S. L. Chuang, J. A. Kong, J. K. Lee
Department of Electrical Engineering and
Computer Science and Research Laboratory
of Electronics
Massachusetts Institute of Technology
Cambridge, Massachusetts 02139

In the active microwave remote sensing of earth terrain, anisotropic behavior occurs in many experimental data. To explain such behavior, we can either model the terrain medium as a random medium with anisotropic background dielectric or with isotropic background but having anisotropic correlation functions or both. Furthermore, in the case of vegetation field, the anisotropy exhibited in the backscattering cross-sections in radar returns can best be interpreted with anisotropic rough surface effects. It is the purpose of this paper to explore all these cases according to the different types of experimental data.

For vegetation fields with row structures, we find that for looking angles near normal incidence, the anisotropy in surface roughness is dominant while at larger incident angles, the data can be explained by using anisotropic correlation functions with three different correlation lengths for the random-medium model. In the case of sea ice, the volume scattering effects are better treated with the model of an anisotropic two-layer random medium characterized by a dyadic permittivity $\underline{\underline{\epsilon}}(\vec{r}) = \langle \epsilon \rangle + \underline{\underline{\epsilon}}_f(\vec{r})$ where $\langle \underline{\underline{\epsilon}}_f \rangle = 0$ and $\langle \epsilon \rangle$ is uniaxial. Using the formalism of Dyadic Green's functions an iterative procedure is carried out to calculate analytical expressions for backscattering cross sections that include depolarization effects. All these theoretical results are used to match experimental data collected from sea ice and vegetation fields.

MODIFIED RADIATIVE TRANSFER THEORY FOR ACTIVE REMOTE
SENSING OF A TWO-LAYER RANDOM MEDIUM

M. A. Zuniga, J. A. Kong
Department of Electrical Engineering and
Computer Science and Research Laboratory
of Electronics
Massachusetts Institute of Technology
Cambridge, Massachusetts 02139

Modified radiative transfer (MRT) equations which govern the electromagnetic field intensity in a two-layer random medium are important at least for the following two reasons: (1) the ordinary radiative transfer (RT) equations ignore coherent effects due to wave interactions. In applications to less scattering dominant terrain media such as ice fields, it is known that coherent interference results are present in most experimental data and a more coherent theory than the ordinary RT equations must be developed. (2) It is imperative from the theoretical point of view to see that the incoherent RT theory can be deduced from the coherent MRT result. We derive the MRT equations from the ladder approximated Bethe-Salpeter equation together with the non-linear Dyson equation. The zeroth order mean field solutions to Dyson's equation are substituted into the Bethe-Salpeter equation under the ladder approximation. Constructive interference terms in the ladder operator are dominant provided the rate of absorption is much less than the propagation constant. Selectively equating the constructive interference terms in the Bethe-Salpeter equation results in the MRT equations for the electromagnetic field intensity. The MRT equations are then solved in the first order renormalization approximation to obtain analytical results for the backscattering cross sections of the two-layer random medium with arbitrary three dimensional correlation functions. The coherent effects of MRT theory are illustrated and comparisons are made with back-scattering cross sections obtained with the first Born approximation to the wave equation.

WEDNESDAY AFTERNOON
June 4, 1:30 - 5:00

SURFACE/UNDERGROUND PROPAGATION
DKN 2C

Combined Session F.4/AP-S

Chairman: R.J. King
University of Wisconsin
Madison, WI

The following papers belong to the IEEE AP-S Symposium and the summaries are included in the IEEE AP-S Digest under Combined Session F.4/AP-S.

1. EARTH CONDUCTIVITY EFFECT ON THE FIELD OF A LONG HORIZONTAL ANTENNA, A. Mohsen, Department of Electrical Engineering, University of Manitoba, Winnipeg, Canada.
2. MONOPOLE ANTENNAS OVER LOSSY GROUND, H.K. Schuman and T.E. Baldwin, Atlantic Research Corporation, 5390 Cherokee Avenue, Alexandria, Virginia 22314.
9. SCATTERING OF RADIO WAVES FROM AN EARTH MODEL WITH A PERIODIC ROUGH SUBSURFACE, M.S. El Tanany, M. El Said, S.F. Mahmoud, Electronic and Communications Department, Cairo University, Giza, Egypt.

EXPERIMENTAL AND THEORETICAL STUDIES OF LATERAL-WAVE PROPAGATION

M. F. Brown, R. W. P. King, L. C. Shen, and T. T. Wu
Gordon McKay Laboratory, Harvard University, Cambridge, MA 02138

An apparatus has been constructed for the study of lateral-wave propagation of electromagnetic waves along an air-salt water boundary that may be smooth, undulating, or provided with bumps, depressions, or other irregularities or with a thin layer of a third material. The first tests are designed to compare measured values of the radial electric field in the water and the vertical electric field in the air generated by a horizontal dipole in the water with both accurate theoretical values and approximate formulas including those of Baños (R. W. P. King and J. T. deBettencourt, IEEE Trans. Geosci. Electr., GE-17, 86-92, 1979). The choice of frequency locates the range of measurement in Baños' intermediate field where the decrease in amplitude with distance is smallest. After the measurements using a smooth interface are understood in terms of the theory, they will be extended to surfaces that are not smooth or are modified by an intermediate layer. A description of the apparatus, a discussion of accurate and approximate theoretical formulas, and a report on measurements and their correlation with theory will be given.

DIFFRACTION AT A SURFACE IMPEDANCE DISCONTINUITY.
APPLICATION TO SEA-LAND RADIOWAVE PROPAGATION (†).

Giorgio Franceschetti and Vittorio G. Vaccaro
Istituto Elettrotecnico, Università di Napoli (Italy)

Full solution of plane-wave diffraction by a surface impedance discontinuity is presented. The solution is given for both normal and oblique incidence, the diffraction integral being evaluated asymptotically in a closed form. This solution extends previous results of Malyuzhinets (Sov. Phys. Dokl. 3, 752-755, 1958), valid only for normal incidence, and singular at reflection boundaries.

For practical applications to radiowave propagation over the Earth, the field close to the surface is of interest. This requires the asymptotic evaluation of an integral along a Sommerfeld contour with two poles nearby one saddle point, and three poles nearby the other. The evaluation can be performed using an appropriate modification of the Bleistein's method (J. Math. Mech., 17, 533-559, 1967). The total field is then described in terms of the five pole contributions: an incident field, two reflected (from the two half-planes) fields, a surface field, and an extra component field, this last characteristic of the surface impedance discontinuity. The first four components are the usual (optical or quasi-optical) terms times a transition function; the extra component is a new term, which could be called discontinuity field. In addition, a cylindrical wave (saddle point contribution) scattered by the discontinuity is present.

(†) This work has been sponsored by the European Research Office, United States Army, under Grant DA-ERO-78-G-097.

COUPLED MODES ANALYSIS FOR A NON-UNIFORM TROPOSPHERIC WAVEGUIDE

James R. Wait
ERL/NOAA/CIRES
U.S. Dept. of Commerce
Boulder, CO 80303, USA

We employ a two-dimensional cylindrical model to analyze the normal modes in a laterally non-uniform tropospheric duct. The utilization of the surface impedance boundary condition at the earth's surface permits us to use a field representation in terms of discrete modes only. These modes are chosen to be locally orthogonal so that a tapered type non-uniformity can be handled with a systematic accounting of the mode conversion as demonstrated in the profound work of E. Bahar. The relationship of this method to the mode-matching procedure is pointed out. Explicit formulae are given for the coupling coefficients that have a clear physical interpretation. The present formulation can be applied to non-uniform underwater acoustic waveguides and to uneven atmospheric ducts that support acoustic gravity waves. Special attention is paid to the effect of modal degeneracies which required special handling as pointed out by K.G. Budden and V.V. Shevchenko.

UHF LONG DISTANCE DUCT PROPAGATION

Mauro S. Assis
 Centro de Tecnologia Promon
 Praia do Flamengo 154
 22210 Rio de Janeiro - RJ
 Brasil

Duct propagation is an important mechanism for long distance interference studies. In the microwave band the theoretical analysis of this problem is very difficult since several modes should be taken into account. However, for frequencies below 1GHz only a few modes are trapped and a simple mathematical solution can be established. Based on the first mode of the rigorous theory, this paper presents a semi-empirical model for long distance duct propagation in the 300-1000 MHz band. According to this model the electric field (E) relative to free-space (E_0) is given by

$$\frac{E}{E_0} = 2\sqrt{\pi x} e^{-cx} f_r \cdot f(h_1) \cdot f(h_2)$$

where

$$x = \left[\frac{\pi}{\lambda} \right]^{1/3} \frac{d}{a_e} 2/3 ; d = \text{distance}; \lambda = \text{wavelength}$$

a_e = effective earth radius; c = attenuation coefficient

f_r = roughness factor; $f(h_{1,2})$ = height gain functions

With data from over-water paths in England it was fixed the dependence between the attenuation coefficient and refractivity gradient. The extrapolation for other climatic areas is discussed in the text. Also using experimental results the effect of terrain roughness is considered in a dB per km basis. The model seems to be useful to the study of interference problems in UHF broadcast services and UHF point-to-point radio links largely used in developing countries to cover areas of low telephone traffic density.

FIELDS OF A HORIZONTAL LOOP OF ARBITRARY SHAPE
BURIED IN A TWO LAYER EARTH

James R. Wait and David A. Hill
ERL/NOAA and ITS/NTIA
U.S. Department of Commerce
Boulder, Colorado 80309

In communicating with and/or locating trapped miners, we had earlier suggested that a feasible source would be a wire loop that could be excited by a portable transmitter (J.R. Wait, IEEE Trans. GE-9, 95-98, 1971). A great deal of effort has gone into the problem by various groups in the U.S. and elsewhere. An accessible and very well written account can be found in the prize-winning paper by Large, Ball and Farstad (IEEE Trans. COM-21, 194-202, 1973). In a previous analysis, we considered the problem of a small horizontal loop or vertical magnetic dipole located in the bottom region of a two-layer earth. The results were quasi-static in the sense that all significant distances in the problem were small compared with a free space wavelength. Using numerical integration, the magnitude of the ratio of the horizontal to the vertical magnetic field was examined for an observer on the earth's surface. This was shown to have diagnostic features that could be used as the basis of a source location technique, in spite of the fact that the curves were modified to some extent by the layer structure (J.R. Wait and K.P. Spies, IEEE Trans. AP-19, 717-718, 1971). Here we extend the earlier analysis to allow for the finite extent of the source loop. Also, we derive explicit expressions for the fields that are valid everywhere. In order to render the problem some generality, displacement currents in the air and in the ground are retained at least in the initial formulation. First of all we deal with a circular loop of radius a . When a tends to zero we then recover the field expressions given earlier for a magnetic dipole. We then consider a loop of finite size with any specified shape. In particular, we deal with one of rectangular form. The numerical results indicate that small rectangular and circular loops produce similar surface fields, but that differences appear as the loop size is increased. In particular, the azimuthal symmetry, that exists for circular loops, is lost when the loop is rectangular. Also, an azimuthal component of magnetic field is produced by the rectangular loop. This field component could present a problem in source location. Also, an important limitation of the present formulation is that the current in the loop is assumed to be uniform. This is justified on the basis that the loop wire conductor is covered by insulation and that the circumference of the loop is extremely small compared with the wavelength in the insulation. At radio frequencies and higher, this assumption is clearly violated and another approach, such as the integral equation technique (D.C. Chang, IEEE Trans., AP-21, 871-874, 1974) would have to be implemented.

PROCEDES ELECTROMAGNETIQUES DE DETECTION DE FILONS
METALLIFERES : ETUDE NUMERIQUE DE L'INFLUENCE DU
PENDAGE DU GISEMENT POUR DIFFERENTS
DISPOSITIFS D'EXCITATION

M. CAUTERMAN, P. DEGAUQUE, B. DEMOULIN et R. GABILLARD
Université des Sciences et Techniques de Lille, Département
Electronique, 59 655 Villeneuve d'Ascq Cedex.(France)

Nous avons mis au point depuis quelques années des modèles numériques tridimensionnels permettant de simuler la réponse d'une anomalie de forme quelconque située dans le sol à un champ électromagnétique émis par un dipôle électrique ou magnétique (M. Cauterman et al., *Proc. of the IEEE*, 67, 7, 1009-1015, 1979). L'anomalie est divisée en parallélépipèdes élémentaires suffisamment petits pour que le champ électrique puisse être supposé constant au sein de chacun d'eux. Le champ dans l'anomalie est solution d'une équation intégrale qui se ramène dans ce cas à un système matriciel. Nous avons également montré que si l'hétérogénéité est un parallélépipède rectangle, une réduction considérable du temps calcul est obtenu grâce à des propriétés de symétrie de la matrice. Un tel modèle ne permet pas cependant d'étudier l'influence du pendage. Nous avons donc modifié les programmes en conséquence en effectuant des changements de base de manière à conserver un temps de calcul minimum.

Après avoir décrit brièvement la méthode suivie, nous donnons sur un exemple, l'influence d'un pendage de 45° et de 60° sur la répartition du courant induit dans l'anomalie et sur la réponse de celle-ci à une excitation de type électrique ou magnétique. Nous comparons les formes des courbes de réponse dans ces différents cas pour savoir si une estimation de l'angle de pendage est possible.

D'autre part, les études numériques simulant des gisements miniers font souvent appel au concept de plaque mince. Ceci revient à supposer une distribution superficielle des sources secondaires équivalentes à l'anomalie réduisant ainsi les coûts d'exploitation des modèles numériques. Nous essayons de mettre en évidence les limites de validité de cette technique de calcul en étudiant notamment l'influence de la position relative de l'émetteur par rapport à l'anomalie, ce qui revient à modifier l'angle d'incidence des filets de courant primaire sur la plaque.

THURSDAY MORNING

June 5, 8:30 - 12:00

LINE-OF-SIGHT PROPAGATION

DKN 2C

Combined Session F.5/AP-S

Chairman: R.K. Crane
Environmental Technology Res.Lab.
Concord, MA

The following papers belong to the IEEE AP-S Symposium and the summaries are included in the IEEE AP-S Digest under Combined Session F.5/AP-S.

2. REMOTE SENSING OF RAINDROP SIZE DISTRIBUTING FROM MICROWAVE SCATTERING MEASUREMENTS-II, Y. Furuhashi, T. Ihara and Tohma, Radio Research Laboratories, Ministry of Posts and Telecommunications, Koganei-shi, Tokyo 184, Japan.

6. THE PREDICTION OF CLEAR-AIR FADING FOR TERRESTRIAL LINE-OF-SIGHT AND LOW-ANGLE SATELLITE RADIO PATHS, Claus Fenger, Department of Electrical Engineering, McGill University, Montreal, Quebec H3A 2A7.

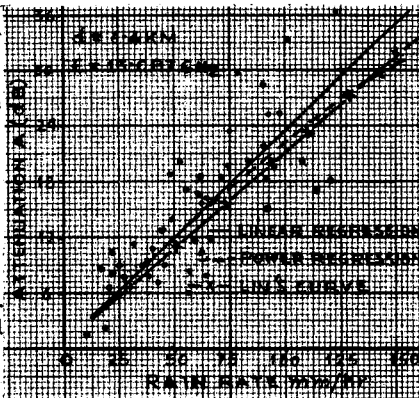
RESULTS OF RAIN ATTENUATION MEASUREMENTS
AT 13 GHz

Y.Kumar and DPS Seth,TRC,IPT,N.Delhi

To introduce Digital Microwave Interexchange junction working at 13 GHz contemplated for the Indian P&T network, a path engineering procedure based on reduction coefficient approach was proposed for rain attenuation effects. A number of methods have been proposed in the literature. Since considerable deviation exists between various approaches, experimental measurements were required to evolve a suitable formula applicable to the Eastern region of India (specifically city of Calcutta) where intense rainfall during monsoons (May-September) is common. Rain gauge observations were taken along a 6.4 Km route at four locations on an operational 13 Ghz horizontally polarized Digital Microwave System during May-September, 1979.

Results of Measurements: Strip chart recordings of the received signal strength were analysed to obtain the signal attenuation at various instants. At the selected instant the highest rain rate of the four rain gauges within a 5 minute period centred at the instant considered, is taken since the rain gauges and recorder were not synchronized.

Figure shows measured attenuation points plotted against corresponding rain rates. For comparison a curve based on Lin's method (Lin, BSTJ,56,1581-1604, 1977) has been included. The attenuation as a function of rain rate is given by $A = Y a R^b$, where $A =$ attenuation in dB, $Y =$ reduction coefficient, $a = 0.0209$, $b = 1.151$, $d =$ distance = 6.4 Kms and $R =$ rainfall rate (mm/hr). 'a' and 'b' are derived from (Olsen, Trans IEEE, AP March '79). For the 6.4 Km route, Lin's expression for the reduction coefficient works out to $Y = 1 / (.985 + 0.0024R)$ and the measured curve gives $Y = 2.88R^{-0.27}$. Reduction factor calculated from these two expressions tally very closely except at low rain fall rates. This is partly because in our experiments unprotected antennae have been used whose attenuation becomes significant at low rain fall rates.



COMPLEX PERMITTIVITY OF SAND - STORM MODELS AT 9 GHz

A. Kumar
 The Higher Institute of Electronics
 Beni Walid
 Socialist People's Libyan Arab Jamahiriya

The complex permittivity of sand-storms has been of increasing interest due to its effect on microwave propagation. Recently, there has been a great demand to analyze the propagation behaviour between earth and satellite through sand-storms, rain, fog and snow at microwave frequencies. In practice, it is very difficult to estimate accurately the amount of sand and compositions in the atmosphere and therefore, we have used models of different compositions of sand and polystyrene foam in the laboratory.

In this paper the complex permittivity of polystyrene foam - sand mixtures has been measured and related with Wiener's theory. The complex permittivity of sand-storms has been also estimated for pure air on the basis of Wiener's theory.

Polystyrene foam - dry sand models were made in the laboratory. We have used a 10, 20,, 80 percent of sand by volume basis in the polystyrene foam. It is assumed that the mixtures are homogeneous. The real and imaginary parts of the complex permittivity of sand has been measured using the evanescent waveguide technique. The cavity perturbation technique has been used to measure the complex permittivity of polystyrene foam and sand-storm models.

In Wiener's theory, the uncertainty in the electric field in the particles is accounted for by a factor C called the mixing condition. For polystyrene - sand, or air - sand mixtures, we assume the mixing condition $C = \infty$ which corresponds to the case where the inclusion particles occur as thin cylinders, planes or ellipsoids with the major axis parallel to the direction of the applied electric field. The complex permittivity is given by

$$\epsilon = V_1 \epsilon_1 + (1 - V_1) \epsilon_2 \quad (1)$$

where ϵ is the complex permittivity of mixture, ϵ_2 is the complex permittivity of polystyrene foam or air, ϵ_1 is the complex permittivity of sand and V_1 is the volumetric concentration of sand in polystyrene or air. The above equation is valid if ϵ , ϵ_1 and ϵ_2 are complex.

The experimental results were compared with Wiener's theory and detailed information will be given at the Conference.

PROPAGATION OF MICROWAVES UNDER ADVERSE SAND-
STORM CONDITIONS OF IRAQ

H. T. Al Hafid, S. C. Gupta and M. Ibrahim
Department of Electrical Engineering, Mosul
University, Mosul, IRAQ.

Attenuation of microwave signal, propagating under adverse sand-storm conditions is estimated theoretically up to 40 GHz. This effect is more predominant at frequencies higher than 10.0 GHz. Scattering and absorption coefficients are obtained and attenuation is obtained for different radii of sand particles.

Performance of Nasiriya-Baghdad link is studied during the adverse storm conditions of the year, when the visibility was dropping to 100 meters. It was observed that the received signal was fading up to -10 to -15 dB for short duration. Meteorological data were also recorded during the experimental work.

DIRECTION FINDING OF MULTIPATH PROPAGATION

Kazuaki TAKAO

Dept. of Electrical Engineering, Kyoto University, Kyoto, JAPAN

Multipath propagation is one of the important problems in mobile communication and TV broadcasting. Among the parameters of the component waves, the angles of arrival of several major ones are of interest in the present paper.

In the VHF or UHF region where the wavelength is not short enough, we are faced with some difficulties in the field measurements (especially in urban areas) because of the transportation of the measuring system as well as the on-the-spot surroundings:

- (1) Highly directional antennas cannot be used.
- (2) Large space is not available for the conventional aperture synthesis.
- (3) Homogeneity of the fields does not spread wide due to near-by scatterers.

The author introduced a new technique to achieve high angular accuracy with a small antenna and small space. (K. Takao et al., Int. Symp. on Antennas & Propagation, Japan, 191-194, 1978) The method may be called "mini" aperture synthesis with a probe antenna scanning along a circle of a small diameter (typically a wavelength). The data form a periodic function of the azimuthal angle with a period of 2π . Their higher harmonics contribute to the angular discrimination of component waves. Under assumption of finite number of multipath waves, Prony's method is used to obtain sharp peaks that correspond to the directions of those waves.

The present paper shows the detail of the performance of the method based on the results of computer simulation with a number of combinations of parameters. The aim is to clarify the angular resolution and accuracy. Also investigated is the criterion to judge the confidence of estimation of each case that may have been harmed either by the low SNR of the data or the excess number of incoming waves.

"A New Method for Evaluating Refractivity Profiles
from Surface Measurements"

M.T. Badr
Telecommunications Research Center,
Dokki Exchange Bldg.
Dokki, Cairo, Egypt.

The knowledge of propagation conditions from surface measurements has been of interest for workers in the field of microwave propagation. In this respect a relation between surface values of refractivity and refractivity at other heights has been investigated. The new suggested method depends on two facts. The first is that one must have information about a preceeding part of the daily cycle in order to evaluate profiles from surface data at the time considered. The second is that the values of atmospheric parameters vary but only little at elevated heights beyond level of stability.

Thus new surface parameters are chosen in order to obtain measures of refractivity at the other heights. The theoretical background for the choice of these parameters is illustrated, and a statistical study is carried for the suggested relations. The statistical study includes construction of scatter diagrams, using observations in three different sites in the Arab Republic of Egypt. Other forms of study, e.g. comparison of monthly averages are investigated also. All the results indicate that the suggested method is suitable for use, and gives better results than methods suggested previously.

MODELING THE INCREASE IN LOSS CAUSED BY
PROPAGATION THROUGH A GROVE OF TREES

by Mark Weissberger and Juergen Hauber
of the IIT Research Institute Staff at the
Department of Defense
Electromagnetic Compatibility Analysis Center
Annapolis, Maryland 21402

The additional loss caused by the intervention of a small (< 200 meter) grove of trees between two antennas is often modeled as (Eq. 1) $L = \alpha(F) \cdot D$ where L is the added loss in dB, α is the differential attenuation in dB/m, F is the frequency in GHz, D is the depth of the grove in meters. Measurements in forests at temperate latitudes were reviewed and new insights into the applicability of this formula were gained. These include:

1. The most-cited data set (Saxton & Lane, *Wireless World*, May 1955) covers $0.1 < F < 3.2$ and $24 < D < 200$, but $F \cdot D$ is always less than 80. The data are from England and Pennsylvania.
2. LaGrone's (*Proc. IRE*, June 1960) curve fit to the Saxton data, $\alpha = 0.26 F^{0.77}$ (Eq. 2), also satisfies the $F \cdot D < 80$ portion of a data set taken by McQuate (*ERL 65-ITS 58-1*, ITS, March 1968) in Colorado. The equation predicts too much loss for larger values of $F \cdot D$, however.
3. $\alpha = 1.33 F^{0.284} D^{-0.412}$ (Eq. 3) describes the entire McQuate data set ($3 < F \cdot D < 840$) as well as the entire Saxton data set. The McQuate data encompassed $15 < D < 90$ and $0.2 < F < 9.2$.
4. The California measurements of Frankel (SRI, *Packet Radio Note 254*, May 1978) are more accurately described by an equation of the form of Eq. 3 than they are by an equation of the form of Eq. 2. In this case, $F = 1.8$, $50 < D < 150$, $90 < F \cdot D < 280$.
5. The data in these three sets involved blockage by branches with leaves. Propagation through clusters of bare tree trunks causes, on the average, less loss.
6. The decrease of α with D in Eq. 3 is not predicted by the theory of propagation through an infinite medium -- whether it is filled with discrete scatterers or a lossy-dielectric continuum. A reasonable physical explanation of the diminishing α is that it represents an increasing percentage of the energy being propagated outside the branchy region -- either in free space or a region occupied by bare trunks.

THURSDAY AFTERNOON

June 5, 1:30 - 5:00

PRECIPITATION ATTENUATION AND DEPOLARIZATION

DKN 2C

Combined Session F.6/AP-S

Chairman: K.S. McCormick
Communications Research Center
Ottawa, Ontario

The following papers belong to the IEEE AP-S Symposium and the summaries are included in the IEEE AP-S Digest under Combined Session F.6/AP-S.

1. MODELING RAIN ATTENUATION OF EARTH-SPACE MICROWAVE LINKS, M.A. Weissberg and R.H. Meidenbauer, IIT Research Institute Staff of the Department of Defense, Electromagnetic Compatibility Analysis Center, Annapolis, MD. 21402.
5. THE ANALYSIS ABOUT THREE TYPES OF POLARIZATION CORRECTORS FOR SATELLITE COMMUNICATION WITH FREQUENCY REUSE SYSTEMS, Zhang Ri-rong, Shijiazhuang Communication Laboratories, Shijiazhuang, Hebei, China.

SPATIAL RAIN RATE DISTRIBUTION
MODELING FOR EARTH-SPACE LINK
PROPAGATION CALCULATIONS

S. O. Lane and W. L. Stutzman
Virginia Polytechnic Institute and State University
Department of Electrical Engineering
Blacksburg, Virginia 24061

Millimeter wave signals experience attenuation and depolarization when precipitation occurs along an earth-space path. This paper presents the prediction of average rain propagation effects using spatial and time statistics of the rainfall. The time distribution of rain rate at the earth station is assumed to be known in a statistical sense, either from direct measurement or from extrapolation from rain accumulation data. The spatial distribution of rain rate is modeled by a cell of gaussian shape with a random location of the peak rain rate. The extent of this typical rain cell decreases with increasing peak rain rate.

The average total attenuation for the propagation path is then computed using only the statistics of the rain cell.

Comparisons between predictions and measured data will be presented.

WAVELENGTH DEPENDENCE OF SLANT PATH
RAIN ATTENUATIONS AT MILLIMETER WAVELENGTHS

E.E. Altshuler and L.E. Telford

Rome Air Development Center, Electromagnetic
Sciences Division, Hanscom AFB, Massachusetts 01731

The main objective of this paper is to examine the wavelength dependence of slant path rain attenuation at millimeter wavelengths in order to determine how well the attenuation at one wavelength can be predicted from that of another. Also, some inferences on the drop size distribution of rain can be drawn from simultaneous attenuation measurements at two wavelengths. The theory of rain attenuation is reviewed and it is noted that the attenuation is a complex function of drop size, shape, orientation, index of refraction and rain intensity along the path. Attenuation ratios are computed based on both drop size and rain rate for wavelengths at which there are measured data. Results obtained by other investigators are reviewed and it is found that frequently attenuation ratios have been measured that would not have been predicted based on a surface rain model such as a Laws and Parsons and indicate that attenuation is often produced from a widely dispersed distribution of large raindrops. During eight rainy days in 1975-76 over 10,000 simultaneous measurements of 2 cm and 8.6 mm wavelength attenuations were recorded in the Boston area. On the basis of these results it is concluded that it is not possible to represent the drop size distribution of rain along a slant path in the Boston area by a Laws and Parsons model, since the ratios of the 8.6 mm to 2 cm attenuations are significantly below those that would have been predicted by that model. The ability to predict slant path rain attenuation at one wavelength based on that at another is shown to be a function of wavelength separation, climatology and whether cumulative or real-time statistics are desired.

Simplification of calculations of rain-induced
differential attenuation and cross polarization
at millimeter waves propagation

A.M. Ghuniem, I.E. Salm, Abd EL-SAMIE Mostapha
Telecommunication Research Center
Dokki Exchange Bldg.
Dokki, Cairo, Egypt.

In this method of calculation, the spheroidal vector wave functions were used for the solution of the scattering of plane electromagnetic waves having orthogonal polarizations, by oblate spheroidal raindrops. The far scattered fields from the oblate spheroidal raindrops were calculated as expansions of the oblate spheroidal vector wave functions.

The application of this method has the following advantages:

1. The spheroidal wave functions are suitable for expressing the variations of the fields in the different directions, because of the spheroidal shape of the raindrops.
2. The boundary conditions are applicable in an easy and direct manner.
3. The infinite series expressing the scattered field are rapidly convergent, i.e. the first few terms of the expansion are sufficient to give high accuracy.

The forward scattering functions for the two orthogonal polarizations were calculated, using this method, for different frequencies in the millimeter wave band, and the results were compared with the calculations based on the previous authors' methods, and they were found to be in agreement with them.

Using this method, it was found that the calculations are more simple and need much less time and memory size on the computer, than the methods used by the previous authors.

TAMPA TRIAD 19-GHz RAINY SEASON DIVERSITY RESULTS FOR 1978-1979

D. D. Tang, D. Davidson
GTE Laboratories Incorporated, Waltham, MA 02154

S. C. Bloch
University of South Florida, Tampa, FL 33620

This paper covers 1978-1979 results with the Tampa Triad which has three baselines - 11, 16 and 20 km long. Reception of the COMSTAR 19-GHz beacon at high elevation angle during two rainy seasons indicates that monthly diversity effectiveness can vary significantly and may be dependent on just one rain event. A preferred baseline emerges for the case of pair diversity. Site-to-site differences within a month tend to improve diversity action even though long-term site attenuation distributions behave similarly. Detailed review of the singular sustained rain event of May 8, 1979 will be given.

CHARACTERIZING THE RAIN MEDIUM

P. H. Wiley and S. C. Ahalt
Virginia Polytechnic Institute and State University
Department of Electrical Engineering
Blacksburg, Virginia 24061

To minimize the effects of rain depolarization on dual polarized satellite links, it is necessary to determine the angles at which linearly polarized receiving antennas should be oriented. These angles are related to those signal polarizations which are coincident to the major and minor axes of the oblate spheroidal raindrop. A knowledge of the effective raindrop canting angle for a specific site should allow the receiving antenna to be oriented in such a way as to minimize rain depolarization.

This paper presents a method by which it should be possible to characterize the effects of the rain medium and determine an effective (or mean) rain drop canting angle. Using data collected from the 19 GHz COMSTAR satellite beacon, a FORTRAN program which implements the mathematical model and calculates Beckmann's complex polarization coefficients, and those polarizations unaltered by the medium has been developed.

DEPOLARIZATION OF THE 28.56 GHz COMSTAR BEACON
SIGNAL BY ICE PARTICLES AT WALLOPS ISLAND, VIRGINIA

Julius Goldhirsh
Applied Physics Laboratory
The Johns Hopkins University
Laurel, Maryland

Cross polarization measurements associated with the COMSTAR beacon signal at 28.56 GHz have been made since January 1979 at Wallops Island, Virginia. These measurements are implemented with a system that employs a Faraday switch at the receiving antenna feed output. By applying current pulses through a coil in the switch, both co- and cross-polarized signal levels are periodically sampled on a continuous basis and recorded on magnetic disk via an HP 9825 minicomputer.

In this paper we examine experimental results pertaining to ice depolarization, i.e., measurements in the absence of rain or during periods of small rain attenuation (<2 dB). Statistics associated with variations in "Isolation Levels" (cross-polarized minus co-polarized signals relative to the co-polarized free space value) are presented. The depolarization signals received by the antenna are assumed to be caused by differential phase shifts through ice crystals in clouds and are presumed therefore to be either "in" or "out of phase" with the residual cross-polarized signal (free space case). The residuals are subtracted out of the cross-polarized levels and statistics associated with the "depolarization signal" for both "in phase" and "out of phase" cases are also presented.

Correlations with radar measurements along the earth-satellite path at S-band are also presented. Some of these measurements are made during periods in which considerable variations in isolations are observed. Preliminary time sequences of reflectivity profiles and RHI's indicate considerable amounts of ice above the zero degree isotherm accompanying the isolation events.

SUMMARY OF 1979 ATTENUATION AND DEPOLARIZATION
MEASUREMENTS MADE WITH THE CTS (11.7 GHz) AND
COMSTAR (19.04 AND 28.56 GHz) BEACONS

E. A. Manus, P. H. Wiley, C. W. Bostian,
W. L. Stutzman, J. R. Dent, R. E. Marshall, and P. Santago
Electrical Engineering Department
Virginia Polytechnic Institute and State University
Blacksburg, Virginia

This paper summarizes attenuation, depolarization, and rain rate data collected during the 1979 calendar year on the CTS and COMSTAR downlinks. It discusses the statistical relationships between attenuation and rain rate and between attenuations measured at different frequencies.

Percent-of-time statistics are presented for 11.7 and 28.56 GHz polarization isolation data taken in 1979 as well as during prior years.

SIMULTANEOUS EARTH-SPACE PROPAGATION MEASUREMENTS
USING THE 28.5 GHZ COMSTAR BEACON AND A 16.5 GHZ
POLARIZATION DIVERSITY RADAR

Y.M.M. Antar, A. Hendry
Division of Electrical Engineering
National Research Council of Canada
Ottawa, Canada, K1A 0R8
J.J. Schlesak, R.L. Olsen, R.C. Bérubé
Communications Research Centre
Department of Communications
Ottawa, Canada, K2H 8S2

There have been few reported experiments involving concurrent radar and satellite-beacon measurements of propagation effects through precipitation. Radar measurements, especially with a dual channel polarization diversity system, provide additional insight into the precipitation structures during different events. This information is of importance to the design of satellite communications systems.

We report here on measurements made at the National Research Council in Ottawa, using the linearly polarized 28.5 GHz Comstar beacon and a Ku-band polarization diversity radar. A specially designed beacon receiver, co-located with the radar, is employed to measure the differential attenuation and phase shift between the linear orthogonal components of the received signal, as well as the co-polar attenuation. The 12-range-gate radar, which is operated in the circular polarization mode, is capable of determining the complex correlation between the returned same-sense and opposite-sense polarizations. The radar reflectivity, cancellation ratio, degree of preferred orientation and frequently the mean orientation angle of the hydrometeors, can be obtained.

Several occurrences of differential phase shift were observed before and after periods of precipitation attenuation. Other depolarization events, showing differential phase shifts exceeding 20° , were observed in the absence of significant rain attenuation. Simultaneous radar observations indicated the presence of high altitude ice particles during these events. There were also several thunderstorms accompanied by severe rain attenuation and by depolarization due to both rain and ice particles. Distinct changes in differential phase shift coincident with lightning were also observed. Satellite beacon receiver and radar data taken during these events as well as analyses of the phenomena involved will be presented.

TUESDAY AFTERNOON
June 3, 1:30 - 5:00

IONOSPHERIC MODIFICATION AND IRREGULARITIES

DKN 2A

Session G.1

Chairman: G. Lyon
University of Western Ontario
London, Ontario

PLASMAPAUSE AND AURORAL OVAL IRREGULARITIES
DURING MAGNETIC STORMS

Zwi Houminer* and Jules Aarons
Air Force Geophysics Laboratory
Hanscom AFB, MA 01731

Eileen MacKenzie
Emmanuel College
Boston, MA 02115

Scintillation observations of VHF and UHF transmissions from geostationary satellites at auroral (Goose Bay, 60° invariant latitude) and subauroral (Sagamore Hill, 53° invariant latitude) stations, show a typical diurnal behaviour of scintillation during magnetic storms. The diurnal variation at Goose Bay has two peaks of scintillation activity. One peak occurs during the afternoon hours on the day of the storm commencement, as well as several days after it. The second peak occurs during the night and is clearly associated with auroral oval electron density irregularities. The Sagamore Hill diurnal pattern exhibits only one peak in scintillation, roughly at midnight.

Examination of the total electron content (TEC) diurnal behaviour during magnetic storms, shows that the afternoon scintillation at Goose Bay as well as the midnight scintillation at Sagamore Hill, occur when the southern wall of the electron density trough, or the plasmopause, passes through the line of sight to the satellite.

Topside ionospheric sounding data from ISIS-2 during the December 1971 magnetic disturbances, taken simultaneously with scintillation observations, indicate a clear relation between the electron density trough and scintillation. The observed double hump nature of the diurnal variation in scintillation at Goose Bay is due to the movement of the trough through the line of sight to the geostationary satellite. Minimum scintillation occurs when the line of sight passes through the trough itself. The trough, then, separates two regimes of electron density irregularities during magnetic storms, auroral oval and plasmopause irregularities.

The scintillations associated with the plasmopause are probably due to magnetospheric heat conduction into the ionosphere during magnetic storms, which produces field-aligned irregularities.

* NRC Senior Research Associate currently on leave from the Radio Observatory, Haifa.

A Case Study of Multi-frequency
Ionospheric Scintillations

C. H. Liu and K. C. Yeh
Department of Electrical Engineering
University of Illinois at Urbana-Champaign

As the multifrequency ionospheric scintillation data accumulate, it becomes feasible to attempt more quantitative comparisons between theoretical predictions and observational results. According to the existing scintillation theory, analytic solutions for the average complex field $\langle u \rangle$ and the mutual coherence function $\Gamma_2 = \langle u_1 u_2^* \rangle$ can be obtained for all levels of scintillation strength, provided that the forward scatter approximation is valid. When compared with the observed phase and amplitude scintillation data, these expressions can be used to yield information about the parameters characterizing the irregularities. These parameters can then be applied to construct a model for the irregularities. Using this model in the propagation code for transionospheric scintillation, other statistical quantities for the complex fields can be computed. The consistency of the model and the validity of the theory can then be checked by comparing the computational results and observational data. Such a study is carried out using data from the DNA Wideband satellite radio beacon experiment.

Preliminary results from the NRL MADRE HF radar
for the HEAO-C launch

by: D.R. Uffelman and J.R. Davis
Naval Research Laboratory
Washington, D.C. 20375
U.S.A.

The NRL MADRE radar which is located on the Chesapeake Bay in Maryland was used to monitor ionospheric modification below the F-region peak due to the launch of the HEAO-C spacecraft on 19 Sept 1979. Preliminary results indicate that a modification in the doppler spectrum of the earth backscatter (clutter) at twice the range of the launch vehicle was observed for a period of at least 7 minutes starting with the ignition of the hydrogen/oxygen launching stage. In addition, a signal was observed which may be an interfering signal reflected into the receiving antenna through the modified region. Spectrum analysis indicates the bandwidth of the unwanted signal was approximately 3 hz and it was observed for approximately 3 minutes commencing about 2 minutes after ignition of the modifying launch vehicle. Doppler shifts of the unwanted signal with time indicate the reflecting region was receding from the receive antenna. Variation of the clutter indicates both approaching and receding components in the modified region.

INTERPRETATION OF BERMUDA POLARIMETRY DATA
FOR THE HEAO-C IONOSPHERIC HOLE

M. H. Reilly
Naval Research Laboratory
Washington, D. C. 20375

Naval Research Laboratory (NRL) measurements in Bermuda of the Faraday rotation of VHF signals from ATS-3 and ATS-5 satellites show large TEC reductions associated with the HEAO-C booster rocket release of H₂O and H₂ in the ionosphere at F-region heights on September 20, 1979. TEC values were calculated from the measured Faraday rotation angles. The inherent baseline ambiguity is partially resolved by detailed comparison with Patrick Air Force Base TEC measurements. In order to quantify the relationship of this data to the dynamics of the ionospheric hole generation, the geometrical orientations of the satellite beacons with respect to the booster rocket trajectory were computed. It was found that the rocket passed as close as 49 km to the ATS-3 ray path at an altitude of 389 km. and as close as 222 km to the ATS-5 ray path at an altitude of 464 km. TEC reductions within the first half-hour of passage of rocket were computed to be about 90% for ATS-3 and 50% for ATS-5. Simple diffusion calculation results are compared with the data for the hole dynamics.

ANALYSIS OF UNUSUAL SIGNAL STRENGTH VARIATIONS OBSERVED IN THE 14 AND 21 MHz BANDS FOLLOWING AN ATLAS-CENTAUR ROCKET LAUNCH: D.B. Odom, N.P. Viens, Raytheon Company, Wayland, Mass. 01778 and J.A. Klobuchar, AFGL (PHP), Hanscom AFB, Mass. 01731

During the early morning hours of September 20, 1979 the ionospheric propagation effects due to the exhaust of an Atlas-Centaur rocket launched from Kennedy Space Center were monitored by over 150 volunteer radio operators from the U.S. and Canada. The signals monitored by the volunteer observers were broadcast from Puerto Rico on frequencies ranging from 3.6 to 21.1 MHz. The objective of this experiment was to determine the spatial extent of the rocket disturbance phenomenon which was strong enough to interrupt the transmissions from Puerto Rico. Approximately 50% of the observations were made on 14.1 MHz, where a two-minute duration power stepped transmission repeated every four minutes was employed. The 21.1 MHz transmissions were monitored during the launch period by 15% of the operators. The 21.1 MHz frequency, in contrast to 14.1 MHz, was on continuously at a fixed power level. 35% of the operators monitored either 3.6 or 7 MHz, where few positive results were obtained. At 14.1 MHz less than 20% of the operators reported any variation in their received signal strength following the launch, possibly because of an interruption in the transmission which occurred at this time. In contrast, at 21.1 MHz, which did not have signal transmission interruption, over 40% of the operators indicated unusual signal strength variations near the time the rocket entered the ionosphere.

HF ray tracing, using observed ionospheric profiles obtained from the Wallops Island ionosonde data collected during launch, indicates that excellent coverage of the launch corridor was available in the eastern half of the U.S. and in parts of southeastern Canada on both 14.1 and 21.1 MHz. The 21.1 MHz frequency placed the ionospheric skip in the region of Georgia, while the tangent ray associated with the greatest one-hop F-region propagation intersected the southern part of Quebec. A family of geographic coverage maps with the associated locations of the volunteer observers and the corresponding designation of quiet and disturbed areas will be shown. The results of the experiment indicate that, although the rocket disturbance phenomenon may be widespread during the nighttime period, the data supporting the existence of a large scale well developed hole in the bottom side of the nighttime ionosphere is not present. The results of the ray tracing and the model of the rocket exhaust induced disturbance which is being used in the analysis will be described.

Recent Ionospheric Modification Experiments
Conducted at Platteville, Colorado

by

C. M. Rush, E. J. Violette, J. C. Carroll, and R. H. Espeland
U. S. Department of Commerce
Institute for Telecommunication Sciences
Boulder, CO 80303

The ionospheric heating facility at Platteville, Colorado, was one of the first facilities to be used to intentionally modify the ionosphere for plasma diagnostic purposes. Numerous efforts conducted in the late 1960's and early 1970's have led to a much increased knowledge about the response of the ionosphere and ionospheric processes to the influence of high power HF radio waves. In recent years, the Platteville Facility has been utilized to modify the ionosphere expressly for the purpose of assessing resultant effects on the performance of selected telecommunications systems.

Detailed investigations centered at Platteville have been undertaken to assess the likelihood of effectively employing high power radio waves to launch HF signals into ionospheric ducts or to recover HF signals that propagate over large distances within ionospheric ducts. These studies are directed toward developing knowledge that can be used to determine the improvement that is afforded by long-distance HF propagation via ionospheric ducts compared to conventional propagation mechanisms. Ionospheric heating centered at Platteville has been used to assess the impact of the operation of the proposed Satellite Power System (SPS) upon the lower ionosphere. Experimental studies that have been undertaken have addressed the performance of ground-based ELF, LF and MF systems and satellite-based VHF systems operating under simulated SPS conditions.

Results from these experiments will be reviewed and interpreted in terms of the existing understanding of ionospheric modification processes.

DETERMINATION OF ELECTRON DENSITY PROFILE
FROM THE RESONANCE SCATTER OF RADIO WAVES
AND THE VERTICAL-INCIDENCE IONOGRAMS

V.V. Belikovich, E.A. Benediktov, G.I. Tyorina,
Radio Research Institute,
Gorky, U S S R
and T.L. Gulyaeva

Institute of Terrestrial Magnetism, Ionosphere and
Radio Wave Propagation, USSR Academy of Sciences,
Troitsk, Moscow Region, U S S R .

This paper describes the results of combined determination of the ionospheric electron density profile using the resonance scattering of radio waves by heater-induced plasma irregularities and the ionograms of vertical-incidence sounding (V.V. Belikovich et al, Geomag. and Aeronomy, 19, 1012-1015, 1979).

Method of resonance scatter is based on generation of artificial periodical irregularities of the ionospheric plasma and resonance scattering of the probing radio waves by these. The exciting and probing transmitters must emit the different modes (ordinary and extraordinary). Varying frequencies of the transmitters and registering virtual height of a signal scattered make it possible to obtain the virtual height versus plasma frequency of the ionosphere for the wide range of the plasma frequencies including the E region and the inter-layer E - F valley (V.V. Belikovich et al, Radiofizika, 21, 1220-1221, 1978).

Using the experimental data obtained at Gorky, a good consistency of results determined by the methods of resonance scatter and the vertical-incidence sounding is shown. Even use of single measurements of the electron density by the resonance scattering technique enables reliability of determining the electron density profile by method of vertical-incidence sounding to be greatly enhanced.

WEDNESDAY MORNING

June 4, 8:30 - 12:00

M. LINDEMAN PHILLIPS MEMORIAL SESSION
ON IONOSONDE TECHNIQUES

DKN 2E

Session G.2

Chairman: K. Toman
NOAA
Boulder, CO

AUTOMATIC PROCESSING OF DIGITAL IONOGRAMS

Bodo W. Reinisch, University of Lowell, Center for
Atmospheric Research, 450 Aiken Street,
Lowell, Massachusetts 01854

Digisonde ionograms are processed on-line or off-line in a variety of ways dependent on the content of the ionogram data. Automatic scaling of ionospheric parameters like foF2, MUF(3000) and hmin has been performed on some 1000 ionograms and it was shown that the scaling algorithm works fairly well even under disturbed ionospheric conditions. An important prerequisite for a reliable foF2 determination was the o and x flagging of the echoes in the Digisonde recording. The MUF(3000) is relatively easy to find by simply converting the vertical into an oblique ionogram. This is achieved by multiplying the frequency coordinate of the echo trace by $M(h')$ the transmission factor which is deduced from the URSI MUF(3000) curves.

Conversion of the $h'(f)$ trace into the vertical electron density profile is performed in the microcomputer unit of the Digisonde. The conversion algorithm is based on the lamination technique for a monotonous profile assuming that $z(fn)$, i.e. height as function of plasma frequency, is continuous and steady at the slab transitions and that the second derivative of z with respect to fn is constant within each slab. The technique was successfully applied in 1978 during an equatorial spread F observation program in Kwajalein, M.I. The algorithm also determines the scale length at the bottomside of the F layer.

Methods for display and analysis of digital ionosonde data.

The 'Dopplionogram'

J.W. Wright & M.L.V. Pitteway
U.S. Department of Commerce
NOAA/Environmental Research Labs.
Boulder, Colorado 80303

A system for the analysis of tape-recorded digital ionosonde data is described. It is applicable to measurements made by instruments which follow the Dynasonde concepts of: (a) flexibly-programmed data acquisition patterns; (b) an adequate description of each echo in terms of time-of-arrival, phase angle and amplitude (or complex amplitude), together with their spatial, temporal, and frequency dependencies. In particular, we describe the 'dopplionogram' obtained from the Dynasonde B-mode of data acquisition, in which the time-rate of change of echo phase (doppler) is expressed in a full ionogram format. Effects of dynamic activity are particularly evident.

NEW DATA PROCESSING ROUTINES FOR THE DIGITAL NOAA IONOSONDE

A.K. Paul
U.S. Department of Commerce
NOAA - ERL
Boulder, Colorado 80303 U.S.A.

The new ionosonde in a typical mode of operation with 4 receiving antenna provides the possibilities for new data processing routines like doppler profile estimates, ordinary and extraordinary echo discrimination and separation, computation of critical frequencies and M(3000) etc. Those methods will be outlined and some first results will be presented.

FIRST RESULTS FROM THE NOAA HF RADAR

F. T. Berkey, J. R. Doupnik and G. S. Stiles
Center for Atmospheric and Space Sciences
Utah State University
Logan, Utah 84322

A newly developed, minicomputer controlled HF radar system has been operational at Logan, Utah since July 1979. The instrument was designed and constructed at the Space Environment Laboratory of the National Oceanic and Atmospheric Administration in Boulder, Colorado and was described in detail at the Helsinki URSI meeting by R. N. Grubb. The radar will be permanently located at Siple Station, Antarctica (after a period at Roberval, Quebec) for extensive co-operative experiments in high latitude ionospheric and magnetospheric physics.

The purpose of our presentation is to demonstrate the versatility of the instrument; we will discuss a number of examples which illustrate its various operating configurations. In the ionosonde mode the amplitude, phase and group delays of the returned echo are measured, enabling us to derive the direction of arrival and the polarization of the echo, in addition to the virtual height information.

Operating in the kinesonde mode, transmissions can be made on up to 10 individual frequencies in the range 0.1 - 30 MHz. If the frequencies are carefully chosen then it becomes possible to monitor various wave propagation modes in the 100-700 km regime using Doppler techniques. We are presently using a travelling wave antenna 100 meters in length for transmitting, and four spaced 10 meter dipoles for receiving. We will conclude with a discussion of the application of these techniques to our long range scientific goals.

Commission G
IONOGRAM SCALING ALGORITHMHarvey Waldman
RCA Laboratories
David Sarnoff Research Center
Princeton, New Jersey 08540H. R. Mathwich
RCA Astro Electronics
Princeton, New Jersey 08540

The present method of manual topside ionogram analysis or scaling requires a high degree of skilled operator effort and is slow and costly. New sounding systems under development are expected to transmit ionograms at a high rate. Ionosondes in low altitude satellites may be obtained separated by as low as 1° of latitude or approximately every 17 seconds.

Topside ionograms present several unique problems to scaling. In addition to the desired reflection trace (usually the X-trace), ionograms contain other traces (the Z- and O-traces), ionospheric resonances and earth interference. The start of the X-trace may range from 1 to 6 MHz, while, f_{x2} may range from 2 to 20 MHz. The presence of these other features presents a confusing and formidable problem to an automated scaling process. A chief task of the algorithm must be to separate the X-trace from these other features. One favorable factor, however, is that the shape of the X-trace usually falls into one or two main types. The scaling algorithm discussed in this paper removes Z-trace data, all of the resonances except for harmonics of f_H and the low frequency portion of the O-trace by estimating the minimum frequency on the X-trace from the resonance data. It then iteratively approximates the X-trace. The first iteration provides a very rough approximation to the trace and allows the algorithm to remove only a few points that can positively be identified as not belonging to the X-trace. Successive iterations improve this approximation. The final set of confirmed X-trace points are fit to a curve by regression. This process results in a smooth curve that describes the X-trace.

Many types of ionograms are obtained by sounding systems. They range from ionograms having well defined traces, easily scalable, to those that are highly obscured and difficult to scale manually. It is expected that the automatic scaling process will be successful on as low as 10 to as high as 90% of ionograms depending on the region of the earth sampled.

In addition to a discussion of the scaling algorithm, a comparison between automated scaling results and that obtained by skilled human operators will be presented using sample ISIS ionograms.

A COMPUTER BASED IONOSPHERIC SOUNDING AND H.F. NOISE
MEASURING SYSTEM

Dr. G.F. Earl
Defence Research Centre, Salisbury,
South Australia, Australia, 5091

A system for the automated collection of ionospheric backscatter sounding and H.F. noise measurement data will be described. The system is configured around a PDP 11/40 minicomputer and modified Barry Research FMCW sounding equipment. The real time digital signal processing associated with the backscatter sounder and noise measurement systems will be presented, as well as a discussion of off-line processing for the suppression of RFI in backscatter ionograms. The data are displayed and recorded in a calibrated mode, and examples will be presented. Deficiencies noted in the operation of the system, and plans for the introduction of oblique and vertical incidence sounding will conclude the presentation.

PERFORMANCE MEASURES FOR AN AUTOMATED SOUNDER SYSTEM

Roger L. Merk
Naval Ocean Systems Center
San Diego, CA 92152

Renewed interest by the Navy in the HF Radio Band has raised questions about the utility an HF Sounder System as part of the new systems of the 1980 and 1990 decades. The signal transmitted by this HF Sounder System is essentially a channel probe meant to characterize the ionospheric path. The received signals contain information about path losses, time delays and frequency dispersion. From these basic parameters one can construct a channel model that can be used to estimate communication performance for any HF circuit.

Three performance measures for this HF Sounder System are evaluated: (1) the probability of detection; (2) the probability of false alarm; and (3) the timing resolution. The evaluation begins by describing a model of the Sounder receiver and a "list of L" detection algorithm. It is shown that a detection threshold set at the rms plus 6 dB noise level produces too high a false alarm rate. A threshold level of at least 3σ is required and an equivalent probability of detection of 0.99 requires a 13.6dB signal-to-noise ratio. Since the rms value of the noise must be estimated using samples, the error in this estimate is related to window durations. A window duration of less than 3 milliseconds will degrade receiver performance below acceptable levels. The timing resolution of the peak amplitude of an arriving signal is ± 20 microseconds. This resolution, determined by the sampling rate, can be significantly improved with signal processing. For example, the peak of a 20 dB signal theoretically can be resolved within ± 4 microseconds.

WEDNESDAY AFTERNOON

June 4, 1:30 - 5:00

IONOGRAM INTERPRETATIONS, IONOSPHERIC
DRIFTS, AND DISPERSION

DKN 2A

Session G.3

Chairman: K. Davies
NOAA
Boulder, CO

GRAVITY WAVE EFFECTS OBSERVABLE WITH MODERN IONOSONDES

J.E. Titheridge

Space Environment Laboratory, NOAA, Boulder, CO. 80303
(On leave from the Radio Research Center, University of
Auckland, New Zealand)

In a horizontally irregular ionosphere, ionosonde signals deviate from the vertical to avoid regions of decreased electron density. Thus standard ionosondes considerably underestimate the ionospheric changes produced by acoustic-gravity waves. With modern instruments the angle of arrival of the echoes can be measured. Extrapolation of this direction does not, however, give the true position of the reflection point. Additional refraction occurs in the ionosphere, and lateral magneto-ionic deviation of the ray path must also be considered. The latter effect is typically 5 to 50 km, and may be sufficient to shift the reflection point from the trough to the peak of a disturbance.

Accurate ray tracing calculations, with 3-dimensional ray-paths in an arbitrarily disturbed ionosphere, have been carried out to evaluate the observable effects of atmospheric waves. Results are needed for different latitudes and ionospheric conditions, and for different phase and amplitude variations in the atmospheric wave. This becomes manageable by using high order prediction/correction ray-path integration, and a procedure which does not require iteration to find rays which return to the receiver.

Results show that height variations in the phase and amplitude of the atmospheric wave are the main cause of profile distortions. Thus a wave amplitude of 8 km, with a vertical wavelength of 200 km, can alter the height of peak electron density by 100 km. Changes deduced from the corresponding virtual height curve, assuming vertical propagation, are much less. Increased accuracy is obtained by using observations of the change in phase or in arrival angle. The period and direction of propagation of a disturbance are most readily obtained from the fluctuations in arrival angle, with some correction for lateral variations caused by magneto-ionic deviation.

LEAST-SQUARES CALCULATION OF N(h) PROFILES

J.E. Titheridge

Space Environment Laboratory, NOAA, Boulder, CO. 80303
(On leave from the Radio Research Center, University of
Auckland, New Zealand)

Current methods of ionogram analysis use only the ordinary ray echo, for the main profile calculation. This discards up to half of the available information, and can be a serious limitation with digitally-acquired data where the higher of two nearby echoes may not be recorded. Profiles are calculated as discrete steps between scaled frequencies. This can give a slightly disjointed result if scaling intervals are too large or ill-chosen. Use of too many data points, with finite errors, gives spurious, small-scale structure in the profile. Manual pre-smoothing of the data has been used to reduce this jitter, but is not acceptable for routine work.

With least squares techniques the amount of profile detail is specified independently of the number of data points. This eliminates jitter. All available data is incorporated in a single one-pass analysis. Where a change from one ray component to the other occurs, spurious discontinuities are appreciably suppressed by use of a tapered weighting function. This also prevents sudden changes due to erroneous data points. A slight extension to current programs could detect and discard bad data before it had any effect on the result. Real-height data can also be incorporated directly, with any desired weight. This should be valuable for obtaining good time-sequences from ionograms of variable quality. Calculated profiles can be adjusted to agree with known real heights, or to have other physically-desirable features. Such constraints are imposed (or removed) with any desired degree of rigour, and with negligible increase in computing time.

Dynasonde Studied of Chemical Depletion of the Ionosphere

J.W. Wright and M.L.V. Pitteway
U.S. Department of Commerce
NOAA
Environmental Research Laboratories
Boulder, CO 80303

Two rocket-borne releases of H_2O in the evening F region were accomplished by the Los Alamos Scientific Laboratory at Kauai, Hawaii in Sept. 1977. Among other diagnostics, the prototype Dynasonde operated near by throughout the experiments. Characteristic ionogram signatures of ray paths within the depletion were observed in both cases. A ray-tracing synthesis permits matching model parameters (and their time dependence) to the digital ionograms and to the observed echo arrival directions.

GRAVITY WAVES PROPAGATION AT E-REGION

A.E.Giraldez ,LIARA,Av.Libertador 327,
Vte Lopez (Bs As) ARGENTINA

Travelling Ionospheric Disturbances monitored by a chain of ionospheric stations covering a 3200Km North-South path,are studied,with special emphasis on E-Region effects.Results show that at E-Region Wind Pattern Disturbances introduced by gravity waves affects Sporadic-E layers electron density as spected according with Wind Shear theory. Results indicate that gravity waves spectrum is discrete in nature,with a few allowed frequency modes.Allowed frequency bands seems not to be fixed by ionospheric parameters,but to depend on latitudinal source location and movement.

Millstone Hill Incoherent Scatter Observations of the Auroral Ionosphere*

J. V. Evans, J. M. Holt, W. L. Oliver and R. H. Wand

Lincoln Laboratory M.I.T. Lexington MA 02173

The Millstone Hill radar, Westford, Massachusetts ($\Lambda = 56^\circ$) has been upgraded for observations in support of the International Magnetosphere Study (IMS) by means of the addition of a 150 ft. diameter fully-steerable antenna. This antenna allows measurements of the F-region properties at auroral latitudes using the existing UHF (68 cm wavelength) radar. The paper describes attempts to measure the electron density and electric field in the auroral zone which commenced in January 1978. This effort entailed making observations to the north of Millstone at very low elevation angles over periods of >24 hours. To secure estimates of both the E-W and the N-S components of the drifts, measurements were made initially in two directions separated by $\pm 15^\circ$ from the magnetic meridian, and (to achieve the desired coverage in latitude) at two elevation angles for each of these azimuths. The separation in time and space of the two components of the drift that are observed introduces a difficulty in interpreting the results. This was overcome by matching the observations, in a least mean squares sense, by analytical functions describing the components of the electric field, each of which has 102 degrees of freedom. The results obtained thus represent the variation of the auroral electric fields over 24 hours local time smoothed both with respect to latitude and time. By May 1978 the technique had been developed to the point where it was possible to secure useful results over the interval $60^\circ < \Lambda < 75^\circ$ and eleven maps, obtained during the period May - December 1978 during moderately quiet periods, have been studied in some detail. Commencing in January 1979 a new method of making these observations was introduced in which the antenna is moved back and forth through an azimuth sector centered on the magnetic meridian alternately being fixed at one of two elevations. This "windshield wiper" mode offers the capability of constructing a map of the electron density and electric fields within the field of view of the radar in about 30 minutes and updating this every subsequent 30 minutes. In this way it is hoped it will be possible to separate U.T. and L.T. variations, albeit still with limited temporal resolution. To illustrate the method we present results obtained during the February 26, 1979, total solar eclipse. On this day the Millstone Hill incoherent scatter radar was operated in the continuous scanning mode, with the radar elevation fixed at 4° and the azimuth swept continuously from 299° to 349° . The path of totality crossed the center of the region swept by the radar beam. Electric field components have been extracted from the radar line-of-sight component of the ion drift by assuming that the electric field may be represented in terms of a quasi-static two-dimensional electrostatic potential with the potential assumed constant along geomagnetic field lines. The resulting time dependent field pattern is characterized by much larger electric fields than usually are observed from Millstone during the day.

*This work was supported by the Atmospheric Science Section of the National Science Foundation under Grants ATM75-02579, ATM75-22193 and ATM79-09189.

TIME SPREADING OF TRANSIENT PULSES BY THE IONOSPHERE

Robert E. McIntosh, Department of Electrical and Computer Engineering, University of Massachusetts, Amherst, MA 01003

Interest in pulse distortion by the ionosphere originated with early telegraph and ionospheric sounding work and continues with the development of sophisticated radar, HF and microwave transionospheric communications systems and the study of EMP phenomenology. In this paper we summarize various aspects of ionospheric pulse dispersion and attempt to define limitations to our current understanding. In doing so, we discuss the transmission and reflection of impulse signals, carrier pulses and frequency-modulated pulses by the ionosphere. We review the contributions of investigators who have considered separately the effects of intrinsic plasma dispersion, geomagnetic field effects and refractive and diffractive (random) multipath. We conclude that the time duration of transmitted pulses is most seriously affected by diffractive multipath effects.

WEDNESDAY MORNING
June 4, 8:30 - 12:00

MEASUREMENTS OF MAGNETOSPHERIC AND SPACE PLASMAS:
PROBES, VLF AND HF

DKN 1E

Session H.1

Chairman: R.W. Fredricks
TRW
Redondo Beach, CA.

THE WISP/HF SYSTEM FOR SPACELAB

H.G. James
Communications Research Centre
Department of Communications
Ottawa, Ontario K2H 8S2 Canada

The National Research Council of Canada has proposed to supply to NASA the High-Frequency (HF) component of the WISP (Waves in Space Plasmas) system, to be used for radio experiments on Shuttle/Spacelab missions. This equipment will generate, receive and process radio signals in the 0.3 to 30 MHz range, and thereby permit the study of injection, propagation and detection of electromagnetic and electrostatic waves in the ionospheric plasma.

The WISP/HF system will be designed to accept a command from an external source and generate signals of variable frequency, intensity and modulation. Transmission frequency and amplitude will be swept, stepped or held constant and will be accurately known. The Orbiter-based system will amplify these signals and actively maximize power transfer to a dipole whose length can be varied up to 300 m tip-to-tip and which will be shared with an external Very-Low-Frequency transmitter. When perfect matching between the output amplifier and the antenna is obtained, the system will deliver about 0.5 kW of pulse power. A receiver is required for most experiments; the frequency, gain and bandwidth settings of reception will be variable and accurately known. Phase-coherent transmission and reception will be employed for Doppler measurements. The equipment will possess its own controller for storing measurement routines and coordinating all functions of the system. The controller will also process housekeeping and received signal data and will transfer internal data of all types to its information output. Real-time commands will be initiated either by the Shuttle Payload Specialist in the Orbiter or by scientific personnel in the Payload Operations Control Center on the ground.

Many innovative plasma experiments will be possible with the WISP/HF system. Cooperative procedures with direct-measurement probes mounted on the Remote Manipulator System should provide understanding about the plasma near an active antenna. Experiments will be carried out on the basic properties of electrostatic waves over moderate distances between the Orbiter-based transmitter and the receiver on a subsatellite (Remote Plasma Diagnostics Package). Over large distances, the system will be used to perform phase-coherent or coded-pulse measurements on ionospherically reflected signals, and this will constitute a considerable improvement in the technique of remote sounding. By virtue of simultaneous operation of other plasma-related instruments on the same flight, such as the ion and electron guns (SEPAC) or the Chemical Release Module, the possibilities for interesting experiments with the WISP/HF are very promising.

IONOSPHERIC WAVE MEASUREMENTS WITH
SATELLITE-BORNE CROSS-POWER SPECTRUM ANALYZERS

K. J. Harker and F. W. Crawford
Institute for Plasma Research
Stanford University
Stanford, California 94305

It is known that the wave spectrum of the fluctuations in a plasma can be measured in the following fashion. The signals from two probes placed in the plasma a certain distance apart are passed through a cross-power spectrum analyzer. The output of the spectrum analyzer, the cross-power spectral density, is recorded as a function of frequency. This procedure is repeated for a series of probe separations. The cross-power spectra are then spatially Fourier-transformed with the aid of a digital computer to obtain the wave spectrum as a function of wave number and frequency.

It has been suggested that this technique can be applied to the ionosphere by placing a cross-power spectrum analyzer on an orbiting satellite. The usefulness of this measurement stems not only from the importance of measuring the wave spectrum in space in its own right, but also from the fact that one can determine from it also the macroscopic characteristics of the surrounding plasma. This method can be considered as an *in situ* alternative to measuring the wave spectrum in the ionosphere by the incoherent scatter technique.

In this paper we assess the feasibility of using this technique in the ionosphere by determining the integration time required to make the measurement. The theory considers in particular spherical probes biased into the electron saturation region. The method consists in assuming an equilibrium plasma wave spectrum, from which the power spectrum directed to each spherical probe and the available power at the amplifier input are determined. Using statistical theory, this information is used to determine the integration time needed to measure the cross-power spectral density at the output terminals of the cross-power spectrum analyzer to a specified accuracy. For typical experimental conditions the integration times are found to increase from 0.1 s to 1000 s as the probe spacing increases from 2 Debye wavelengths to 10 for ion wave frequencies. For electron plasma wave frequencies the corresponding increase is from 10 s to 10^4 s. This implies that single-channel operation will be severely limited.

RADIATION EFFICIENCY AND PATTERN OF A VLF
ELECTRIC DIPOLE ANTENNA IN THE MAGNETOSPHERE
U. S. Inan and T. F. Bell, Radioscience
Laboratory, Stanford University, Stanford,
California 94305

A variable length VLF electric dipole antenna in the magnetosphere is considered. Such an antenna would be an important part of VLF transmitters to be placed on the space shuttle for studying wave-particle interactions and wave propagation in the magnetosphere and the ionosphere.

The Power integral method (T. N. C. Wang and T. F. Bell, J. Geophys. Res., 77(7), 1174-1189, 1972) is used in the presence of multiple ion species to calculate the VLF whistler mode radiation resistance and the large scale radiation pattern for various values of frequency, antenna orientation, plasma composition, density and static magnetic field. The effects of the ion sheath formed around the antenna are separately accounted for and a circuit model of the antenna terminal impedance is developed. Radiation efficiencies calculated on the basis of this model show that the dipole antenna would be very efficient (> 30%) for certain ranges of the parameter values.

Our results show that relatively small sized (< 1 km) radiating structures can be used to generate whistler mode waves of intensities that are required for triggering strong non-linear wave-particle interactions in the magnetosphere.

A Numerical Study of Satellite Reception
of VLF Signals Using Waveguide Concepts

Richard A. Pappert, W. F. Moler,
and J. A. Ferguson
EM Propagation Division
Naval Ocean Systems Center
San Diego, CA 92152

Full wave methods and waveguide concepts are used to calculate the nighttime 17.8 kHz radio fields along the 40°W parallel of longitude at 500 km altitude. The fields are generated by the ground based transmitter at Cutler, Maine. The results are compared with data obtained by the OGO-4 satellite and with results of Souza and Scarabucci which were calculated using other methods. Waveguide leakage accounts for general features of measurements made in the northern geomagnetic hemisphere. Measurements made in the southern geomagnetic hemisphere suggest that those fields can be estimated by assuming lossless whistler mode propagation of waveguide leakage fields at the geomagnetic conjugate.

THE METROLOGY OF LINEAR RANDOM
WAVE FIELDS IN SPACE PLASMAS (invited)

L.R.O. STOREY

Centre National de la Recherche Scientifique
Centre de Recherches en Physique de l'Environnement
45045 Orléans, France

This paper reviews the information that can be got from direct measurements of the linear random fields of natural plasma waves in space, and explains how the experimental data should be acquired and analysed. The starting-point is the related theoretical problem of finding the simplest complete statistical description of the field. The answers to these questions are different for electromagnetic (EM) and for electrostatic (ES) waves. Linear random EM wave fields are described by a pair of *wave distribution functions*, one for each of the two wave modes. These functions can be estimated from the cross-spectral matrix of multi-component electric and magnetic field measurements at a single point ; they contain information about the origin and propagation of the waves. Linear random ES wave fields are described by a set of *particle distribution functions*, one for each of the charged particle species in presence. These functions can be estimated from the cross-spectrum of two-point measurements of a single electric field component ; they provide full information about the local state of the plasma. In both cases, the analysis of the data to estimate the relevant distribution function involves an inverse problem with a constraint of positivity.

PRELIMINARY RESULTS FROM CONTROLLED VLF EXPERIMENTS IN THE MAGNETOSPHERE USING THE NEW TRANSMITTER AT SIPLE STATION, ANTARCTICA
R. A. Helliwell, J. P. Katsufarakis, D. L. Carpenter,
U. S. Inan, T. F. Bell, and T. R. Miller,
Radioscience Laboratory, Stanford University,
Stanford, Calif. 94305

New nonlinear effects have been observed in the magnetosphere in controlled experiments using VLF waves injected from Siple Station, Antarctica. Prior controlled experiments were limited to frequency modulation only, in 10 ms wave train segments. With the new transmitter both AM and FM are available in 1 ms wave train segments for each of two frequency synthesizers. Examples of new findings are:

- (1) Wide ranging frequency ramps showed signal growth and emission triggering over a limited band of frequencies. For ramp slopes exceeding 0.5 kHz/s no triggered emissions were seen. The upper cutoff frequency was significantly higher (by ~300 Hz) for positive ramps than for negative ramps of the same slope.
 - (2) Two signals spaced 5 Hz in frequency showed amplitude growth between the nulls of the beat and emission triggering at each null.
 - (3) Two converging frequency ramps showed mutual interaction in the form of sidebands at multiples of the difference frequency when the frequency separation was less than ~60 Hz, thus providing a new measurement of the 'coherence' bandwidth.
 - (4) Satellite observations have shown that wave-particle interactions involving nonducted waves can also result in amplification and VLF emission triggering and that the spectral characteristics of these emissions can be different from those triggered by ducted waves.
- Spectrographic examples of these results will be presented.

WHISTLER-MODE SIDEBAND GENERATION IN
THE MAGNETOSPHERE

C. G. Park, Radioscience Laboratory,
Stanford University, Stanford, CA
94305

A VLF transmitter at Siple, Antarctica ($L \sim 4$) and a receiver at the conjugate station, Roberval, Quebec, are used to investigate sideband generation in the magnetosphere. The results show that sideband generation is a fairly common phenomenon, with the frequency separation ranging from ~ 2 Hz to ~ 50 Hz (carrier frequency = ~ 2 kHz to 5 kHz). The sideband intensity is quite variable and occasionally exceeds the carrier intensity. Multiple pairs of symmetric sidebands may appear, but their frequency separations from the carrier are not always harmonically related. The lower sidebands are usually weaker than upper sidebands, sometimes falling below the threshold of detection. Sideband structures may turn on and off suddenly without changing their frequency. This can occur at remarkably regular intervals (~ 0.5 second period). Finally, the sideband frequency does not depend on the carrier amplitude. Several theories on whistler-mode sideband generation will be reviewed in light of the above experimental results.

VLF ELECTROMAGNETIC WAVE DISTRIBUTION FUNCTIONS
IN THE MAGNETOSPHERE

F. Lefeuvre

Radioscience Laboratory, Stanford University,
Stanford, California 94305, USACentre de Recherches en Physique de l'Environnement,
Avenue de la Recherches Scientifique, Orleans, 45100, FRANCE

VLF electromagnetic fields observed onboard GEOS are assumed to be random. They are considered as being composed of a continuum of superimposed plane waves of different frequencies and propagating in different directions. They are characterized by a function called the Wave Distribution Function (WDF) which specifies, in any narrow band frequencies, how the wave energy is distributed with respect to the direction of propagation $\vec{k} = \vec{k}/|\vec{k}|$, \vec{k} being the wave number vector (L. R. O. Storey and F. Lefeuvre, *Geophys. J. R. Astr. Soc.*, 56, 255-269, 1979). WDFs are estimated from the continuous measurement of the three magnetic and of one or several electric components of the field. Typical WDFs encountered in the magnetosphere, at the GEOS-1 orbit, are presented. When the plane wave approximation can be considered as valid, they are compared to the wave normal direction \vec{k} calculated from classical methods. The emphasis is put on the two-peak WDFs, very often observed in that particular experiment, and on the new insight it yields into the problem of wave-particle interaction.

OBSERVATION OF POLAR VLF EMISSION OBSERVED
BY SEMI-POLAR ORBITAL SATELLITE "KYOKKO"

Takeo Yoshino, Takashi Shibata and Kazuyuki Nakagawa
University of Electro-Communications,
Chofu-shi, Tokyo 182, Japan.

The IMS contributed satellite EXOS-A "KYOKKO" was launched into a semi-polar orbit from Kagoshima Space Center on February 4, 1978. The telemetry data reception of polar VLF emission detector which on boarded as one of the payload, have started at Syowa Station by the 19th Japanese Antarctic Research Expedition Party since two days after launch. The orbit of the polar orbital Ionospheric Sounding Satellite ISIS-1 and 2, and the semi-polar orbital Scientific Satellite EXOS-A "KYOKKO" was always intersected each other on a perpendicular lines at the coast region of Antarctic Continent. The latitudinal characteristics of polar VLF emission data have obtained from ISIS-1 and 2, and the longitudinal characteristics have obtained from EXOS-A "KYOKKO". The simultaneously observation of polar VLF emission distribution between ISIS-1 or 2 and EXOS-A "KYOKKO" at Antarctica have been able to obtain the variation data of the location and the size of auroral oval at every magnetic local time and Kp index variations.

Our results shows that the distribution pattern of polar VLF hiss and saucer emission in summer and winter at the polar cap region gives a very good agreement between the expansion of location and size of the auroral oval and the variation of Kp index value.

WEDNESDAY AFTERNOON

June 4, 1:30 - 5:00

PLASMA RELATED THEORETICAL STUDIES

DKN 2D

Session H.2

Chairman: R. Gagné
Université Laval
Québec, Québec

BOUNDARY CONDITIONS AND ANTENNA MODELS
IN A WARM ISOTROPIC PLASMA

N. SINGH, Physics Department, Utah State University,
Logan, Utah 84321, USA

The electron-transparent and electron-reflecting models of antennas in a warm isotropic plasma are reexamined. It is shown that a purely electrical treatment of both the models without an explicit use of the boundary condition on electron velocity yields the same results as previously obtained through an electro-mechanical treatment. The essential difference between the two models is that for the electron-reflecting model fields are non-zero only in the exterior region while for the electron-transparent one they are non-zero both in the exterior and interior regions of the antenna. This distinction helps in clarifying some misconceptions about these models of antennas in warm isotropic plasma.

ELECTRON TEMPERATURE DERIVED FROM INCOHERENT SCATTER
RADAR OBSERVATIONS OF THE PLASMA LINE FREQUENCY.

Tor Hagfors
Department of Electrical Engineering
Norwegian Institute of Technology
N-7034 Trondheim-NTH, Norway

M. Lehtinen
EISCAT Scientific Association
Geophysical Observatory
SF-99600 Sodankylä, Finland

Most of the information derived by incoherent scatter radar (ISR) comes from careful study of the ion-acoustic part of the fluctuation spectrum. In many cases it is advantageous to be able to fix one or more of the parameters derived from the ion line, either in order to establish a greater number of parameters or in order to increase the accuracy.

One possible way of establishing one of the parameters by independent means is to observe that the frequency of the plasma line is dependent on the product $(k \cdot D)^2$, D being the Debye length and k being the wave vector of the plasma wave giving rise to the plasma line scattering. Since D^2 is directly proportional to the electron temperature it will be possible to derive this temperature provided the same plasma volume can be observed at the same time with different values of k .

For a non-magnetized plasma it is easy to show that the necessary range of k -values can be achieved either by simultaneous monostatic and bistatic observations, or by simultaneous backscatter observations at two different transmitter frequencies. When the magnetic field is taken into account complications arise particularly when the electron gyro-radius becomes comparable with the Debye length. Nevertheless, the method should be quite useful provided the correct theory is applied for the interpretation of the data.

We show in turns of several worked examples what frequency separations to expect for different geometries and ionospheric parameters.

It appears conceivable that an extension of the method can be applied to the detection of possible anisotropies in the thermal electron velocity distribution ($T_{e||} \neq T_{e\perp}$).

PROPAGATION IN A GYROMAGNETOELECTRIC MEDIUM

Paul R. McIsaac
 School of Electrical Engineering
 Phillips Hall
 Cornell University
 Ithaca, NY 14853

The electromagnetic properties of a fluid composed of molecules possessing both an electric and a magnetic dipole moment are discussed. The model assumes that each molecule's angular momentum, magnetic moment and electric moment are co-linear. It is well-known that such a medium cannot exhibit a direct magnetoelectric effect (T. H. O'Dell, The Electrodynamics of Magneto-electric Media. Amsterdam: North-Holland, 1970). It is shown here that if co-linear dc electric and magnetic fields, E_0 and H_0 , are applied, then the medium will exhibit an ac gyromagnetoelectric effect.

The four ac susceptibility dyadics, χ_{ee} , χ_{mm} , $\chi_{me} = \chi_{em}$, are derived, and their relation to the fluid parameters explored. It is found that each ac susceptibility has two resonant frequencies. If either E_0 or H_0 is zero, then only a single resonant frequency is obtained, and the ac magnetoelectric effect is lost ($\chi_{me} = \chi_{em} = 0$).

Plane wave propagation in the medium is discussed. For a propagation direction making a non-zero angle with the axis of E_0 and H_0 , the fields are elliptically polarized, and the wave is not TEM. There will be two characteristic waves with different dispersion curves. In the general case, the field relations are fairly complex.

The special case of plane wave propagation parallel to the axis of E_0 and H_0 is examined. In this case, the two characteristic waves are TEM CW and CCW circularly polarized waves. Effective scalar susceptibilities are derived for these waves. For one wave, the effective susceptibility has two distinct resonances, while for the other, the effective susceptibility has no resonance. The ω - β diagrams are presented for a particular set of parameters. The first wave has two stopbands determined by the susceptibility resonances, while the second wave has no stopband. Because the characteristic waves are CW and CCW circularly polarized, Faraday rotation can occur in the passband regions. The effective impedances for the CW and CCW waves are also discussed. Relevant to this is the fact that the instantaneous electric and magnetic fields are not oriented orthogonal to each other. Some of the implications of the propagation characteristics for this type of medium are discussed.

COVARIANT FORMULATION OF WAVE-PARTICLE
INTERACTION FOR RELATIVISTIC PLASMAS

A. K. Sinha

Communications Satellite Corporation, Washington, D.C.

Interaction of the electromagnetic wave with a highly energetic or relativistic plasma is involved in many cases of theoretical and practical importance. Such interactions can be studied with the help of coupled Maxwell-Boltzmann equations. While manifestly covariant formulation of Maxwell's field equations is well familiar, a similar representation of the Boltzmann equation seems missing from the literature.

In this paper, the derivation of a manifestly covariant formulation of the Boltzmann equation is presented. Mathematical elegance and simplicity associated with the use of the resulting covariant set of Maxwell-Boltzmann equations for studying a wide range of wave-particle interaction phenomena in the relativistic domain are delineated. Examples of possible applications for theoretical analyses of electromagnetic wave interaction with relativistic plasmas are suggested, including astrophysical problems, parametric amplification, travelling-wave-tubes, and laser-fusion. Further generalization of the results is indicated.

HEATING OF A PLASMA BY A DOUBLE LAYER

N. SINGH, Physics Department, Utah State University,
Logan, Utah 84322, USA
H. THIEMANN, IPW, Freiburg, West Germany

Results from numerical simulations of a double layer in an inhomogeneous plasma are reported. The simulation was carried out over a finite extent of plasma of size $0 \leq x \leq d = 65 \lambda_{d0}$. With a constant potential difference $\varphi(x=d) - \varphi(x=0) = 15 k_B T_{e0}/e$ maintained across it, where k_B is the Boltzmann constant, T_{e0} and λ_{d0} are respectively the electron temperature and Debye length associated with the Maxwellian electrons streaming into the simulation region at $x=0$. The simulation starts at $t=0$ with the region $0 \leq x \leq d$ empty of plasma and with prescribed Maxwellian velocity distribution functions for appropriate free and trapped particles entering the region at $x=0$ and d . A double layer forms within a time of about $600 \omega_{p0}^{-1}$, where ω_{p0} is the electron plasma frequency at $x=0$. The double layer is always found to be anchored at $x=0$. The electrons accelerated by the double layer excite strong oscillations through e-e interactions on the high potential side of the layer. The non-linear evolution of the oscillations shows amplitude modulations, which eventually decay into side bands. It is observed that by the time the modulations begin to develop the velocity distribution functions of the beam and trapped electrons overlap resulting in a strong nearly flat tail to the bulk distribution function. The mechanism leading to the formation of tail is identified to be the resonant and non-resonant acceleration of trapped electrons and resonant deceleration of the beam electrons. The electron distribution functions seen in the simulation are qualitatively similar to those as measured during inverted-V events.

MONDAY MORNING
June 2, 8:30 - 12:00

VERY LONG BASELINE INTERFEROMETRY
DKN 2D

Combined Session J-1/AP-S

Chairman: N.W. Broten
Herzberg Institute of Astrophysics
National Research Council
Ottawa, Ontario

The following paper belongs to the IEEE AP-S Symposium and the summary is included in the IEEE AP-S Digest under Combined Session J.1/AP-S.

6. PHASE SCINTILLATION MEASUREMENT SYSTEM USING REAL TIME VLBI, N. Kawano, F. Takahashi, T. Yoshino, and N. Kawajiri, Kashima Branch, Radio Research Laboratories, Kashimamachi Ibaraki 314, Japan.

CANADIAN LONG BASELINE INTERFEROMETER
D.N. Fort, Herzberg Institute of Astro-
physics, National Research Council of
Canada, 100 Sussex Drive, Ottawa,
Canada K1A 0R6

A description of the present and future state of Canadian LBI hardware including both recording and playback systems is given. Special attention is paid to the new 4 x 4 level digital cross-correlator which has now replaced the analog correlation techniques previously used.

THE PROPOSED CANADIAN VLB ARRAY
T.H. Legg, Herzberg Institute of
Astrophysics, National Research
Council of Canada, 100 Sussex Dr.
Ottawa, Canada K1A 0R6

The proposal put forward by the Canadian Astronomical Society/Société Canadienne d'Astronomie, for a very-long-baseline array of radio telescopes, will be outlined, and the present status of this proposal reported. The value of redundant baselines in forming reliable images will be discussed.

VLBI ARRAY STUDIES

Marshall H. Cohen, California Institute
of Technology, Pasadena, California
91125 U.S.A.

K.I. Kellermann, NRAO, Box 2, Green Bank,
WV 24944, U.S.A.

A new study of a modern array for very-long-baseline interferometry is being undertaken by a group of Caltech and JPL, together with major assistance from many others in the radio astronomy community. Both U.S. and international systems are being considered. The main conclusions will be presented.

THE MARK III VLBI SYSTEM - A WIDEBAND DATA RECORDING AND
PROCESSING SYSTEM FOR VERY-LONG-BASELINE INTERFEROMETRY

A.R. WHITNEY
HAYSTACK OBSERVATORY
WESTFORD, MASS 01886

for the EAST COAST VLBI GROUP

The Mark III system is a digital data recording and processing system for VLBI which has been developed to make, initially, a more than five-fold improvement (compared with the Mark II system) in the sensitivity of VLBI for astrophysical, astrometric, and geophysical applications. The Mark III uses instrumentation tape recorders presently outfitted with 28-track heads; each track is used to record a 2-MHz bandwidth with a longitudinal density of 33,000 bits per inch so that the total recorded bandwidth is 56-MHz. The system is quite flexible in allowing slower record speeds, and the corresponding narrower bandwidths, for operations that do not require the full bandwidth.

Each recorded track is used to record the upper or lower sideband video output from one of the I.F.-to-video converters in the Mark III acquisition terminal. The analog video signals are clipped, sampled and formatted in the same way for each recorder track so that each track can be decoded independently. The Mark III serial data format contains complete time of day, auxiliary data, cyclic-redundancy check bits and parity check bits along with the sampled-video data bits.

The Mark III system has 14 video converters, each with built-in synthesized local oscillators which have a range of 100 to 500 MHz. In the normal wideband-continuum mode all 14 upper and all 14 lower sideband video outputs are used, one going to each recorder channel. Other modes are ones in which fewer tracks are recorded simultaneously if fewer frequency bands are needed. In these modes all the physical tracks on the tape are recorded after many forward and reverse passes of the tape. For example if one 2 MHz bandwidth channel is adequate for a given experiment, 6.5 hours of data can be recorded on one 9600-foot reel of tape by shuttling the tape back and forth while recording one track at a time.

In order to improve the area packing density on the tape there is an ongoing development to increase the number of physical tracks on the tape by using narrower track widths. The number of tracks will be increased to 112 so that the wideband mode (56 MHz bandwidth at 135 inches/sec) can be used for 4 passes of the tape.

The Mark III acquisition is controlled by a built-in minicomputer so that mode changes, tape motion and data logging can be carried out automatically.

THE MARK-III DATA ANALYSIS SYSTEM -
A COMPLETE SYSTEM FOR THE RECOVERY OF GEODETIC AND
ASTROMETRIC INFORMATION FROM VLBI OBSERVATIONS

James W. Ryan for the East Coast VLBI Group
Goddard Space Flight Center

The MARK-III data analysis system is a complete system for the geodetic and astrometric analysis of VLBI observations produced by the MARK-III data acquisition and processing systems. It consists of a series of programs which are linked by the MARK-III Data Base Handler. Among these programs are CALC and SOLVE. CALC computes theoretical VLBI observations and partial derivatives of the observations with respect to various geometric, astrometric, and environmental parameters. It is perhaps the most complete program in existence today for modelling VLBI delay and rate observations. SOLVE is an interactive least squares parameter estimation program specifically designed for the geodetic and astrometric applications of VLBI. It has the capability of combining VLBI data taken on diverse baselines over many years to produce a single regression analysis. The system also provides for various calibrations of VLBI observations. Surface weather and water vapor radiometry data are used to correct for the effects of tropospheric refractions. Dual frequency VLBI observations are used to correct for the effects of ionospheric refraction. Finally, cable calibration measurements are used to account for the effects of the time varying electrical length of the cable carrying timing pulses from the frequency standard on the ground to the receiver on the antenna. Shortly, the use of radio source maps will be included in the system to account for the effects of radio source structure.

The MARK-III data acquisition, processing, and analysis have combined to produce geodetic baseline length estimations with an accuracy of better than 5 centimeters and radio source positions with an accuracy of a few milliseconds of arc.

RADIOMETRIC SYSTEM FOR MEASUREMENT OF
INTEGRATED WATER VAPOR AND LIQUID
ON EARTH-SPACE PATHS

D. C. Hogg and F. O. Guiraud
Environmental Radiometry
Wave Propagation Laboratory
NOAA/Environmental Research Laboratories
Boulder, CO 80303

A dual-channel (21 and 32 GHz) radiometer which measures simultaneously and independently integrated water vapor and cloud liquid on an earth-space path is discussed. Measurements show that the operational stability of the instrument is equivalent to about 0.1 mm of integrated vapor over periods of hours. Calibration of the vapor channel using U. S. National Weather Service radiosondes, and of the liquid channel using absorption of the COMSTAR-C 28 GHz beacon (J. B. Snider et al., Radio Science, January 1980) is emphasized. Examples of measurements of precipitable water vapor and cloud liquid are given. Design of an efficient all-sky coverage radiometric antenna is described. Application of the instrument in providing phase-shift correction for wide-baseline arrays is discussed.

TWO YEARS OF BASELINE COMPONENTS AND EARTH ROTATION PARAMETERS
OBTAINED FROM ANALYSES OF 35-KM INTERFEROMETER OBSERVATIONS
D.D. McCarthy, G.H. Kaplan, F.J. Jostics, W.J. Klepczynski, D.
Matsakis, P. Angerhofer, U.S. Naval Observatory
K.J. Johnston, J.H. Spencer, Naval Research Laboratory

The connected element interferometer of the National Radio Astronomy Observatory in Green Bank, West Virginia has been used by the U.S. Naval Observatory and the Naval Research Laboratory in a joint program to apply radio interferometric techniques to the determination of variations in Earth rotation parameters. Two years of data are now available for a preliminary evaluation. These show that Universal Time and polar coordinates may be obtained in the form of two or three-day averages with an internal precision of about 1 ms for UT and an external precision equal to that currently available from the most precise optical instruments. Comparison with results from the Bureau International de l'Heure (BIH) shows that systematic differences do exist between the two data sets. The nature of these systematic effects is now under investigation. These two years of data indicate that regular radio interferometer observations such as these can be extremely useful in obtaining improved Earth rotation parameters and in understanding the relationship between Earth-fixed reference frames and those defined in space by positions of stars or radio sources.

MONDAY AFTERNOON
June 2, 1:30 - 5:00

RADAR ASTRONOMY

DKN 2D

Session J.2

Chairman: T.W. Thompson
Planetary Science Institute
Pasadena, CA.

PIONEER VENUS RADAR RESULTS: ALTIMETRY AND IMAGING

Peter G. Ford and Gordon H. Pettengill, Dept. of Earth and Planetary Sciences, M.I.T., Cambridge, Mass. 02139; Harold Masursky, Branch of Astrogeologic Studies, U.S. Geological Survey, Flagstaff, Arizona, 86001.

The radar altimeter aboard the Pioneer Venus orbiter spacecraft has yielded a series of maps covering 83% of the planet's surface, much of it inaccessible to Earth-based observations. A topographic map, with a linear resolution of better than 200 km and vertical accuracy of about 200 m, shows extremes of relief (i.e. center-of-mass-to-surface radius) from a low of 6048.5 km to a high of 6062 km. The planetary oblateness is less than 1.5×10^{-4} , and 60% of the total surface lies within 500 m of the modal radius value of 6051.1 km, 20% within 125 m. Highland areas, elevated 2 km or more above the mean radius value of 6051.39 ± 0.10 km, constitute only about 5% of the observed surface.

The radar altimeter also yields a map of the distribution of average surface slopes, at the scale of one meter, in a one to ten degree range, with the same linear resolution and global coverage as the topographic map. Highland areas are generally found to have the higher values of average slope, and, with some exceptions, the spacecraft observations, taken at near vertical incidence, correlate well with Earth-based imaging. Of great interest, and not hitherto observed, are a number of narrow and relatively straight parallel features, extending, in some cases, over more than 1000 km.

Three-station radar images of Venus:
resolution limits and a proposed 1km resolution mapping system

R. F. Jurgens, G. Morris, and R. M. Goldstein
Jet Propulsion Laboratory, Pasadena, California

During the 1978 inferior conjunction of Venus, eight radar images of Venus were made using the 3-station interferometer at the Goldstone deep space tracking facility. These images, having a resolution near 10km, show several new mountains, craters, and irregular ridges. Detailed analysis of the radar system and data reduction algorithms indicate that resolutions approaching 1km are possible for regions within 3° of the subradar point near the time of inferior conjunction. Altimetry maps having accuracies between 30 and 400m are possible within this region, and high quality reflectivity images should be possible within 5° of the subradar point. A radar system having such high resolution capability could be available in time for the 1981-2 inferior conjunction of Venus.

Radar Mapping of Mars at JPL: Plans and Progress

G. S. Downs

Jet Propulsion Laboratory
California Institute of Technology
Pasadena, California 91103

Radar observations are confined to the latitudes between $\pm 25^\circ$, probing approximately 40% of the Martian surface. Efforts to probe the surface by radar necessarily require intense activity during the months bracketing each opposition during the 17 year interval between favorable oppositions. Backscattered power in both circular polarizations, orthogonal to and the same as that transmitted, should be measured. Planetary surfaces are best characterized if the radar observations are made at two or more wavelengths an order of magnitude apart. The end-products are (1) surface elevations, (2) an estimate of root-mean-square (rms) surface slopes, (3) reflectivity, (4) a local estimate the small scale roughness, and (5) a global estimate of the small scale roughness. Latitudes 21°S to 14°S were well covered in one polarization at 12.6 cm wavelength during 1971 and 1973. Considerable analysis of the measured elevations has stimulated much rethinking of the Martian surface (L. Roth, et al. 1980, submitted to Icarus), while good correlations between the scattering parameters and the types of terrain evident in Viking TV images has been found (G. Schaber 1980, submitted to Icarus). Considerable work remains to be done with the scattering data. Partial coverage in the lower latitudes was obtained at 12.6 cm and 3.5 cm during 1975 - 1976. Global scattering in one polarization was measured at 3.5 cm during 1976. Nearly 3/4 of a rotation was obtained at 11°N during 1978 at 3.5 cm. One full rotation near latitude at 22°N is expected for the 1980 opposition, mostly at 12.9 cm wavelength, with some coverage at 3.5 cm. Expansion of the usual range-Doppler observations to the same polarization as that transmitted are expected. Plans for the 1980's include extension of past capabilities, with intensive observations during the oppositions of 1982, 1984 and 1986. An extended season in 1984 with an upgraded 3.5 cm transmitter, to cover low Southern latitudes, is hoped for.

BISTATIC RADAR STUDIES OF PLANETARY SURFACES
R.A. Simpson and G.L. Tyler
Stanford Center for Radar Astronomy, Stanford
University, Durand Bldg., Stanford, CA 94305

Oblique radiowave scattering from planetary surfaces permits study of specular processes at locations inaccessible to earth-based radar as well as under geometrical conditions other than normal incidence. Considerable experience with bistatic radar was obtained on the moon using transmitters aboard Explorer 35 ($\lambda = 2.2\text{m}$), Luna 11 (and subsequent spacecraft in that series at $\lambda = 1.7\text{m}$), and the Apollo command modules ($\lambda = 13$ and 116 cm). A wavelength dependence in scattering was observed, while various geologic provinces were shown to exhibit different behaviors - highlands typically appeared 2-4 times as rough as maria. More recently, Soviet investigators have applied bistatic radar to Venus, inferring surface roughness (and less directly) large scale topography. Our own early examination of Viking bistatic radar data from the Hellas Basin on Mars showed it to have roughness and dielectric constant properties similar to Chryse Planitia (site of Viking Lander 1) and to lunar maria. More recent examination of data acquired in the north polar region suggests surface morphologies as diverse as those encountered near the equator in earth-based radar studies - surface roughness changes of 10 to 1 and complex reflectivity behavior have been observed.

OUTER-SOLAR-SYSTEM RADAR ASTRONOMY: 1979 RESULTS

Steven J. Ostro
National Astronomy and Ionosphere Center
Cornell University
Ithaca, New York 14853

Observations made with the Arecibo Observatory's S-band (12.6-cm-wavelength) radar system during the past year have yielded important results for bodies in the outer solar system.

Minor planet 4 Vesta was detected in November 1979. Preliminary analyses of data indicate a normalized radar cross section: $\hat{\sigma}_{OC} = 0.23 \pm 0.07$ for at least one side of the target, considerably larger than the value, 0.04 ± 0.01 , determined for another main-belt asteroid, 1 Ceres.

Observations of the outer three (icy) Galilean satellites since 1976 have yielded weighted-mean values of critical 12.6-cm properties averaged over the entire surface of each target. Europa and Ganymede have nearly identical circular-polarization properties, while Callisto and Ganymede are indistinguishable in terms of roughness (i.e., scattering laws). Several albedo and/or polarization features are prominent in some spectra and are being correlated with Voyager images. Each satellite is more limb-darkened (i.e., smoother) in the "OC" sense of circular polarization than the "SC" sense. The strongest detection to date of Io suggests a Lambert scattering law, contrary to previous impressions. Results of observations of the Galilean satellites planned for early 1980 will be presented.

Radar observations of Saturn's rings at intermediate tilt angles rule out large-particle monolayer models of the rings. Extant observational results indicate that the rings' radar polarization depends on wavelength or tilt angle, or both, and provide restrictions on ring-particle shape which are more severe for monolayer models than for extended-layer models.

VOYAGER I RADIO OCCULTATION EXPERIMENT
OF SATURN'S RINGS

E.A. Marouf, G.L. Tyler, and V.R. Eshleman, Center for Radar Astronomy, Stanford University, Stanford, CA 94305

In the early morning hours of November 13, 1980 (UT), the Voyager I spacecraft will emerge from Earth occultation by Saturn and will start propagating the first man-made radio signals ever through the ring system. For a period of about 25 minutes the radio beam will pierce the rings all the way from the top of the atmosphere to the outer edge of ring F. On Earth, the received perturbed signal will be simultaneously recorded at two coherent wavelengths (3.6 and 13 cm) for both the co-polarized and cross-polarized components of the transmitted circular polarization. When segmented over short time intervals, the temporal record of the received signal can be regarded as sample functions of a locally stationary complex gaussian process whose mean and power spectrum are determined by the particles' material, sizes, shapes, and by the column density of the region probed. The behaviour of the mean and spectrum is analysed for a ring model composed of a polydispersion of spherical ice particles that sparsely populate a layer that is either one particle or many particles thick. Detectable changes in the power of the mean, or coherent, signal provide a high resolution map of the radio opacity as a function of the radial distance. Simultaneous measurement of the coherent signal phase allows the decoupling of the particle size information from the column density if the particles are lossless and small compared to the wavelength. The decoupling can also be achieved for particles of effective diameter in the range of the two probing wavelengths from differential measurement of the radio opacity. Larger particles of effective diameter exceeding about 50 cm strongly rescatter the lost coherent power in directions close to the forward direction. This incoherent signal is received spread in frequency because of the relative motion of the particles and the spacecraft. The shape of its power spectrum is actually a high resolution map of the radial variation of the ring's radar cross-section. Estimates of the latter, together with the measured radio opacity, may be used to separate particle size information and to distinguish a monolayer from a multilayer vertical distribution. The column, or surface, density may also be recovered if the particles are nearly monodispersed. Over regions where multiple scattering is not dominant, the spectral width becomes a direct measure of particle size if the effective particle diameter exceeds the diameter of the spacecraft antenna (366 cm). The distinct behaviour of the measured averages over different ranges of particle size and opacity render this experiment most useful in exploring a system for which these parameters remain largely unknown.

CORONAL OCCULTATIONS OF SPACECRAFT RADIO SIGNALS

D. Routledge
Electrical Engineering Dept.
University of Alberta
Edmonton, Canada

and

H. M. Bradford
Canadian Coast Guard College
Sydney, Nova Scotia, Canada

Simultaneous angular and spectral broadening measurements are reported, of radio signals from spacecraft observed during solar coronal occultation. Observations made close to the sun at 13 cm wavelength with the Owen's Valley Radio Observatory 700m variable-spacing interferometer and a digital cross-power spectrometer of 14 Hz resolution are discussed. Solar wind speeds are derived from the measured values of angular and spectral broadening, which were obtained at various separations of the line of sight from the photosphere, and various heliographic latitudes.

Results from three coronal occultations near solar maximum are discussed, these being the first in what is intended to be a series of such observations spanning the present maximum and next minimum of the solar activity cycle. The principle objective will be to determine the importance of coronal scattering in accounting for the long-standing discrepancy between the heights and frequencies of solar 'plasma frequency' radio bursts.

TUESDAY AFTERNOON
June 3, 1:30 - 5:00

SPECTROMETRY AND TECHNICAL DEVELOPMENT

DKN 2D

Session J.3

Chairman: A.T. Moffet
California Institute of Technology
Pasadena, CA.

Spectrometry With the VLA

L. R. D'Addario, P. J. Napier and A. Rots
National Radio Astronomy Observatory

The VLA radio telescope in west-central New Mexico is now nearing completion, and facilities are becoming available which allow simultaneous spatial- and frequency-domain Fourier synthesis. The frequency synthesis is accomplished in hardware and real-time software, which are now operational. Total bandwidths of $2^{-k} \times 50$ MHz can be synthesized for $0 \leq k \leq 9$; 16×2^k channels are obtained for $0 \leq k \leq 3$, and 256 channels for $k \geq 4$. Polarization measurements are possible by allocating one-fourth of the channels to each of the elements of the polarization matrix.

The spatial synthesis is accomplished for each frequency channel in off-line digital processors, which compute an interpolation to a grid in the (u,v)-plane, followed by a discrete Fourier transform. This processing involves several mini-computers and array processors, and is still under development.

Present and projected capabilities of the system will be described.

JPL 2¹⁶ Channel 20 MHzBandwidth Digital Spectrum Analyzer*

George A. Morris, Jr. and Helmut C. Wilck

Jet Propulsion Laboratory
California Institute of Technology
Pasadena, CA 91103
U.S.A.

A 65,536 (2^{16}) channel, 20 MHz bandwidth, digital spectrum analyzer has been constructed at Jet Propulsion Laboratory (JPL). The design, fabrication, and maintenance philosophy of the modular, pipelined, Fast Fourier Transform hardware are described. The spectrum analyzer will be used to examine the region from 1.4 GHz to 26 GHz for Radio Frequency Interference (RFI) which may be harmful to present and future tracking missions of the Deep Space Network. The design will have application to the Search for Extraterrestrial Intelligent (SETI) signals and radio science phenomena.

A WIDEBAND DIGITAL AUTOCORRELATOR FOR SPECTRAL ANALYSIS

Philip A. Ekstrom, Staff Scientist
Battelle-Northwest Laboratories
P.O. Box 999, Richland, Washington 99352

A project to develop a wideband digital spectral analysis capability has produced a delay-multiply-accumulate correlator unit cell which operates in excess of 400 MHz clock rate. This speed, a large fraction of the 100K series ECL flipflop toggle rate, required a traveling-wave circuit design and the use of or-tie gating. Clock distribution employs a cascade instead of the more usual clock tree, allowing free interchange of the four-unit-cell circuit boards. The clock buffer circuit developed specifically for cascade operation is stable against the effects of propagation delay asymmetry. Construction is single plane microstrip on conventional glass-epoxy circuit board with a power distribution and bypass layer bonded to the ground plane.

Signal representation is 3-level, or $1\frac{1}{2}$ bits, implying an observing time penalty of 57% when compared with an infinite precision representation.

The completed instrument, comprising 64 four-cell boards, will perform 10^{11} arithmetic operations per second and offer 1% spectral resolution at up to 200 MHz instantaneous bandwidth. Two-way input multiplexing will extend this to 400 MHz at 2% resolution. Extensive self-test capability will allow automated fault detection and location of a failing logic package.

THE DESIGN OF ACOUSTO OPTICAL SPECTROMETERS
FOR RADIO ASTRONOMY

Colin R. Masson
California Institute of Technology
Pasadena, California 91125

The principle of using acousto optical devices to produce radio frequency spectrometers has been known for about 2 decades. Despite the simplicity of the acousto optical approach, it is only recently that acousto optical spectrometers (AOS) have been used for radio astronomy. The main reason for this slow progress has been the extreme stability required for the long integrations used in radio astronomy.

Recent work at Caltech has been devoted to a careful study of the various sources of mechanical and thermal drifts in AOS. From the results of this work, it is possible to design AOS with stability adequate for frequency switching or beam chopping rates as low as 0.01 Hz. This is a significant improvement over the first generation of AOS, which require chopping at ~ 1 Hz to cancel drifts. AOS can be built with bandwidths of up to 1 GHz, using commercially available components.

To demonstrate these techniques, a prototype 100 MHz, 1024 channel spectrometer has been built at Caltech. Measurements of the performance of this instrument will be presented.

Future work at Caltech will include development of a correlating version of the AOS for use with the new millimeter interferometer.

A LOW NOISE S-BAND RADIOMETER
K.F. Tapping, J.M. Bastien,
E.J. Stevens, and C.S. Philipson.
Herzberg Institute of Astrophysics,
National Research Council of Canada,
100 Sussex Drive, Ottawa, Canada
K1A 0R6

A low noise, S-Band radiometer has been developed for use on the 46 m. antenna at the Algonquin Radio Observatory. The system noise temperature is about 30°K. The first amplifier is a dual-stage, cooled parametric amplifier. This is followed by a GaAs FET amplifier which brings the total gain before the mixer to about 60 dB, rendering the mixer noise contribution negligible and reducing the effect of spurious mixer responses on the receiver performance as a line receiver. Provision is made for remote receiver tuning and noise temperature measurement.

In order to improve receiver flexibility and servicability, a digital control and status system is used and the receiver subsystems built as stand-alone modules. Faults can be diagnosed and system reconfigurations can be made remotely.

THE HAYSTACK OBSERVATORY COMPUTER SYSTEM
A Modular Approach to Telescope Control

B. G. Leslie
Haystack Observatory
Westford, Mass. 01886, U.S.A.

We have replaced the original computer used for pointing and data acquisition at the 37.5 meter telescope at the NERO Haystack Observatory with a modern mid-size computer. The multi-task capability of the new system allows both on-line and post-real-time processing to be carried out in parallel with real-time observations.

Programs and subroutines have in general been written to separate control and execution functions in real-time subsystems. This allows the user to use the same control software with different receiver back-ends, or to develop a specialized control system if desired without the necessity of rewriting the device handlers.

Processing programs are written in an interactive mode to provide the shortest possible learning curve for new users while maintaining the flexibility needed for more complex experiments. Whenever possible, the software handles differences in receivers transparently to the user.

This software is based on the same computer system as the MK-III VLBI terminals. It will operate either separately or in parallel with the MK-III checkout and data acquisition programs.

WEDNESDAY MORNING

June 4, 8:30 - 10:00

RADIO STARS

DKN 2D

Session J.4

Chairman: J.L. Yen
University of Toronto
Toronto, Ontario

WEDNESDAY AFTERNOON
June 4, 1:30 - 5:00

RADIO ASTRONOMY ANTENNAS

DKN 2E

Session J.6

Chairman: T.H. Legg
Herzberg Institute of Astrophysics
National Research Council
Ottawa, Ontario

Developments in High Precision Large Space Telescope Design

T. B. H. Kuiper, P. N. Swanson, P. D. Batelaan
Jet Propulsion Laboratory, California Institute of Technology

M. K. Kiya, J. P. Murphy, M. W. Werner
NASA Ames Research Center

We are investigating the technology readiness for submillimeter and infrared astronomical space telescopes in the 10-30 m class. The possibility of such systems is suggested by the results of studies funded by the Defense Advanced Research Project Agency directed toward large aperture IR ($\lambda > 2 \mu\text{m}$) optical systems. Problem areas which have been addressed include: primary mirror materials, surface finish mass production techniques, figure sensing and control, vibration damping, and deployment mechanisms. After a survey of the industry we concluded that large IR telescopes are technically feasible. We are now concentrating on evaluating the trade-offs between performance (e.g. minimum wavelength and maximum aperture for coherent imaging) versus cost and risk (i.e. probability of successful deployment and operation). A contract study is currently being carried out at the Lockheed Palo Alto Research Laboratory. We will report our findings and the results of the Lockheed study. A scenario for the development of a 10-15 m class submillimeter wavelength telescope for use circa 1990 will be presented.

ELECTROSTATICALLY-CONTROLLED ANTENNAS

David H. Staelin and Jeffrey H. Lang*
Massachusetts Institute of Technology
Cambridge, Massachusetts 02139

Conventional large reflector antennas are limited to beamwidths typically greater than ~ 1 arc minute by thermal and gravitational distortion effects, although clever engineering has occasionally exceeded these limits by modest factors. Controlled antenna systems can require large numbers of sensors and actuators in order to significantly exceed these same limits. In electrostatically controlled antennas (J. H. Lang, J. R. Gersh, and D. H. Staelin, Electronics Lett., 14, 665-666, 1978) large numbers (10^2 - 10^4) of very simple fast actuators can be realized economically and reliably. Because such antennas can exhibit Rayleigh-Taylor instabilities, these must also be controlled electronically.

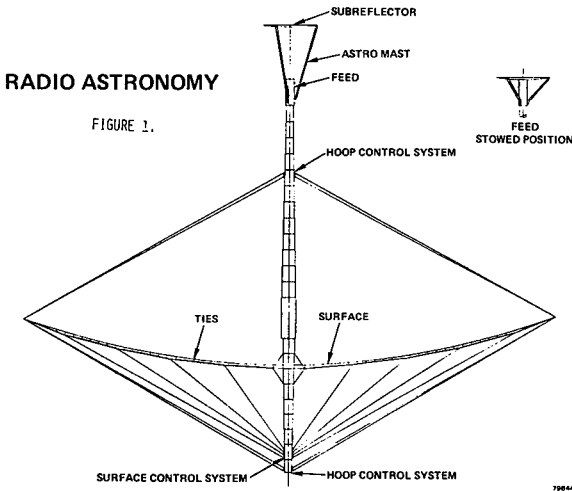
It has been shown that the resolution limit of an electrostatically-controlled antenna is $\sim (900/AM^2(f/D))^3$ arc sec, where A is a factor near 10, M is the number of controlled unstable modes, f is the antenna focal length, and D is its diameter. Our laboratory demonstration of the control of three unstable modes in a thin mesh 1-m square suggests that antennas with $f/D \approx 2$ could yield beamwidths of ~ 2 arc sec.

*On leave to the Charles Stark Draper Laboratory
from M.I.T.

A 30 METER HOOP/COLUMN EARTH ORBITING
 VERY LONG BASELINE INTERFEROMETER

Larry D. Sikes
 Harris Government Electronic Systems Division
 P.O. Box 37
 Melbourne, FL 32901

Very Long Baseline Interferometry (VLBI) has been used by radio astronomers utilizing earth based observatories over the last decade to obtain celestial radio sources at previously unrealizable levels of angular resolution. Of late, increased interest in obtaining higher resolution maps of radio sources with less ambiguity has directed investigations toward large earth orbiting VLBI systems. The longer baselines measured between fixed earth and orbiting radio observatories results in this higher resolution. Studies have been performed which indicates that 30 meter diameter earth orbiting antenna operating in the frequency range of 1.4 to 30 GHz fulfills the mission scenario (Figure 1). This antenna would be delivered to a 400 kilometer earth orbit via Shuttle/IUS and deployed before boost to the specified altitude.



AN INTERFEROMETER FOR MILLIMETER WAVELENGTHS

W.J. Welch, D.D. Thornton, W. Hoffman, M.C.H. Wright, D.R.W. Williams,
R.L. Plambeck, and J.H. Biegling

Radio Astronomy Laboratory, University of California, Berkeley, CA
94720

A description is given of the Hat Creek Interferometer. It is an earth-rotation aperture synthesis instrument with the antennas movable on a T-shaped roadbed. The system is designed to operate in the range 1-15 mm. During the last two years the telescopes have been instrumented to work in the band 85-90 GHz (3.4 mm) using solid state local oscillators and room temperature mixers. The system has been used to make maps of both radio continuum sources and of spectral line emission from molecular clouds. The performance of the instrument at these wavelengths is discussed and some initial results are shown. Atmospheric and thermal effects and the problems of calibrations are discussed in particular.

A Simple and Accurate Antenna Theodolite

Chuang-Jy Wu and S. Gerylo

Herzberg Institute of Astrophysics
National Research Council of Canada
Ottawa, Ontario, Canada

Many techniques of measuring paraboloidal reflecting surface accuracy had been reported during last decades. In order to determine the relative position of a point on a well behaved almost paraboloidal surface, two independent quantities; i.e. the distance and the relative height between the point and the reference point, are required. Distances between the target on the paraboloidal surface and the reference point are generally obtained either by using accurate measuring tape or by measuring time delay of an electromagnetic wave. The relative height between the target and the reference point is usually obtained by using optical angular measurement equipments.

Despite of various indirect measurement methods proposed recently, such as the microwave holographic technique, the trolley method, etc., the survey theodolite is still the basic measurement equipment during alignment of the paraboloidal reflecting surface. One of the difficulty in using the survey theodolite is reading the angle micrometer. Special care is needed in order to obtain accurate readings. In this report a simple method which can display the theodolite relative angle accurately is described.

An accurate LVDT (Linear variable differential transformer) model PCA-220-020, Schaevitz Engineering, is mounted on the theodolite base (Watts Microptic Theodolite No 2 Mk 2), and the direction of LVDT's core movement is approximately perpendicular to the axis of theodolite telescope. The relative angular measurement then becomes the core displacement measurement. Since the LVDT is a device which transforms the linear displacement into voltage, the target relative angle may be obtained by measuring the output voltage of LVDT. A $6\frac{1}{2}$ digits digital voltmeter is employed in the experiment. The system has been used at Algonquin Radio Observatory to adjust the reflecting surface of 150-ft diameter antenna. Better than 1 arc second display accuracy of the target relative angle has been achieved.

OBSERVING RADIO STARS WITH THE ARECIBO INTERFEROMETER

Kenneth C. Turner, Arecibo Observatory, P. O. Box 995, Arecibo, Puerto Rico 00612

The high sensitivity made possible by the large collecting area of the Arecibo Interferometer, together with the possibility of making position measurements with accuracies of a small fraction of a second of arc, make this instrument ideal for the study of radio stars.

Currently in use at 2380 MHz., its 10.6 km. baseline (almost N-S) gives a fringe spacing of 2.4 arc seconds. Maser receivers yielding 50K system temperatures produce measured fluctuations of 5 mJy. rms for 10 sec. averages about a 10 min. mean. Phase stability is adequate for integrations of at least 30 to 40 minutes.

Two programs of observations of radio stars have commenced using this instrument. The first, initiated by M. M. Davis of Arecibo Observatory and the author is a search for emission due to ionized material ejected from high luminosity stars by stellar winds.

The second, due to Y. Terzian of Cornell University and myself, is a study of recent and old galactic novae, looking for evidence of nearby ionized material detectable at radio wavelengths.

Preliminary results for a number of stars will be presented.

AN IMPROVED RADIO SOURCE CATALOGUE BASED ON
35 km INTERFEROMETER OBSERVATIONS
G.H. Kaplan, F.J. Josties, W.J. Klepczynski,
D. Matsakis, P. Angerhofer, D.D. McCarthy,
U.S. Naval Observatory
K.J. Johnston, J.H. Spencer, Naval Research
Laboratory

The connected element interferometer of the National Radio Astronomy Observatory in Green Bank, West Virginia, has been used by the U.S. Naval Observatory and the Naval Research Laboratory in a joint program to apply radio interferometric techniques to the determination of variations in Earth rotation parameters. An important part of the program is the determination of improved positions for the observed sources. Using data obtained during October-November 1978, the positions for 19 sources were improved. These improved positions were based on single frequency observations and, hence, were uncorrected for differential ionospheric effects. Recently, using dual frequency observations, the positions for 14 sources were improved based on data obtained during October-December 1979. The steps taken and the results obtained for this latter phase will be presented.

AUTHOR INDEX

Aarons, J.	288	Brown, G.S.	102
Aboul-Atta, O.A.	71	Brown, M.F.	265
Adams, A.T.	51	Buettner, H.M.	184
Agrawal, A.K.	120	Burke, G.J.	119
Ahalt, S.C.	283	Burke, H.K.	248,249
Al Hafid, H.T.	274	Burt, E.C.	42,159
Ali, A.A.	209	Bussgang, J.J.	217
Altshuler, E.E.	280	Butler, C.M.	25,26,58,59
Angersofer, T.	333,359	Campbell, R.W.	93
Antar, Y.M.M.	286	Cancellieri, G.	27
Araki, K.	191	Carpenter, D.L.	316
Arnold, J.M.	32,33	Carroll, J.C.	293
Assis, M.S.	268	Carver, K.R.	186
Audet, J.	9,144	Cashman, J.	41
Avrin, J.S.	219	Cauterman, M.	270
Badr, M.T.	276	Chan, C.K.	165
Bahar, E.	104	Chang, D.C.	50,70,113
Balanis, C.A.	46	Chang, R.K.	139
Baldwin, T.E.	264	Chang, S.	106
Bansal, R.	153	Chao-Dong Z.	54
Barber, P.W.	139	Chaudhuri, B.B.	66
Barrington, R.E.	3	Chaudhuri, S.K.	159
Bastien, J.M.	347	Checcacci, P.F.	84
Batelaan, P.D.	353	Chen, H.C.	24
Beard, C.T.	251	Chen, K.C.	157
Beilfuss, J.	226	Chen, K.M.	143
Belikovich, V.V.	294	Cheung, R.	101
Bell, T.F.	313,316	Chew, W.C.	150,190
Benediktov, E.A.	294	Chive, M.	9
Bennett, C.L.	119,122,146	Choi, C.W.	154
Berkey, F.T.	299	Chou, T.J.	51
Bérubé, R.C.	286	Chow, Y.L.	96,138
Bevensee, R.M.	178	Christopher, P.F.	205
Bieging, J.H.	356	Chu, R.S.	186
Blachman, N.M.	216	Chu, T.H.	165
Blamont, J.	214	Chuang, S.L.	258,262
Blanchard, Y.	231	Chu-Fang, X.	107
Bloch, S.C.	282	Cipolla, F.W.	186
Block, H.	143	Citerne, J.	67
Boerner, W.M.	74,159	Clarricoats, P.J.B.	115
Bojarski, N.N.	125,179	Clowes, K.J.	202,203
Bolomey, J.Ch.	9,41,144,152	Coffey, E.I.	47,95,119
Bostian, C.W.	285	Cohen, M.H.	329
Botros, A.Z.	72	Cole, J.	74
Bradford, H.M.	341	Collin, R.E.	133
Brand, J.C.	171,172	Conradi, J.	196
Brenci, M.	84	Constantinou, P.	206
Bringi, V.N.	100	Cooper, G.R.	220
Brittingham, J.N.	151	Cordaro, J.T.	119
Brown, G.J.	230	Cornbleet, S.	111

Cosnard, E.	67	Epseland, R.H.	293
Coyle, C.	168	Eshleman, V.R.	340
Cramer, P.,JR.	167	Evans, J.V.	308
Crawford, F.W.	312	Falciai, R.	84
Crone, G.A.E.	32	Fantini, P.	27
Currie, N.C.	235	Farhat, N.H.	165
D'Addario, L.F.	343	Favre, F.	81
Dagenais, J.C.	203	Fedors, J.C.	242
D'Ambrosio, G.	7	Feit, M.D.	110
Dando, J.	226	Feldman, H.	23
Daniele, V.	77	Feldman, P.A.	350
Das, S.	118	Fellinger, P.	53
Das, Y.	162,182	Felsen, L.B.	30
Davidson, D.	282	Fengler, C.	271
Davis, J.R.	290	Ferguson, J.A.	314
Davis, W.A.	119	Ferrara, G.	7
Deadrick, F.J.	119	Ferrari, R.L.	87
Decker, M.T.	244	Fleck, J.A., JR.	110
Degauque, P.	270	Ford, P.G.	335
DeInore, V.E.	241	Fort, D.N.	327
Demarest, K.R.	52	Franceschetti, G.	77,266
Demoulin, B.	270	Franklin, C.A.	2
Dent, J.R.	285	Furuhama, Y.	271
Deschamps, G.A.	43	Gabillard, R.	270
De Souza, E.G.	75	Galeati, P.	35
Dike, G.A.	42,159	Gardner, R.L.	257
Di Meglio, F.A.	7	Gaunaurd, G.C.	130
Dinger, R.J.	106	Gelin, P.	60
Direskeneli, H.	100	Geryl, S.	357
Dod, L.R.	247	Ghuniem, A.M.	281
Dombroski, E.J.	140	Giraldez, A.E.	307
Dombrowski, M.	250	Glisson, A.W.	121
Dorey, J.	231	Goddard, W.R.	74
Douppnik, J.R.	299	Goldhirsh, J.	284
Downs, G.S.	337	Goldstein, R.M.	336
Doyle, M.	250	Govind, S.	136
Duchene, B.	144	Grankov, A.G.	254
Durment, J.	224	Gray, K.G.	21
Durney, C.H.	8	Griffin, D.W.	106
Dyer, F.B.	235	Guiraud, F.O.	332
Earl, G.F.	301	Gulyaeva, T.L.	294
Eckerman, J.	250	Gupta, G.S.	115
Edgerton, A.T.	248,249	Gupta, S.C.	176,274
Ekstrom, J.L.	218	Gurbaxani, S.H.	120
Ekstrom, P.A.	345	Habashy, T.M.	150
El Habiby, S.	41,152	Hagfors, T.	322
Elliott, R.S.	187	Hansen, P.M.	222
El Said, M.	264	Hardy, K.R.	248
El Tanany, M.S.	264	Harger, R.O.	233
En-Yao, Y.	54	Harker, K.J.	312

Harrington, R.F.	134,241,242	Jordan, A.K.	129
Hauber, J.	277	Joshi, G.H.	226
Hauser, J.P.	225	Josties, J.	333,359
Hayre H.S.	208	Jurgens, R.F.	214,336
Hayward, R.A.	164	Kahn, W.K.	55
Heller, M.	213	Kajfez, D.	25,26
Helliwell, R.A.	316	Kalahdar Rao, T.C.	91,120
Hendry, A.	286	Kamal, A.A.	57
Herndon, D.H.	140	Kang-hou, M.	174
Hessel, A.	108	Kao, C.	194
Hill, D.A.	269	Kaplan, G.	333,359
Hill, K.O.	117	Katsuftrakis, J.P.	316
Hillaire, F.	152	Kawajiri, N.	326
Ho, C.M.	159	Kawano, N.	326
Ho, J.H.	249	Kawasaki, B.S.	117
Hofer, W.J.R.	63	Kellerman, K.J.	329
Hofer, R.	245	Kelly, F.J.	225
Hoffman, W.	356	Kennaugh, E.M.	22,40
Hogg, D.C.	244,332	Keshavamurthy, T.L.	58,59
Holt, J.M.	308	Kim, J.G.	234
Hoorfar, A.	70	King, H.E.	106
Houminer, Z.	288	King, J.L.	246
Hower, R.T.	171	King, R.J.	14
Hsu, S.V.	62	King, R.W.P.	49,153,265
Huang, J.	37	Kiya, M.K.	353
Huchital, G.S.	185	Kleinman, R.E.	128,137
Hung, R.J.	239	Klepczynski, W.K.	333,359
Hung-chia H.	79	Klobuchar, J.A.	292
Hutchins, R.L.	119	Knepp, D.L.	103
Ibrahim, M.	274	Ko, W.L.	170
Ihara, T.	271	Kong, J.A.	150,190,258,260,262,263
Imai, M.	116	Kouyoumjian, R.G.	38,39
Imbriale, W.A.	92	Kressel, H.	195
Inan, U.S.	313,316	Krowne, C.M.	186
Ishimaru, A.	99,101	Krueger, R.J.	127
Iskander, M.F.	8	Ksienski, A.A.	147
Itoh, H.	110	Kubacsi, M.	261
Itoh, K.	110	Kuester, E.F.	70,113
Itoh, T.	191	Kuga, Y.	101
Iyer, R.	200	Kuhfeld, J.	10
Jacobsen, G.	34	Kuiper, T.B.H.	353
Jaggard, D.L.	82,199	Kumar, A.	273
James, H.G.	311	Kumar, Y.	272
Jamnejad, V.	173	Laine, E.F.	181
Javed, A.	200	Lakhtakia, A.	8
Jecko, B.	119	Lamontagne, Y.	180
Jedlicka, R.P.	186	Lamsakis, M.	333,359
Jirapunth, T.	38	Landt, J.A.	119
Johnston, K.	333,359	Lane, S.O.	279
Jones, W.L.	241	Lang, J.H.	354

Langenberg, K.L.	53	McIsaac, P.R.	323
Larson, C.J.	106	Meadors, J.G.	155
Leader, J.C.	98	Medgyesi-Mitschang, L.N.	135
Lee, C.Q.	11	Medynski, D.	231
Lee, J.K.	262	Meidenbauer, R.H.	278
Lee, K.S.H.	158	Merk, R.L.	302
Lee, L.S.	207	Meyers, W.D.	106
Lee, S.W.	167,169,173	Mezzetti, M.	27
Lefevvre, F.	318	Michalski, K.A.	142
Legg, T.H.	328	Mieras, H.	119,122
Lehman, T.H.	47,48,95,119	Mieziis, R.	247
Lehtinen, M.	322	Miller, E.K.	119
Lennon, J.F.	105	Miller, T.R.	316
Lenz, P.A.	159	Mishra, S.R.	228
Leroy, Y.	9	Mittra, R.	89,90,170,173
Leslie, B.G.	348	Mitzner, K.M.	20
LesseLier, D.	144,152	Mohsen, A.	73,264
Leuven, K.U.	188,189	Moler, W.F.	314
Lewis, J.E.	83	Monsen, P.	210
Liang-Ming, Z.	54	Montgomery, J.P.	15,175
Lilly, J.D.	46	Montrosset, I.	77
Lin, H.C.	147	Morgan, M.A.	21
Lindström, C.	197	Morris, G.A., JR.	336,344
Liu, C.H.	289	Moser, P.J.	130
Long, S.A.	186	Mostapha, A.E.S.	281
Look, C.M.	198	Munk, B.A.	106
Lyons, R.	119	Murphy, J.D.	130
Lytle, R.J.	181	Murphy, J.P.	353
MacCartney, D.	333	Nagl, A.	130
Mach, I.M.	80	Nair, R.A.	176
Mack, R.B.	137	Naito, Y.	191
Mackenzie, E.	288	Nakagawa, K.	319
MacPhie, R.H.	18	Napier, P.J.	343
Mahmoud, S.F.	72,264	Neiswander, R.S.	16
Maile, G.L.	87	Nguyen, T.H.	31
Makita, F.	13	Njoku, E.G.	245
Malindzak, G.	10	Noad, J.P.	198
Mann, E.B.	48	Norvell, S.	211
Manus, E.A.	285	Nyquist, D.P.	62
Marouf, E.A.	340	Odom, D.B.	292
Marshali, S.A.	57	Okada, J.T.	181
Marshall, R.E.	285	Oliver, W.L.	308
Martin, L.U.	251	Olsen, R.G.	69
Masson, C.R.	346	Olsen, R.L.	286
Massoudi, H.	8	Orr, G.	250
Masursky, H.	335	Ostro, S.J.	339
McFee, J.E.	162,182	Papa, R.J.	105
McGillan, M.E.	259	Papiernik, A.	119
McGree, T.P.	220	Pappert, R.A.	314
McIntosh, R.E.	309	Parhami, P.	136

Park, C.G.	317	Saad, S.S.	57
Park, P.K.	187	Salm, I.E.	281
Parsons, J.D.	227	Sankar, A.	119
Pathak, P.H.	38	Santago, P.	285
Paul, A.	61	Sanzgiri, S.	15
Paul, A.K.	298	Sarkar, T.K.	159,221
Paul, D.K.	66,114	Satoh, T.	13
Pavlasak, T.J.F.	228	Scheggi, A.M.	84
Peake, W.H.	155	Schlesak, J.J.	286
Pearson, L.W.	142	Schmale, D.M.	141
Pelosi, G.	39	Schrieber, P.W.	156
Peng, S.Y.	186	Schuman, H.K.	264
Petenzzi, M.	60	Schutt, J.	250
Peters, L., JR.	145	Seliga, T.A.	100
Pettengill, G.H.	335	Sengupta, D.L.	229
Philipson, C.S.	347	Senior, T.B.A.	19,229
Pichot, Ch.	9,144	Seth, D.P.S.	272
Pitteway, M.L.V.	297,306	Shafai, L.	71,186
Plambeck, R.L.	356	Sheikh, A.U.H.	227
Poe, G.	249	Shen, L.C.	186,265
Poe, M.T.	186	Sheshadri, M.	173
Pogorzelski, R.J.	44,92	Shevgaonkar, R.K.	114
Presby, H.M.	28	Shibata, T.	319
Price, H.J.	91,120	Shields, M.	187
Pues, H.F.	189	Shih, Y.C.	63
Purton, C.R.	351	Shin, R.	260,261
Rahman, F.	186	Shlanta, A.	236
Rahmat-Samii, Y.	168,169	Shmoys, J.	108
Rao, S.M.	121	Shnitkin, H.	106
Rech, K.D.	53	Shoamanesh, A.	186
Reilly, M.H.	129,291	Shumpert, T.H.	141
Reinisch, B.W.	296	Shutko, A.M.	254
Rengarajan, S.R.	83	Shuwen, Y.	85
Rhoads, F.J.	225	Sikes, L.D.	355
Riggs, L.S.	141	Simpson, R.A.	338
Ri-rong, Z.	278	Sindoris, A.R.	186
Rispin, L.W.	50	Singh, N.	321,325
Rizzoli, V.	35	Sinha, A.K.	201,324
Robillard, M.	9	Sinha, B.P.	18
Roemer, L.	10	Sio, L.F.	11
Roger, A.	131	Sleeman, B.D.	128
Rope, E.L.	164	Smith, C.P.	77
Rosenkranz, P.W.	253	Smith, E.W.	140,171,172
Rots, A.	343	Smith, R.E.	239
Routledge, D.	341	Smyth, D.C.	224
Rowe, H.E.	80	Smyth, J.B.	224
Rulf, B.	23	Smythe, G.	238
Rush, C.M.	293	Som, S.C.	161
Rushdi, A.M.	90	Someda, C.G.	35
Ryan, J.M.	331	Spencer, J.	333,359

SpringThorpe, A.J.	198	Tyorina, G.I.	294
Staelin, D.H.	354	Uberall, H.	130
Stalzer, H.J., JR.	108	Uffelman, D.R.	290
Stark, A.	106	Ulaby, F.T.	240
Stephene, H.	203	Umashankar, K.	94
Stevens, E.J.	347	Vaccaro, V.G.	266
Stiles, G.S.	299	Van de Capelle, A.	188,189
Stone, W.R.	124	Van Lil, E.	188
Storey, L.R.O.	315	Varadan, V.K.	100
Strauch, C.	244	Varadan, V.V.	100
Stutzman, W.L.	279,285	Viens, N.P.	292
Suratt, R.E.	109	Violette, E.J.	293
Swanson, P.N.	353	Volakis, J.	145
Swift, C.T.	241,242	Wait, J.R.	267,269
Tabbara, W.	144	Waldman, H.	300
Taflove, A.	76,94	Wallenberg, R.F.	42,159
Takahashi, F.	326	Walton, E.K.	148
Takao, K.	275	Wand, R.H.	308
Tang, D.D.	282	Wang, J.	250
Tang, R.	186	Wang, J.J.H.	88,154
Tapping, K.F.	347	Warhola, G.T.	82,199
Tarnawecy, M.Z.	71	Weigan, L.	64,65,112
Tatekura, K.	110	Weil, H.	156
Taylor, L.S.	160	Weissberg, M.A.	278
Telford, L.E.	280	Weissberger, M.	277
Thiemann, H.	325	Weissman, D.E.	234
Thio, C.	74	Welch, W.J.	356
Thornton, D.D.	356	Werner, M.W.	353
Tiberio, R.	39	West, G.F.	5,180
Tien, P.K.	29	Weston, V.H.	126
Tihanyi, P.	197	Wetzel, L.B.	237
Tijhuis, A.G.	143	Whitney, A.R.	330
Titheridge, J.E.	304,305	Wilck, H.C.	344
Tohma, K.	271	Wiley, P.H.	283,285
Toldalagi, P.M.	252	Williams, D.R.W.	356
Tomar, R.S.	61	Wilton, D.R.	121
Tong, T.C.	119	Wong, J.L.	106
Toomey, J.P.	146	Wong, N.S.	186
Tranfaglia, A.	7	Woo, K.	167
Trapani, L.P.	186	Woo, R.	99
Trebits, R.N.	235	Wright, M.C.H.	356
Tremblay, Y.	117	Wright, J.W.	297,306
Tricoles, C.	164	Wu, C.J.	357
Trivedi, N.B.	75	Wu, D.C.	109
Tsang, L.	258,260	Wu, F.T.	236
Tsao, C.H.	89	Wu, T.T.	153,265
Tseng, F.I.	221	Xunxian, X.	212
Turner, K.C.	358	Yang, F.C.	99
Tutt, M.	96,138	Yeh, C.	78
Tyler, G.L.	338,340	Yeh, K.C.	289

Yen, J.L.	4	Zbontar, T.	25,26
Yen, Y.H.	14	Zich, R.	77
Yip, G.L.	31,202,203	Zimmerman, W.R.	48,119
Yoshino, T.	319,326	Ziołkowski, R.W.	43
Yu, C.L.	37	Zrnic, D.S.	238
Yu, J.S.	163,183	Zuniga, M.A.	262,263
Yu, W.M.P.	236	Zygielbaum, A.I.	214

Forthcoming URSI and URSI-Related Meetings
(where known, the name of a contact is given in parentheses)

- 23-27 June 1980 Conference on Precision Electromagnetic Measurements, Braunschweig, FRG.
- 30 June-4 July 1980 International Symposium on the Biological Effects of Electromagnetic Waves, near Paris, France (A & B cosponsorship).
- 17-24 July 1980 Sixth International Symposium on "Equatorial Aeronomy", Puerto Rico (S. Matsushita).
- 28 July-1 August 1980 Commission F International Symposium on "Middle atmosphere dynamics and transport", Urbana, USA (T.E. Van Zandt).
- 26-29 August 1980 Commission B International Symposium on Electromagnetic Waves, Munich, FRG (H. Hochmuth - FRG).
- 2-5 September 1980 European Conference on Circuit Theory, Warsaw, Poland (T. Morawshi - Poland).
- 8-12 September 1980 European Microwave Conference, Warsaw, Poland.
- 14-18 September 1980 Bioelectromagnetic Society Symposium, San Antonio, TX.
- 17-19 September 1980 Fifth International Wroclaw Symposium on Electromagnetic Compatibility, Wroclaw, Poland.
- 7-9 October 1980 IEEE International Symposium on Electromagnetic Compatibility, Baltimore, MD.
- 5-8 January 1981 Commission F International Symposium on "Signature problems in remote sensing of the surface of the earth", Lawrence, KA (R.K. Moore).
- 12-15 January 1981 USNC/URSI National Radio Science Meeting, Boulder, CO (T.B.A. Senior)
- 15-22 April 1981 IUCRM Colloquium (with COSPAR): "Wave-dynamics, radio probing of the ocean surface, and related topics", Miami, FL (O.M. Phillips).
- 15-19 June 1981 National Radio Science, IEEE AP-S and IEEE MTT-S Meetings, Los Angeles, CA (R.S. Elliott).

NOTES

NOTES

NOTES



ROOM TIME	DKN 1A	DKN 1B	DKN 1D	DKN 1E	DKN 2A	DKN 2B	DKN 2C	DKN 2D	DKN 1271 - 1289 (Poster Sessions)	BUSINESS AND SPECIAL MEETINGS
MONDAY 8:30 - 12:00 a.m.	B.1 Scattering I		AP.1 Millimetre Wave Antennas	AP.2 Dipole and Slot Antennas	A Bio electro- magnetics	B.2/AP-S Optical Commun. I		J.1/AP-S VLBI		SUNDAY 4:00 p.m., VCH 1045 AP-S WPSC Meeting 6:30 p.m., Salon Prof. USNC/URSI Exec. Comm. 8:00 p.m., Salon Prof. USNC/URSI Business
MONDAY 1:30 - 5:00 p.m.	B.3 HF Scattering	B.4 Wire Antennas I	AP.3 Satellite Antennas	AP.4 Adaptive Antenna Systems		C.1/D Optical Commun. II	F.1 Remote Sensing- Active	J.2 Radar Astronomy	B.5 Guided Waves	MONDAY 7:00 p.m., VCH 1045 AP-S WPSC Meeting 8:00 p.m., DKN 1A Electromag. Soc. Meeting
MONDAY 5:30 - 7:00 p.m.	Cocktail - Jardin Géologique									Cocktails - Geological Garden
TUESDAY 9:00 - 12:00 a.m.	Plenary Session - Radio Science in Canada - Théâtre de la Cité Universitaire									TUESDAY 12:00-noon, Salon Prof. AP-S Reviewers Lunch 5:00 p.m., Salon du Recteur AP-S Local Chapter
TUESDAY 1:30 - 5:00 p.m.		B.6 Induction from Overhead Conductors	AP.5 Phased Arrays	AP.6 Scattering and Diffraction	G.1 Ionospheric Modification and Irreg.	B.7/AP-S Optical Commun. III	F.2 Remote Sensing- Passive	J.3 Spectrometry and Technical Development	AP.7 Horn Antennas	5:30 p.m. B Business, DKN 1248 F Business, DKN 1252 Geosc.-Rem. Sens., DKN 1255 6:00 p.m., Salon Prof. Ad. Com. Meeting

ROOM TIME	DKN 1A	DKN 1B	DKN 1D	DKN 1E	DKN 2A	DKN 2B	DKN 2C	DKN 2D	DKN 2E	DKN 1271-1289 (Poster Sessions)	BUSINESS AND SPECIAL MEETINGS
WEDNESDAY 8:30 - 12:00 a.m.	B.8 Analyt. and Num. Techniques	B.9 Random Media	AP-S/B.10 HF-to-UHF Arrays	H.1 Magnetosph. and Space Plasmas	C.2 Satellite and Radio Transmission	B.11/AP-S Optical Commun. IV	F.3 Radiative Transfer and Lightning	J.4 Radio Stars A/J.5 Large Ant.	G.2 Ionosonde Techniques	AP.8 Ant. Meas. and Calculations	THURSDAY 5:00 p.m. DKN 1255 Electromagn. Consulting
WEDNESDAY 1:30 - 5:00 p.m.	AP-S/B.12 Transients	B.13 Inverse Scattering I	AP.9 Antenna Synthesis	AP.10 Radar-D.F. AP.11 Adapt. Ant.	G.3 Ion. Int. Ion. Drifts and Disp.	C.3 Signal Processing	F.4/AP-S Surface/ Underground Prop.	H.2 Plasma rel. Theor. Studies	J.6 Radio Astron. Antennas	AP.12 Satellite Antenna Systems	5:30 p.m. DKN 1248 G Business 5:30 p.m. DKN 1252 H Business
WEDNESDAY 7:30 p.m.	Banquet - Château Frontenac										Conference Banquet - Château Frontenac
THURSDAY 8:30 - 12:00 a.m.	B.14 Scattering II	B.15/AP-S Inverse Scattering II	AP.13 Reflector Antennas I	AP.14 Vehic. Antennas	E Noise and Interf.		F.5/AP-S Line-of- Sight Prop.				5:30 p.m. VCH 1045 CNC/URSI B Business
THURSDAY 1:30 - 5:00 p.m.		B.16 Special Topics	AP.15 Offset Ref. and Lens Antennas	AP.16 Microstrip Antennas	AP.17 GTD and Ray Methods		F.6/AP-S Prec. Atten. and Depolar.			B.17/AP-S Inverse Scattering III	8:00 p.m. VCH 1045 USNC/URSI Exec. Comm.
THURSDAY 7:30 p.m.	Vin et fromages - Pavillon Pollack										Wine and Cheese - Pavillon Pollack
FRIDAY 8:30 - 12:00 a.m.	B.18 Reflector Antennas II	B.19 Inverse Scattering IV		AP.18 Wire Antennas II						AP-S/B.20 Microstrip Ant. and Arrays	

Division des publications
Service des relations publiques
RPDP-80-179
Université Laval, Québec, Canada

QUÉBEC, JUIN / JUNE 2-6, 1980



UNION RADIO SCIENTIFIQUE INTERNATIONALE
INTERNATIONAL UNION OF RADIO SCIENCE